

https://dspace.org/

Sequential adeno-associated virus deliverd HIV-1 subtype C ENV glycoproteins as novel vaccine immunogens

Moodie, Melanie

2018
https://hdl.handle.net/10539/27024

Downloaded from a DSpace repository. https://dspace.org/

Sequential Adeno-Associated Virus delivered HIV-1 subtype C Env Glycoproteins as Novel Vaccine Immunogens.

Melanie Moodie

A Dissertation submitted to the Faculty of Health Sciences,

University of the Witwatersrand, Johannesburg

In fulfilment of the requirements for the degree of

Master of Science in Medicine

Johannesburg, October 2018

“We are just an advanced breed of monkeys on a minor planet of a very average star. But we can understand the Universe. That makes us something very special.”

Stephen William Hawking

(8 January 1942 – 14 March 2018)

Declaration

I, Melanie Moodie, declare that this Dissertation is my own, unaided work. It is being submitted for the Degree of Master of Science in Medicine at the University of the Witwatersrand, Johannesburg. It has not been submitted before for any degree or examination at any other University.



Melanie Moodie

18 day of October 2018.

Publications and presentations arising from this study

Conference presentations:

1. M. Moodie, T. A. Scott, M. A. Killick, and M. Papathanasopoulos. Sequential Adeno-Associated Virus delivered HIV-1 subtype C Env Glycoproteins as Novel Vaccine Immunogens. October 2017, 8th Cross-faculty postgraduate symposium, WITS University, JHB, SA. Oral presentation.
2. M. Moodie, T. A. Scott, M. A. Killick, and M. Papathanasopoulos. Sequential Adeno-Associated Virus delivered HIV-1 subtype C Env Glycoproteins as Novel Vaccine Immunogens. November 2017, Molecular Biosciences Research Thrust, postgraduate research day, WITS University, JHB, SA. Poster presentation.

Abstract

An efficacious HIV-1 vaccine that can elicit broadly neutralizing antibodies (bNAbs) targeting the HIV-1 envelope glycoprotein (Env) is likely to provide protection from infection. To date, no vaccine immunogen has elicited bNAbs against HIV-1. Recent evidence from infected individuals suggests that bNAbs develop over time in response to constant antigenic challenge provided by an evolving Env that drives the somatic hypermutation of these antibodies and is necessary for their development. Env sequences required to engage the unmutated germline B-cells and drive the somatic hypermutation required to develop a bNAb response are available. Recombinant adeno-associated viral (rAAV) vectors present an attractive novel strategy for *in vivo* delivery and long-lived expression of sequential HIV-1 Env immunogens. Thus, this study aimed to provide proof-of-concept that rAAV can be used for the delivery and expression of sequentially-derived HIV-1 Env sequences in mammalian cells. Five sequential Env sequences (from a total of 292), over an infection period of 78 weeks, replicating *in vivo* viral evolution from patient CH505 who was infected with HIV-1 subtype C, were selected, codon optimized, and cloned into pcDNA3.3 for mammalian expression of Env. Recombinant Env glycoproteins were transiently expressed in HEK293 T cells, purified, and biochemically characterized by SDS-PAGE, Western Blotting and ELISA. The matched *env* sequences were also sub-cloned into the rAAV-Luc vector, allowing for the production of rAAV following a polyethylenimine (PEI)-based triple transfection protocol of HEK293 T cells. rAAVs were purified via polyethylene glycol (PEG) precipitation, followed by iodixanol gradient centrifugation, and quantified via droplet-digital PCR (ddPCR). These rAAVs were used to transduce HEK293 T cells and characterize the expression of Env *in vitro* by ELISA. Consensus Env sequences were generated from all time points, and following bioinformatics analyses, sequences from weeks 4, 20, 30, 53, and 78 post infection were selected. All pcDNA3.3-CH505 Env constructs were successfully expressed and purified, apart from the week 4 Env. Binding of the recombinant Envs to a panel of bNAbs, as determined by ELISA, confirmed they were functional and conformationally intact. Interestingly, differences in antibody binding were noted between weeks 20 – 78, highlighting potential changes in epitope exposure. All 5 *envs* were successfully sub-cloned into the pAAV backbone vector with intact ITRs, as confirmed by restriction enzyme digest analysis. The *env* transgenes were then packaged into serotype 2 rAAV vectors, and rAAVs were successfully produced and purified, with an average yield of $1{,}4 \times 10^{11}$ genome copies/ml, as quantified by digital droplet PCR. Transduction assays and characterization revealed that they were functional and produced recombinant Env

glycoproteins, with the exception of week 4, with optimal expression between 6-8 days post-transduction. Overall, these results provide the first evidence that HIV-1 Env can be successfully cloned into rAAV, and the associated recombinant proteins can be expressed in HEK293 T cells. Moreover, we provide reagents for future prime-boost immunizations using a panel of sequential Env expressing AAVs with matched recombinant proteins for testing in small animal models.

Acknowledgements

I would like to express my deepest gratitude and sincerest appreciation to all the people involved in making it possible for me to carry out this project.

To my supervisor, Prof. Maria Papathanasopoulos, thank you for your patience, guidance, expertise, and support. I would also like to thank you for always coming through with everything I needed, as well as the opportunities you have afforded me over the years. And thank you for always managing to calm me down in moments of anxiety and panic. Your continued support and encouragement of my scientific endeavours is greatly appreciated.

To my co-supervisor, Dr. Mark Killick, thank you for the technical assistance, detailed discussions, and helping me to improve all my skills, particularly my writing. A special thank you for always challenging me and for instilling a sense of critical evaluation in me and helping me become a better research scientist as a result. Your friendship and continued encouragement of my scientific endeavours is greatly appreciated.

To my co-supervisor, Dr. Tristan Scott, thank you for your patience and guidance, especially with the most challenging aspects of viral production and analysis, and troubleshooting required to get there. Thank you for challenging me to think critically and always consider the unexpected options.

To my friends and colleagues in the HIV Pathogenesis Research Unit, both past and present, for your continued friendship, encouragement, and support throughout the years. Special thanks in particular to Mark, Tristan, Lorraine, Fiona, Nancy, and Roberto who have always been there to mentor and guide me; to Britt and Tumelo who have started this journey with me; and to everyone who was always there to make me laugh and making the long hours' worth it.

To my dearest Rob, thank you for all your love, patience, understanding, continuous support, and proof-reading skills. You always motivate and inspire me to be a better person and I cannot thank you enough.

To my family and friends: specifically, my parents, Ansie and Neal; my sister, Jennifer; and "big brother" Dries; who have always and continue to be there for me.

Table of Contents

Declaration **i**

Publications and presentations arising from this study **ii**

Abstract **iii**

Acknowledgements **v**

Table of contents **vi**

List of Figures **xi**

List of Tables **xiii**

List of Abbreviations **xiv**

Chapter 1: Introduction **1**

1.1) The HIV-1 Pandemic 1

1.2) Current Treatment and Prevention Strategies 3

1.3) HIV-1 Structure, Function, and Lifecycle 4

1.3.1) HIV-1 Virion Structure 4

1.3.2) HIV-1 Lifecycle 5

1.4) HIV-1 Transmission, Disease progression, and Immune responses 6

1.4.1) HIV-1 Acquisition and Transmission 6

1.4.2) Pathogenesis and Disease Progression 7

1.4.3) Immune Response to HIV-1 9

1.4.4) Immune Correlates of Protection 12

1.4.5) Implications for vaccine design 13

1.5) Vaccine History, Developments, and Different strategies 13

1.5.1) General 13

1.5.2) Traditional vaccine approaches 15

1.5.3) Genetic vaccination 16

1.5.4) Current HIV-1 Human Vaccine Trials 17

1.6) HIV-1 Envelope Glycoprotein as vaccine immunogen 18

1.6.1) Native Env structure and function 18

1.6.2) Challenges associated with HIV-1 Env immunogens 19
1.7) Broadly Neutralizing Antibodies (bNAbs) 20
1.7.1) Description and Characteristics/ Structural features 20
1.7.2) Neutralizing epitope targets on HIV-1 Env 22
1.7.3) Development and evolution of bNAbs 23
1.7.4) Sequential immunization 26
1.8) Adeno-associated Viruses (AAVs) and Vaccines 27
1.9) Rationale for study, aims, and objectives 28

Chapter 2: Materials and Methods 30

2.1) General information 30
2.2) Plasmids used in this study 30
2.3) Design and construction of HIV-1 envelope glycoprotein (Env) constructs 30
2.3.1) Selection and design of HIV-1 subtype C *env* constructs 30
2.3.2) HIV-1 Subtype C CH505 *env* construct design 31
2.4) Transformation of the recombinant plasmids into *Escherichia coli (E. coli)* DH5α cells and large-scale recombinant plasmid isolations and characterization 32
2.4.1) *E. coli* DH5α Transformations 32
2.4.2) Plasmid isolation (Maxiprep) 32
2.4.3) Restriction enzyme digest screening of pcDNA™3.3 (+) Env plasmids 33
2.5) Restriction sub-cloning of the CH505-w4 insert into the pcDNA™3.1 backbone for expression comparison 34
2.5.1) Digestion of backbone and insert 34
2.5.2) Ligation of insert and backbone fragments 35
2.5.3) *E. coli* DH5α Transformations 35
2.5.4) Screening of positive bacterial colonies 36
2.5.5) Screening and selection of positive colonies by restriction enzyme digest 36
2.6) Recombinant HIV-1 Env expression and purification 37
2.6.1) Plasmids used for protein expression 37

2.6.2) General Mammalian cell culture 37
2.6.3) Transient Transfections 38
2.6.4) Enzyme-linked immunosorbent assay (ELISA) 39
2.6.5) Lectin-affinity chromatography purification of recombinantly expressed HIV-1 Env 39
2.6.6) Total protein concentration determination 40
2.6.7) Characterization of recombinant Envs via Sodium dodecyl sulphate-polyacrylamide gel electrophoresis (SDS-PAGE) and Western blot 41
2.6.8) Characterization of recombinant Envs via ELISAs 42
2.7) Restriction sub-cloning of the CH505 inserts into the pAAV backbone 44
2.7.1) Digestion and Ligation of backbone and insert 44
2.7.2) *E. coli* SURE2 Transformations and Screening of positive bacterial colonies 44
2.7.3) Screening and selection of positive colonies by restriction enzyme digest 45
2.7.4) Optimized Chloramphenicol plasmid isolation protocol 45
2.8) Transformation of additional plasmids into *Escherichia coli (E. coli)* SURE2 cells and large-scale recombinant plasmid isolations for rAAV production 46
2.8.1) *E. coli* SURE2 Transformation and Optimized Chloramphenicol plasmid isolation protocol 46
2.8.2) Restriction digest screening of AAV helper plasmids 46
2.9) AAV Production 47
2.9.1) Plasmids used for rAAV production 47
2.9.2) Mammalian cell culture and Large-scale polyethyleneimine transfections 47
2.9.3) rAAV Purification 48
2.10) Droplet Digital Polymerase Chain Reaction (ddPCR) 49
2.10.1) Primers and Probes 49
2.10.2) Droplet digital PCR genome titre assay 50
2.11) Viral Transduction assays 51
2.11.1) Mammalian Cell Culture and Optimising *In vitro* infections 51
2.11.2) Enzyme-linked immunosorbent assay (ELISA) 52

Chapter 3: Results

3.1) Design and construction of HIV-1 envelope glycoprotein (Env) constructs 54
3.1.1) Selection of sequentially derived HIV-1 Subtype C *env* constructs 54
3.1.2) HIV-1 Subtype C CH505 *env* construct design 56
3.2) Restriction enzyme digest screening of pcDNA™3.3 (+) Env constructs 56
3.3) Recombinant HIV-1 Env expression 57
3.3.1) Transient expression of HIV-1 Subtype C CH505 Env constructs 57
3.3.2) Enzyme-linked immunosorbent assay (ELISA) for the detection of recombinantly expressed CH505-Envs 61
3.3.3) HIV-1 Env glycoprotein purification 62
3.3.4) Biochemical characterization of purified recombinant Envs via ELISAs 63
3.4) Restriction sub-cloning of the CH505 inserts into the pAAV backbone 68
3.5) Isolation and purification of pAAV-GFP reporter, rep/cap and adenohelper plasmids for large-scale recombinant rAAV production 71
3.6) rAAV Production and Isolation 73
3.7) Droplet Digital Polymerase Chain Reaction quantification of rAAVs 74
3.8) rAAV Viral Transduction Assay of HEK293 T cells 75
3.8.1) *In vitro* optimization 75
3.8.2) Recombinant Env expression from *in vitro* rAAV-CH505 transduction studies 76

Chapter 4: Discussion 79

4.1) Design and construction of HIV-1 Env constructs 79
4.1.1) Selection of sequentially derived HIV-1 Subtype C *env* constructs 79
4.1.2) HIV-1 Subtype C CH505 *env* construct design 81
4.2) Expression and purification of the matched CH505 recombinant Env 82
4.3) Antigenicity and functionality assessment of recombinantly expressed CH505 Envs 85
4.4) Generation of recombinant AAV vector containing the HIV-1 CH505 Env transgenes 87

4.5) Quantification of rAAV CH505 vectors 88
4.6) rAAV mediated transgenic expression of CH505 Envs in *vitro* 89
4.7) Concluding remarks and future directions 91

References **92**

Appendices **119**
Appendix A: Supplementary Figures 119
Appendix B: Standard protocols and recipes 129
Appendix C: Ethics Approval 140

List of Figures

Figure 1.1: World map displaying the global HIV-1 prevalence per region in 2016. Image obtained from [6]. 2

Figure 1.2: Structure of the HIV-1 virion showing the associated viral proteins. Image obtained from [22]. 5

Figure 1.3: HIV pathogenesis and disease progression to AIDS, showing the three stages of disease over time [41]. 8

Figure 1.4: Schematic representation of a typical antibody structure [160]. 21

Figure 3.1: The predicted amino acid sequence alignment of selected envelope glycoprotein (Env) sequences derived from an HIV-1 subtype C infected individual (CH505w*n*gp140), an inferred subtype C founder virus Env consensus sequence (Founder vi), and a reference genome (HXB2). 55

Figure 3.2: A schematic representation of the engineered trimeric Env constructs (w*n*gp140) used for this study. 56

Figure 3.3: Restriction enzyme digest analysis of the pcDNA3.3w*n*gp140 expression vectors. 57

Figure 3.4: Western Blot analysis of FVgp140 and selected CH505gp140 envelope glycoproteins. 58

Figure 3.5: Western Blot analysis of FVgp140 and CH505gp140w78 envelope glycoproteins**.** 60

Figure 3.6: SDS-PAGE (A) and Western Blot (B) analysis of *G. nivalis* lectin-affinity purified FVgp140 and CH505gp140 envelope glycoproteins. 63

Figure 3.7: Indirect ELISA showing the antigenicity and functionality of the purified FV and CH505-Envs. 65

Figure 3.8: CD4i/17b binding ELISA evaluating the conformational integrity and CD4 binding functionality of the purified FV and CH505-Envs. 67

Figure 3.9: Restriction enzyme digest analysis of the pAAV-CH505 w*n*gp140 cis-expression vectors. 70

Figure 3.10: Restriction enzyme digest analysis of the pAAV-GFP, AdenoHelper5 (pHelper), and Rep/Cap2 expression vectors. 72

Figure 3.11: Schematic representation of large-scale rAAV large-scale vector production and isolation. 73

Figure 3.12: Relative transduction efficiency of the rAAV-GFP vector *in vitro*. 76

Figure 3.13: rAAV transduction and recombinant Env glycoprotein evaluation in HEK293 T cell line. 78

Supplementary Figure 1: pcDNA3.3-CH505w*n*gp140 and corresponding pAAV-CH505w*n*gp140 vector maps. 119

Supplementary Figure 2: pcDNA3.1-FVgp140 vector map. 122

Supplementary Figure 3: pAAV-Luc vector map. 123

Supplementary Figure 4: pAAV-GFP vector map. 124

Supplementary Figure 5: Replication/ capsid (rep/cap) serotype 2 vector map. 125

Supplementary Figure 6: AdenoHelper vector map. 126

Supplementary Figure 7: Restriction digest analysis of the pAAV-Luc expression vector, showing intact ITRs. 127

Supplementary Figure 8: Corresponding bright field images for the relative transduction efficiency of the rAAV-GFP vector *in vitro*. 128

List of Tables

Table 3.1: Recombinantly expressed CH505-Env detection and concentration estimation via indirect ELISA using the VRC01 primary antibody. 62

Table 3.2: ddPCR quantification of final rAAV yields, in average genome copies per ml (GC/ ml). 75

Table B1: Restriction enzymes and corresponding buffers used for restriction enzyme digests of plasmids, all from Thermo Fisher Scientific (Waltham, MA, USA). 131

Table B2: Running and Stacking gel recipes for 1.5- and 0.75-mm gels. 134

Table B3: Preparation of iodixanol gradients. 137

Table B4: The fluorescent dyes and quencher used in the ddPCR probes, obtained from Thermo Scientific (Waltham, MA, USA). 138

Table B5: Primary and secondary antibodies used in this study. 139

List of Abbreviations

(e)GFP: enhanced green fluorescent protein

µ: micro

1dCD4: single domain CD4

6-FAM: 6-Carboxyfluorescein fluorescent reporter dye

AAV: adeno-associated virus

AAV2: adeno-associated virus, serotype 2

Ad: adenovirus

ADCC: antibody-dependent cell-mediated cytotoxicity

AIDS: acquired immunodeficiency syndrome

AM: affinity maturation

A_n: absorbance

APCs: antigen presenting cells

ART/ HAART: antiretroviral therapy and highly active antiretroviral therapies

BCR: B cell receptor

bNAb: broadly neutralizing antibody

bp: base pairs

BSA: bovine serum albumin

CAG: chimeric chicken-β-actin promoter

Cap: capsid

CCR5: cellular chemokine co-receptor type 5

CD4+: human CD4 positive T lymphocytes

CD4bs: CD4-binding site

cDNA: complementary deoxyribonucleic acid

CDR: complementarity-determining regions

CDRH3s: heavy-chain complementarity-determining regions 3

CMV: cytomegalovirus immediate early promoter

CTL: CD8+ cytotoxic T lymphocyte

CTT: cytoplasmic tail

CXCR4: cellular chemokine co-receptor type 4

ddPCR: droplet digital polymerase chain reaction

dH_2O: distilled water

DMEM: Dulbecco's Modified Eagle Medium

DNA: deoxyribonucleic acid

E. coli: *Escherichia coli*

EC: elite controllers

ED: ectodomain

ELISA: enzyme-linked immunosorbent assay

env: HIV-1 envelope gene

Env: HIV-1 envelope protein

FCS: foetal calf serum

FDC: follicular dendritic cells

FV: founder virus

G. nivalis: *Galanthus nivalis*

GALT: gut-associated lymphoid tissue

GC/ ml: genome copies per ml

GC: germinal centre

GIT: gastrointestinal tract

gp: glycoprotein

GT: genital tract

HEK: human embryonic kidney

HEPS: highly exposed persistently negative

HIV-1: human immunodeficiency virus type-1

HLA: human leukocyte antigen

HR1/HR2: heptad repeat region

HRP: horse-radish peroxidase

HVTN: HIV Vaccine Trials Network

iCoP: immune correlates of protection

IFN: type I interferon

IgH/ IgL: antibody heavy and light chain genes

INSTIs: integrase strand transfer inhibitors

ITR: inverted terminal repeat

kDa: kilo-Dalton

LB: Luria-Bertani

LTNP: long-term nonprogressors

LTR: long terminal repeat

Luc: luciferase gene

M: molar

MAPK: mitogen-activated protein kinase

MHC: major histocompatibility complex

MMC: medical male circumcision

MMP: methyl α-D-mannopyranoside

MOI: multiplicity of infection

MPER: membrane-proximal external region

MSD: membrane-spanning domain

Mw: molecular weight marker

n: nano

NAb: neutralizing antibody

NF-κB: nuclear factor kappa B

NHP: non-human primate

NNRTIs: non-nucleoside reverse transcriptase inhibitors

NRTIs: nucleoside reverse transcriptase inhibitors

PAMPs: pathogen-associated molecular patterns

PBS: phosphate buffered saline

PBS-T: Dulbecco's phosphate buffered saline containing Tween 20

PEG: polyethylene glycol

PEI: polyethylenimine

PEP: post-exposure prophylaxis

PIs: protease inhibitors

PMTCT: prevention of mother-to-child transmission

PNGs: potential N-linked glycosylation sites

Poly(A): polyadenylation

PR: protease

PrEP: pre-exposure prophylaxis

PRRs: pattern recognition receptors

QSY™: dark quencher

rAAV: recombinant adeno-associated virus

Rep: replication

RIG: retinoid acid-inducible gene

RLRs: retinoid acid-inducible gene-like receptors

RNA: Ribonucleic acid

RNaseH: Ribonuclease H

RP: rapid progressors

RT: reverse transcriptase

SDS-PAGE: sodium dodecyl sulphate-polyacrylamide gel electrophoresis

SFMII: serum-free media II

SHM: somatic hypermutation

STI: sexually transmitted infections

SU: surface glycoprotein

Tfh: T follicular helper cells

TLRs: toll-like receptors

Tm: melting temperature

TM: transmembrane glycoprotein

T-TBS: Tris-buffered saline containing Tween 20

UBC: ubiquitin C promoter

UCA: unmutated common ancestor antibody

UV: ultraviolet

VIC™: 2′-chloro-7′phenyl-1,4-dichloro-6-carboxy-fluorescein fluorescent reporter dye

VIP: vectored immunoprophylaxis

VNP: viremic nonprogressors

w.p.i: weeks post-infection

WHO: World health organization

Chapter 1: Introduction

1.1) The HIV-1 Pandemic

Since the discovery of human immunodeficiency virus type-1 (HIV-1) as the causative agent of acquired immunodeficiency syndrome (AIDS) in 1983, there has been a significant amount of research dedicated to the prevention and treatment of this disease [1, 2].

Current statistics indicate that by the end of 2016 there were 36.7 million people infected with HIV-1 globally, with 1.8 million people newly infected in this year alone [3, 4] (Figure 1.1). The African region has the highest prevalence of HIV-1, with 25.6 million people living with HIV-1 [3]. Within this region, South Africa has the highest number of infected individuals, and burden of disease, with approximately 7.1 million people living with HIV/ AIDS [5].

To date, approximately 35 million people have already died from HIV/ AIDS [3, 4], however, there has been an overall decline in incidence, morbidity, and mortality rates since the pandemic reached its' peak in 2005 [4]. Almost paradoxically there has been an increase in overall prevalence, which is due to the improved morbidity and mortality rates, because of increased access to, and improved antiretroviral drug treatments available, translating into enhanced HIV-1 patient survival.

However, despite these extensive efforts to combat the disease, the high number of new infections every year indicates that HIV/ AIDS remains a serious global health problem. Thus, novel prevention strategies are a key component particularly in the Sub-Saharan African region.

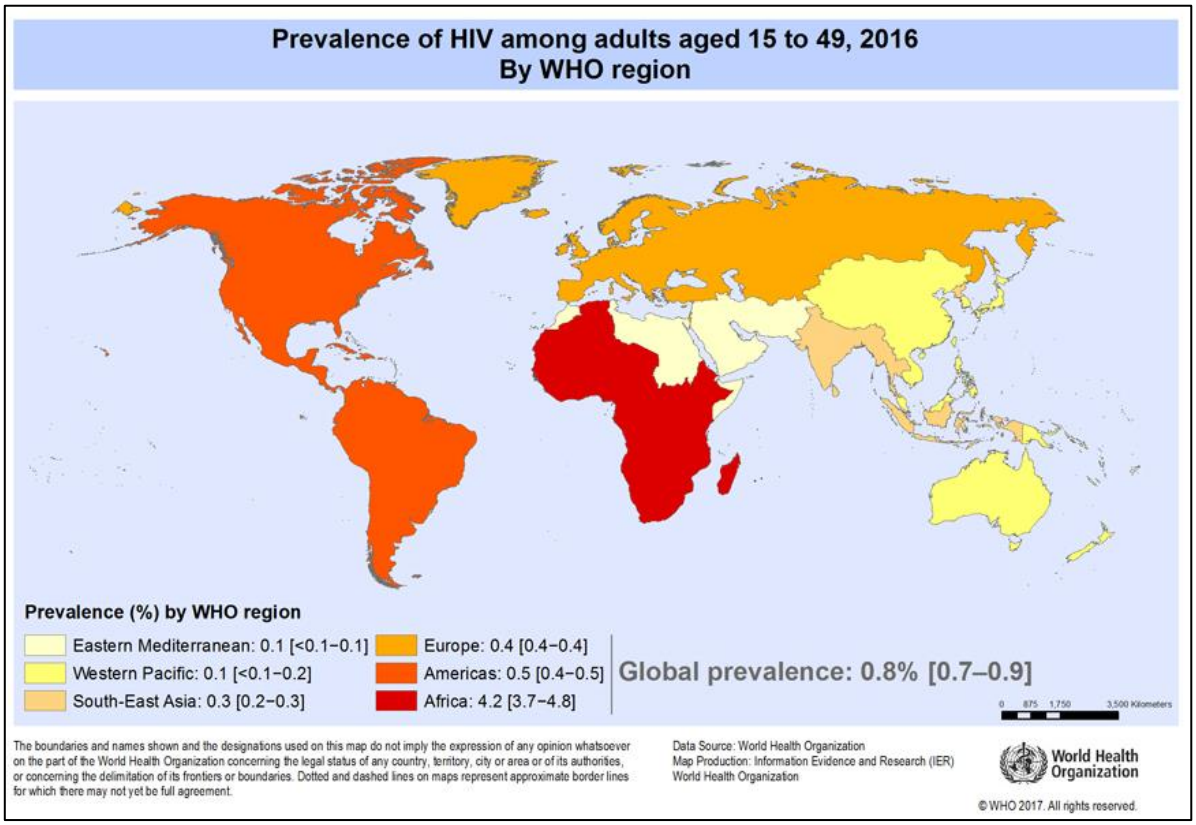


Figure 1.1: World map displaying the global HIV-1 prevalence per region in 2016. Image obtained from [6].

One of the main reasons that HIV/ AIDS is such a challenging problem, is that access to the main preventative and treatment strategies (especially antiretroviral therapy and highly active antiretroviral therapies (ART/ HAART)) remains restricted, particularly in resource-limited settings such as South Africa. Current WHO recommendations state that all patients who have been identified as HIV positive should be put onto a treatment plan, but there are still only 18.2 million people on ART/ HAART (of the 36.7 million infected) globally, as of mid-2016 [7]. This imbalance between the numbers of people living with HIV, the new infections every year, and the people who are receiving treatment, indicates that there is an important gap that needs to be addressed to effectively control the HIV-1 pandemic.

Although continued investment into these existing strategies will continually improve patient and public health outcomes, there remains a demand in finding novel treatments, specifically preventative or curative options. Most importantly, the development of an effective vaccine that can prevent HIV-1 infection, as this could be the best possible option to eradicating HIV. This is of importance within more resource limited areas that also experience the greatest burden of disease and the greatest barriers to obtaining traditional treatment options.

1.2) Current Treatment and Prevention Strategies

Current strategies to prevent HIV-1 infection employ a diverse array of methods that include social and biomedical interventions, to construct an overall combinatorial approach that can be used not only to prevent infection, but also treat those who are already infected [8, 9].

The social interventions include, but are not limited to: (i) information, education, and communication about various topics (safe sexual behaviour and practices, gender based violence, condom usage, sexually transmitted infection (STI) symptoms, health-seeking behaviour, etc.), (ii) needle exchange programs and safe injection sites, (iii) social marketing (specifically aimed at improving accessibility to treatment and healthcare services), and (iv) policy changes [10, 11, Reviewed in: 12]. Biomedical prevention strategies encompass medical male circumcision (MMC), which have shown to reduce the risk of HIV-1 acquisition in heterosexual men by between 48-61% [13-15]; ART-based strategies including (i) pre-exposure prophylaxis (PrEP) [16, 17], (ii) post-exposure prophylaxis (PEP) for high-risk individuals, and (iii) prevention of mother-to-child transmission (PMTCT); as well as associated testing and counselling services [Reviewed in: 12].

The only effective treatment currently available for HIV-1 positive individuals includes various combinations of antiretroviral (ARV) drugs as part of ART or HAART. These drugs fall under 6 different classes, namely: non-nucleoside reverse transcriptase inhibitors (NNRTIs), nucleoside reverse transcriptase inhibitors (NRTIs), protease inhibitors (PIs), fusion inhibitors, CCR5 antagonists or entry inhibitors, and integrase strand transfer inhibitors (INSTIs). ARVs are designed to target various susceptible points in the viral lifecycle, however there are several limitations to their use. These include: poor access in resource limited settings, drug inefficiencies, acquisition of drug resistance mutations following sub-optimal drug levels or prolonged usage, the inability to cure infection and eliminate the latent viral reservoir thus failing to fully restore immune health and function.

These prevention methods work best within the mentioned combinatorial approach, because the social interventions are generally aimed at the population level or community-based level to change behaviours, attitudes, and ideas; whereas the biomedical interventions are generally aimed at the individual level to suppress viral load [Reviwed in: 11, 12]. Despite the relative success of these combinatorial approaches and the decline seen in HIV-1 incidence and prevalence, an effective vaccine would still be needed to fully address the problems described.

1.3) HIV-1 Structure, Function, and Life Cycle

1.3.1) HIV-1 Virion Structure

HIV-1 is classified as a member of the *Lentiviridae* genus, part of the *Retroviridae* family. Morphologically, the HIV-1 virion is a rounded, irregularly shaped particle, which is enclosed in a lipid bilayer derived from the host cell membrane (which virus obtains from budding from the cell surface) (Figure 1.2). The HIV-1 genome is composed of two positive, single ribonucleic acid (RNA) strands, each one with a 5' cap and a 3' polyadenylation (poly(A)) tail [18, 19].

The genome is comprised of 9 genes that encode for at least 16 proteins, flanked by two long terminal repeats (LTRs) [19-21]. These proteins can be classified according to their main function (Figure 1.2) [19]: (i) Structural proteins; Pol (encodes for viral enzyme protease, reverse transcriptase, RNaseH, and integrase), Gag (encodes for the capsid proteins, p17, and p24), and Env (encodes for envelope glycoproteins); (ii) Regulatory proteins; Tat and Rev which are the necessary regulatory factors for viral gene expression. (iii) Accessory proteins; Nef, Vpr, Vpu, and Vif, which are not considered to be necessary for viral replication, but aid in replication efficiency. The genome is enclosed within conical capsid (Figure 1.2, red), comprised of p24 protein [18, 22]. This structure is surrounded by the p17 matrix protein, which is then encapsulated by the host-derived envelope glycoprotein [22]. Within the envelope, the viral envelope glycoprotein (Env) trimeric spikes are embedded which are heterodimers composed of non-covalently linked gp120 and gp41 proteins essential for viral entry and determine viral tropism.

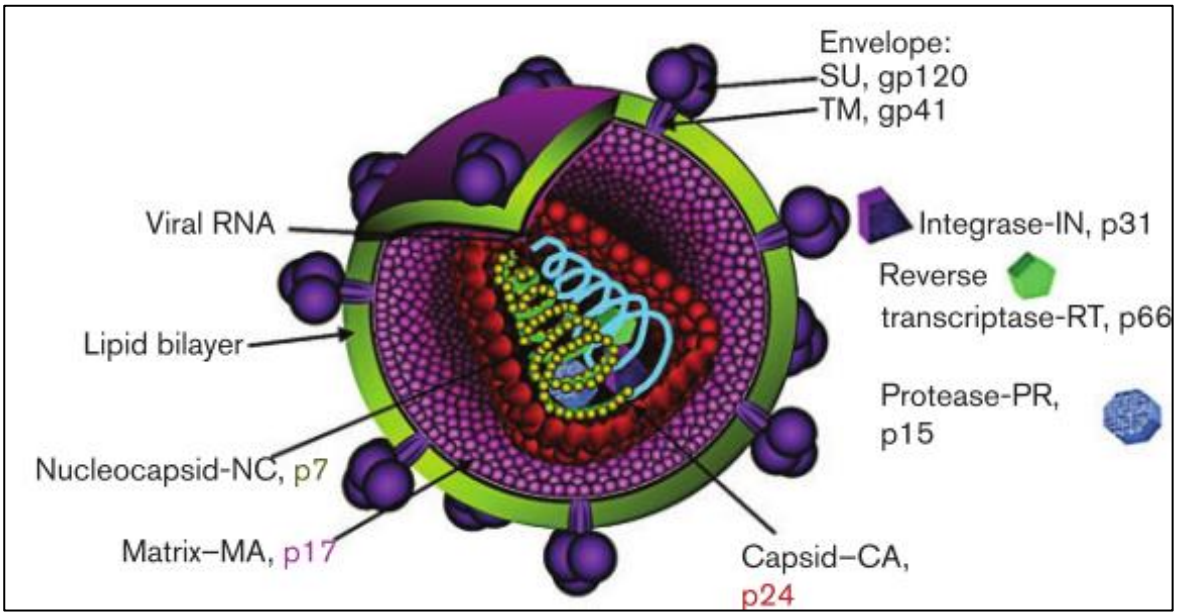


Figure 1.2: Structure of the HIV-1 virion showing the associated viral proteins. Image obtained from [22].

1.3.2) HIV-1 Life cycle

HIV-1 infects CD4 positive (+) cells, predominantly the CD4+ T lymphocytes due to the high levels of CD4 receptor expressed on their surface but infection of immune cells with a lower density of CD4 such as dendritic cells and macrophages is common [23]. A thorough understanding of the HIV lifecycle is critical if we are to develop novel effective therapeutic and preventative strategies.

During the viral lifecycle, HIV-1 utilizes the Env spike to gain entry into host cells through membrane receptor binding (or attachment) and subsequent membrane fusion [24]. This binding is initiated when Env recognises, and binds the surface exposed CD4 receptor on the host cell membrane [22]. This specific cell tropism of HIV-1 is determined by the Env, as this is the viral receptor that interacts with the host receptor to gain entry into host cells [24, 25]. This initial binding step alone is not sufficient for viral entry, and subsequent conformational changes need to occur in the Env spike that will allow for subsequent exposure and binding of the co-receptor (most commonly CCR5 or CXCR4, although there have been implications that other receptors may have some contribution towards infection [26-28]). This triggers further conformation changes in Env, and the establishment of a "fusion-active" state, thus allowing for fusion of the host and viral plasma membranes [22].

Following fusion, the virus enters the cytosol of the host cell and is decapsidated [18]. The RNA genome is then reverse transcribed into complementary DNA (cDNA), by the viral

reverse transcriptase (RT) enzyme, an error prone process resulting in viral quasispecies. This newly formed cDNA is translocated into the nucleus where the integrase (I) enzyme non-reversibly integrates the viral DNA into the host genome as a viral progene (which can be replicated or remains latent in the cell). This integrated viral genome copy allows for the host mediated transcription of viral genes, which are transported to the cytoplasm for translation of viral proteins. Furthermore, some proteins in the cytoplasm undergo post-translational modifications, such as glycosylation. These newly transcribed viral proteins, along with two full copies of the viral RNA genome, are then assembled into new immature (non-infectious) viral particles. As the immature viral particles bud off from the host cell, viral protease (PR) cleaves the Gag and GagPol precursor proteins (protease-mediated maturation), allowing for the formation of matured (infectious) viral particles [25]. The mature virus is now able to initiate a new replication cycle.

It is important to fully understand the mechanism of viral replication, as these mechanisms present opportunities for drug or vaccine targets, which could allow us to prevent infection completely.

1.4) HIV-1 transmission, disease progression, and immune responses

1.4.1) HIV-1 Acquisition and Transmission

HIV-1 transmission occurs predominantly via sexual contact (both hetero- and homosexual), and is affected by many variables [29]. Interestingly, up to 80% of infections is a result of a single transmitted virus, which is termed the founder virus (FV), despite the recipient being exposed to diverse viral quasispecies [30-33]. The reasons for a single FV being responsible for establishing infection is unclear, however the severe restriction in genetic variation that occurs within the recipient results in selection of the "fittest" viral strain which is best suited for successful systemic infection [30].

For the FV to successfully initiate infection during heterosexual transmission, it needs to transverse the mucosal surface of the genital tract (GT) and infect the sub-epithelial vulnerable cell populations. The epithelial cell layer is an effective physical barrier to infection, and direct crossing of this barrier is probably a rare event (between 0.0005 – 0.0026 per coital act) [34, 35]. However, the virus may potentially gain entry through this layer at naturally occurring thinner sites (endocervix and upper female reproductive tract) [36], or due to the presence of

other vulnerabilities such as trauma (due to physical abrasions) [37], or the coincidence of genital tract infections (increased availability of immune cells and through barrier disruption) [38, 39].

1.4.2) Pathogenesis and Disease Progression

Once the FV effectively establishes infection, the virus population begins to expand as the virus-infected cells, reach the surrounding draining lymph nodes. This leads to subsequent systemic dissemination to the secondary lymphoid tissues/organs, central nervous system, and the genitourinary tract [40, 41]. Specifically, once in the lymph nodes and lymphoid tissues, exponential growth of the viral population begins as there are more CD4 + T lymphocyte target cells available. This results in a strong initial immune response (discussed below) which causes generalized lymphadenopathy, due to increased T lymphocyte recruitment and destruction of these cells in the lymph nodes (by HIV-1 or CTL responses), as well as the release of inflammatory cytokines, and general flu-like symptoms or febrile illness [42].

This acute phase of infection (approximately 2- 10 weeks post-infection [w.p.i]) coincides with peak viremia levels throughout the lymphoid tissues and in the peripheral blood (Figure 1.3). Following this, there is significant damage inflicted on the immune system due to mass CD4 + T lymphocyte destruction (Figure 1.3A, blue and green lines, from 3 w.p.i), specifically within the gut-associated lymphoid tissue (GALT) of the gastrointestinal tract (GIT) (Figure 1.33A, green line) [38, 43]. This site is of importance, as approximately 80% of the CD4+ T cells are destroyed within this site following the initial 3 weeks, and the GALT does not fully recover from this [44, 45]. Importantly, the CD4+ cell numbers may recover in the peripheral system (discussed below), but they fail to recover in the GIT, making patients susceptible to opportunistic infections [46]. Importantly, this is when the virus establishes a latent reservoir of infected memory T lymphocytes [47, 48].

The initial decrease in CD4+ T cell numbers is due both to destruction by HIV-1 infection, as well as destruction due to CD8+ cytotoxic T lymphocyte (CTL) responses that eliminate HIV-1 infected cells (Figure 1.3B, red and green lines). This rise in the CD8 + T specific lymphocytes coincides with a decrease in in the peripheral blood viral load and recovery of the CD4 + T lymphocytes, although they seldom reach pre-infection levels (Figure 1.3A, blue line, ~9 w.p.i). The viral load then decreases to a viral load set point (Figure 1.3A, red line, ~9 w.p.i) [49, 50]. These two indicators, the recovering CD4 levels and viral load to set point, mark the beginning of the secondary or asymptomatic phase of HIV-1 infection.

During the asymptomatic phase of infection, patients are generally well as the patient's immune systems controls viral replication (Figure 1.3). This phase generally occurs 9-12 w.p.i and can last up to 10 years. However, as general immune dysfunction and destruction progresses, along with chronic activation and inflammation, the immune system becomes overwhelmed (Figure 1.3B). Towards the end of the asymptomatic phase, the viral load steadily begins to increase during this time (Figure 1.3A, red line), with progressive depletion of CD4+ and CD8+ T lymphocytes (Figure 1.3A and B), and susceptibility to opportunistic infections. This functional impairment eventually leads to the development of AIDS, and eventually death (usually within 2 years of an AIDS diagnosis, for patients not on ART) [51].

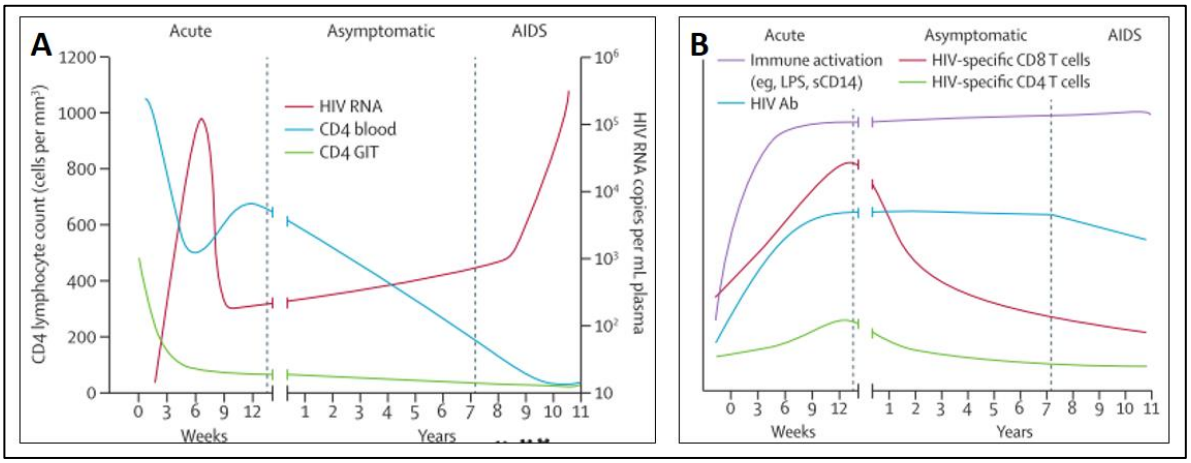


Figure 1.3: HIV pathogenesis and disease progression to AIDS, showing the three stages of disease over time. (A) Shows the changes in viral load in HIV RNA copies/ ml (red) from acute infection through to development of AIDS (initially in weeks then in years), with the corresponding changes in CD4+ lymphocytes (cells per mm^3) in the peripheral blood (blue) and the GIT (green). (B) Shows the immune responses observed from acute infection through to development of AIDS (initially in weeks then in years). These responses include levels of immune activation (purple), HIV antibody development (blue), CD8+ T lymphocyte responses (red), and CD4+ T lymphocyte responses (green) *[Picture adapted from: 41]*.

Disease progression profiles

Despite this general disease progression profile, there can be dramatic differences between natural disease progression rates for various patients [Reviewed in: 52]. These overall disease outcomes and progression rates can also be dramatically affected by ART.

Elite controllers (EC) are those patients who manage to maintain an undetectable viral load, long after seroconversion. Long-tern nonprogressors (LTNP) and viremic nonprogressors (VNP) do have detectable viral loads but manage to maintain functional CD4+ T cells and

remain asymptomatic for a much longer period. For these three patient groups (EC, LTNP, and VNP) progression to AIDS may be delayed to 12 years or more. On the other end of the progression spectrum a small percentage of patients have been observed to progress to AIDS within 1-4 years and are termed rapid progressors (RP) [53]. Interestingly, a percentage of individuals are considered to be highly exposed persistently seronegative (HEPS), where their immune responses suggest that they were exposed/ transiently transfected, but they are not considered HIV positive [52, 53].

This variety in responses depends on various factors, both host and viral, and may offer significant clues in the design of novel immunogens or alternate vaccine approaches that may lead to an effective prophylactic vaccine against HIV-1.

1.4.3) Immune response to HIV-1

During an acute infection, the immune system usually protects the host by eliminating the pathogen or reducing the effects the pathogen may have [Reviewed in: 54, 55]. Although the immune system does respond in various ways to HIV-1 infection (chronic), the mechanisms are generally ineffective at preventing infection, and while differences in disease progression may vary as described above, there has been no documented evidence of natural clearing of HIV-1 infection in humans [32, 54, 56-58]. Thus, the correlates of immune protection against HIV-1 infection are unclear, and a deeper understanding these mechanisms are required to inform how a potential vaccine could best stimulate the immune system for the most effective response.

The innate immune response

The innate immune system is the first line of defence encountered by HIV-1, and this response is critical for containing early replication, as well as inducing and enhancing the adaptive immune response [Reviewed in: 59]. The innate response constitutes 3 parts: the epithelial barrier (such as the genital mucosa), the complement system, and phagocytotic and antigen presenting cells (such as dendritic cells and natural killer cells) [Reviewed in: 54].

One of the key features of the innate immune response is that of pattern recognition receptors (PRRs) [Reviewed in: 54]. The role of this mechanism is to recognize the relatively conserved structures on pathogens, called pathogen-associated molecular patters (PAMPs) [Reviewed in: 54, 55]. These PRR molecules on host cells include toll-like receptors (TLRs), which are membrane bound host receptors capable of identifying pathogen-specific hydrophobic molecules (such as viral proteins) or pathogen nucleic acids (DNA and RNA). Other PRRs are

located in the cytosol of cells and facilitate the identification of intracellular pathogens and include DNA receptors and retinoid acid-inducible gene (RIG)-like receptors (RLRs) [Reviewed in: 54, 55].

The engagement of these various receptors leads to the activation of various signalling pathways, including the mitogen-activated protein kinase (MAPK) and nuclear factor kappa B (NF-κB) pathways [60-64]. These pathways are responsible for activating important transcription factors, which in turn allows for the production of cytokines, chemokines, cell adhesion molecules, and type I interferons (IFN), all of which have important antiviral effects [65].

HIV-1 is quite adept in evading the innate immune response, specifically because the initial recognition of the intact virion by PRRs is limited due to glycan shielding of important viral Env epitopes and the fact that the remainder of the viral membrane is composed of "self" [Reviewed in: 54, 59]. HIV-1 is also able to regulate various innate immune response pathways to alter them as needed during infection, by impairing pathway activation, transcription factor binding, or interfering with the actions of products of these pathways [66, 67].

Ultimately, these responses are not the most effective in preventing acquisition of HIV-1 or controlling infection, but they play a vital role in activating the adaptive immune response. The innate immune response does this through antigen presentation (via antigen presenting cells, or APCs such as DCs or natural killer cells), recruiting the cells of the adaptive immune system to the sites of infection, and providing priming signals to the adaptive immune response cells [32, 54, 55, 57, 58].

Adaptive immune response

The adaptive immune response responds to HIV-1 infection via two main mechanisms- using T and B lymphocytes, which constitute cellular and humoral immunities, respectively [Reviewed in: 68].

T-cell responses

The CD8+ T cell response is the first adaptive response observed against HIV-1 infection, usually around the time of peak viremia [56, 69]. As a result, it is initially responsible for controlling HIV-1 replication, and thus the initial decline in viremia to the viral set point. During the acute phase of infection, the CTL response is narrow, usually targeting a few epitopes on the transmitted virus [41, 56, 69]. The response does broaden as infection continues into the chronic phase, but also due to the development

of mutations and viral quasispecies. Overall, the anti-HIV CD8+ CTL response fails to achieve full viremic control [56, 69].

CD4+ T cells (or T helper cells) assist other lymphocytes, via the secretion of cytokines, in regulating various immunological processes [70]. This includes recruitment of immune cells to the infection site, aiding in B cell maturation and stimulation of antibody production, and the activation of CD8+ T cells and macrophages [71]. However, as these are the main cell population targeted during HIV-1 infection they are significantly depleted (either due to direct infection or from other cells, such as CD8+ cells) and their response becomes deficient and less potent over time [70, 71]. This has detrimental effects on the regulation of the other functions of the adaptive and innate immune response, thus contributing to the overall immune dysfunction observed during disease progression to AIDS.

B-cell responses

The main function of the B cell response is to produce antibodies specific for the antigens presented by APCs [72]. These antibodies can respond to HIV-1 in a variety of ways, and the overall response may vary dramatically between different individuals [Reviewed in: 73]. The main mechanism of action is that of neutralization, where antibodies (targeting extracellular virions and free circulating virus), bind to critical epitopes on the virus thereby preventing viral entry into host cells and infection.

During the natural course of infection, antibodies begin to develop from plasma cells as early as 8-14 days post-infection [72, 74]. These initial responses (binding antibodies) are usually directed towards free circulating virus and are ineffective at neutralising the virus as they generally target linear or irrelevant epitopes. The response then evolves into a response that is directed towards several HIV-1 proteins such as p24, Integrase, as well as gp41 and then gp120 [74]. An autologous neutralizing antibody (NAb) response against viral Env emerges approximately 3 months post-infection [75-78]. The NAbs can neutralize the autologous or founder virus by targeting immunodominant variable loop regions of Env and preventing viral entry, but this response is generally quite narrow and generally selects for viral escape mutants [64-67]. Approximately 10-30% of individuals go on to develop further NAb responses, ranging from moderate to broad and of these around 1% develop highly potent and broad neutralizing antibodies (bNAbs) that target highly conserved regions on the HIV-

1 Env, capable of neutralising a wide range of clinically relevant HIV-1 subtypes [75, 76, 78-81].

Besides these neutralizing capabilities, antibodies are also able to target HIV-1 through other antibody mediated effector functions, namely: agglutination, complement activation, and antibody-dependent cell-mediated cytotoxicity (ADCC) [73]. Once bound to a pathogen, antibodies may render the attack ineffective via agglutination (by forming large clumps that render the pathogen ineffective), which makes the pathogen an attractive target for opsonization. Antibodies can activate the complement system through binding to the pathogen and recruiting components of the complement system, ultimately resulting in opsonisation and phagocytosis, or cell lysis. The last mechanism of viral destruction is that of ADCC. This mechanism involves an effector cell of the immune system (such as a natural killer cell) actively lysing the target cells, whose antigens on the membrane has been coated with the specific antibodies [82, 83].

1.4.4) Immune correlates of protection

The combination of protective effects of both adaptive and innate responses above contribute to immune correlates of protection (iCoP). iCoP are measurable signs of an immune response that are responsible for protection from an infection (from establishing infected or developing disease/symptoms) [84-86]. Correlates of infection risk, often used in conjunction with/ interchangeably with iCoP, are the immune responses that increase or decrease the risk of infection [84].

As highlighted above, the immune response to a pathogen is often complex, with multiple components of the immune response acting either sequentially or simultaneously during the different stages of infection. Therefore, the iCoP may be complex, and there may be more than one factor that contributes to protection (either partial or complete protection. As mentioned previously, the iCoP for HIV-1 infection have largely been unidentified, because there have been no recorded spontaneous recovery cases in humans, no patients have ever regained full immune function, and there are no appropriate animal models [86, 87].

Briefly, analysis of the results obtained from the RV144 vaccine trial (described in detail below) identified four potential iCoP, which would need to be further confirmed [84, 88-92]. These responses were identified as follows: (i) V1V2-specific IgG Abs correlated inversely with infection risk; (ii) Env-specific IgG3 correlated inversely with infection risk; (iii)

polyfunctional CD4+ T-cells correlated inversely with infection risk; and (iv) IgA Abs which correlated directly with infection risk and decrease vaccine efficiency.
Other studies (including studies performed in non-human primates (NHP), studies analysing LTNPs, and other initial HIV-1 vaccine trials) have identified other potential iCoP [Reviewed in: 93]. These include the quality of the adaptive immune response (the efficiency of the CD8+ T cells); genetic polymorphisms, such as the 32 base-pair deletion in the CKR-5 (CCR5) gene; human leukocyte antigen (HLA) types of individuals, such as the HLA-B* 27 and HLA-B*57 types (associated with a protective role, or slower disease progression, respectively); and the development of bNAbs .

From these data, it is largely accepted that the adaptive immune response is the primary determinant of protection, with NAbs preventing infection, and cell-mediated responses that control disease progression. Of these adaptive immune responses, bNAbs are of interest, as they have been shown to prevent HIV-1 acquisition in animal models following passive immunization studies [94-100] – highlighting that sterilizing immunity may be possible.

1.4.5) Implications for vaccine design

Overall, understanding the complexities of the immune response to HIV-1 infection, as well as the complex interplay between host genetics, variations and diversity in viral sequences, variable vaccine responses and responses to other treatments such as ART, antiretroviral drug resistance development, and disease progression, will reveal key insights in developing an efficient vaccine.

These factors must be taken into consideration with regards to the length of time needed to act- as there is a small window of opportunity during acute infection (well within the first ~14 days) in which a vaccine must effectively prevent the integration of the viral genome in order to derive maximum benefit and ultimate protection against HIV-1 acquisition

1.5) Vaccine History, Developments, and Different strategies

1.5.1) General

Following the discovery of HIV-1 in 1983, it was thought that a vaccine would be available within 2-3 years. However, despite almost 35 years of intensive research into different immunogen designs and vaccine strategies, limited success has been achieved in human clinical trials.

An effective vaccine should stimulate a protective immune response, similar to one that would naturally occur during infection. Classical vaccine strategies for other infectious diseases have imitated these protective responses, hence successful vaccines are available for diphtheria, yellow fever, influenza, poliomyelitis, measles, mumps, rubella, etc [Reviewed in: 101, 102]. However, due to the many complexities inherent to HIV-1 infection described above, this "natural protection" may be limited (as noted in LTNPs or ECs), or may not exist (as noted for most chronic infections where patients do not recover) [95]. In some patients, responses have only been observed following superinfection by another HIV-1 strain, and this may affect the immune system in ways we do not yet understand and may have significant implications for vaccine design (i.e. merely replicating the immune response may not be protective alone) [103-105]. Because of this lack of an effective natural immune response against HIV-1, an effective vaccine may be required to stimulate immune responses in a way that is different to what occurs during natural infection. In addition to the requirement of providing protection from infection, a vaccine should also be cost-effective (production, storage, distribution costs), easily administered, and safe to use.

HIV-1 vaccine research has examined a variety of strategies and immunogen designs, with different goals in mind. Potential vaccines are classified as either (i) preventative/ prophylactic vaccines (which is given to a healthy person to prevent infection) or (ii) therapeutic vaccines (given to those already infected in the hopes of boosting/ guiding immune responses) [Reviewed in: 106], both of which are of importance to help further treat those already infected, and to prevent new infections altogether.

The different goals for each vaccine strategy involve some debate about the best suited immune responses required for the control or to prevent infection- these aims correspond to the 3 main strategic vaccine "waves" we have seen over the years of research and development, namely: (1) First vaccine wave, which focused on the induction of a bNAb response; (2) Second vaccine wave, which focused on the induction of anti-HIV CD8+ CTL responses; and (3) currently the third vaccine wave, which is a combinatorial approach of eliciting both the humoral and cellular arms of the immune system [Reviewed in: 68, 106].

Ideally, regardless of the immune response elicited, sterilizing immunity would be the ultimate goal of an HIV-1 vaccine, although a functional cure may be more easily achieved [Reviewed in: 107]: Sterilizing immunity involves complete protection against HIV-1 acquisition

following vaccination or the complete elimination of the latent viral reservoirs following acute infection. Alternatively, a therapeutic vaccine may result in a functional cure where control over viral replication is achieved and prevents the need for ART altogether. A therapeutic vaccine would thus lower the risk for subsequent transmission.

1.5.2) Traditional Vaccine Approaches

Tradition approaches include the following main strategies: attenuated, inactivated, and subunit vaccines [Reviewed in: 68, 101].

Briefly, vaccine research typically begins by looking for a live, attenuated vaccine (where the pathogen has reduced pathogenicity and virulence) [Reviewed in: 68, 101]. Despite being able to potentially induce robust and effective humoral and cell-mediated immune response to HIV-1, this approach carries a significant risk of the pathogen reverting back to its disease-causing form [108]. This is of concern because of the high mutation rate associated with HIV-1 replication.

The alternative, an inactivated vaccine, uses virus that has been destroyed by various mechanisms to eliminate infectivity, yet preserving the natural antigenicity [Reviewed in: 101]. Inactivated vaccines display better safety profiles and increased stability over attenuated vaccine approaches [109]. However, there is a risk that not all particles are inactivated, and costs are generally increased as they require booster shots to achieve the same duration of immunity and robustness to that of attenuated vaccines.

Lastly, the subunit vaccine approach which has successfully been employed against Hepatitis B virus and influenza viruses, utilizes protein fragments/immunogens to stimulate an immune response [102]. Although subunit vaccines have improved safety profiles over the other two traditional vaccine approaches, the major disadvantage is their relatively low immunogenicity, thus requiring "booster" immunizations and adjuvants to supplement the response and increase its effectiveness. The lack of engagement of the CD8+ T-cell responses and insufficient/inappropriate antibody responses following subunit based vaccination, may suggests limited use against HIV-1 [108].

Newer approaches to vaccine design aimed at stimulating both the humoral and cell-mediated adaptive immune responses are being pursued. These include DNA and recombinant vector vaccine strategies, which is discussed in more detail below.

1.5.3) Genetic vaccination

DNA vaccines and recombinant vector vaccines, collectively referred to as "genetic vaccines" [110, 111], are similar vaccination strategies in that they both make use of DNA sequences (derived from the pathogen of choice) that encode relevant proteins required to develop a bNAb or cellular immune response, but their methods of delivery differ.

DNA vaccines are DNA-encoded plasmids that are injected into the patient, via use of gene guns or electroporation, or incorporated into DNA-liposomes, DNA-coated polymers, or DNA-coated metal complexes, for protein expression in cells to produce the relevant immune responses [110, 112-116]. Recombinant vector vaccines (also called live vectored vaccines) also incorporate DNA sequences for protein expression, but these are introduced into replication-deficient (attenuated) recombinant viral vectors (such as adenoviruses (Ad), adeno-associated viruses (AAVs), poxviruses, polioviruses, Venezuelan equine encephalitis virus, etc.) [117-121].

These various methods all result in the DNA sequences being delivered into cells, entering the nucleus, and transcribing the immunologically relevant proteins. The host cell then recognises these proteins as foreign and presents them on the cell surface using the major histocompatibility complex (MHC) class I or II molecules, thereby initiating an immune response against the desired antigens [113, 116, 121-124].

Genetic vaccination has many advantages over traditional vaccine approaches, including improved safety profiles, relative ease of production, ability to stimulate cellular and humoral immunity, and can be administered in prime-boost combinations [125]. These vaccine strategies are particularly important because of their role in MHC presentation (prime) and their ability to effectively stimulate cellular responses against HIV-1 [126-135], boosted with subunit vaccine immunogens to elicit a bNAb response [111].

Recombinant vectors are preferable to typical artificial delivery methods, because the vectors allow for long-term transgene expression, and the conferred immunity lasts longer and typically shows stronger responses [108, 117-121]. AAVs have many advantages over traditional

vectors, including but not limited to: these are the only non-pathogenic vectors available, their vector genomes are simple and contain no endogenous AAV viral genes, they are easy to administer, have improved safety profiles, they can efficiently express transgenes in tissues long-term, and they can target many tissue types depending on the AAV serotype used (brain, muscle, lung, liver, retina) [136-138].

1.5.4) Current HIV-1 Human Vaccine Trials

The lack of efficient humoral and cellular adaptive responses obtained with traditional vaccine approaches [Reviewed in: 139, 140], and the insufficient responses obtained with naked DNA vaccines, has led to the evaluation of more effective prime-boost strategies. These strategies involve an initial priming of the immune system (with a genetic vaccine), and subsequent boosting of this response with further genetic or protein subunit vaccines. The priming is thought to focus the immune response on a specific antigenic target of the disease, with the boosting providing an enhancing response. Only five efficacy trials have been completed to date, with varying results. Below is summary of these clinical trials.

Briefly, the VAX004 [141, 142] and VAX003 [88-91] trials were based solely on a protein subunit approach using recombinant gp120 immunogens (AIDSVAX B/B and B/E respectively), however, there was no clear efficacy noted and the vaccine immunogens elicited an overall weak neutralizing antibody (NAb) response against tier 1 viral isolates (not clinically relevant). The STEP [143-146] and HVTN 503 [147] trials both used a recombinant Ad-vector (Ad5), to deliver the *gag, pol, and nef* genes, but neither vaccine showed any efficacy and they had only weak CD8+ T cell responses, of narrow breadth. These trials were also halted prematurely due to safety concerns, as they observed a trend for increased risk of HIV-1 infection in vaccinees [144, 147]. Moreover, they highlighted the differences in vaccine immune responses between humans and NHP models. The RV144 trial [84, 92, 148, 149], which used a canarypox vector prime (with *env, gag, and pol* genes) and a protein subunit boost (AIDSVAX B/E gp120) showed mild efficacy (31%), but the overall cellular response was moderate, with a weak humoral response. More recently, the HVTN 505 trial [150] used a DNA prime (*gag, pol, nef,* and *env* genes) and a recombinant adeno-viral vector boost (expressing Gag, Pol, and Env). However, this trial was also stopped prematurely as the vaccine showed no efficacy and no reduction in viral load set point in those individuals that received the vaccination, but subsequently became infected. Ongoing studies include the HVTN705 trial in South Africa, which is based on the vaccine used for the RV144 trial, but includes HIV-1

subtype C sequences (the predominant circulating subtype in South Africa, to make it locally relevant), as well as other study improvements to increase the breadth and duration of the immune response [151].

Although the RV144 trial revealed a moderate efficacy rate, as well as being the first proof-of concept successful HIV-1 vaccine, there are many challenges remaining before progress towards a fully efficient HIV-1 vaccine. It is widely accepted that the most effective ways to design an efficacious HIV vaccine would be to include an immunogen that elicits bNAbs towards the HIV-1 Env glycoprotein. The challenges that remain to be addressed in order to design an effective HIV-1 vaccine include the extensive viral diversity and ability of the virus to effectively escape the host immune response; the lack of a natural protective response and the poor understanding of iCoP; and the need for improved animal models to further understanding and testing capabilities.

1.6) HIV-1 Envelope Glycoprotein as vaccine immunogen

1.6.1) Native Env structure and function

The HIV-1 Env glycoprotein is expressed as a precursor polypeptide, the 160 kiloDalton (kDa) or gp160 protein. This protein undergoes cleavage by host proteases (furin or furin-like proteases) in the Golgi apparatus, which results in two mature subunits: the gp120 surface glycoprotein (SU) and the gp41 transmembrane glycoprotein (TM) [152-154] (Figure 1.2). These subunits assemble via non-covalent and hydrophobic bonds to form a trimer of heterodimers known as the Env spike [152]. The Env spikes are incorporated into the host-derived cell membrane and envelope the virus as it buds from the cell during the last phase of the viral life cycle. However, the amount of Env spikes per virion is relatively low (~ 10 spikes/ virion), which likely aids in immune recognition evasion and decreased cytotoxicity [155, 156]. These low spike numbers also mean they are more sparsely located, which can affect recognition and effectiveness of neutralizing antibodies [157, 158].

The gp120 SU contains regions that are both highly conserved (constant regions C1-C5) and regions that show a high degree of variability (variable loops V1-V5) [22, 159, 160]. The gp120 SU also contains the key binding sites for CD4 (CD4bs) and co-receptors on the host cells, and is thus responsible for viral transmission, cell tropism, and entry into the host cell [25, 161] . The gp41 TM is divided into 3 regions, the extracellular ectodomain (ED), the transmembrane region or membrane-spanning domain (MSD) and the cytoplasmic tail (CTT) [24]. The gp41

TM contains the hydrophobic fusion peptide sequence and two heptad repeat regions (HR1 and HR2) which are key regions that aid in viral and host cell membrane fusion, and the HR regions aid in the trimeric quaternary structure formation of the Env spike.

As Env is the only viral encoded protein displayed on the HIV-1 virion surface, it is the logical target for antibody-mediated immune recognition. However, its use as an immunogen for vaccine design presents many challenges.

1.6.2) Challenges associated with HIV-1 Env immunogens

A major obstacle in developing an effective HIV-1 vaccine is the high degree of genetic variation of viral isolates circulating worldwide. The Env region is the most variable region of the viral genome, where diversity can typically range from 25- 35% within HIV-1 subtypes [24]. Viral diversity arises as a result of the error prone RT process leading to a high mutation rate of HIV-1 and presents the major challenge of selecting an appropriate "representative sequence" capable of targeting all the circulating clinically relevant HIV-1 worldwide. Sequence diversity is also used as an immune evasion strategy. Moreover, HIV-1 Env is also extensively glycosylated, where up to 50% of the molar mass of Env can be attributed to the presence of glycans [152, 162]. This glycan shield can block up to 97% of the Env surface from immune recognition [163].

Another mechanism employed by HIV-1 to avoid immune recognition is by displaying Env in a variety of forms, from functional Env trimeric spikes, to monomeric gp120 antigens and gp41 stumps [164, 165]. The functional Env spikes also "pulse" through different conformations as viral fusion and entry occurs (from pre-fusion to fusion-active states, mentioned in section 1.3.2). This transient exposure of vulnerable epitopes and decoy forms of Env results in antibodies that are directed to non-functional epitopes and/or display decreased or no neutralizing activity.

The above-mentioned factors all contribute towards Env being less immunogenic and allowing HIV-1 to continuously avoid immune recognition. As a result, the development of "structure-based immunogen design" strategies have been employed to address these various challenges [166]. This approach uses modern structural biology techniques to gain further understanding into the immunobiology of Env and inform optimal vaccine design. The strategies to address the various problems with HIV-1 immunogen design are grouped into 4 areas: (i) Env trimer, (ii) antibody epitope, (iii) glycan, and (iv) germline B-cell receptor -based immunogen design strategies [166].

Despite these challenges associated with using Env as a vaccine immunogen, antibodies that target highly conserved epitopes of Env have improved neutralization breadth and are capable of cross-reactive neutralizing activity, as evidenced by natural infection [104, 167-181].

1.7) Broadly Neutralizing Antibodies (bNAbs)

1.7.1) Description and Characteristics/ Structural features

The viral Env (or Env derivatives) is the only immunogen that can stimulate the humoral immune response to make bNAbs. These are antibodies that can neutralize the majority of strains and subtypes (referred to as cross-neutralization), of a highly diverse pathogen such as HIV-1 [182].

These bNAbs have been shown to develop during the natural course of infection in a minority of HIV-1 infected individuals (10-25%), but only after chronic antigen exposure for several years, with multiple cycles of viral immune escape, and extensive antibody affinity maturation [75, 78-81, 183, 184]. This suggests that in some individuals, the immune system can overcome the various immune mechanisms employed by HIV-1, and that conserved regions of Env are able to be effectively targeted.

A typical antibody structure is illustrated in Figure 1.4. Each antibody consists of paired heavy (IgH) and light (IgL) chains. These two regions both contain variable regions, which form the antigen binding sites, collectively called the Fv regions. These regions are particularly important because they contain the complementarity-determining regions (CDR) which can accommodate significant amino acid mutation, hence they are referred to as hypervariable regions [185]. The heavy and light chains also contain constant regions, which determine the isotype (IgM, IgD, IgA, IgG, and IgE) of the antibody.

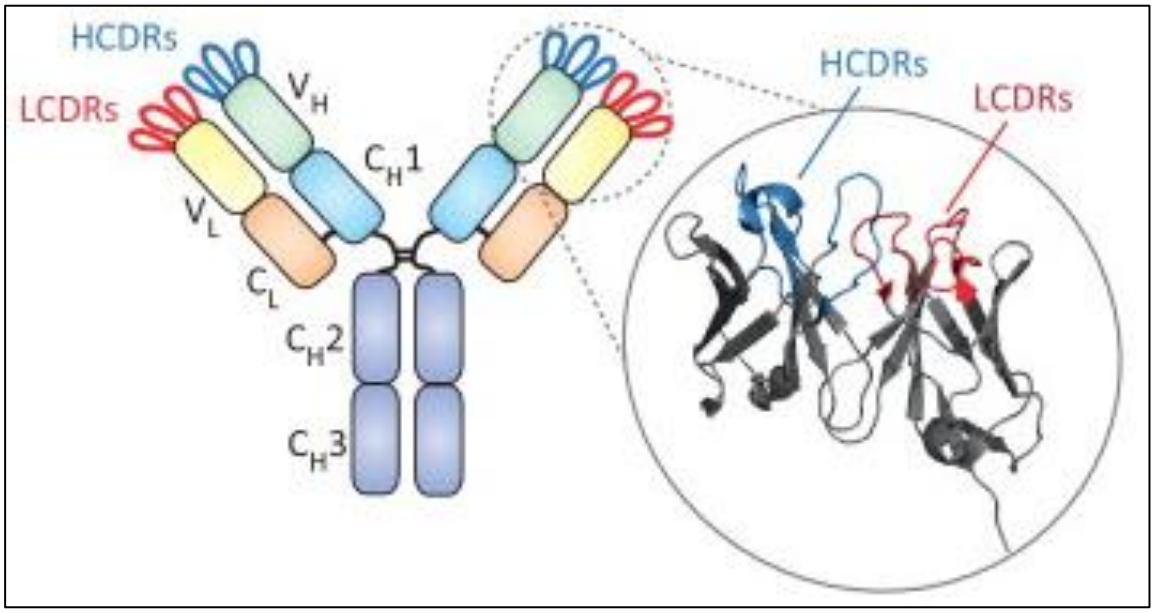


Figure 1.4: Schematic representation of a typical antibody structure. The heavy (H) and light (L) chains are indicated, along with the constant (C) and variable (V) regions. The complementarity-determining regions (CDR) are indicated for the heavy and light chains. Figure obtained from [186].

Compared to non-neutralizing or autologous neutralizing antibodies, bNAbs differ in several ways due to unique features. These include extensive somatic hypermutation (SHM), long heavy-chain complementarity-determining regions 3 (CDRH3s), and polyreactivity [79, 103, 187-189]. The first generation of bNAbs obtained from patients, were isolated via phage display and human hybridomas [182], showed limited potency and breadth but did reveal these common features [99, 100, 190-193]. These studies also revealed that overall, bNAbs were capable of preventing infection and decreasing the viral load to some degree, but that they failed to clear established HIV-1 infection [99, 100, 190-193]. Second generation antibodies, isolated via improved memory B cell culture and Env-specific B cell sorting methods [182], have shown enhanced breadth and potency. Preclinical studies have evaluated bNAb-mediated passive immunization in monkeys [96-100, 194-197] and humanized mice [198-201], and have shown it to be effective at achieving sterilizing immunity. A Phase I human trial was performed with a CD4-binding site (CD4bs) antibody (3BNC117), which showed a moderate reduction in viral load, with viremia that was reduced up to 28 days following transfusion [202]. Similar studies have analysed the safety, tolerability, and pharmacokinetics of the CD4bs VRC01 in humans, both short [203] and long-term [204]. These two studies also found that the antibody was effective, with a range of anti-HIV effects [204].

Although these studies have demonstrated the effectiveness of bNAbs via passive immunization, the ultimate goal of an ideal HIV-1 vaccine would be to elicit this protective response by stimulating the immune system to mimic the development of bNAbs in any individual.

1.7.2) Neutralizing epitope targets on HIV-1 Env

Through various methods mentioned above, numerous bNAbs have been isolated, with a wide range of potency and breadth. This has resulted in the identification of five defined epitopes on the Env spike, including the CD4bs, membrane-proximal external region (MPER), the gp120-gp41 interface region, the high mannose path (including the N332 supersite and V3 loop), and the apex region (V1/V2 loop) [Reviewed in: 205]. These epitopes are the most conserved regions of the Env spike and afford the antibodies that target these regions extensive neutralization breadth of circulating HIV-1 subtypes.

CD4bs

The CD4bs is a functionally conserved site found on gp120 and is critical for Env to bind to the CD4 receptor on host cells. The first bNAb targeting this site, b12 was identified in 1994 [168], and this site has been a key focus of bNAb and Env vulnerability research since. Antibodies targeting this site acts by directly competing for binding with the CD4 receptor. However, this Env site is located in a recessed pocket, surrounded by glycans and variable loop regions, reducing accessibility and making it a difficult target for bNAbs to neutralize. Despite these challenges, newer antibodies of this class that act in a similar way have been isolated due to improved techniques, including VRC01 and VRC01-like antibodies [206], NIH45-46 and 3BNC117 [178], CH103 [187], and more recently, N6 [207]. These antibodies have CDR regions that vary in length, varying degrees of SHM (but usually relatively higher than other bNAb classes), and some polyreactivity. The neutralization breadth of these antibodies is similar, with most being able to neutralize at least 90% of pseudoviruses (exceptions are CH103 which neutralizes 55%, and b12 neutralizing 75%). The most effective of these antibodies, N6, was able to neutralize 98% of isolates tested.

MPER

The MPER is a highly conserved region found on the gp41 subunit of the Env spike and is important for viral fusion to occur. Antibodies targeting this site include 2F5, 4E10, and Z13 [176, 179, 208, 209]. These antibodies typically react with linear epitopes in this region and have been shown to be polyreactive. A newer antibody isolated in 2012 called 10E8 [172],

showed a different pattern of recognition to the rest of the MPER-directed antibodies (as it did not bind phospholipids, and bound cell-surface envelope) and it did not display the same polyreactive qualities, yet it showed the highest potency (neutralizing 98% of tested viruses).

gp120-gp41 interface:

The gp120-gp41 interface contains a key glycan, N276, that forms an epitope for bNAbs 8ANC195 [177, 178], 35O22 [171], PGT151 [167, 169], and VRC34 [173]. This epitope spans both subunits of Env, incorporating portions of gp41 and key glycans adjacent to the CD4bs on gp120. The mechanism of antibody mediated neutralization is through the prevention of the necessary conformational changes required for efficient viral entry. These antibodies can neutralize approximately 50-60% of pseudoviruses tested and show relatively high levels of SHM.

Apex region (V1/V2 loop):

This region lies at the apex of the Env spike on gp120. This site is primarily responsible for providing a shielding effect for neutralizing epitopes, and thus for evading immune recognition through mutations. However, the N160 glycan within this site occurs in a conserved subdomain of the variable loop region and is the primary target of various bNAbs. As these epitopes occur at the apex, these antibodies are often specific to the quaternary structure of this epitope. These bNAbs include PG9 and PG16 [174, 181], PGT141-145 [180], CAP256-VRC26 [103], and CH01-04 [210]. These antibodies show varying amounts of SHM, but all typically have long CDRH3 regions (to penetrate the glycan shield and contact the protein epitopes) and are polyreactive. The neutralization breadth varies from 50-70%.

High mannose patch (N332 supersite and V3 loop):

Similar to the gp120-gp41 interface described above, there is a critical glycan (N332) located at the base of the V3 loop. These bNAbs include the PGT family (PGT121, PGT124, PGT128, PGT135, 10-1074) [175, 180]. These antibodies share similar mechanisms of neutralization to those described above (apex region), specifically because of their shared features of long CDRH3 regions. These antibodies can neutralize up to 72% of HIV-1 isolates.

1.7.3) Development and evolution of bNAbs

Antibodies are produced by B lymphocytes. The development of bNAbs requires a microevolutionary process called affinity maturation (AM), which is the process of selecting and mutating B cell receptors (BCR) [211-213].

Briefly, this process begins when naïve B-cells bind to, and internalize, the antigens that are presented by follicular dendritic cells (FDC). These activated B-cells can then undergo the process of AM whereby the BCR affinity toward the target antigen is improved through SHM of the CDR regions. Following this process, the various B-cells will compete for T follicular helper cells (Tfh) co-stimulation. This stimulation allows for the B-cell to receive survival signals from the Tfh cell-derived chemokines and cytokines. The BCRs that bind with better affinity to their corresponding antigens are able to capture more antigen, preferentially selecting them for positive selection. Each successive round of AM selects for antibodies that have enhanced binding affinity to their cognate antigen [211-213].

The isolated bNAbs against HIV-1 (as mentioned previously) typically display high levels of SHM and their delay in emergence from the initial infection time point suggests that multiple rounds of affinity maturation are required to achieve the levels of neutralization breadth and potency. The extensive maturation process required for the development of these bNAbs is also highlighted by the other unusual features mentioned, including long CDR regions, polyreactivity, etc. [214]. As HIV-1 mutates and evolves rapidly in response to immune pressure, the antibodies required for neutralization need to continuously evolve the corresponding paratopes. Many studies have documented this HIV-1/ antibody co-evolution, where this continual viral escape drives the affinity maturation of the antibody response *in vivo* [103, 187, 215].

HIV-1 and antibody Co-evolution: implication for vaccine development

Human HIV-1 vaccine trials, incorporating Env based-immunogens, have thus far failed to elicit bNAbs despite capitulating and exposure of these critical epitopes. This discordance between HIV-1 Env, bNAbs antigenicity and immunogenicity (eliciting antibody responses that target the bNAbs conserved epitopes) was perplexing, however research into viral and antibody coevolution has revealed the virological and immunological characteristics of bNAbs development. [103, 187, 216-218]. The two key studies that were initially done include analysing the CH103 antibody lineage by Liao [187] and colleagues in 2013, and the CAP256-VRC26 antibody lineage by Doria-Rose [103] and colleagues in 2014.

Briefly, in the Liao study [187], they analysed the evolution of the CH103 bNAb lineage towards to CD4-binding site, in an individual (CH505) infected with HIV-1 subtype C FV. The CH103 CD4bs bNAb lineage was isolated and sequenced, which revealed that these bNAbs contained fewer mutations than typical CD4bs bNAbs. The initial unmutated common ancestor

(UCA) antibody of the lineage bound the FV Env sequences, which initiated bNAb development. Early members of this lineage were found as early as 14 weeks post-infection, with limited neutralization activity towards the autologous virus. These early autologous NAbs triggered subsequent viral mutations and escape. The lineage continued to increase in heterologous neutralizing breadth, while still maintaining the ability to neutralize the autologous virus. The founder CH505 Env bound well to the unmutated ancestor, and subsequent Envs bound with increasing affinity to later members of this lineage. This led to extensive evolution in Env, near the relevant epitope region site, which preceded the acquisition of neutralization breadth- defined by its ability to neutralize 55% of a panel of 196 geographical and genetically diverse Envs [187].

Later studies [215, 219] showed the development of a second bNAb lineage alongside CH103 named CH235. This lineage allowed for the selection of Env sequences that were resistant to itself (the CH235 bNAb), but that were more sensitive to neutralization via the CH103 lineage. This phenomenon is known as “B-cell lineage cooperation” [220].

The second study by Doria-Rose [103], revealed a similar mechanism of antibody and virus co-evolution. The authors analysed the evolution of the CAP256-VRC26 bNAb lineage towards the V1-V2 loop of Env, in an individual (CAP256) infected with a primary, HIV-1 subtype C FV and superinfected with a second subtype C virus 15 weeks later. Members of the VRC26 bNAb lineage were isolated and sequenced (between 15-206 w.p.i), which revealed a long CDRH3 region and moderate SHM. Using phylogenetic analyses, they found that this lineage arose 30-38 weeks post-infection and its unmutated ancestor already carried the long CDRH3, as a result of VDJ recombination and not through successive rounds of SHM. It is unknown, but likely that the superinfecting virus was responsible for initially engaging the naïve B cell bNAb lineage, due to the combination of the antibodies recapitulating the observed neutralization observed [103]. However, due to the recombination between the two viruses, there was considerable autologous virus diversity which led to significant viral diversification, allowing for expanding antibody neutralization breadth. The earlier clones of this lineage were not as effective at binding these diverse Env sequences, leading to cycles of antibody selective pressures and viral escape, and subsequent affinity maturation of the lineage to improve viral neutralization

These studies highlighted the importance of constant antigenic challenge and indicate the importance of engaging specific naïve B cell repertoires, and the multiple, successive rounds of AM are required to mature the antibody response. These findings are particularly relevant in the HIV-1 vaccine field, because the Env-based vaccine regimens used were not sufficient to engage the UCA or provide enough antigenic stimulation to drive the appropriate responses. Current thinking is that specific Env sequences can be deployed as a priming step, to engage specific naïve B cell lineages; followed by mimicking the natural Env evolution and driving the AM of these antibodies. This process is known as a sequential immunization strategy.

1.7.4) Sequential immunization

From the previous studies analysing bNAb lineage evolution, there is some data available on the Env sequences capable of engaging with precursor B-cells, and the possible sequential Env sequences which would correlate with the emergence of bNAb activity [103, 187, 215-220]. Thus, a lineage-based design (based off the analysis of bNAb lineage development), such as sequential immunization, is a logical step towards a rational based vaccine design.

Sequential immunization aims to recapitulate the key events of the bNAb evolution process. This entails the use of consecutive and subsequent immunizations with the appropriate Env sequences over time (as they would naturally evolve in the infected individual), which would likely drive the extensive somatic hypermutation required to produce bNAbs against HIV-1. This requires details of the antibody and the viral sequences evolution over time; the UCA, inferred intermediate antibodies, and finally the development of bNAbs; and the exact sequential Env sequences that influenced their development.

In a study done by Malherbe and colleagues, they hypothesized that immunizing with a variety of sequential HIV-1 *env* variants that arose *in vivo* during infection, would result in a broader level of NAb activity compared to single *env* genes alone [221]. They tested the quasi-species vaccine concept by comparing the antibody responses in 3 groups: (i) those exposed to the sequential evolution on Env clones (sequential group), (ii) those receiving a cocktail of Env clones that were present in a quasi-species (mixture group), and (iii) those repeatedly exposed to the same Env sequence (clonal group) [221]. Overall, they found that the sequential method of immunization performed better than the other strategies, resulting in the development of autologous and weak heterologous NAbs that replicated some NAb response features as seen in the SHIV infected animal (from where the sequences were derived). This was the first indication that a sequential method of immunization may better educate the humoral response,

but the failure to elicit broader NAbs may have been due to the vaccine delivery system and the fact the sequences were SHIV-derived.

Subsequent studies have also shown promise for sequential immunization vaccine strategies [222-230]. Combined, these studies showed that sequential immunization is a successful vaccine strategy to produce bNAbs, using specific germ-line targeting Envs to engage with precursor or naïve B-cells, and boosting Envs to further drive antibody evolution and selection through intermediate NAbs to bNAbs. The authors have found that the sequential vaccine strategy is able to guide bNAb maturation, as the subsequent Env boosts result in successive rounds of SHM and the ability to refine the bNAbs to recognize Env. One particular study found that the most effective Envs to use for boosting occur prior to, or simultaneously with, the development of approximately 50% neutralization breadth [223], which reveals that these earlier timepoints are a promising source for future immunogens. Some potential challenges that remained to be addressed using these strategies include engineering or selection of Envs that can engage the precursor B-cells, and that immune tolerance mechanisms typically restrict the development of bNAbs due to polyreactivity.

Despite these challenges, these sequential immunization strategies show promise in eliciting bNAbs. Possible improvements and refinements to the current sequential immunization strategies include the vaccine delivery mechanisms, using sequences from HIV-infected individuals with more potent bNAb responses, and the use of key individual sequences as immunogens, for educating the B-cell response for improved NAb maturation.

1.8) Adeno-associated Viruses (AAVs) and Vaccines

AAVs were discovered in 1965, and since then there has been a significant amount of research into these parvoviruses and their applications [Reviewed in: 231]. These non-enveloped, single-stranded DNA (approximately 4,7 kb) viruses are members of the *Dependoparvovirus* genus, which require the aid of a helper virus (such as adenovirus) to replicate [232]. These viruses contain two open reading frames: *rep* (for replication) and *cap* (for capsid formation), flanked by two inverted terminal repeats (ITRs), which are required for efficient viral replication [233]. Recombinant (r)AAVs are particularly attractive options in gene therapy applications, as they have been "gutted" and DNA sequences of interest can be inserted for delivery of expression cassettes, and they do not contain any viral genes thereby making it a type of "protein-nanoparticle", which accounts for the improved safety profiles seen compared

to other vectors and making them attractive options for further clinical use (as described in section 1.5.3).

Recombinant AAVs were first used for gene-therapy treatment of hemoglobinopathies, cystic fibrosis, and other human diseases (by delivering self-genes to replace defective or non-functional genes) [234-241]. Since then the application of rAAV has expanded into vaccine research and the delivery of gene-encoded immunogens to stimulate an immune response or immunoglobulin genes to produce the required antibodies as immunoprophylaxis [136]. As mentioned in section 1.5.3, these vectors are particularly attractive for vaccine use, mainly as they are non-pathogenic, non-replicative, and can effectively transduce many tissue types [Reviewed in: 111]. Despite these numerous advantages there are some limitations, including a small packaging size, some pre-existing immunity to certain serotypes that reduce their field application, and the fact that they generally result in low titre stocks [Reviewed in: 111]. There have been various improvements to try and alleviate these challenges, such as capsid modifications, using different serotypes to circumvent pre-existing immunity, and newer production methods to enhance viral titres [242].

Recombinant AAV vectors are currently being been used in number of HIV-1 vaccine and preventative strategies. Examples include the vectored immunoprophylaxis (VIP) approach [95, 243, 244], involving the use of AAVs to deliver bNAb encoding genes, such as eCD4-Ig [245], circumventing the traditional vaccine approach, yet providing antibody-mediated protection through prolonged transgenic expression. HIV-1 vaccine approaches include packaging different immunogens into the AAV vectors, such as *env*, *gag*, and *pol* [108] or the use of hybrid vectors packaged with *gag* or *gp140* [246]. To our knowledge, rAAVs have not been used for the delivery of sequentially-derived HIV-1 Env immunogens.

1.9) Rationale for study, aims, and objectives

We hypothesise that developing an effective bNAb response relies on the ability to engage the unmutated germline B-cells and drive the somatic hypermutation required to develop a bNAb, through a sequential immunization strategy, replicating an evolving Env response. Therefore, the use of sequential Env sequences (such as those described in Doria-Rose *et al* (2014) and Liao *et al* (2013)) packaged into various AAV vectors, and to be used for a sequential immunization vaccine design, may lead to improved cellular and humoral responses, and may better educate the B-cell responses translating into improve neutralizing breadth and/or potency.

Thus, the overall aim of the project is to provide proof-of-concept that rAAV can be used for the delivery and expression of sequentially-derived HIV-1 Env sequences in mammalian cell lines for future use as vaccine immunogens.

This was achieved using the following objectives:

- To design and generate sequential Env sequences, replicating HIV-1 Env evolution during natural infection.
- To express, purify and characterise the matched recombinant HIV-1 Env proteins.
- To design and construct recombinant AAV vectors, comprising the AAV2 Cap serotype for *in vitro* expression of the selected sequential HIV-1 Env sequences.
- To characterise the transduction efficiency of the generated HIV-1 Env rAAVs in vitro (mammalian HEK293 T cell line) and confirm the expression of the HIV-1 Env transgenes.

Chapter 2: Materials and Methods

2.1) General information

All DNA concentrations were quantified using the NanoDrop® Spectrophotometer ND-1000, software version 3.8.1 (Thermo Fisher Scientific, Waltham, MA, USA). All water used, unless otherwise stated, was Sabax injection water (Adcock Ingram, ZA).

2.2) Plasmids used in this study

The pcDNA™3.3 (+) vector (Life Technologies, Carlsbad, CA, USA), was used for matched recombinant protein expression of the CH505-Env sequences.

The pcDNA™3.1 $gp140_{FVC}$GCN4(+) plasmid containing the HIV-1 subtype C, founder virus consensus sequence has previously been described [247], and herein after referred to as **FVgp140 or simply FV**, and was available to be used as a control for transient transfection and expression during matched recombinant envelope glycoprotein production (see Appendix A for plasmid map).

The pAAV-Luc plasmid (AAV2 plasmid backbone with luciferase transgene); pAAV-GFP plasmid (AAV2 plasmid backbone with GFP transgene); pHelper plasmid (with adenovirus helper functions) (Applied Viromics, Fremont, CA, USA); and the rep/cap plasmid (serotype 2/2) needed for recombinant AAV production were available in our laboratory (see Appendix A for plasmid maps).

2.3) Design and construction of HIV-1 envelope glycoprotein (Env) constructs

2.3.1) Selection and design of HIV-1 subtype C *env* constructs

Published sequence data, consisting of bNAb and viral Env sequence co-development [49, 79, 103, 187, 221, 223, 248-253], was analysed during the literature review process and the sequential Env sequences described by Liao and colleagues (2013) [187] were selected for this study.

Patient CH505 was infected with HIV-1 subtype C, and was followed from the time of infection for 3 years [187]. Both the HIV-1 *env* and bNAb sequences were analysed at specific timepoints, including 4, 14, 20, 22, 30, 53, 78, 100, 136, and 160 w.p.i. This patient was infected with a single subtype C transmitted founder virus and developed autologous NAbs by

week 14, CD4bs-Abs that bound to recombinant Env were isolated from week 53, and cross-reactive neutralizing antibody activity emerged between 41-92 w.p.i.

A total of 292 published, full gp160 *env* sequences (accession numbers KC247375-KC247667) were downloaded from GenBank (https://www.ncbi.nlm.nih.gov) as FASTA files. The individual *env* sequences were aligned for each timepoint using ClustalX 2.0 [254]. Consensus *env* sequences for each time point were manually generated and subsequently translated in GeneDoc to obtain the corresponding amino acid sequences (Env, gp160). These consensus Env sequences were aligned in ClustalX 2.0 and viewed in GeneDoc [255].

Following this analysis, 5 representative time points were chosen that best select the potential sequential sequences that could drive the evolution of bNAbs, and mimic the response seen by these investigators. The final selection was as follows: 4, 20, 30, 53, and 78 w.p.i. These time points were chosen because the week 4 Env sequence was the one responsible for initially engaging the naive B cell receptor; the week 20 Env sequence allowed for autologous neutralization and heterologous neutralization against tier 1 viruses; weeks 30 and 53 correspond to the expanding heterologous neutralization, specifically tier 2 viruses; and week 78 for full neutralization breadth [187].

2.3.2) HIV-1 Subtype C CH505 *env* construct design

The selected HIV-1 subtype C CH505 consensus *env* sequences, corresponding to relevant timepoints, were used to design 5 constructs, termed **CH505w*n*gp*140*-GCN4+** (*n* corresponds to the week post-infection) hereafter referred to as **w*n*gp140 or w*n***. For recombinant trimeric Env expression by transient transfection of a mammalian cell line or by delivery of recombinantly produced AAV vector, Env sequences containing the gp140 from each selected time point (4, 20, 30, 53, and 78 w.p.i) were designed with the following modifications:

As each of these were gp140 sequences, they contained the original consensus gp120 envelope sequence and the ectodomain of gp41 (for that time point), with the trimeric GCN4 leucine zipper sequence (amino acid sequence NH_3-GMKQIEDKIEEILSKIYHIENEIARIKKLIGEV-COOH) fused to the carboxyl terminus of the gp41 ectodomain [256-258]. These gp140 sequences retained the intact furin-cleavage amino acid sequence (REKR), hence the + sign.

The native N-terminal signal peptide (amino acid sequence NH_3-MRVMGIQRNYPQWWIWSMLGFWMLMICNG-COOH) was replaced with the

heterologous human CD5 antigen leader peptide (amino acid sequence NH_3-MPMGSLQPLATLYLLGMLVASVLA-COOH), which has previously been shown to facilitate optimal expression and secretion of Env proteins [259, 260].

The amino acid sequences were sent to GeneArt (Thermo Scientific, Carlsbad, CA, USA), where they were codon optimised for human/ mammalian expression. The DNA cassettes, encoding the open reading frame for the selected 5 codon-optimized HIV-1 *envs* at each of the selected 5 time points, were synthesized and sub-cloned by GeneArt into the pcDNA™3.3 (Invitrogen, Life Technologies, Carlsbad, CA, USA) mammalian expression vector using the *Bam*HI and *Not*I restriction sites.

Matched Recombinant envelope glycoprotein (Env) expression and purification

2.4) Transformation of the recombinant plasmids into *Escherichia coli (E. coli)* DH5α cells and large-scale recombinant plasmid isolations and characterization

2.4.1) *E. coli* DH5α Transformations

The five pcDNA™3.3 (+) lyophilized w*n*gp140 plasmids were resuspended in sterile distilled water, at a final concentration of 0.1 μg/ μl. Two hundred nanograms (ng) of each of the five w*n*gp140 plasmids were used to transform 20 μl of chemically competent *E.coli* DH5α cells (Invitrogen, Life Technologies, Carlsbad, CA, USA) (see Appendix B1.1-1.3 for further details). The transformed cells were cultured on selective LB-agar plates (Appendix B1.6), supplemented with 100 μg/ ml ampicillin (Roche, Mannheim, Germany) (Appendix B1.7.1) and incubated overnight at 37°C.

2.4.2) Plasmid isolation (Maxiprep)

The recombinant plasmid DNA was purified from the transformed *E. coli* DH5α cells using the Maxi plasmid purification kit (Qiagen, Hilden, Germany), as per the manufacturer's instructions. Briefly, a single transformed bacterial colony was selected per plasmid and used to inoculate a starter culture of 5 ml LB media, supplemented with 100 μg/ ml ampicillin, and incubated for 6 hours 37°C, in a high-rotation shaking incubator at 250 rpm. One ml of the starter culture was added to a sterilised Erlenmeyer flask containing 250 ml of LB media,

supplemented with 100 µg/ ml ampicillin. These flasks were then incubated overnight at 37°C, in a high-rotation shaking incubator at 250 rpm. The bacterial cells were harvested by centrifugation at 6000 x g for 15 minutes at 4°C. The supernatant was subsequently discarded, while the pellet was resuspended in 10 ml P1 buffer containing RNase A (final concentration of 100 µg/ ml). The cells were lysed under alkaline conditions with the addition of 10 ml P2 lysis buffer (200 mM NaOH, 1% SDS (w/v)) and incubated for 5 minutes at room temperature. Genomic DNA, proteins, and cell debris was precipitated with the addition of 10 ml pre-chilled P3 buffer (3 M potassium acetate, pH 5.5) and incubated on ice for 20 minutes, followed by centrifugation at 20 000 x g for 30 minutes at 4°C. The clarified supernatant with the recombinant plasmid was captured on a QBT-equilibrated (10 ml), anion-exchange chromatography Qiagen-tip 500 column by gravity flow. This was followed by 2 x 30 ml washing steps with QC buffer, to remove RNA and protein contaminants. The bound recombinant plasmid was eluted from the Qiagen-tip 500 with 15 ml QF elution buffer. The DNA was precipitated with the addition of 0.7 volumes of isopropanol (Sigma-Aldrich, St. Louis, MO, USA) and centrifuged at 13 000 x g, for 30 min at 4°C. The residual isopropanol was removed by washing with ethanol (70% [v/v]; Sigma-Aldrich, St. Louis, MO, USA) and centrifuged at 13 000 x g, for 10 min at 4°C, followed by air-drying the pellet for 10 min. This pellet was gently resuspended in distilled water (dH_2O), and the concentration was determined by UV absorption at A_{260nm}. Plasmids were stored in aliquots at -20°C (general storage) and -80°C (long-term storage).

2.4.3) Restriction enzyme digest screening of pcDNA™3.3 (+) Env plasmids

The plasmid integrity was then checked by performing standard restriction enzyme digests as follows: (i) *Bam*HI and *Not*I double digest (to check plasmid size and successful ligation), *Bam*HI single digest (to check the correct size of plasmid), along with undigested plasmid as a control (all enzymes and corresponding buffers were obtained from Thermo Fisher Scientific, Waltham, MA, USA; see Appendix B2, Table B1). Briefly, 1 µg of DNA was digested for each reaction; with 10U (units) of *Bam*HI enzyme (for single digests) or 10U of *Bam*HI and 20U of *Not*I (for double digests); 2 µl (10X) of Unique *Bam*HI buffer; made up to a total reaction volume of 20 µl (with dH_2O). Restriction reactions were incubated for 1 hour at 37°C. The products were subsequently resolved on a 1% agarose gel as detailed in Appendix B3. DNA bands were visualised under UV light following ethidium bromide staining and images

captured using the ChemiDoc™ MP imaging system from Bio-Rad (CA, USA) and the QuantityOne version 4.6.9 Software Programme (Bio-Rad, CA, USA).

2.5) Restriction sub-cloning of the CH505-w4 insert into the pcDNA™3.1 backbone for expression comparison

2.5.1) Digestion of backbone and insert

Two micrograms of DNA was digested for the w4gp140 plasmid, along with 10 µg of the pcDNA™3.1 backbone vector, using the *Not*I (5') and *Bam*HI (3') restriction enzymes (all enzymes and corresponding buffers from Thermo Fisher Scientific, Waltham, MA, USA; see Appendix B2, Table B1). This was done to further analyse why the expression levels were insufficient in the pcDNA™3.3 backbone vector.

Digestion reactions were set up in a final volume of 20 µl; using the Unique *Bam*HI 10 x buffer, 20U *Bam*HI of and 40U *Not*I (according to the manufacturer's recommendations). The reactions were incubated at 37°C for 90 min. The products were subsequently resolved on a 1% agarose gel as detailed in Appendix B3. DNA bands were visualised under UV light following ethidium bromide staining and images captured using the ChemiDoc™ MP imaging system from Bio-Rad (CA, USA) and the QuantityOne version 4.6.9 Software Programme (Bio-Rad, CA, USA).

Gel extraction of the insert (w4gp140 construct) and backbone (pcDNA™3.1) bands was performed with the QIAQuick Gel Extraction kit (Qiagen, Hilden, Germany), as per the manufacturer's instructions. Briefly, the DNA fragment was excised from the agarose gel using a sharp scalpel and weighed. Three volumes of QG buffer was added to 1 gel volume (300 µl buffer to 100 mg gel) and incubated at 50°C until fully dissolved. One gel volume of isopropanol (Sigma-Aldrich, St. Louis, MO, USA) (100 µL isopropanol to 100 mg gel) was added to the sample and vortexed for 10 seconds. To bind the DNA, this solution was applied to a QIAQuick Spin column and centrifuged for 1 min at 16 000 x *g* until all the sample had passed through the filter. The flow-through was discarded and 500 µl of QG buffer was applied to the column and centrifuged for 1 minute at 16 000 x *g*. The flow-through was discarded before washing the column filter with 750 µl PE buffer and centrifuged for 1 min at 16 000 x *g*. The flow-through was discarded and the column filter re-centrifuged to remove any residual wash buffer. The column was then placed into a clean microcentrifuge tube, and 25 µl of dH_2O was used to elute the DNA. The tube was incubated at room temperature for 2 minutes, before

centrifugation for 2 minutes at 16 000 x *g*. The concentration was determined by UV absorption at A_{280nm} using the NanoDrop® Spectrophotometer ND-1000 (see section 2.1).

2.5.2) Ligation of insert and backbone fragments

Ligation of the fragments was performed using a 1:3 molar ratio of (vector backbone DNA: insert DNA), to maximise the likelihood of vector insert assembly. The volumes of DNA required were calculated from the femtomoles of DNA obtained from the gel extraction.

Briefly, the molecular weight was determined using the online calculator Oligo Calculator, version 3.27 [261]. The femtomoles/ µl were then calculated using the following equation:

Femtomoles/ µl = [(concentration in ng/µl x 1000)/ molecular weight] x 1000

Forty femtomoles of vector backbone DNA was used, with 120 femtomole of insert DNA (to give the 1:3 ratio mentioned above). To get the volumes of DNA required, the following equation was used:

volume of DNA in µl = femtomoles required/ (femtomoles/ µl from gel extraction)

A negative control containing no insert DNA, but the same volume of digested backbone, was used to verify that the subsequent clones were not because as a result of undigested or re-ligated backbone.

DNA ligation reactions were performed using T4 ligase (New England Biolabs® Inc., MA, USA) according to the manufacturer's instructions. Briefly, reactions were set up in a final volume of 20 µl: comprising 40 femtomoles of backbone DNA to 120 femtomoles of insert DNA (1:3 molar ratio), 1U of NEB T4 ligase, and 2 µl T4 DNA ligase buffer (New England Biolabs® Inc., MA, USA), with the final volume adjusted to 20 µl with nuclease-free water (Ambion, Thermo Fisher Scientific, Waltham, MA, USA). The reactions were incubated in the GeneAmp® PCR system 2700 Thermal Cycler (Applied Biosystems, Thermo Fisher Scientific, Waltham, MA, USA) at 22°C for 1 hour, followed by heat inactivation at 65°C for 10 minutes.

2.5.3) *E. coli* DH5α Transformations

Eight microliters of the ligation reaction (CH505-w4gp140 pcDNA™3.1) plasmid was used to transformed 100 µl chemically competent *E. coli* DH5α cells (see Appendix B1.1-1.3). The transformed cells were cultured as described previously in section 2.4.1.

2.5.4) Screening of positive bacterial colonies

The recombinant plasmid DNA was purified from the transformed *E. coli* DH5α cells using the HighPure Plasmid Isolation kit (Roche, Mannheim, Germany) as per the manufacturer's instructions.

Briefly, three single transformed bacterial colonies were selected per plasmid, and used to inoculate three sterilised tubes containing 3 ml of 2YT LB media (see Appendix B1.5) and supplemented with 100 μg/ml ampicillin (Roche, Mannheim, Germany) (see Appendix B1.7.1). These tubes were incubated overnight at 37°C in a high-rotation shaking incubator at 250 rpm. The bacterial cells were harvested by centrifugation at 6000 x g for 5 minutes at 4°C. The supernatant was subsequently discarded, while the pellet was resuspended in 250 μl Suspension/RNase buffer. The cells were then lysed under alkaline conditions with the addition of 250 μl Lysis buffer and incubated for 5 minutes at room temperature. Genomic DNA, proteins, and cell debris was precipitated with the addition of 350 μl Binding buffer and incubated for a further 5 minutes on ice before centrifugation at 13 000 x g for 10 minutes. The supernatant was then transferred to a High Pure Filter Tube and centrifuged at 13 000 x g for 1 minute. The flow through was discarded and the filter washed with 500 μl of Wash buffer I, followed by centrifugation at 13 000 x g for 1 minute. This washing procedure was repeated using 700 μl of Wash buffer II, plus additional centrifugation for 1 minute after the flow through was discarded. The bound recombinant plasmid was eluted with 25 μl dH_2O and the concentration was determined by UV absorption at A_{280nm}. Plasmids were stored in aliquots at -20°C (general storage) and -80°C (long-term storage).

2.5.5) Screening and selection of positive colonies by restriction enzyme digest

The colonies for the newly cloned CH505-w4gp140 pcDNA™3.1, were then screened by performing a standard restriction enzyme digests using *Bam*HI and *Not*I as described previously in section 2.4.3.

If clones were identified as positive (confirming the correct plasmid size and contained the correctly sized *env* gene insert), the isolated DNA was used to re-transform *E. coli* DH5α cells as previously described (section 2.4.1).

The recombinant plasmid DNA (CH505-w4gp140 pcDNA™3.1) was purified from the transformed *E. coli* DH5α cells using the Maxi plasmid purification kit, and digested, as described previously for section 2.4.2 and 2.4.3 respectively.

2.6) Recombinant HIV-1 Env expression and purification

2.6.1) Plasmids used for protein expression

The plasmids used for the transient transfections of mammalian cells included the **FVgp140** (as a positive control), and the five **w*n*gp140** plasmids (in the pcDNA™3.3 (+) backbone). Recombinant HIV-1 Env expression and purification procedures were based on methods described previously by Killick et. al (2015) [262].

2.6.2) General Mammalian cell culture

General Maintenance

All mammalian cell culture maintenance and experiments were carried out at 37°C using a humidified, water jacketed incubator (Thermo Fisher Scientific, Waltham, MA, USA) in an atmosphere supplemented with 5% CO_2 (Medical CO_2, Afrox, Selby, South Africa).

HEK293 T cells were obtained through the NIH AIDS Reagent Program (Germantown, MD, USA). These cells are derived from human primary embryonic kidney cells that have been transformed by sheared human adenovirus type 5 (Ad 5) DNA [263]. The HEK293 T cells express the large T antigen, which is important for plasmids that contain the SV40 enhancer of protein expression.

HEK293 T cells were maintained in Dulbecco's Modified Eagle Medium (DMEM) (Gibco, Life Technologies, Carlsbad, CA, USA), supplemented with 10 % foetal calf serum (FCS) (Gibco, Life Technologies, Carlsbad, CA, USA), 2 mM L-glutamine (GlutaMax, Gibco, Life Technologies, Carlsbad, CA, USA), and penicillin (100 units/ ml) and streptomycin (0.1 mg/ ml) (Sigma-Aldrich, St. Louis, MO, USA). Cells were sub-cultured twice a week (when cultures were between 70-90% confluent, as determined by visual, microscopic inspection). Briefly, the cells were rinsed with Dulbecco's Phosphate Buffered Saline (PBS) (Sigma-Aldrich, St. Louis, MO, USA) and trypsinized for 3 minutes at 37°C with 0.25% TrypLE (Gibco, Life Technologies, Carlsbad, CA, USA). Trypsinization was stopped by the addition of DMEM, with the resuspended cells then split as required (re-seeded at a ratio of 1/5-1/10).

Cell counting procedure

Cells were enumerated manually by staining the cell suspension at a 1:1 ratio with 0.4% trypan blue solution (Sigma-Aldrich, St. Louis, MO, USA). Viable cells were then

enumerated by microscopic examination of the stained cell suspension on the Countess II FL cell counter (Life Technologies, Carlsbad, CA, USA).

Cryostorage

For long-term cell storage, cell suspensions were prepared with freezing mix at a final concentration of 1-2 x 10^6 cells/ ml (see Appendix B4.1), and aliquoted in cryovials (Nunc, Roskilde, Denmark). The cryovials were cooled at a rate of -1°C/ minute using a Mr Frosty™ freezing container (Thermo Fisher Scientific, Waltham, MA, USA), according to the manufacturer's instructions. Cell lines were replaced after passage 45 and replaced with fresh aliquots by rapidly thawing the frozen cells and diluting them into 10 ml pre-warmed media in a T25 tissue culture flask (Nunc, Roskilde, Denmark).

2.6.3) Transient Transfections

For the expression and characterization of the founder virus Env (FVgp140) and the 5 CH505-w*n*gp140 Env glycoproteins, transient transfections were carried out with HEK293 T cell lines. These transfections were carried out in T175 tissue culture flasks (Nunc, Roskilde, Denmark) using the Polyethylenimine (PEI) Max (linear, MW 25 000) transfection reagent (Polysciences, Warrington, PA, USA) according to the manufacturer's instructions (see Appendix B4.2).

Briefly, 24 hours prior to transfection, 12 × 10^6 cells were seeded into 30 ml media in a T175 flask. Thirty micrograms of purified plasmid DNA was combined with 90 µl PEI Max in a final volume of 400 µl of OptiMEM (Life Technologies, Carlsbad, CA, USA); final DNA: PEI ratio = 1:3. The transfection complexes were vortexed for 10 seconds and incubated for 5 minutes at room temperature, before addition to the flasks. Twenty-four hours post-transfection, the media was replaced with 15 ml serum-free media II (SFMII; Gibco, Life Technologies, Carlsbad, CA, USA), supplemented with 2mM L-glutamine (GlutaMax, Gibco, Life Technologies, Carlsbad, CA, USA), and incubated for a further 48 hours. The supernatants containing the Env glycoproteins were then harvested, and the media replaced with fresh SFMII (repeated every second day for ~ 7 days). This harvested media was clarified by centrifugation at 1,000 × g for 10 mins, filter sterilised through an Acrodisc syringe filter with a 0.8 µm Supor® membrane (PALL Life Sciences, Port Washington, NY, USA), and stored at -20˚C until analysis/ purification. Expression was confirmed by enzyme-linked immunosorbent assay (ELISA), as described below.

2.6.4) Enzyme-linked immunosorbent assay (ELISA)

Standard, indirect ELISA protocols were followed for initial Env protein expression confirmation [264]. Briefly, medium binding, flat-bottomed, 96-well, maxisorp Immuno plates (Nunc, Roskilde, Denmark) were coated overnight with 100 µl per well of *Galanthus (G.) nivalis* lectin, concentration= 2 µg/ ml (Sigma-Aldrich, St. Louis, MO, USA), at 4°C. The plates were subsequently blocked with 250 µl blocking buffer (see Appendix B7.1) per well, for 1 hour at room temperature. The blocking buffer was removed, and plates were washed with PBS-T (see Appendix B7.2); 3 × 300 µl per well using a BioTek, ELx 50 automated plate washer (BioTek, Winooski, VT, USA).

Purified FVgp140 (available in the laboratory) was used as a positive control and to construct a standard curve. A two-fold dilution of FVgp140 protein was prepared in Dulbecco's PBS (concentration range 1000 – 7,1825 ng/ml) and run in duplicate. Non-Env containing wells were included as a negative control. The harvested media from the HEK293 T cells (w*n*gp140 Envs) was run as is (undiluted) and a two-fold dilution (diluted). Following an hour-long incubation at room temperature, unbound proteins were removed by washing each well 5 times with 300 µl PBS-T.

Following washing, each well (except for the no primary antibody control) was incubated with 100 µl primary antibody, VRC01 (see Appendix B11, Table B5) at a concentration of 1 µg/ml (made up in PBS-T) per well for 1 hour at room temperature. Following washing (5 x 300 µl PBS-T), each well was incubated with 100 µl of horse-radish peroxidase (HRP)-conjugated polyclonal anti-human Fc antibody (secondary antibody, see Appendix B11, Table B5) at a 1: 2000 dilution (made up in PBS-T) per well for 1 hour at room temperature. The unbound secondary antibody was removed by washing each well 5 times with 300 µl PBS-T.

The bound secondary antibody was then detected by chromogenic methods using the TMB Chromogen Solution for ELISA (Thermo Fisher Scientific, Waltham, MA, USA) and a 1M sulphuric acid stop solution. Absorbance values were quantified spectrophotometrically at 450 nm using the BioRad iMark™ microplate reader (BioRad, Hercules, CA, USA) to inform further confirmation analysis.

2.6.5) Lectin-affinity chromatography purification of recombinantly expressed HIV-1 Env

The Envs were purified via optimized lectin-affinity chromatography, using protocols established within the laboratory. Briefly, a separate lectin bound resin was used for each Env

to be purified. Two ml of *G. nivalis* lectin cross-linked to a 4% beaded agarose (Sigma-Aldrich, St. Louis, MO, USA), was incubated in harvested culture supernatant (~ 500 ml) containing the expressed Env glycoprotein, with stirring overnight at 4˚C. The resin was then collected and packed into a Luer-lock, non-jacketed liquid chromatography column (Dimensions: internal diameter (i.d.) 2.5 × 10 cm) (Sigma-Aldrich, St. Louis, MO, USA).

All subsequent washing and elution procedures were carried out manually, and all buffers (see Appendix B8) were maintained on ice. The packed resin bead was washed with 20 column bed volumes (~50 ml) of 0.5 M NaCl (see Appendix B8.1), followed by 20 column bed volumes of 1.0 M NaCl (see Appendix B8.2), followed by 20 column bed volumes of 1 x PBS (see Appendix B8.3). The bound Env glycoproteins were eluted with 7.5-bed volumes of PBS containing 1.0 M methyl α-D-mannopyranoside (MMP) (Sigma-Aldrich, St. Louis, MO, USA) (see Appendix B8.4). The eluted Env was filter-sterilized using an Acrodisc syringe filter, with a 0.45 µm Supor® membrane (PALL Life Sciences, Port Washington, NY, USA), and concentrated to approximately 100 µl in volume using an Amicon® Ultra Centrifugation Filter Unit (Millipore, Billerica, MA, USA) with a 50 kDa molecular weight cut-off.

The purified and concentrated Envs were quantified (see below), snap-frozen in liquid nitrogen and stored at -80˚C until needed.

2.6.6) Total protein concentration determination

The total protein concentration of each purified recombinant Env was determined using the BCA™ Protein Determination Kit (Pierce, Thermo Fisher Scientific, Waltham, MA, USA) according to the manufacturer's microplate protocol.

Briefly, a dilution series of the bovine serum albumin (BSA) was prepared (according to the manual), with the standards ranging in concentration from 25 - 2000 µg/ml, using the 2 mg/ml BSA ampule supplied by the manufacturer. These BSA standards were diluted in sterile PBS and stored at 4°C for up to two months.

The purified CH505 Env glycoproteins were not diluted. The BSA standards and unknown samples were assayed in duplicate by transferring 10 µl of each sample to a flat-bottomed, 96-well, polysorp Immuno plate (Nunc, Roskilde, Denmark). Two hundred microliters of the BCA working reagent was added to each sample and incubated at 37°C on an orbital shaker (THERMOstar Microplate incubator, BMG Labtech, Ortenberg, Germany) at 300 rpm for 1 hour. Following the incubation, plates were allowed to cool to room temperature before the absorbance at 570 nm was determined using the BioRad iMark™ microplate reader (BioRad,

Hercules, CA, USA). The protein concentration of unknown samples was determined using a standard curve, which was generated by linear regression analysis using GraphPad Prism 7 version 7.03 for Windows (GraphPad Software, La Jolla, CA, USA) of the prepared standards of known concentration and the corresponding A_{570nm} values. Protein concentrations of unknown samples were determined by interpolating the A_{570nm} against the derived standard curve.

2.6.7) Characterization of recombinant Envs via Sodium dodecyl sulphate-polyacrylamide gel electrophoresis (SDS-PAGE) and Western blot

The purified FVgp140 and the 5 w*n*gp140 HIV-1 Env glycoproteins were evaluated by SDS-PAGE, followed by Western blotting or Coomassie blue staining. The mammalian tissue culture supernatants, containing the transiently expressed glycoproteins, were prepared in 2 x Laemmli sample buffer (see Appendix B5.6), boiled for 5 minutes, and resolved on a 10% SDS-PAGE gel (see Appendix B5) [265].

For Coomassie staining, the SDS-PAGE gel was stained overnight on an orbital shaker in Coomassie blue stain (see Appendix B5.10.1). The gels were then placed in destaining solution (see Appendix B5.10) for at least 6 hours until bands could be clearly seen. Images of the Coomassie stained protein bands were captured using the ChemiDoc™ MP imaging system from Bio-Rad (CA, USA) and the QuantityOne version 4.6.9 Software Programme (Bio-Rad, CA, USA).

For Western blotting, the gels were removed from the gel casting apparatus and equilibrated for at least 10 minutes in Transfer buffer (see Appendix B6.1) at room temperature. The resolved bands were transferred to a nitrocellulose membrane (BioRad, Hercules, CA, USA) at 20 V for 30 minutes, using the XCell II™ Blot Module (Invitrogen, Life Technologies, Carlsbad, CA, USA). The membranes were then blocked overnight in 5% blocking solution (fat-free milk powder) in T-TBS (made from a 10 X TBS stock, see Appendix B6.2 and 6.3). The blocking solution was discarded, and the nitrocellulose membrane washed with T-TBS for 10 minutes on an orbital shaker. The resolved Env glycoproteins were detected using either anti-gp140 rabbit sera, 10E8, 4E10, or HIV-1 positive patient sera as the primary antibody (see Appendix B11, Table B5), at a concentration of 1 µg/ml (made up in T-TBS), and incubated at room temperature for 1 hour. Non-specific bound antibody was removed by 3 x 5-minute washes, on an orbital shaker, with T-TBS. The bound antibodies were detected using a 1: 2000

dilution of either anti-rabbit or anti-human secondary antibody (see Appendix B11, Table B5), incubated at room temperature for 1 hour.

Protein detection was performed by standard chemiluminescence methods, using the SuperSignal™ West Pico Chemiluminescent Substrate kit (Thermo Fisher Scientific, Waltham, MA, USA). Images were capture using the ChemiDoc™ MP imaging system from Bio-Rad (CA, USA) and the QuantityOne version 4.6.9 Software Programme (Bio-Rad, CA, USA).

2.6.8) Characterization of recombinant Envs via ELISAs

ELISAs were performed to further characterize and test the functionality of the purified recombinant Env glycoproteins. These included indirect ELISAs using various CD4-bs antibodies, and a 17b/ soluble, single domain (1d) CD4 ELISA protocol (established in our laboratory) [264].

CD4bs- ELISAs

Briefly, plates were coated with *G. nivalis* lectin [concentration= 2 µg/ ml] (Sigma-Aldrich, St. Louis, MO, USA), and blocked as described previously (section 2.6.4) [264].

A five-fold dilution series was prepared for each Env glycoprotein (including the FVgp140 as a positive control) in Dulbecco's PBS (concentration range from 1 000 – 8 ng/ml). Samples were run in duplicate (100 µl per well), and non-Env containing wells were included as a negative control. Following an hour-long incubation at room temperature, unbound proteins were removed by washing each well 5 times with 300 µl PBS-T.

Following washing, Env-bound wells (except for the no primary antibody control wells) were probed with 100 µl/ well volume of the following primary antibodies: VRC01, IgG1b12, 3BNC117, or NIH45-46 G54W (see Appendix B11, Table B5) at a 1 µg/ ml final concentration (prepared in PBS-T) for 1 hour at room temperature. Following washing (5 x 300 µl PBS-T), bound primary antibody was detected with 100 µl/ well of HRP-conjugated polyclonal anti-human Fc antibody (secondary antibody, see Appendix B11, Table B5) at a 1: 2000 dilution (made up in PBS-T) per well for 1 hour at room temperature. Unbound secondary antibody was removed by washing each well 5 times with 300 µl PBS-T.

The bound secondary antibody was then detected by chromogenic methods and quantified as described in section 2.6.4.

17b/ 1dCD4 ELISA

Briefly, plates were coated with *G. nivalis* lectin [concentration= 2 µg/ ml] (Sigma-Aldrich, St. Louis, MO, USA), and blocked as described in section 2.6.4 [264].

A five-fold dilution series was prepared for each Env glycoprotein (including the FVgp140 and purified HIV-1 subtype B BaL gp120 (available in our laboratory), as incorporated as appropriate positive controls) in Dulbecco's PBS (concentration range from 10 000 – 4.57 ng/ ml). Each dilution was incubated with an equal volume of soluble 1dCD4 [266] (prepared at 2 µg/ ml) at room temperature for 1 hour.. Another set of Env dilutions, adjusted to the same concentration using PBS-T, was run alongside this. Samples were run in duplicate and non-Env containing wells were included as a negative control. Following an hour-long incubation at room temperature, unbound proteins were removed by washing each well 5 times with 300 µl PBS-T.

Following washing, each well (except for the no primary antibody control) was incubated with 100 µl primary antibody, 17b (see Appendix B11, Table B5) (1: 2000 dilution, made up in PBS-T) per well for 1 hour at room temperature [267, 268]. Following washing (5 x 300 µl PBS-T), each well was incubated with 100 µl of HRP-conjugated polyclonal anti-human Fc antibody (secondary antibody, see Appendix B11, Table B5) at a 1: 2000 dilution (made up in PBS-T) per well for 1 hour at room temperature. The unbound secondary antibody was removed by washing each well 5 times with 300 µl PBS-T.

The bound secondary antibody was then detected by chromogenic methods and quantified as described in section 2.6.4.

Recombinant AAV (rAAV) production

2.7) Restriction sub-cloning of the CH505 inserts into the pAAV backbone

2.7.1) Digestion and Ligation of backbone and insert

Two micrograms of DNA was digested per w*n*gp140 plasmid (w4gp140, w20gp140, w30gp140, w53gp140, and w78gp140), along with 10 µg of the backbone vector pAAV- Luc, using the *Not*I (5') and *Bam*HI (3') restriction enzymes (all enzymes and corresponding buffers from Thermo Fisher Scientific, Waltham, MA, USA; see Appendix B2, Table B1).

Digestion reactions for the plasmids and the gel extraction of the insert (w*n*gp140 constructs) and backbone (pAAV) bands, were set up as described previously in section 2.5.1. Ligation of the extracted fragments was performed as described previously in section 2.5.2.

2.7.2) *E. coli* SURE2 Transformations and Screening of positive bacterial colonies

Eight microliters of the ligation reaction (pAAV-CH505-w*n*gp140) or pAAV-GFP plasmid was used to transformed 100 µl chemically competent *E. coli* SURE2 cells (see Appendix B1.1-1.3). The transformed cells were cultured on selective LB-agar plates (see Appendix B1.6), supplemented with 100 µg/ ml carbenicillin (Thermo Fisher Scientific, Waltham, MA, USA) (see Appendix B1.7.2) and incubated overnight at 37°C.

The presence of the AAV ITRs in the pAAV backbone vectors (pAAV-CH505w*n*gp140 and pAAV-GFP) necessitated the use of a recombinase- and endonuclease- deficient cell line such as *E. coli* SURE2 (Agilent Technologies, Santa Clara, CA, USA). These ITR sequences form hairpin loop secondary structures, that are unstable in *E. coli* and prone to deletion during replication. To further ensure ITR retention, the plasmids are grown no longer than 12 hours, and on plates supplemented with carbenicillin, which has improved stability over ampicillin (specifically for large-scale growth) [269].

For the screening of positive bacterial colonies, the recombinant plasmid DNA was purified from the transformed *E. coli* SURE2 cells as described previously in section 2.5.4. Changes of note to the protocol include the substitution of ampicillin with carbenicillin.

2.7.3) Screening and selection of positive colonies by restriction enzyme digest

The colonies for each plasmid, either the pAAV-GFP or the newly cloned pAAV-w*n*gp140, were then screened by performing a standard *Sma*I digest for both plasmids to check ITR integrity.

In addition to the *Sma*I digest, the pAAV- GFP was digested with *Bam*HI (to confirm plasmid size). For pAAV-w*n*gp140 additional digests were as follows: *Bam*HI and *Not*I double digest (to confirm plasmid size and successful ligation of the *env* insert), and *Bam*HI single digest (to check the correct size of plasmid) (see Appendix B2, Table B1 for corresponding buffers).

Five hundred nanograms of DNA was digested for each reaction; with 5U of *Sma*I, 5U of *Bam*HI and 10U of *Not*I (for double digests), or 5U *Bam*HI enzyme (for single digests); 2 µl (10X) of corresponding buffer; made up to a total reaction volume of 20 µl (with dH_2O). Restriction reactions were then completed as described in section 2.4.3.

If clones were identified as positive (containing intact ITRs, confirming the correct plasmid size, and contained the correctly sized *env* gene insert), the isolated DNA was used to re-transform *E. coli* SURE2 cells as previously described (section 2.7.2). The transformed cells were cultured on selective LB-agar plates (see Appendix B1.6), supplemented with carbenicillin (Thermo Fisher Scientific, Waltham, MA, USA) at a final concentration of 100 µg/ ml (see Appendix B1.7.2). The plates were then incubated overnight at 37°C.

2.7.4) Optimized Chloramphenicol plasmid isolation protocol

The recombinant plasmid DNA (pAAV-GFP, and pAAV-w*n*gp140) was purified from the transformed *E. coli* SURE2 cells using the Maxi plasmid purification kit (Qiagen, Hilden, Germany) as per the manufacturer's instructions. The plasmid isolation protocol was modified (from the maxiprep isolation procedure described in section 2.4.2) to improve DNA yields. The protocol was adapted because the DNA yields were initially much lower than expected with standard protocols, and the addition of chloramphenicol has been reported to improve DNA yields [269]. The low yields were as a result of the plasmids being low-copy-number plasmids, due to the pMB1 origin of replication. The addition of chloramphenicol inhibits the bacterial host protein synthesis, but as the plasmid replication is independent, it's replication will continue.

Briefly, a single transformed bacterial colony was selected per plasmid and used to inoculate a starter culture of 5 ml 2 YT LB media (see Appendix B1.5), supplemented with 100 µg/ml

carbenicillin (Thermo Fisher Scientific, Waltham, MA, USA) (see Appendix B1.7.2), and incubated for 6-8 hours at 37°C, in a high-rotation shaking incubator at 250 rpm. One millilitre of the starter culture was added to a sterilised Erlenmeyer flask containing 250 ml of 2 YT LB media (see Appendix B1.5), supplemented with 100 μg/ml carbenicillin (see Appendix B1.7.2). These flasks were then incubated for a further 8-10 hours at 37°C, in a high-rotation shaking incubator at 250 rpm. This was followed by the addition of 170 μg/ml chloramphenicol (see Appendix B1.7.3) and incubated for a further 12 hours at 37°C, in a high-rotation shaking incubator at 250 rpm. The bacterial cells were then harvested and plasmid DNA isolated, as described previously (section 2.4.2). Final DNA stocks were stored in aliquots at -20°C (general storage) and -80°C (long-term storage).

2.8) Transformation of additional plasmids into *Escherichia coli (E. coli)* SURE2 cells and large-scale recombinant plasmid isolations for rAAV production

2.8.1) *E. coli* SURE2 Transformation and Optimized Chloramphenicol plasmid isolation protocol

Two hundred nanograms of each of Adenohelper or the rep/cap plasmid 2/2 were used to transform 20 μl of chemically competent *E. coli* SURE2 cells (as described in section 2.7.2).

The recombinant plasmid DNA was purified from the transformed *E. coli* SURE2 cells using the modified Maxi plasmid purification kit (Qiagen, Hilden, Germany) as per the manufacturer's instructions (as described in section 2.7.4).

2.8.2) Restriction digest screening of AAV helper plasmids

The plasmid integrity was confirmed by performing standard restriction enzyme digests as follows:

Adenohelper 5 plasmid: (i) *Bam*HI digest (2 restriction sites), and (ii) *Xho*I digest (1 restriction site), both to check the correct size of plasmid, along with undigested plasmid as a control.

Rep/Cap serotype 2: (i) *Nco*I digest (2 restriction sites), and (ii) *Bam*HI digest (1 restriction site) both to check the correct size of plasmid), along with undigested plasmid as a control (all enzymes and corresponding buffers from Thermo Fisher Scientific, Waltham, MA, USA; see Appendix B2, Table B1). One microgram of DNA was digested for each reaction; with 10U of *Xho*I or *Bam*HI enzyme (for single digests), or 10U of *Bam*HI or *Nco*I (for double digests); 2

µl (10X) of corresponding buffer; made up to a total reaction volume of 20 µl (with dH_2O). Restriction reactions were then completed as described in section 2.4.3.

2.9) AAV Production

All recombinant adeno-associated viral (rAAVs) vectors were prepared via triple transfection of HEK293 T cells (with the *cis*, *trans*, and helper plasmids described below), followed by purification via the Iodixanol gradient method [270, 271].

2.9.1) Plasmids used for rAAV production

The plasmids used for the rAAV triple transfections were as follows: (i) ***Cis* plasmids** containing the transgene of interest, either an (a) enhanced green fluorescent protein (EGFP) (pAAV-GFP, section 2.6.6) or an (b) Env (pAAV- w*n*gp140 cloned plasmids, section 2.6) expression cassette flanked by the AAV2 ITRs; (ii) ***Trans* plasmid** containing the AAV serotype 2 replication (rep) gene, and the capsid gene from AAV serotype 2 to produce pAAV2/2 (for *in vitro* work) (section 2.7); and (iii) **adenovirus helper plasmid**, AdenoHelper5 (section 2.7), used to aid in viral replication.

2.9.2) Mammalian cell culture and Large-scale polyethyleneimine transfections

Mammalian cell lines were cultures and maintained as described in section 2.6.2

Recombinant AAV vectors were produced by large-scale transient transfections of HEK293 T cells. Seventy-two hours prior to transfection, 3.5 x 10^6 HEK293 T cells were seeded per 15 cm^2 plate (Fisher Scientific, Thermo Fisher Scientific, Waltham, MA, USA), with 4 plates allocated per virus for production. Once the cells had reached 80% confluency, transfections were carried out using the PEIMax transfection reagent.

Briefly, at least 2 hours prior to transfection the media was replaced with 15 ml of fresh, pre-warmed media, which was added in a drop-wise manner to avoid disturbing the cell monolayer. Plasmids at a ratio of 1 : 1.3 : 1.6 (6 µg *Cis* plasmid : 8 µg Helper plasmid : 10 µg *Trans* plasmid), where *Cis*, *Trans*, and Helper plasmids as defined in section 2.8.1, were added together and the final volume adjusted to 500 µl with Ambion nuclease-free water (Thermo Fisher Scientific, Waltham, MA, USA). Three-point-five millilitres of OptiMEM (Life Technologies, Carlsbad, CA, USA) was added to the DNA, followed by 500 µl of PEImax for the 4 plates (1 mg/ ml) (at a ratio of 5:1 to DNA). The transfection complexes were vortexed for 10 seconds, followed by incubation for 5 minutes at room temperature. This was then added in a dropwise manner to the 15cm^2 plate. The plate was rocked gently to distribute the

complexes over the full surface area and laid flat (to ensure even growth) in the incubator for 24 hours. The media was harvested and replaced with 25 ml pre-warmed media every alternate day for up to 7 days (24, 72, 120, and 168 hours post-transfection), and stored at 4°C until further processing.

2.9.3) rAAV Purification

rAAVs were harvested from both the media collected (as described in section 2.9.2) and the cells, to maximise virus collection and titres [270, 271].

Harvesting from cells

The HEK293 T cells were mechanically dislodged from the culture plates using 30 ml PBS (across all 4 plates per virus) and a cell scraper, and pelleted via centrifugation at 400 x g, for 15 minutes at 4°C. The cells were resuspended in 5 ml viral lysis buffer (see Appendix B9.1), followed by 5x freeze-thaw cycles, with liquid nitrogen (-196 °C) and a water bath (37 °C). The lysate was sonicated for 80 seconds in a Bandelin Sonorex sonicating water bath (RK 103 H) at 35 kHz (Bandelin Electronic, Berlin, Germany), treated with Benzonase® nuclease (Sigma-Aldrich, St. Louis, MO, USA) at a final concentration of 250 Units/ µl, at 37°C for 1 hour (vortexed every 10 minutes) to remove any contaminating DNA and RNA. The lysate was centrifuged at 2 500 x *g* for 15 minutes at 4°C to remove any cellular debris. The supernatant was collected and re-centrifuged at 2 500 x *g* for 15 minutes at 4°C, again before placing the lysate on ice (which was used to resuspend the pellet obtained from the harvested supernatant mentioned below).

Harvesting from culture supernatant

The rAAV in the collected culture supernatant was clarified by filter sterilisation using the Nalgene™ Rapid-Flow™ Sterile Disposable Filter units with polyethersulfone (PES) membrane (0.2 µm pore size) (Thermo Fisher Scientific, Waltham, MA, USA), into a sterile 500 ml bottle, before the addition of 5 x polyethylene glycol (PEG) Sigma-Aldrich, St. Louis, MO, USA) (see Appendix B9.3: 12.5 ml PEG per 50 ml collected media) and allowed to precipitate at 4°C for 24 hours. The PEG precipitation allows for the removal of any cellular debris and the soluble proteins [270].

The precipitant was harvested by centrifugation at 4 000 x *g* for 30 minutes at 4°C. After the supernatant was discarded, the cell lysate (from the cell harvesting) was used

to resuspend the precipitated protein pellet, which was then transferred to a Quick-Seal centrifuge tube (Beckman Coulter, CA, USA) using a glass Pasteur pipette.

Preparation and centrifugation of Iodixanol (discontinuous) gradient

Four iodixanol step gradients were prepared by underlying and displacing the less dense cell lysates with iodixanol, prepared from a 60% solution of OptiPrep (Sigma-Aldrich, St. Louis, MO, USA) (see Appendix B9.4-9.6). Layering of the iodixanol gradient was performed in the above mentioned Quick-Seal tubes in a "bottom-up" fashion: a 15% gradient (1.5 ml), a 25% gradient (1.5 ml), a 40% gradient (1.5 ml), and a 60% gradient (1.5 ml). The tubes were sealed and placed inside the 70.1 Ti rotor, before ultracentrifugation at 171 000 x *g*, for 2 hours at 4°C (Acceleration: Max; Deacceleration: 1) in an Optima™ L-80 XP Ultracentrifuge (Beckman Coulter, CA, USA).

Once the samples had undergone ultracentrifugation, the functional virus particles were harvested from the 40% Iodixanol fraction by collecting no less than 800 µl (maximum volume 1 200 µl) with a 20G needle. Viral aliquots were stored in aliquots at -20°C (general storage) and -80°C (long-term storage).

2.10) Droplet Digital Polymerase Chain Reaction (ddPCR)

The final purified rAAVs were quantified using the absolute DNA quantification method (ddPCR). The assay uses standard "TaqMan" primer-probe sets in a 20 µl reaction that has been fractionated into approximately 15 000 individual droplets. These are scored as either positive or negative based on probe-derived fluorescence. The portioning of the sample significantly increases assay sensitivity and accuracy [272].

2.10.1) Primers and Probes

For quantification of rAAVs, specific primer sets, and fluorescent hybridisation probes were designed for ddPCR. The pAAV-GFP and pAAV- w*n*gp140 sequences were aligned in ClustalX 2.0 [254] to identify regions that were common in all transgenes. One primer/ probe set was designed specifically for the EGFP-transgene of the pAAV-GFP, and another set was designed for the SV40 region, which is common to all 6 sequences [272]. The two sequences (for GFP and SV40 regions) were inserted into the Primer3Plus primer design tool [273, 274], and all 3 design options selected: right and left (forward and reverse) primers, and hybridization probe options. Once the output sequences were obtained, final sequences were selected based

off the recommended parameters for ddPCR primer and probe design: primer Tm between 50-65°C; probe Tm ± 5°C higher (Drop Digital™ PCR Applications Guide, BioRad, Hercules, CA, USA). These were subsequently ordered from Thermo Scientific (Thermo Fisher Scientific, Waltham, MA, USA).

The following primers and probes were used in this study, where 6-FAM refers to the 6-Carboxyfluorescein fluorescent reporter dye (emission max = 518 nm) on the 5' end of the GFP-specific probe, VIC™ refers to the 2′-chloro-7′phenyl-1,4-dichloro-6-carboxy-fluorescein fluorescent reporter dye (emission max = 552 nm) on the 5' end of the SV40 probe, and QSY™ refers to the dark quencher used (all Thermo Fisher Scientific, Waltham, MA, USA) (see Appendix B10, Table B4).

Green fluorescent protein (GFP) assay

Forward: 5'-GACGACGGCAACTACAAGA-3'

Reverse: 5'-GATGCCCTTCAGCTCGAT-3'

Probe: 5'-6-FAM-AGGTGAAGTTCGAGGGCGACAC-QSY-3'

SV40 sequence assay

Forward: 5'-TCGAGCAGACATGATAAGATAC-3'

Reverse: 5'-GCAATAGCATCACAAATTTCAC-3'

Probe: 5'-VIC-TGGACAAACCACAACTAGAATGCAGTGA-QSY-3'

2.10.2) Droplet digital PCR genome titre assay

Sample preparation and serial dilutions

The purified rAAV vector aliquots were treated with DNase I (New England Biolabs® Inc., MA, USA) to further remove any contaminating DNA and RNA. Two microliters of purified vector were treated with DNase I at a final concentration of 400 Units/ ml, in addition to 2 µl (10X) of corresponding buffer; made up to a total reaction volume of 20 µl (with dH_2O). Reactions were incubated for 30 minutes at 37°C. This reaction constituted the first dilution of vector (10^1). The samples were then further diluted to within the linear range of the ddPCR assay (10^2-10^7), using dilution buffer (see Appendix B10.2). The samples were vortexed for 10 seconds and placed on ice. The reaction mixtures were then assembled with the ddPCR™ Supermix for probes (no

dUTPs, BioRad, Hercules, CA, USA), the TaqMan primers and probes (final concentrations of 900 nM and 250 nM, respectively), 5 µl of template DNA (of the appropriate dilution), and PCR-grade water to a final volume of 20 µl.

Droplet generation and PCR amplification

Each reaction (20 µl) was loaded into a sample well of an 8-well disposable cartridge (BioRad, Hercules, CA, USA). Seventy microliters of droplet generation oil (BioRad, Hercules, CA, USA) was added to the appropriate oil wells, covered with a rubber gasket (BioRad, Hercules, CA, USA), and droplets were formed in the QX 200 Droplet Generator (BioRad, Hercules, CA, USA). A forty microliter sample of the droplets was transferred to a 96-well PCR plate, heat-sealed with plate foil in the PX1 PCR Plate sealer (BioRad, Hercules, CA, USA), and amplified with the C1000 Touch Thermal Cycler (BioRad, Hercules, CA, USA) using the following protocol: Initial denaturation at 95°C for 10 minutes, followed by 42 cycles of 30 seconds denaturation at 95°C, probe/ primer annealing at 60°C for 60 seconds, and primer extension at 72°C for 15 seconds. A final denaturation step was incorporated at 98°C for 10 minutes.

QX200 Droplet reader and analysis

The plate was subsequently scanned on the QX 200 Droplet Reader (BioRad, Hercules, CA, USA) and the data analysed with the QuantaSoft™ Analysis Pro 1.0.596 software (BioRad, Hercules, CA, USA). The copies per microliter (C/ µl) readout was converted to genome copies/ ml (GC/ ml) according to the following formula:

$$\mathbf{X = [(aY)(1000/b)]D}$$

Where:

X: GC/ ml

a: volume of the ddPCR (20 µl)

Y: ddPCR readout in C/ µl

b: volume of the diluted vector in the ddPCR (5 µl)

D: total dilution applied to test material

2.11) Viral Transduction assays

2.11.1) Mammalian Cell Culture and Optimising *In vitro* infections

Mammalian cell lines were cultures and maintained as described in section 2.6.2.

The optimal multiplicity of infection (MOI) was determined by infecting HEK293 cells with various dilutions of rAAV-GFP, based off the concentration of GC/ ml. Cells were visualised with the CKX41 Inverted Microscope (Olympus, Tokyo, Japan) to observed GFP-fluorescence and infer successful GFP expression.

Briefly, 40 000 HEK293 T cells were plated per well in a final volume of 100 µl in a 96-well plate (Nunc, Roskilde, Denmark). After 6 hours, cells were infected with rAAV-GFP at increasing MOIs of 1, 10, 100, 1 000, 10 000, and 100 000 (prepared in a final volume of 100 µl DMEM media, supplemented as previously described). The GFP-fluorescent images were digitally captured using the CC-12 Soft Imaging system (Olympus, Tokyo, Japan) and the analysis LS report software, version 2.8 (build 1235) (Olympus, Tokyo, Japan), at 24, 48, and 72 hours post-transduction.

Once the optimal MOI was confirmed (100 000), the same procedure was used in the *in vitro* infections with the other rAAVs (rAAV-CH505), where expression of the CH505 Envs was monitored via ELISA (see below).

2.11.2) Enzyme-linked immunosorbent assay (ELISA)

Standard, indirect ELISA protocols were followed for detection of protein expression from the rAAV vectors, with coating, blocking, and washes as described in section 2.6.4 [264].

Purified FVgp140 (available in the laboratory) was used as a positive control and to construct a standard curve. A two-fold dilution of FVgp140 protein was prepared in Dulbecco's PBS (concentration range 5000 – 2.28 ng/ml) and run in duplicate. The transduced HEK293 T cell supernatant was run as is (undiluted) and a two-fold dilution (diluted). Negative controls included a sample of the rAAV-GFP transduced cell supernatant, and supernatant from cells that were not transduced. Following an hour-long incubation at room temperature, unbound proteins were removed by washing each well 5 times with 300 µl PBS-T.

Following washing, each well was incubated with 100 µl primary antibody, IgG1b12 (see Appendix B11, Table B5) at a concentration = 1 µg/ml (made up in PBS-T) per well for 1 hour at room temperature. Following washing (5 x 300 µl PBS-T), each well was incubated with 100 µl of HRP-conjugated polyclonal anti-human Fc antibody (secondary antibody, see Appendix B11, Table B5) at a 1: 2000 dilution (made up in PBS-T) per well for 1 hour at room temperature. The unbound secondary antibody was removed by washing each well 5 times with 300 µl PBS-T.

The bound secondary antibody was then detected by chromogenic methods quantified as described in section 2.6.4, to inform further analysis.

Chapter 3: Results

3.1) Design and construction of HIV-1 envelope glycoprotein (Env) constructs

3.1.1) Selection of sequentially derived HIV-1 Subtype C *env* constructs

Selection of sequentially-derived HIV-1 subtype C Env was informed by the research published by Liao and colleagues [187]. Following the bioinformatics analysis of these 292 HIV-1 subtype C CH505 Env sequences [187], a consensus sequence was generated for each timepoint (4, 14, 20, 22, 30, 53, 78, 100, 136, and 160 w.p.i). From these ten timepoints, five were chosen to best select the potential sequential sequences required to recapitulate the evolution of bNAbs following immunization *in vivo* (4, 20, 30, 53, and 78 w.p.i) (Figure 3.1).

The consensus sequences for each timepoint were generated from 52 sequences for w4 group; 28 for w20; 30 for w30; 25 for w53; and 34 for w78. These sequences were aligned to an inferred founder virus sequence for HIV-1 subtype C [247, 262] and the HXB2 reference genome. Key areas highlighted in Figure 3.1 include potential N-linked glycosylation sites (PNGs) (purple regions), and the residues that are important for CD4 binding and the CD4bs-directed bNAb epitopes (red regions).

The derived CH505 Envs had longer V1, V4, and V5 loops (specifically weeks 53 and 78) and an increase in the predicted number of PNGs, particularly in the V1 loop region compared to HXB2 and Founder virus sequences (Figure 3.1). Additionally, these Envs displayed slightly more diversity in the CD4 binding site and CD4bs-directed bNAb epitope regions, when compared to the Founder virus sequence, with amino acid substitution occurring in the D loop constant region 2 (F283I; and A287V or A287G); the V5/β24 region (N466K or N466E; and S468N); and in other key CD4bs-contacts indicated (P376L; V379T; and K436E).

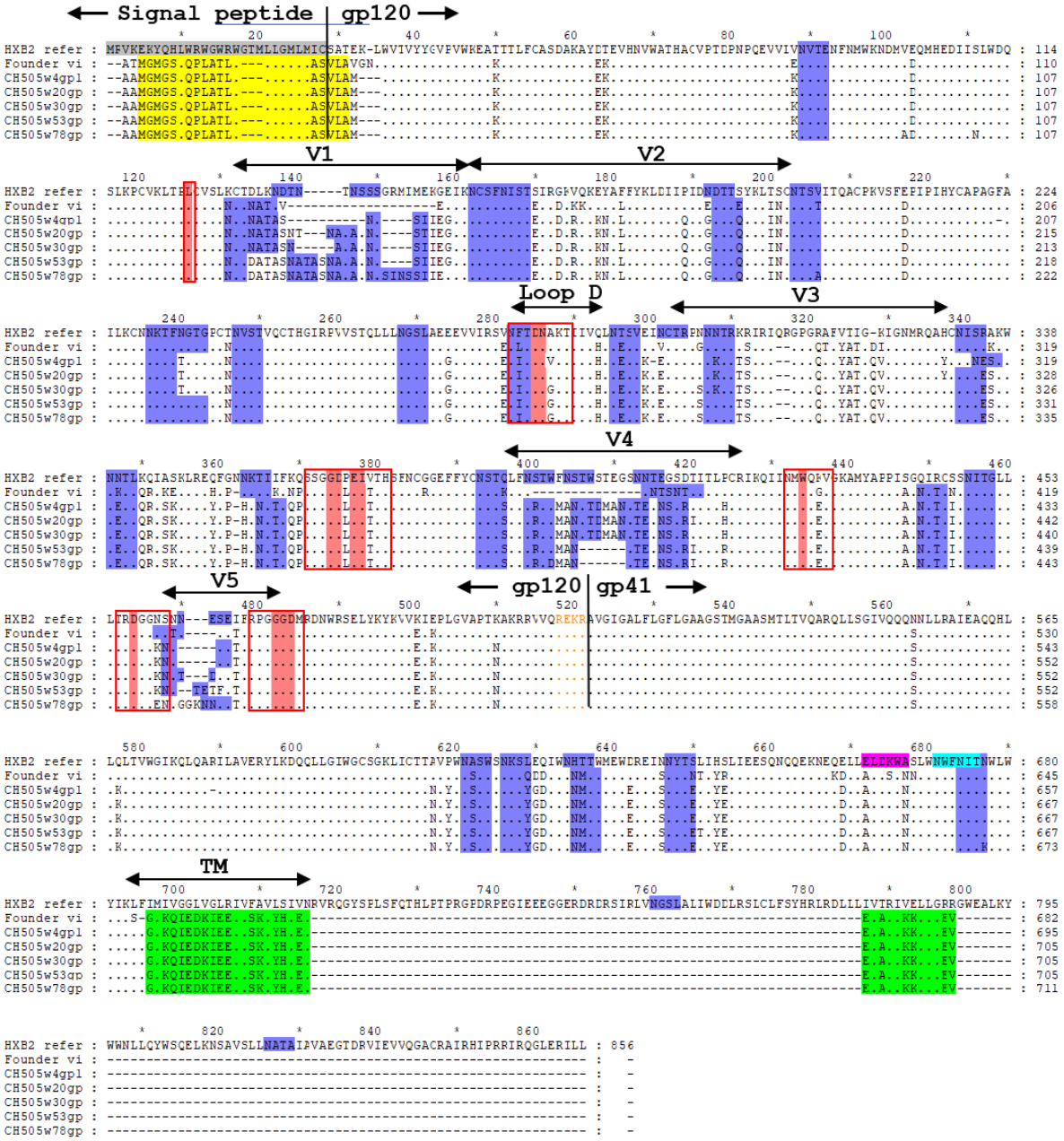


Figure 3.1: The predicted amino acid sequence alignment of selected envelope glycoprotein (Env) sequences derived from an HIV-1 subtype C infected individual (CH505w*n*gp140), an inferred subtype C founder virus Env consensus sequence (Founder vi), and a reference genome (HXB2). The CH505 Env sequences were aligned to the HXB2 reference genome and the inferred founder virus sequence, to aid in orientation and for comparative analysis. The names of key regions are indicated above the sequence with a black arrow. The potential N-linked glycosylation sites (PNGs) are shaded in purple, the native signal peptide in grey, the CD5 antigen leader peptide in yellow, and the GCN4 trimeric sequence in green. Regions that have been boxed in red indicate the residues that are important for CD4 binding and the CD4bs-directed bNAb epitopes (the most critical of these are shaded in red). The linear epitopes of two bNAbs targeting the gp41 MPER region 2F5 (ELDKWA) and 4E10 (NWFDIT) are shown in pink and light blue respectively. The furin cleavage site (REKR motif) is indicated in orange text. (.) indicates the residue is identical to the reference sequence, (-) indicates an insertion/ deletion.

3.1.2) HIV-1 Subtype C CH505 *env* construct design

Constructs, consisting of the codon optimized trimeric gp140 sequences (w*n*gp140 or w*n*), were designed and successfully cloned into pcDNA™3.3 mammalian expression vectors, by GeneArt (Figure 3.2 and Appendix A, Supplementary Figure 1A, C, E, G, and I). The lyophilized constructs were resuspended in sterile distilled water before transformation into chemically competent *E. coli* DH5α cells, followed by large-scale plasmid isolations (results not shown), for downstream mammalian transfection and protein expression of HIV-1 Env glycoproteins; and subsequent sub-cloning of the Env constructs into the pAAV backbone for recombinant AAV production.

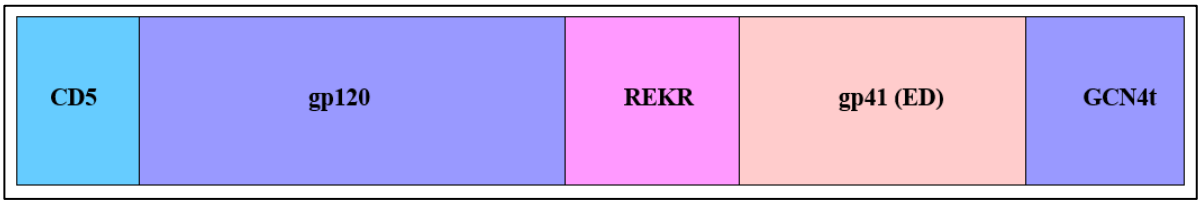


Figure 3.2: A schematic representation of the engineered trimeric Env constructs (w*n*gp140) used for this study. The gp140 constructs comprised the full gp120 sequence (gp120) and the gp41 ectodomain (ED; residues 522-693) sequence, with an intact cleavage site (REKR (+)), and a heterologous trimeric GCN4 leucine zipper sequence (GCN4t) fused to the C-terminus of the gp41 ED. The native Env leader sequence was replaced with the heterologous human CD5 antigen leader peptide (CD5) at the gp120 N-terminus.

Matched Recombinant envelope glycoprotein (Env) expression and purification

3.2) Restriction enzyme digest screening of pcDNA™3.3 (+) Env constructs

Following bacterial transformations, the pcDNA3.3™-w*n*gp140 plasmid DNA (w4gp140, w20gp140, w30gp140, w53gp140, and w78gp140) was extracted and purified, followed by restriction enzyme digest analysis to ensure the integrity of the plasmids and that the necessary transgenes (CH505 Envs) were present (refer to Appendix A, Supplementary Figure 1A, C, E, G, and I; for plasmid map schematics and position of relevant restriction sites). Figure 3.3 shows the agarose gel following restriction enzyme digest analysis of the w*n*gp140 constructs. Plasmids were subjected to both a single digest (with *Bam*HI) and a double digest (with *Bam*HI and *Not*I). Undigested plasmid samples were included as a negative control.

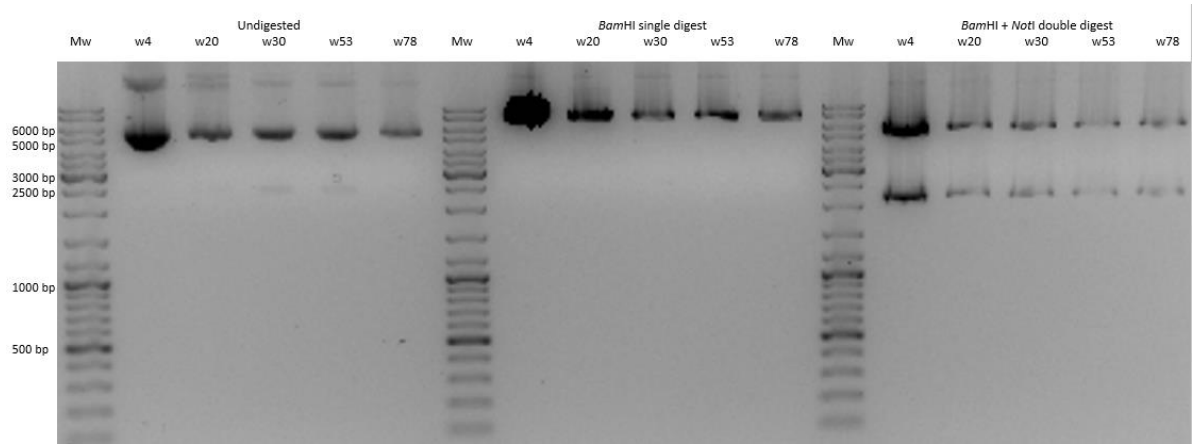


Figure 3.3: Restriction enzyme digest analysis of the pcDNA3.3w*n*gp140 expression vectors. All DNA samples were resolved on a 1% agarose gel and visualised under UV light following ethidium bromide staining. The undigested DNA was run as a negative control. All 5 plasmids were digested with *Bam*HI alone (one restriction site); or *Bam*HI and *Not*I in a double digest reaction. w4-w78 corresponds to the CH505 HIV-1 Env isolate weeks post infection, described previously. The O'Gene Ruler DNA ladder (Thermo Fisher Scientific, Waltham, MA, USA) was used a reference molecular weight marker (Mw) bands are indicated on the left of the image in base pairs (bp).

The wngp140 constructs were successfully linearized by *Bam*HI single digest, (compare undigested and *Bam*HI single digest treatments (Figure 3.3)), and produced a single band that resolved at approximately 7 500 bp (expected sizes of 7 504, 7 534, 7 534, 7 534, and 7 552 bp for w4, w20, w30, w53, and w78 respectively (refer to Appendix A, Supplementary Figure 1A, C, E, G, and I)). The respective CH505 Env transgene was successfully excised using the *Bam*HI and *Not*I double digest and produced bands that migrated at approximately 5 400 and 2 100 bp. The expected sizes include 5 414 bp, for all five constructs; and 2 090, 2 120, 2 120, 2 120, 2 138 bp for the *env* transgene of w4, w20, w30, w53, and w78 respectively (refer to Appendix A, Supplementary Figure 1A, C, E, G, and I).

These successful restriction enzyme digests confirm the plasmid integrity and that the transgenes of interest (CH505 Env w4, w20, w30, w53, and w78) were present. These constructs were used for downstream mammalian transfection, and protein expression of matched recombinant Envs.

3.3) Recombinant HIV-1 Env expression

3.3.1) Transient expression of the HIV-1 Subtype C CH505 Env constructs

Initial transient transfection of HEK293 T cells was performed using selected HIV-1 Env constructs: w*n*gp140, weeks 53, 78) and the FVgp140, as a positive transfection control.

Unpurified culture supernatants were resolved on SDS-PAGE and analysed by Western blot (Figure 3.4). A sample of purified FVgp140 (1 µg) was resolved in parallel and served as a positive control for the Western blotting procedure (Figure 3.4, 140+ lane). Resolved and transferred HIV-1 Envs were detected using anti-FVgp140 rabbit sera [262] as a primary antibody followed by anti-rabbit HRP-linked secondary antibody. Signal was observed for both the purified FVgp140 (140+) and unpurified, culture supernatant FVgp140 (140+(T)) positive controls. A reduced signal was observed in the CH505 Envs, w53 and w78 unpurified culture supernatant samples (Figure 3.4). As expected, under denaturing and reducing SDS-PAGE the protein bands observed for these trimeric constructs migrated at equivalent levels of approximately 140 kDa, corresponding to the monomeric subunits.

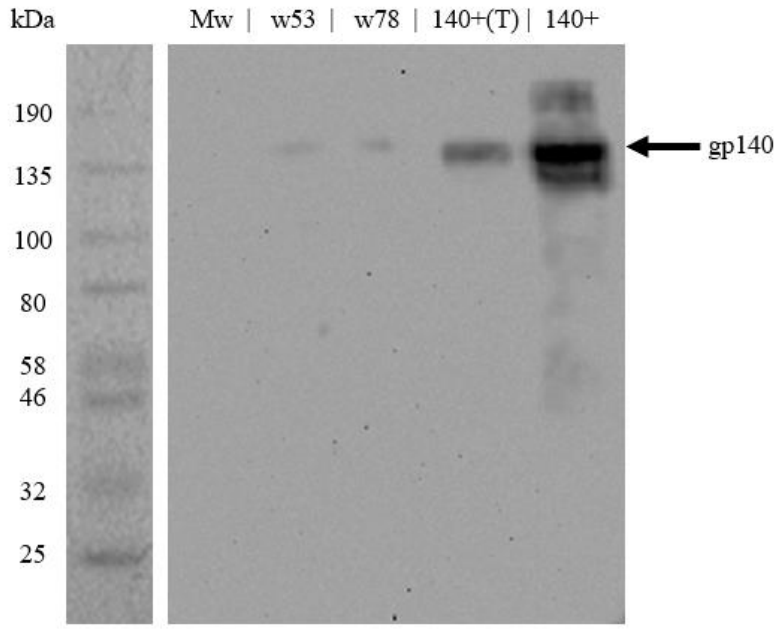


Figure 3.4: Western Blot analysis of FVgp140 and selected CH505gp140 envelope glycoproteins. Following transient transfections of HEK293 T cells, unpurified cell culture supernatants were analysed via Western blot. Protein expression was confirmed by probing for Env using anti-gp140 rabbit sera primary antibody (diluted 1: 1 000). Subsequent detection was done with a horse radish peroxidase (HRP)-conjugated anti-rabbit secondary antibody (diluted 1: 2 000). Controls include: 140+(T) = founder virus gp140 GCN4+, that was transfected along with the other samples; and 140+ (purified founder virus gp140 GCN4+ protein). The molecular weight marker (Mw) corresponds to the prestained protein marker, broad range (New England Biolabs® Inc., MA, USA); bands are indicated on the left in kilodaltons (kDa). Photograph of the pre-stained molecular weight standard on nitrocellulose membrane taken under white light.

Recombinant protein expression of HIV-1 Env was successfully achieved using the transient transfection protocol, albeit to varying degrees of success, as observed by the low signal obtained for the CH505 Env w53 and w78 compared to FVgp140 (Figure 3.4). It is unclear whether this difference in observed expression is a result of inefficiencies in the expression of the selected CH505 constructs or the Western blot detection (detection of the FVgp140 Env would be favoured using anti-FVgp140 rabbit sera over the detection of the CH505 Env sequences) method, or a combination thereof. To explore the sensitivity of the SDS-PAGE and Western blot procedure further, the unpurified, transiently transfected tissue culture FVgp140 and CH505-w78 supernatant samples were resolved and Env detected using three different primary antibodies.

Selected primary antibody sources included HIV+ human patient sera (obtained from the South African National Blood Service, Johannesburg) and two, linear-epitope recognizing, bNAbs 10E08 (which recognizes an epitope which overlaps the 4E10 epitope) [172] and 4E10 (Figure 3.1)[179]. Bound primary antibody was detected using an anti-human secondary HRP-linked antibody. All three primary antibody sources detected the FVgp140 Env in transient transfection control sample, with a clear band observed, corresponding to 140 kDa (Figure 3.5). In contrast, no HIV-1 Env was detected in the CH505w78 culture supernatant samples, using the HIV-1+ positive patient sera, the 10E08, or 4E10 antibodies (Figure 3.5) despite the presence of the 4E10 epitope in the predicted amino acid sequences (Figure 3.1).

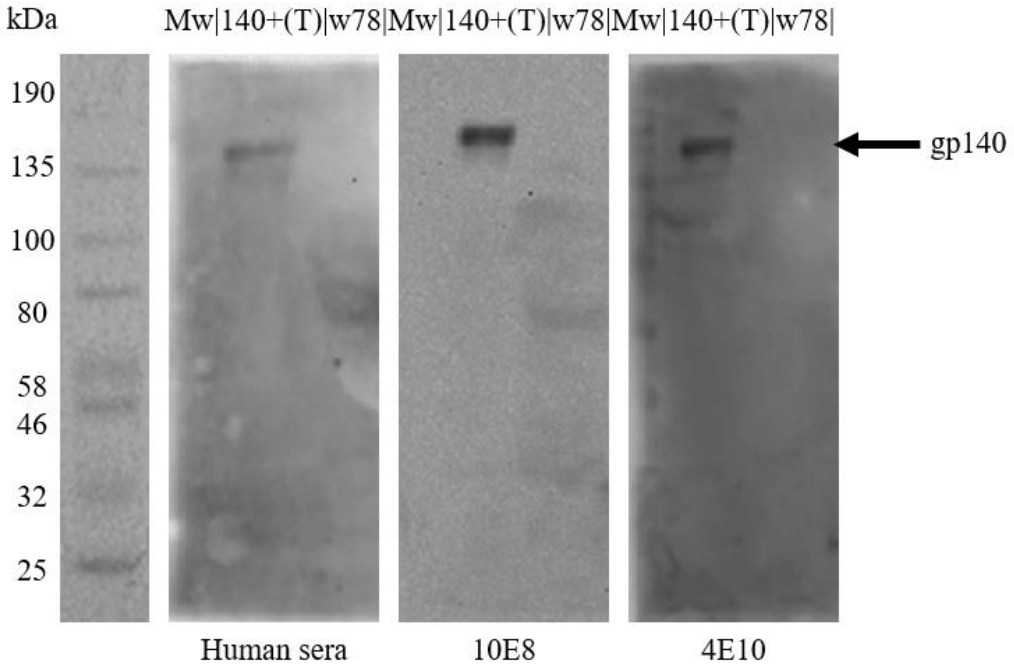


Figure 3.5: Western Blot analysis of FVgp140 and CH505gp140w78 envelope glycoproteins. Following transient transfections of HEK293 T cells, unpurified cell culture supernatants were analysed via Western blot. Protein expression was confirmed by probing for Env using 10E8, 4E10, or HIV-1 positive patient sera as a primary antibody (diluted 1: 1 000). Subsequent detection of primary antibody was done using a horse radish peroxidase (HRP)-conjugated anti-human secondary antibody (diluted 1: 2 000). Mw- prestained protein marker, broad range (New England Biolabs® Inc., MA, USA) and corresponding bands are indicated on the left in kilodaltons (kDa). Photograph of the pre-stained molecular weight standard on nitrocellulose membrane taken under white light.

Based on the varying detection levels of FVgp140 between the primary antibody sources used, the 10E8 antibody was shown to be the most sensitive of the primary antibodies evaluated in the Western blots. Combined, these data suggest that the expression of the CH505 Env constructs may be reduced relative to the FVgp140 control and bordering on the detection limit of our Western blot assay. To this end, we performed an ELISA protocol that showed enhanced sensitivity over the Western blot technique, thus confirming the presence of 4 of the 5 expressed CH505 Envs (w20, w30, w53, w78) while also providing semi-quantitative data regarding Env concentration in the culture supernatant samples.

3.3.2) Enzyme-linked immunosorbent assay (ELISA) for the detection of recombinantly expressed CH505-Envs

Following the detection/ expression challenges noted above, the transient transfections were scaled-up accordingly. Approximately 300 ml of culture supernatant was harvested from transiently transfected HEK293 T cells, followed by clarification via centrifugation and filtration. To confirm Env protein expression and estimate recombinant Env protein concentrations in the unpurified culture supernatants, an indirect ELISA was performed. A standard curve was constructed from the purified FVgp140 protein and used to infer the relative CH505 Env concentrations in the unpurified, CH505 Env containing supernatants. HIV-1 Env was captured using immobilized *G. nivalis* lectin and bound Env probed using the CD4 directed bNAb VRC01 [206] and subsequent primary antibody detection using an HRP-conjugated, anti-human secondary antibody. Wells containing no Env were used as a negative control (blank), and all culture supernatant samples were assayed in duplicate. The inferred CH505 Env concentrations in the unpurified culture supernatants are shown in Table 3.1 and represent the average of the duplicate samples tested.

The CH505-Env w20-w78 proteins were successfully detected using this ELISA protocol, and estimated concentrations were greater than 100 ng/ ml (average concentration = 298.5 ng/ ml), however, concentrations varied considerably between the different CH505 constructs evaluated (Table 3.1). The CH505-w4 construct produced far lower yields of protein (14.6 ng/ ml), than the other constructs tested. Corresponding large-scale transfections for the FVgp140 were not carried out, as the purified stock was available for testing.

In an attempt to improve the expression levels of CH505-w4 Env, the CH505-w4 Env was sub-cloned into the pcDNA3.1 expression vector (CH505-w4 in pcDNA3.1). Given the successful expression of the FVgp140 from the pcDNA3.1 backbone vector, we hypothesised that a substitution of the backbone expression vector for w4, from pcDNA3.3 to pcDNA3.1, may improve expression levels. Small-scale, transient mammalian cell transfections were repeated using the newly sub-cloned CH505-w4 construct in the pcDNA3.1 backbone (w4 in pcDNA3.1) and Env protein expression levels compared to the existing CH505-w4 construct (w4 in pCDNA3.3) and to the FVgp140 (FV in pcDNA3.1) using the ELISA protocol described above. Unpurified, culture supernatants were assayed in triplicate and a change in the expression vector, from pcDNA3.3 to pcDNA 3.1, did not increase the Env expression levels of the CH505-w4 construct, yielding 0.80 ng/ m and 0.65 ng/ ml respectively (Table 3.1). The CH505-w4 construct failed to express at practical levels, despite correct bands observed during

restriction digest screening of the pcDN3.3 constructs. (Figure 3.3). Sanger sequencing was performed, with coverage for the full CH505-w4gp140 transgene (see Appendix A, Supplementary Figure 1B), however, no changes in the sequence were observed that would account for the poor expression levels.

We proceeded to purify the other 4 recombinantly expressed Envs (CH505 w20-w78), however due to the low levels of w4 protein obtained subsequent characterization and analysis of this construct could not be performed.

Table 3.1: Recombinantly expressed CH505-Env detection and concentration estimation via indirect ELISA using the VRC01 primary antibody.

Expression vector used	Protein expressed	Concentration (ng/ mL)	Large- or small-scale transfection
pcDNA3.3	CH505-w4gp140	14,6	Large*
pcDNA3.3	CH505-w20gp140	515,1	Large*
pcDNA3.3	CH505w30gp140	227,7	Large*
pcDNA3.3	CH505w53gp140	132,1	Large*
pcDNA3.3	CH505w78gp140	319,2	Large*
pcDNA3.3	CH505-w4gp140	0,8	Small**
pcDNA3.1	CH505-w4gp140	0,65	Small**
pcDNA3.1	FVgp140	420,2	Small**

* Transfections in T175 flasks, 5 flasks per construct.

**Transfections in T25 flasks, 1 flask per construct.

3.3.3) HIV-1 Env glycoprotein purification

To confirm recombinant protein expression, the w20-w78 Envs glycoproteins were purified from the culture supernatant by *G. nivalis* lectin-affinity chromatography, and concentrated to minimal volume using the Amicon, centrifugation concentrator unit. Total protein concentration for each Env was quantified and used to standardise the loading of SDS-PAGE gels. Analysis of the CH505 purified Envs was performed using SDS-PAGE and Western blot

(Figure 3.6; 4 µg and 2 µg of protein resolved respectively). The CH505 Envs were successfully purified using lectin affinity chromatography, as indicated by the migration of the 140 kDa protein band (compared to the FVgp140 positive control used, Figure 3.6A and B). This 140 kDa protein was confirmed to be HIV-1 Env using the 10E8 primary antibody (Figure 3.6B, Western blot). The SDS-PAGE shows that there was partial cleavage of the gp140 into the gp120 component by the endogenous furin enzyme for all constructs as indicated by the arrow in Figure 3.6 A (lower arrow on the right). However, detection of the gp41 external domain could not be confirmed by SDS PAGE. Western Blotting using the 10E08 antibody confirmed the presence of the gp140 and the suspected gp41 external domain + GNC4 motif for FV, w20 and w78 constructs. As the presence of the gp41 band could not be definitively proven it was not indicated on the figure (Figure 3B). Following confirmation of these purified proteins, functional assessment was performed by ELISA.

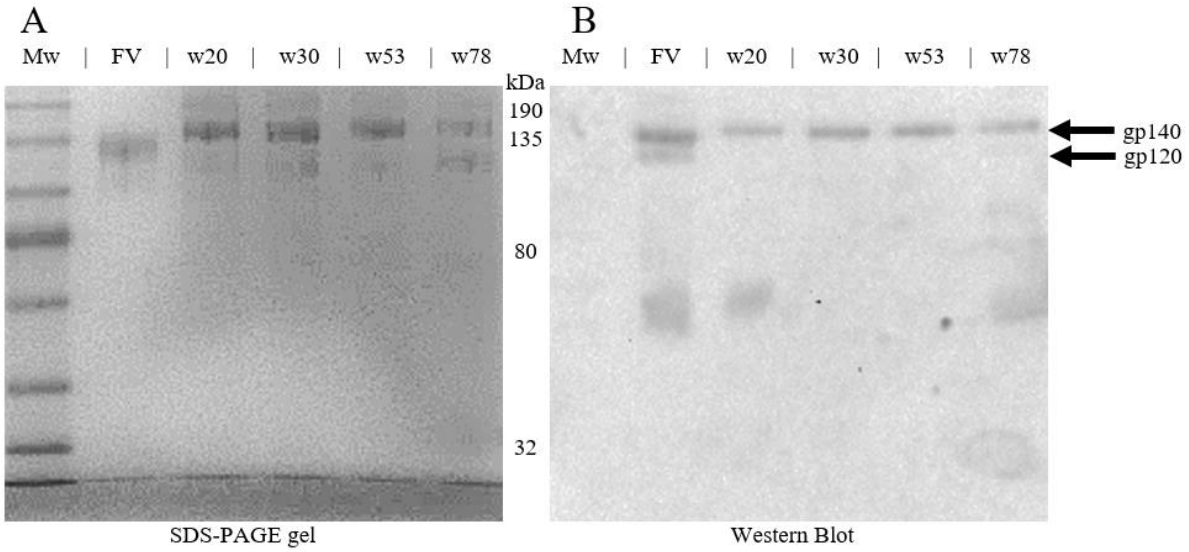


Figure 3.6: SDS-PAGE (A) and Western Blot (B) analysis of *G. nivalis* lectin-affinity purified FVgp140 and CH505gp140 envelope glycoproteins. Following transient transfections in HEK293 T cells, culture supernatant was clarified via centrifugation and filtered through a 0.45 µm filter membrane. **(A) SDS-PAGE: 4** µg of protein loaded on an 8% SDS-PAGE gel and visualised with Coomassie staining. Mw- prestained protein marker, broad range (New England Biolabs® Inc., MA, USA) and corresponding bands are indicated on the left in kilodaltons (kDa). **(B) Western blot**: Protein expression was confirmed by probing for Env (2 µg of protein loaded) using the 10E8 primary antibody (diluted 1: 1 000). Subsequent detection with a horse radish peroxidase (HRP)-conjugated anti-human secondary antibody (diluted 1: 2 000).

3.3.4) Biochemical characterization of purified recombinant Envs via ELISAs

Following SDS-PAGE and Western blot analysis, the antigenicity and functionality of the purified Envs was confirmed via ELISAs, using a panel of bNAb targeting the CD4-bs (Figure

3.7) and the ability of Env to bind to CD4 (domain 1 CD4 – 1dCD4) and induce the native CD4 induced(i)-17b epitope (Figure 3.8).

CD4bs- ELISAs

The HIV-1 Envs were captured using immobilized *G. nivalis* lectin and bound Env probed using a concentration of 1 µg/mL (b12, VRC01, and 3BNC117) or 0.1 µg/mL (NIH45-46) of the indicated primary bNAb and subsequent primary antibody detected using an HRP-conjugated, anti-human secondary antibody. Wells containing no primary antibody and wells containing no Env were used as negative controls. The relative binding of the antibodies to decreasing concentrations of Env (5 000 – 2.29 ng/ ml) are shown in Figure 3.7 and represent the average of the duplicate samples tested.

The IgG1b12 antibody bound well to all the Envs (FVgp140 and CH505 Envs w20-w78) in a dose dependant manner (Figure 3.7, orange dotted line), indicating that this epitope is intact and consistent between all constructs (although w20 shows a reduced maximum absorbance at the highest concentration relative to the other constructs).

For the FVgp140 (Figure 3.7E), the other antibodies bound in a similar fashion, with NIH45-46 binding the best (blue line), followed by 3BNC117 (green line), and lastly VRC01 (red line). However, these three antibodies showed decreased binding to the CH505 Envs relative to the FVgp140 control (compare Figure 3.7 A, B, C, D to Figure 3.7E). Binding of VRC01 to the CH505 Envs was far lower than compared to the FVgp140 control, and fairly consistent between progressive timepoints (Figure 3.7 red line). Interestingly, binding levels of the 3BNC117 and NIH45-46 antibodies decreased relative to evolving Env sequence. Most notably NIH45-46 binding was reduced between w20-w30 (Figure 3.7A and B, blue line) whereas decreasing binding of 3BNC117 was observed over the three-time points, w20, w30 and w53 (Figure 3.7 A, B, C green line). Overall w78 showed the lowest binding to 3BNC117 and NIH45-46 (Figure 3.7D green and blue lines respectively). This result suggests alteration of these specific epitopes over time or an increase in steric occlusion of these epitopes.

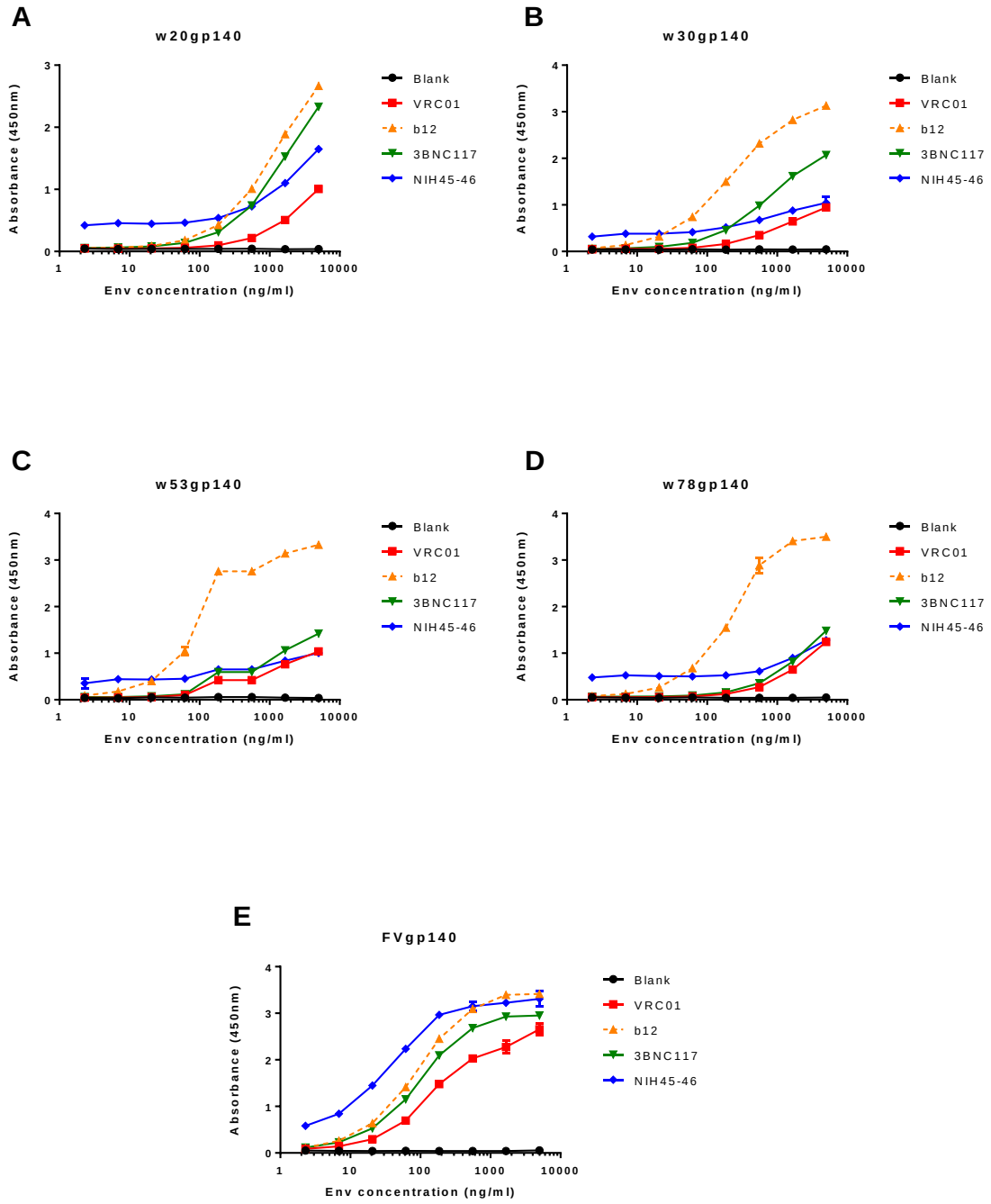


Figure 3.7: Indirect ELISA showing the antigenicity and functionality of the purified FV and CH505-Envs. The interaction of decreasing concentrations (5 000 – 2.29 ng/ µL) of the purified Env glycoproteins with various antibodies (b12 (IgG1b12) = orange line; VRC01 = red line; 3BNC117 = green line; NIH45-46 = blue line; no primary antibody = black line) was analysed via standard indirect ELISA. Each well was tested in duplicate to obtain an average absorbance and standard deviation was used to calculate error bars. The bound antibodies were detected using an HRP-conjugated, anti-human IgG antibody and established TMB/ stop solution chromogenic methods. (A) the w20gp140 Env, (B) the w30gp140 Env, (C) the w53gp140 Env, (D) the w78gp140 Env, and (E) the FVgp140 Env.

17b/ 1dCD4 ELISA

To further confirm CD4 binding functionality, the Envs were assayed using the CD4i/17bELISA, which preferentially detects the CD4 bound, Env conformation. Either Env alone, or Env that had been complexed with 1dCD4 were captured using immobilized *G. nivalis* lectin. Bound Env or Env/1dCD4 complex was probed using a concentration of 1 µg/mL of the 17b primary antibody. Subsequent primary antibody was detected using an HRP-conjugated, anti-human secondary antibody. Wells containing Env, but not probed with primary antibody and wells containing no Env were used as negative controls. In addition, HIV-1 subtype B BaL gp120 was included as a positive control. The relative binding of the 17b antibody to decreasing concentrations of Env (5 000 – 2.29 ng/ ml) or Env/1dCD4 complex (final concentrations 5 000 – 2.29 ng/ ml for Env; 1 µg/ ml for 1dCD4) are shown in Figure 3.8 and represent the average of the duplicate samples tested.

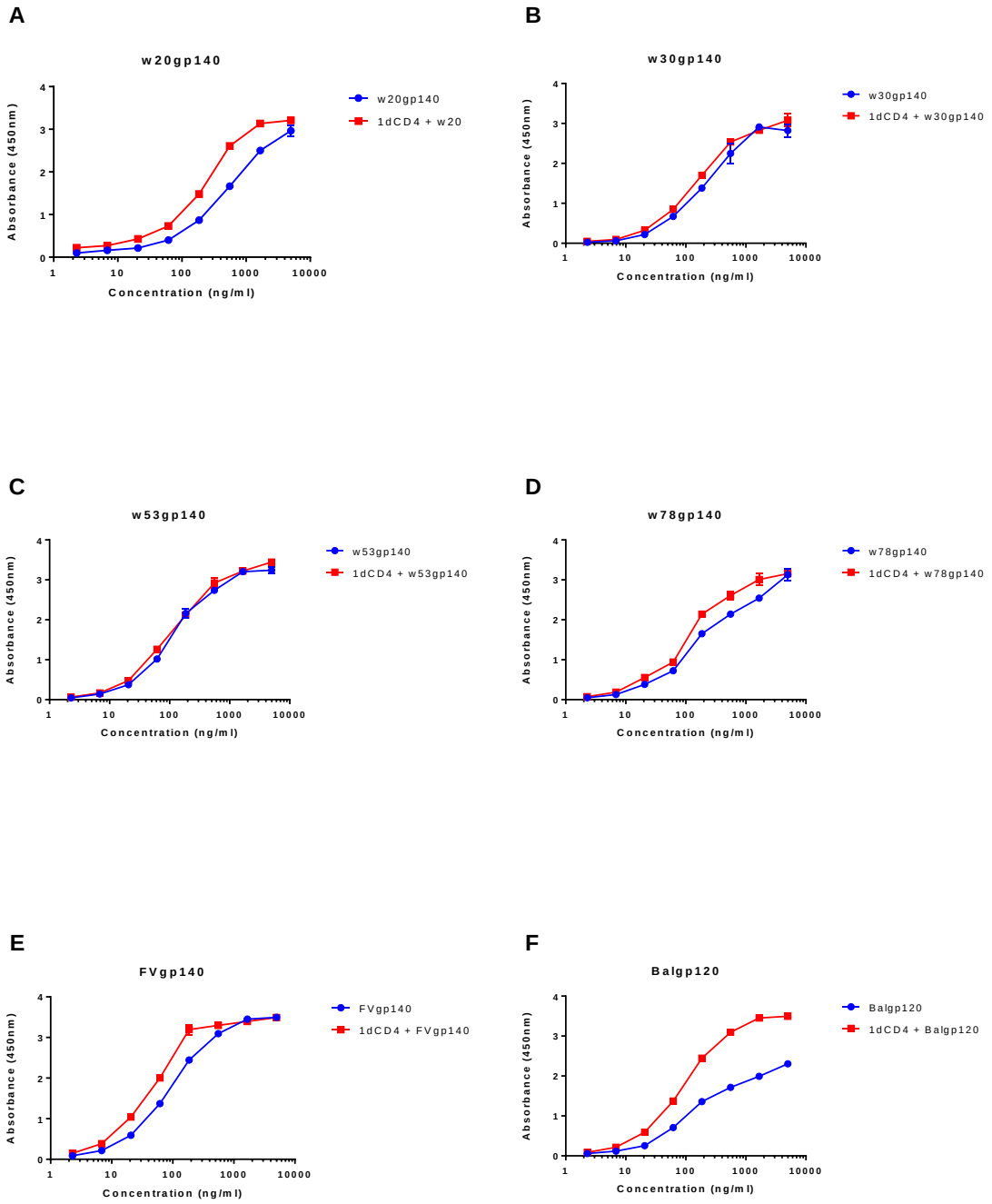


Figure 3.8: **CD4i/17b binding ELISA evaluating the conformational integrity and CD4 binding functionality of the purified FV and CH505-Envs**. The 1dCD4-liganded Env (red) or Env alone (blue) were probed with the 17b antibody, and detected using an HRP-conjugated, anti-human IgG antibody and established TMB/ stop solution chromogenic methods. Each well was tested in duplicate to obtain an average absorbance and standard deviation was used to calculate error bars. (A) w20gp140 Env, (B) w30gp140 Env, (C) w53gp140 Env the, (D) the w78gp140 Env, (E) the FVgp140 Env and (F) the Balgp120 Env.

The BaL gp120 positive control Env shows that 17b binding to the Env/1dCD4 complex was enhanced relative to the Env alone (Figure 3.8F compare red and blue lines). Indicating that the BaL gp120 bound the 1dCD4 and underwent conformational change leading to increased exposure of the 17b epitope.

The 17b antibody bound well to the FVgp140 and CH505 Envs alone (Figure 3.8A-E, CH505w20, w30, w53, w78, and FVgp140 respectively; blue lines), with only a moderate enhancement noted when Envs were complexed to 1dCD4 (Figure 3.8A-E, red lines). This suggests that the 17b epitope is constitutively accessible and does not require CD4 induction on the subtype C Env's tested (FVgp140 and CH505 Env sequences). However, these results were unable to verify CD4 binding functionality of the CH505 Envs, yet the antigenicity of the CD4bs was confirmed albeit at lower levels to the FVgp140 control.

Recombinant AAV (rAAV) production

3.4) Restriction sub-cloning of the CH505 inserts into the pAAV backbone

To generate rAAVs containing the CH505 Env transgene sequences, the Env sequences described in section 2.3 and 3.1 were sub-cloned using restriction digests protocols into the pAAV backbone (see Appendix A, Supplementary Figure 1B, D, F, H, and J). The pAAV-GFP was available in our laboratory (see section 3.5 below; Appendix A, Supplementary Figure 4), but the pAAV-CH505 constructs needed to be constructed by restriction cloning into the pAAV-Luc backbone vector (see Appendix A, Supplementary Figure 3). Before cloning procedures could commence, a restriction enzyme digest analysis was performed to check the integrity of the inverted terminal repeats of the pAAV- Luc backbone vector, as these regions are critical for rAAV production (see Appendix A, Supplementary Figure 7).

Following the preparation of the backbone (pAAV-Luc) and *env* gene inserts (w*n*gp140), sub-cloning was performed via DNA ligation (see Methods, section 2.6) and transformed into *E. coli* SURE2 cells. Several colonies were screened using restriction enzyme digests for the presence of the CH505 Env sequences using *Bam*HI and *Not*I restriction enzymes, and the integrity of the ITR regions for each construct confirmed by *Sma*I digests (results not shown). Positive clones, containing the respective CH505 Env transgene and intact ITR regions were re-transformed into *E. coli* SURE2 cells and large-scale plasmid isolation performed according to the optimised chloramphenicol protocol for pAAV plasmids (see Methods, section 2.6.6).

Isolated pAAV-CH505 plasmids were rescreened to confirm the presence of the CH505 Env transgene and ITR integrity (Figure 3.9A and B respectively).

The pAAV-CH505 plasmids were screened for the presence of the HIV-1 Env transgene by excision of the transgene using *Bam*HI and *Not*I double digests. Undigested and single *Bam*HI digests were included as appropriate controls (Figure 3.9A).

For the *Bam*HI single digest, the linearized vectors resolved at 6 200 bp (expected sizes of 6 264, 6 294, 6 294, 6 294, and 6 312 bp for w4, w20, w30, w53, and w78 respectively). For the *Bam*HI and *Not*I double digest bands, the backbone pAAV expression vector resolved at 4 200 and the HIV-1 CH505 Env genes at approximately 2 200 bp (expected sizes of 4 173 bp [for the first band, all 5 constructs]; and 2 091, 2 121, 2 121, 2 121, and 2 139 bp for w4, w20, w30, w53, and w78, respectively (as observed in Figure 3.3)).

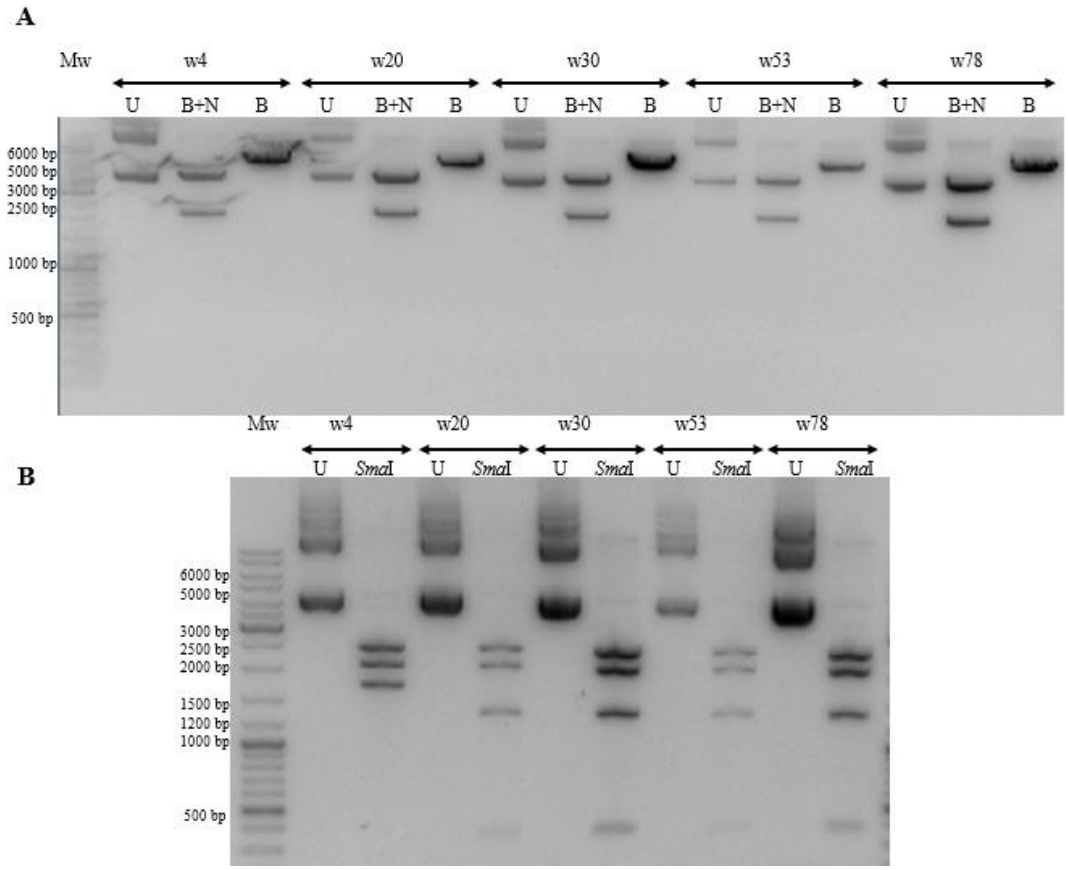


Figure 3.9: Restriction enzyme digest analysis of the pAAV-CH505 w*n*gp140 cis-expression vectors. All DNA samples were resolved on a 1% agarose gel and visualised under UV light. The undigested DNA (U) was run as a negative control. **(A)** All 5 plasmids were digested with *Bam*HI (B) restriction enzyme); and *Bam*HI and *Not*I (B+N) restriction enzymes. **(B)** All 5 plasmids were digested with *Sma*I restriction enzyme to check ITR integrity. w4-w78 corresponds to the CH505 week Env described previously. Mw corresponds to the O'Gene Ruler DNA ladder (Thermo Fisher Scientific, Waltham, MA, USA) used; bands are indicated on the left in base pairs (bp).

The ITRs for each pAAV CH505 construct was confirmed by *Sma*I digest. Undigested plasmid was included as negative digest control (Figure 3.9B). As there are 2 *Sma*I sites in each ITR, digestion with this enzyme will result in a common banding pattern (of approximately 2 500, 2 100, 11, and 11 bp fragments; see Appendix A, Supplementary Figure 1 for plasmid map schematics and position of these restriction sites in the ITR structures). The top two bands for each construct in Figure 3.9B represent the first two fragments, and the 11 bp fragments are not visible on the gel. Additional *Sma*I restriction sites may produce alternate bands, as seen above. The pAAV-w4 construct contained 1 extra *Sma*I restriction site in the w4 Env transgene (at 2 516 bp, see Appendix A, Supplementary Figure 1B); whereas the other pAAV-CH505

constructs contained 2 extra *Sma*I restriction sites in the respective transgenes (for positions see Appendix A, Supplementary Figure 1D, F, H, and J).

For the *Sma*I digest of w4, bands were observed at 2 500, 2 100, and 1 700 bp (expected sizes of 2 437, 2 092, 1 713, 11, and 11 bp) (Figure 3.9B, lane 3). For the *Sma*I digests of the other 4 constructs (w20- w78) bands were observed at 2 500, 2 100, and 1 400 bp (expected sizes of 2 462, 2 458, 2 455, 2 467 bp for the first band respectively; 2 092 and 1 353 bp for the second and third bands each) (Figure 3.9B, lanes 5, 7, 9, 11).

These successful restriction enzyme digests (Figure 3.9) confirm the plasmid integrity and that the transgenes of interest (CH505 Env w4, w20, w30, w53, and w78) are present. Importantly the plasmid amplification protocol used for large-scale plasmid isolations retained ITR integrity as confirmed by the *Sma*I restriction enzyme digest. These pAAV-CH505 env constructs were subsequently used for rAAV production.

3.5) Isolation and purification of pAAV-GFP reporter, rep/cap and adenohelper plasmids for large-scale recombinant rAAV production.

The pAAV-GFP, Adenohelper, and the rep/cap plasmids, were replicated and isolated using the optimised chloramphenicol procedure described in section 2.7.4. Isolated plasmids samples were subjected to restriction enzyme digests specific for each plasmid, to confirm integrity, and an undigested plasmid control was included as appropriate negative control (Figure 3.10).

The pAAV-GFP plasmid, used to generate a GFP reporter rAAV was digested with *Bam*HI to check plasmid size, or *Sma*I to check ITR integrity (see Appendix A, Supplementary Figure 4; for plasmid map schematics and position of relevant restriction sites). The *Bam*HI linearized pAAV-GFP plasmid resolved at approximately 5 600 bp, corresponding to the expected size of 5 582 bp (Figure 3.10, lane 4). *Sma*I restricted fragments were observed at 2 700, 1 400, 1 100, and 369 bp (expected sizes 2 680, 1 383, 1 101, 396, 11, 11 bp) consistent with ITR regions required for efficient packaging of the GFP transgene in to the rAAV capsid (Figure 3.10, lane 3).

Single restriction enzyme digests using *Xho*I or *Bam*HI was used to verify the Adenohelper plasmid (pHelper; see Appendix A, Supplementary Figure 6; for plasmid map schematics and position of relevant restriction sites). The *Xho*I single digest linearized the vector with a single

band observed at > 10 000 bp (expected size 11 635 bp; Figure 3.10, lane 6). The pHelper plasmid contains two *Bam*HI restriction sites and following restriction enzyme digest with *Bam*HI produced the expected fragments of approximately 9 000 and 2 600 bp (precise fragment sizes 9 022 and 2 613 bp; Figure 3.10, lane 7).

The Rep/Cap serotype 2 plasmid (rep/cap2; see Appendix A, Supplementary Figure 5; for plasmid map schematics and position of relevant restriction sites), was verified by single restriction enzyme digest using *Bam*HI or *Nco*I. The *Bam*HI linearized the rep/cap2 plasmid as expected producing a single DNA fragment that resolved at approximately 7 400bp (expected size 7 313 bp; Figure 3.10, lane 10). The *Nco*I restriction digest of rep/cap2 plasmid produced two DNA fragments that resolved at approximately 4 200 and 3 100 bp respectively. This is consistent with the plasmid map, that indicates the position of two *Nco*I sites that should generate fragments of 4 172 and 3 141 bp (Figure 3.10, lane 9).

These successful restriction enzyme digests confirmed the plasmid integrity of the pAAV-GFP, pHelper and rep/cap2 plasmids and that they can be used for subsequent rAAV production.

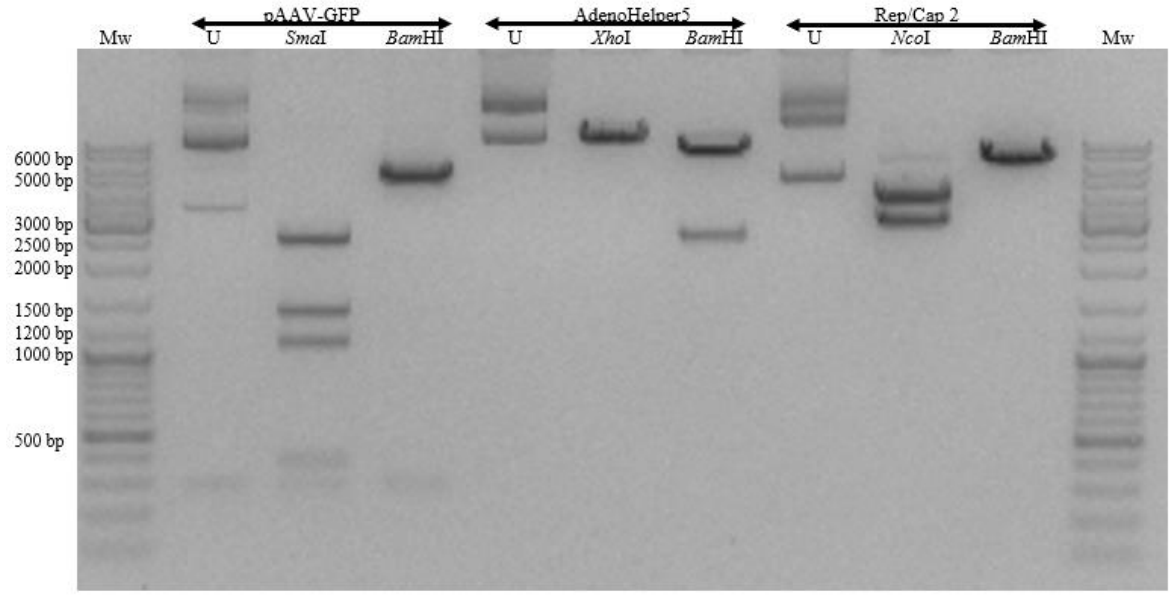


Figure 3.10: Restriction enzyme digest analysis of the pAAV-GFP, AdenoHelper5 (pHelper), and Rep/Cap2 expression vectors. Restriction DNA fragments were resolved on a 1% agarose gel and visualised under UV light. Undigested DNA was included as a negative control. Mw corresponds to the O'Gene Ruler DNA ladder (Thermo Fisher Scientific, Waltham, MA, USA) used; bands are indicated on the left in base pairs (bp).

3.6) rAAV Production and Isolation

The rAAVs were successfully produced using a PEImax-based triple transfection method of HEK293 T cells, followed by purification via iodixanol gradient centrifugation [270, 271] (Figure 3.11).

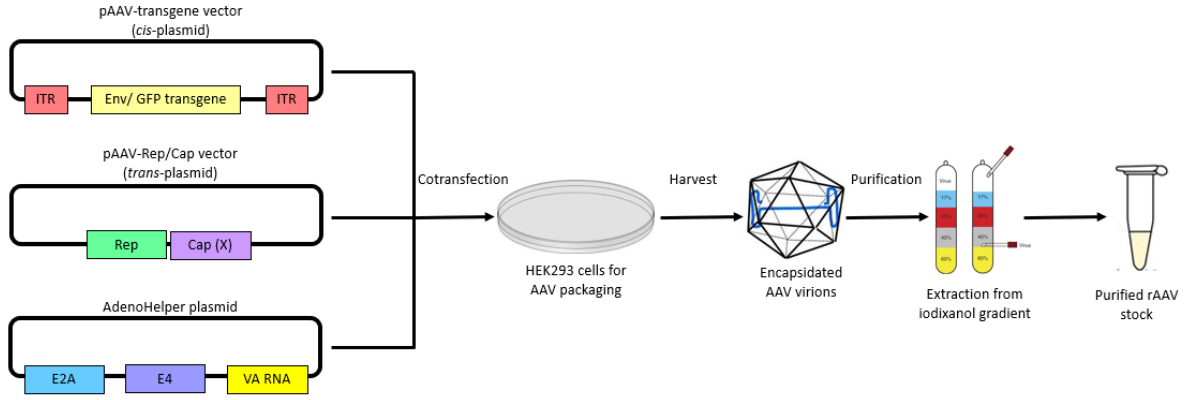


Figure 3.11: **Schematic representation of large-scale rAAV large-scale vector production and isolation.** The "helper-free" method is based on the adenovirus-free transient transfection of HEK293 T cells. This triple plasmid transfection procedure comprises (i) the *cis*-plasmid containing the AAV serotype 2 ITRs flanking the transgene of interest; (ii) the *trans*-plasmid containing the AAV serotype 2 replication (rep) and capsid (cap) genes; and (iii) the adenohelper plasmid that provides helper genes isolated from adenovirus. Following transfection, the rAAV virions are harvested, and purified via iodixanol gradient centrifugation.

Using this established method, the CH505 Env or GFP transgenes (from the *cis*-plasmid) were packaged into serotype 2 rAAV vectors (the *trans*-plasmid) (Figure 3.11). The inclusion of rAAV-GFP was for use as a positive control to assess transfection efficiency during the production of the rAAV (visual inspection of GFP expressing HEK293 T cells during the transfection), as well as for use as a positive control during downstream quantification and confirmation of infectivity (packaged rAAV-GFP). The rAAVs were harvested from the cells and the culture supernatant to maximise rAAV yields, and fractions were combined and purified through the iodixanol gradient centrifugation.

Following the purification via ultracentrifugation, the encapsidated AAV virions (packaged virions containing the transgene of interest) were extracted from the 40% iodixanol gradient (shown in grey, Figure 3.11) and stored at -80 ˚C. The final purified rAAV stocks were quantified by ddPCR before transduction studies could be performed.

3.7) Droplet Digital Polymerase Chain Reaction (ddPCR) quantification of rAAVs

All rAAV stocks obtained in 3.6 were titered using ddPCR. For the rAAV-GFP (positive control) two primer-probe sets were used, (i) one specific for the SV40 poly (A) sequence; and for comparison (ii) one specific for the GFP transgene. The SV40 primer-probe set was used for quantification of the other rAAV vectors containing CH505 HIV-1 env transgenes, as these sequences all share the SV40 poly A sequence in common (see Appendix A, Supplementary Figure 1).

Table 3.2 shows the final rAAV titres obtained, during an experiment run in triplicate. The average genome titres were higher overall for isolated rAAV-GFP vector compared to those obtained for the 5 rAAV-CH505 vectors. The genome titres for the rAAV-GFP differed by approximately 1.0 $x10^{11}$ genome copies/ml between the two different primer sets used: genome titre of 2,96 x 10^{11} for the GFP primer set, and 1,91 x 10^{11} for the SV40 primer set (Table 3.2). A larger degree of variation was observed for the rAAV-CH505 viral titres, with the lowest viral titre obtained for rAAV-w30 (1,85 $x10^{10}$), and the highest viral titre for rAAV-w53 (6,27 x 10^{10}). The overall average genome titre obtained from the rAAV production was 1,04 x 10^{11}. These quantified viral titres were used to inform optimization of *in vitro* transduction assay studies.

Table 3.2: ddPCR quantification of final rAAV yields, in average genome copies per ml (GC/ ml).

rAAV name	Description	Primer set used for detection	Viral titre in genome copies/ ml (GC/ ml)
rAAV-GFP	AAV backbone containing the GFP transgene.	GFP set	$2{,}96 \times 10^{11}$
rAAV-GFP	AAV backbone containing the GFP transgene.	SV40 set	$1{,}91 \times 10^{11}$
rAAV-w4gp140	AAV backbone containing the w4 gp140 Env transgene.	SV40 set	$3{,}51 \times 10^{10}$
rAAV-w20gp140	AAV backbone containing the w20 gp140 Env transgene.	SV40 set	$6{,}49 \times 10^{10}$
rAAV-w30gp140	AAV backbone containing the w30 gp140 Env transgene.	SV40 set	$1{,}85 \times 10^{10}$
rAAV-w53gp140	AAV backbone containing the w53 gp140 Env transgene.	SV40 set	$6{,}27 \times 10^{10}$
rAAV-w78gp140	AAV backbone containing the w78 gp140 Env transgene.	SV40 set	$5{,}85 \times 10^{10}$

3.8) rAAV Viral Transduction Assay of HEK293 T cells

3.8.1) *In vitro* optimization

The purified and quantified rAAVs functionality was evaluated by transduction assays performed by infection of HEK293 T cells. To determine the optimal MOI required for successful transduction, the purified rAAV-GFP was used as the positive control, at various MOIs, and GFP expression was monitored via fluorescence microscopy over 72 hours following infection (Figure 3.12; see Appendix A, Supplementary Figure 8 for corresponding bright field images).

Figure 3.12 shows GFP expression was detected at 24 hours post transduction, particularly at the higher MOIs of 100 000 and 50 000. Generally, GFP expression peaked at 72 hours post-transduction (Figure 3.12, last column), and an MOI of 100 000 inducing the greatest GFP expression (Figure 3.12, top row). An MOIs of 50 000 and 25 000 also showed relatively high levels of GFP expression, although it was overall not as effective, and took longer to reach sufficient levels, compared to an MOI of 100 000 (Figure 3.12, second and third rows). The rAAV-GFP was deemed to be functional and effective at transducing HEK293 T cells at an

MOI >25 000, which was used to inform transduction assays using the rAAV-CH505 Env vectors.

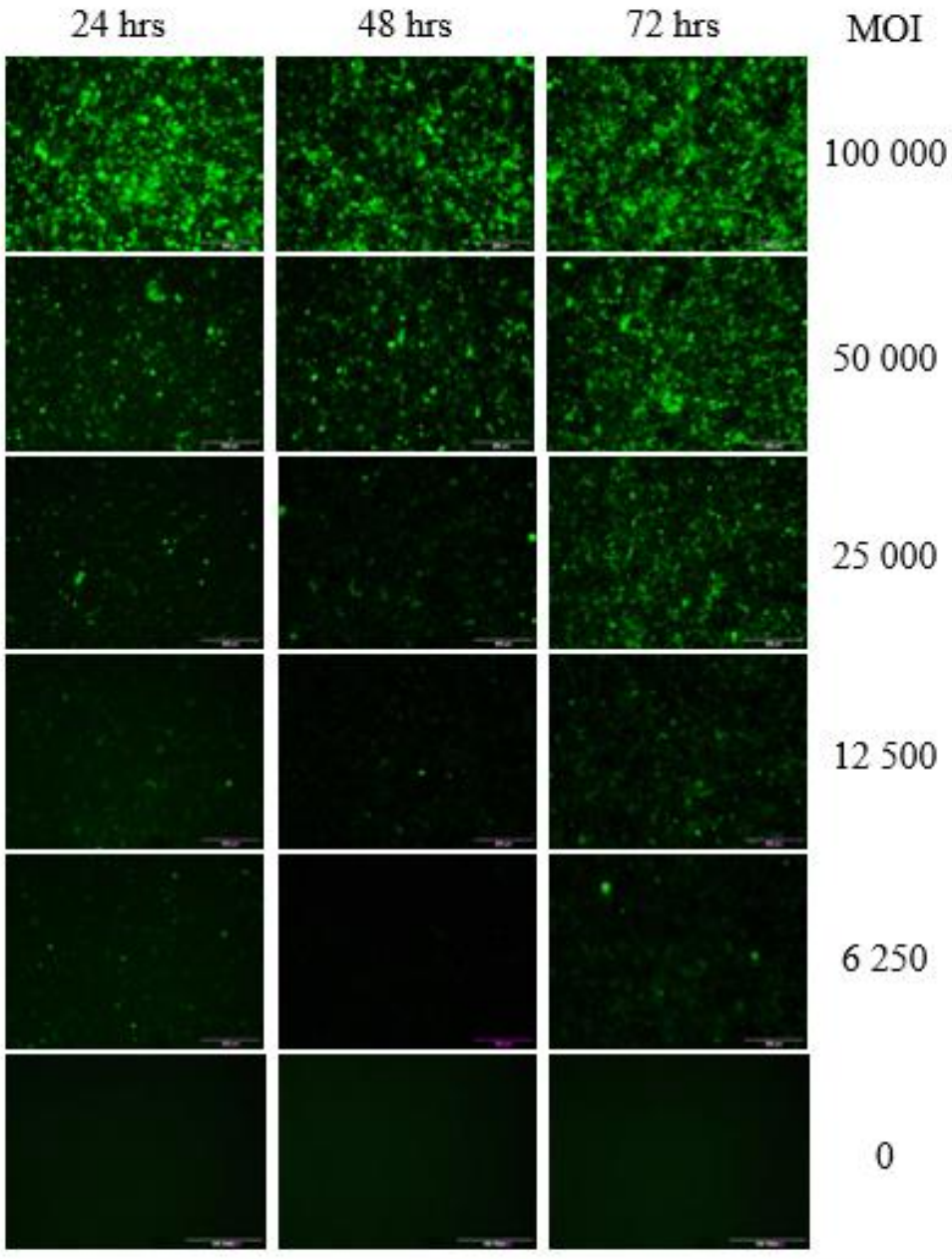


Figure 3.12: Relative transduction efficiency of the rAAV-GFP vector *in vitro*. HEK293 T cells were infected in duplicate at various MOIs (range 100 000 - 0). GFP expressed was monitored was fluorescent microscopy of infected HEK293 T cells: 24, 48, and 72 hours post-transduction (exposure time 2 000 ms). Magnification = 100x. Scale bar (lower right corners) = 200 µm.

3.8.2) Recombinant Env expression from *in vitro* rAAV-CH505 transduction studies

The purified and quantified rAAV vectors were then functionally evaluated by HEK293 T transduction assays and the recombinant expression of HIV-1 Env monitored by indirect

ELISA (Figure 3.13A and B respectively). Viral transductions were performed using the optimized MOI of 50 000 determined above.

The rAAV-GFP was used as a positive transduction control, by monitoring GFP expression levels using fluorescent microscopy for 8 days (Figure 3.13A, top panel). Observed GFP expression peaked at 8 days post-transduction (Figure 3.13A, top right box), and there was no further observation beyond this point due to over confluence of cells and media exhaustion.

The HIV-1 Envs were then captured using immobilized *G. nivalis* lectin and bound Env probed using a concentration of 1 µg/mL of the IgG1b12 primary antibody, as this antibody was determined to be the most sensitive at detecting the CH505 Envs (section 3.3.4). Subsequent primary antibody was detected using an HRP-conjugated, anti-human secondary antibody. Wells containing the cell control supernatant (non-transduced cells) and the rAAV-GFP transduced cell supernatant were used as negative controls. Concentrations were quantified relative to the purified FVgp140.

Figure 3.13B shows the relative Env expression levels over the indicated time period, and each point represents an average of the duplicate samples tested. As expected no HIV-1 Env expression was detection rAAV-GFP cell supernatant. (Figure 3.13, green dotted line). For the w20, w53, and w78 rAAV vectors, expression of the HIV-1 Envs was observed (Figure 3.13, pink, blue, and red lines respectively). Generally, expression of the Envs was low at 2 days post-transduction and increased over time (peak expression was observed between 6-8 days post-transduction). Average total protein expression was ~2095 ng/ ml, which was approximately 7 times higher than that observed for the matched recombinant Env expression noted in section 3.3.

For rAAV-w30, peak expression was observed at 2 days post-transduction (Figure 3.13, purple line), and decreased over time. This result was confirmed when the ELISA was repeated for this rAAV vector. There was no expression detected for the rAAV-w4 vector, which corresponds to the results obtained for the matched recombinant Env expression noted in section 3.3, indicating an issue with this construct.

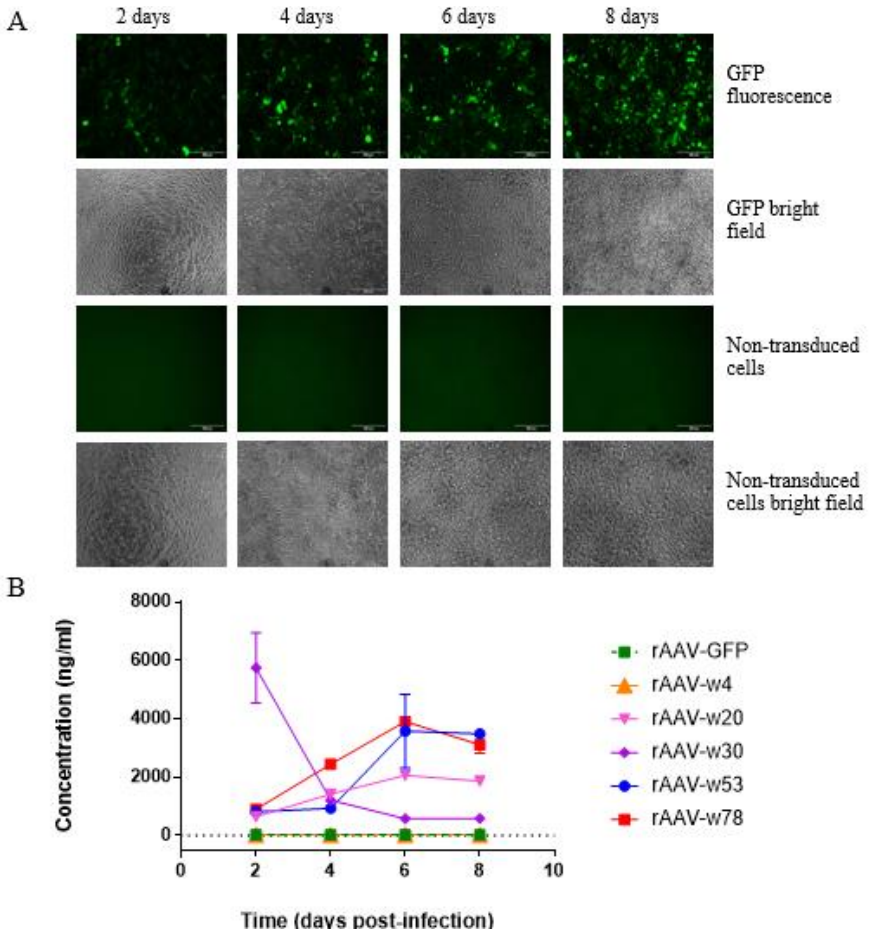


Figure 3.13: rAAV transduction and recombinant Env glycoprotein evaluation in HEK293 T cell line. HEK293 T cells were infected in duplicate at an MOI of 50 000 using the rAAV vectors. GFP expression from the rAAV-GFP vector was monitored by fluorescent microscopy at: 2, 4, 6, 8 days post-transduction (exposure time 2 000 ms). Supernatant was collected from all the assayed wells at the same time points and replaced with fresh media. Magnification = 100x. Scale bar (lower right corners) = 200 µm. **(A) Relative transduction efficiency of the rAAV-GFP vector *in vitro*.** GFP fluorescent and brightfield images for the cells transduced with the rAAV-GFP, and for the non-transduced (control) cells were taken at the indicated timepoints. **(B) ELISA showing the relative concentrations of rAAV vectors over 8 days.** The GFP and CH505-Env proteins produced from the respective rAAVs were tested for interaction with the IgG1b12 primary antibody. Each well was tested in duplicate to obtain an average absorbance and standard deviation was used to calculate error bars. The bound antibodies were detected using an HRP-conjugated, anti-human IgG antibody and established TMB/ stop solution chromogenic methods.

Taken together, these results indicate that the rAAV successfully expressed the HIV-1 Envs in HEK293 T cells.

Chapter 4: Discussion

One of the ultimate goals in the development of an effective HIV-1 prophylactic vaccine remains the ability to elicit a bNAb response following vaccination. As HIV-1 Env is the only virally-encoded protein on the virion surface, it remains the sole target for these bNAbs and thus the focus of HIV-1 subunit vaccines. However, the intrinsic challenges associated with Env based immunogens (such as the high sequence variability, shielding of critical epitopes by glycans, and other immune avoidance mechanisms) have thwarted the effective induction of bNAb responses with previous vaccine candidates. Moreover, it has become apparent that bNAbs naturally arise *in vivo* as a result of continuous antigenic stimulation that effectively drives the extensive affinity maturation and SHM of specific repertoires of naïve B-cells, required for their (bNAbs) development. Sequential immunization strategies provide a method of recapitulating this natural antibody-viral co-evolution observed *in vivo*. This strategy uses viral Env sequences as they have evolved during the course of infection, to prime naïve B-cells to produce UCA antibodies and guide their affinity maturation ultimately to produce bNAbs.

This dissertation describes the design, production, and characterization of recombinant AAV vectors, expressing sequentially derived-HIV-1 Env sequences, and the corresponding matched recombinant Env proteins, for potential use as a therapeutic/ preventative vaccine strategy.

4.1) Design and construction of HIV-1 Env constructs

4.1.1) Selection of sequentially derived HIV-1 Subtype C *env* constructs

As a result of the challenges associated with using HIV-1 Env as a vaccine immunogen (such as the extreme genetic variability of the Env), current research efforts are focused on identifying the most effective immunogens capable of eliciting a bNAb response [24, 275, 276]. Recent research analysing longitudinal viral and antibody sequence evolution in patients that develop a bNAb response indicates that the engagement of the naïve B-cells/ UCA bNAbs repertoires by HIV-1 Env is limited. Thus, the selection of an HIV-1 Env sequence capable of engaging the bNAbs repertoires, accompanied by the subsequent antigenic stimulation to mature response is fundamental in their development [103, 187, 215-218]. Sequential immunization strategies aim to replicate this natural bNAb evolution response by utilizing sequential Env sequences from these patients to recapitulate the bNAb development pathways observed [221-230]. Thus, Env sequence data available from these longitudinal studies may provide the relevant Env sequences to inform immunogen design needed to elicit bNAbs, when used in a sequential immunization vaccine strategy.

Here we describe the selection and construction of five consensus, sequential HIV-1 subtype C Env sequences, based on five key time points analysed during the longitudinal analysis of patient CH505, as described by Liao and colleagues [187]. The time points (and corresponding consensus sequences) were selected for the following reasons: (i) w4 was the transmitted founder virus sequence responsible for infection and likely for the initial engagement of the naïve B cell receptor of the CH103 bNAb lineage; (ii) w20 allowed for the development of autologous neutralization and heterologous neutralization against tier 1 pseudoviruses; (iii) w30 and w53 sequences correspond to the development of expanding heterologous neutralization, specifically tier 2 pseudoviruses; and (iv) w78 was likely responsible for the development of full neutralization breadth [187]. These findings are further supported by a study that found that the most effective Env sequences to use for improved neutralization breadth occur prior to, or simultaneously with, the development of approximately 50% neutralization breadth [223].

The five selected CH505 Env sequences were progressively longer when compared to the FVgp140 and HXBC reference genomes, specifically in the V1, V4, and V5 loop regions (Figure 3.1). This is attributed to the increased amino acid sequence diversity and insertions observed within these regions. Changes in the length of these variable loop regions are often associated with changes in the number and /or relative position of PNGS [277]. Progressive elongation of the V1 loop was noted over time (w4 – w78) and coincided with accumulation of PNGS, with only a single PNGS predicted in the w4 sequences compared to up to four PNGS predicted for w53 and w78 (Figure 3.1). Interestingly, the reverse was observed in the V4 loop structure where w4-w30 displayed the longest loop region and was subsequently shortened by 6 amino acids in the w53 and w78 Envs. This shortening also corresponded with a loss in PNGS (Figure 3.1). The relative position of PNGS altered over time, as one can observe a shift in the second PNGS in the V1 loop for w53 and w78, and in the V5 loop for w78. The elongation of the variable loop structure is consistent with immunological pressure and viral escape mechanisms, as reported by the authors [187].

As originally described by Liao and colleagues, Env diversification at key CD4 contact residues was noted overt time in direct response to the CD4bs-directed antibody pressure (CH103 lineage of antibodies). Several amino acid substitutions were noted in discontinuous CD4 contact residues, for the derived consensus sequences (Figure 3.1, red boxed regions) making up the CD4bs on gp120 [268, 278, 279]. Importantly, the critical residues remained conserved among all the sequences (Figure 3.1, red shaded residues), but the mutations seen

adjacent to these residues and within the contact regions, may have important bNAb binding effects.

Of particular interest, in the D loop CD4-bs region, an acidic amino acid changed to a non-polar (hydrophobic) aromatic amino acid (F283I) and a substitution of alanine at position 287 to valine, to glycine in later sequences was noted. In the CD4-bs regions on either site of the V4 loop, a non-polar amino acid changed to a polar amino acid (V379T); and a basic amino acid changed to an acidic amino acid (K436E). In the CD4-bs region adjacent to the V5 loop, a polar amino acid changed to a basic amino acid (N466K) or an acidic amino acid (N466E). This amino acid substitution resulted in a minor shift in the PNGS position, but most likely arose as a result of immunological pressure and corresponds with the amino acid position that is in direct contact with the CH103 antibody (amino side chain and main chain contacts) [187]. As these mutations can result in a significant difference in charge and/ or protein structure, they may have significant effects on the ability of certain bNAbs to bind to these Env sequences. In addition to these, the additional PNGS and other mutations elsewhere in the Env sequence may effect bNAb binding, as alanine-substitution analysis has demonstrated that mutations in seemingly unrelated residues may affect neutralization sensitivities [280]. This may be as a result of changes in the overall tertiary/quaternary structure of the targeted epitope, which may further enhance or shield their exposure. The major drawback in evaluating these unrelated contact residues is that they require experimental validation. While the significance of these mutations falls outside the scope of this study, it presents a future avenue of research.

Overall, the CH505 Env sequences demonstrated a large degree of conservation to each other, however noticeable differences were observed in the V1, V4 and V5 loop, most likely as a result of immunological pressure. As the patient (CH505) from which these HIV-1 Env sequences were derived, developed a bNAb (CH103) that was directed towards the CD4bs, it was expected that we would observe some changes in associated CD4 contact residues over time.

4.1.2) HIV-1 Subtype C CH505 *env* construct design

The native HIV-1 Env spike is a trimer of heterodimers, composed of the non-covalently linked gp120 and gp41 subunits [152]. Previous vaccine approaches have attempted to use non-native forms of Env such as monomeric gp120 [90, 281] for subunit vaccines, due to the relative ease of design and production, but these have shown a lack of protective immunogenicity in clinical studies [142, 282]. These studies have shown that monomeric gp120 typically elicits non-

neutralizing antibody responses towards epitopes that are generally not accessible or buried on the native spike. Additionally, several bNAbs (PG9, PG16, CAP256.VRC26, PGT 145) target a quaternary epitope on the V1/V2 crown of the native trimeric Env spike [180]. Therefore, in order to elicit effective bNAb responses, improved immunogen design is called for that more closely resembles the native Env spike structure.

The development of trimeric HIV-1 Env immunogens has thus focused on soluble gp140 derivatives [283-287], since the gp160 Env is a membrane bound structure. This gp140 Env is cleaved by furin (as for gp160) and includes the MPER site of gp41 but lacks the transmembrane domain of gp41. Of these gp140 based immunogens, the BG505-SOSIP is the most promising, producing fully cleaved native–like trimers with improved antigenic properties [288, 289]. To stabilize the cleaved gp120 and gp41 subunits, the SOSIP trimers contain an engineered intermolecular disulphide bond between the subunits (SOS) and the substitution of the isoleucine at position 559 to proline (IP).

Other approaches to generate stable trimeric gp140 Env immunogens include the addition of heterologous trimerization motifs, such as GCN4 transcription factor (GCN4) to the C terminal of the protein [256-258, 290, 291]; and the replacement of the native N-terminal signal peptide with the heterologous human CD5 antigen leader peptide [259, 260]. Although the GCN4 motif does not necessarily form the correct quaternary structure, it would not impact on the CD4bs epitope, and still provides an advantage as there is reduced exposure of the gp120 inner domain. Therefore, our Env design included both these features (Figures 3.1 and 3.2) which have been previously shown to generate trimeric Env conformations and facilitate the effective expression and secretion of Env, proteins respectively; in addition to an intact cleavage motif (REKR). Collectively, these features allow for native-like gp140 trimers to be produced.

4.2) Expression and purification of the matched CH505 recombinant Env

The pcDNA3.3 CH505 HIV-1 sequentially derived, consensus Env constructs were confirmed by restriction enzyme digests (Figure 3.3) These constructs and the FVgp140 sequence, were used to recombinantly express functional gp140 trimeric Env glycoproteins *in vitro*. Initial transient transfections failed to express the CH505 recombinant Env proteins as there was little to no signal observed at the expected molecular weight sizes following Western blot analysis (data not shown). There was evidence of the FVgp140 control Env being expressed initially, although limitations in detection were noted. The detection of FVgp140 did improve with

optimization of transfection and western blot procedures (Figure 3.4, 140(+)T). However, detection of the transiently expressed CH505 w53 and w78 remained low, relative to the FVgp140 control (Figure 3.4). This disparity in the detection of the different transiently expressed Envs (FVgp140 vs CH505 w53 and w78) may be attributed to the use of rabbit sera as primary antibody source to detect the transferred HIV-1 Envs. As this rabbit sera was obtained from a rabbit immunized with the FVgp140 immunogen [262], one would expected a greater sensitivity in detecting the autologous Env (FVgp120) compared to a heterologous Env sequence (CH505 w53 and 78). During further optimization, detection levels of the FVgp140 improved with the use of the 10E8 monoclonal antibody, compared to human sera and the 4E10 antibody (Figure 3.5). Unfortunately, this change in primary antibody source did not improve the sensitivity in the detection of the transiently expressed CH505 w78 Env (Figure 3.5) despite both protein constructs containing the 10E08 epitopes. A likely possibility was that there was a lower efficiency of expression with the CH505 Envs used when compared to the FV due to the inconsistencies noted in detection for multiple western blots (Figures 3.4 and 3.5, additional western blots not shown) and this was to be investigated further.

In order to address the suspected, lower efficiency in the expression of the CH505 Env proteins several optimizations were performed including the use of different mammalian cell lines recommended for protein expression (HEK293 F and HEK293 T), the use of different transfection reagents (PEI, Lipofectamine, PolyFect), altering the DNA plasmid to transfection reagent ratios and increasing plasmid overall DNA amounts used in the transfection protocol. Despite these optimization attempts, detection of the transiently expressed CH505 Env remained low by Western Blot (results not shown).

To improve detection sensitivity an in-house indirect ELISA protocol was optimised, and successfully used to detect four of the five CH505 Env glycoproteins (w20, w30, w53, and w78) in culture supernatant following transient transfection (Table 3.1). The expression levels of the w4 Env glycoprotein were considerably lower than expected (Table 3.1) and despite repeated attempts were not detectable on SDS-PAGE or Western blot (data not shown). Furthermore, despite the Env sequence being cloned into the pcDNA3.1 backbone (the same backbone as the FVgp140 Env which showed relatively high expression levels), there was no enhancement in expression of the CH505 w4 Env compared to the pcDNA3.3 expression vector backbone, as determined by the indirect-ELISA (Table 3.1, pCDNA3.3 CH505 w4 large-scale transfection and compare relative Env concentration achieved using the pcDNA3.1 and pcDNA3.3 for w4 in small scale transfection format). Sanger sequencing of the w4 plasmid

construct was performed to ensure that there were no premature stop codons present or interfering insertions and/or deletions that resulted in a frame shift mutation etc. (data not shown). The w4 construct showed 100% sequence identity to the GeneArt ordered construct, and bioinformatic translation of the DNA sequences verified the amino acid sequence to that shown in Figure 3.1, w4. It remains unclear as to the reason for the low levels of CH505 w4 expression, however we suspect that it must be related to the w4 construct sequence given the successful expression of the other CH505 Env constructs used in this study, and that a change in the expression vector did not result in an improvement. Unfortunately, in terms of a sequential immunization strategy, the w4 Env sequence is critical, as it was responsible for engaging the naïve B-cell and initiating the development of the CH103 bNAb lineage [187]. Thus, in terms of future work, it would be important to uncover the precise mechanism accounting for the low-level expression.

Having confirmed the successful expression of the CH505 Env w20-w78, they were successfully purified, to relative homogeny using the *G. nivalis* lectin affinity chromatography (Figure 3.6 A and B). The CH505 Envs were of expected size (140 kDa) as determined by SDS-PAGE. Despite the intact furin cleavage site (Figure 3.1), the SDS-PAGE gel shows that there was inefficient proteolytic cleavage of these four glycoproteins (Figure 3.6, w20 – w78 lanes as indicated), as there was only a very small fraction of the cleaved gp120 Env protein visible on the Coomassie stained SDS-APGE gel (Figure 3.6 A, band that resolved slightly lower than the gp140). The gp41 band may not have been visible due to presumed low concentrations. Despite the presence of the PNGS in the external domain of gp41 (Figure 3.1) the lectin affinity purification method may be inefficient in retaining the cleaved gp41 portion during the purification procedure, thus resulting in reduced detection by SDS-PAGE. Western blotting analysis carried out using the 10E8 primary antibody confirmed that the bands observed on the SDS-PAGE were indeed HIV-1 Env, and apart from the FVgp140 control (which detects the gp140 and suspected gp120 Env) showed A single band equivalent to ~140kDa (Figure 3.6 B). As the 10E8 epitope is located in the gp41 ectodomain, it confirms the migration position of gp140 on SDS-PAGE. This finding is consistent with previous results published by our group [247, 262] and the work of others [288, 292-294]. The work presented here indicates that there may be evidence of the cleaved gp41 ectodomain at approximately 58 kDa (Figure 3.6 B, lower bands). The calculated molecular weight of gp41 is 24 kDa (calculated using Compute pI/Mw [295-297]), but due to the presence of PNGS this may result in an increased the size to that noted in Figure 3.6B. As the 10E8 antibody is gp41 specific, it

does suggest that this band is gp41, however, precise identification of this band would require further investigation. This inefficient cleavage is due to incomplete processing of Env. This incomplete processing occurs as the furin proteases become saturated and are no longer able/available to cleave increased levels of Env, or because of the different processing pathways between transfected and non-transfected cells [36, 47-49]. The efficient cleavage of Env has been shown to impact the final quaternary structure of Env, the antigenicity and recognition by bNAbs [298-300]. This could be remedied by co-transfection of plasmid encoding furin protease [288] or by enhancement of furin recognition by replacing the native cleavage site sequence with six arginine residues (RRRRRR) [288, 301]. However, cleavage does not necessarily affect the CD4 response, hence why the gp140 GCN4 construct is suitable for these Envs and the immune response intended to be elicited.

While the trimeric conformation of the CH505 Envs was not confirmed in this current study, our group has previously shown the GCN4 motif efficiency forms "trimeric sized" conformation using the FVgp140 construct. This was determined by native PAGE and size exclusion chromatography [262]. However future work can verify the trimeric conformation of these CH505 Env sequences using the methodology described previously [262].

4.3) Antigenicity and functionality assessment of recombinantly expressed CH505 Envs

With the exception of the w4 Env, the CH505 purified Env proteins were characterised using two ELISA formats: one analysing the antigenicity of the Env CD4 bs using selected bNAbs targeting this site (Figure 3.7) and the 17b/CD4 ELISA to confirm binding to the native CD4 receptor and subsequently induction/exposure of the CD4i epitope targeted by the 17b antibody [268] (Figure 3.8). It is important for these Envs to be fully functional, to be able to bind CD4 and facilitate fusion, in order to fully mimic native-Envs; and to be immunogenic to initiate an effective immune response for downstream testing [302].

Our analysis showed that the FVgp140 Env bound to the CD4bs antibodies IgG1b12, VRC01, 3BNC117, and NIH45-46 G54W (a clonal variant of VRC01) (Figure 3.7E). As these antibodies all target the CD4bs conformational epitope, their ability to bind to the FVgp140 Env glycoprotein confirms that the CD4bs is conformationally intact and the Env has folded correctly. For the CH505 Env glycoproteins, only the IgG1b12 antibody bound as expected (Figure 3.7A-D, orange line). This indicates that the IgG1b12 epitope is intact and consistently exposed on the different CH505 Envs at the selected time points (w20-w78). However, a slight

reduction in the maximum binding activity was noted for w20 against IgG1b12 relative to the other CH505 Envs. (Figure 3.7 compare the orange line in A with B, C and D) between all the Envs tested. Interestingly, the other CD4bs bNAbs showed poor binding to the CH505 Envs (Figure 3.7, A-D). Furthermore, this data demonstrates a decrease in the binding of 3BNC117 and NIH45-46 relative to Env evolution, with w53 and w78 showing equivalent low-level binding of VRC01, 3BNC117 and NIH45-46 antibodies. The NIH45-46 antibody binding decreased from w20 to w30 and stabilized at this level for w53 and w78. This suggests that an alteration in the Env sequence between these two-time points (w20 and w30) affected critical residues targeted by this antibody, or perhaps unrelated mutations reduced the epitope accessibility. Similarly, 3BNC117 binding reduced in a more stepwise fashion, as indicated by a subsequent decrease in maximal binding from w20, to w30 before plateauing at w53. This suggest an accumulation of mutations in the Env sequence was required over time to reduce the binding of 3BNC117, again these could have been at critical contact residues or at unrelated sites that affect accessibility (Figure 3.1). Unbeknownst to us at the time, this figure also indicates that VRC01 was a poor choice for the estimation of transiently expressed Env in culture supernatant using ELISA (Table 3.1) as this VRC01 consistently shows reduced binding to the CH505 Envs relative to the FVgp140 control (Figure 3.7 Compare red line in A-D to E). Thus, it is likely that the concentrations of CH505 Envs reported in Table 3.1 are underestimated.

This reduction in binding levels of the CD4bs directed bNAbs is not completely unexpected given that these sequences were derived from a patient who developed CD4bs directed antibody response (CH103 lineage) over the course of the infection. In the original paper, Liao and colleagues describe the evolution of the transmitted virus Env sequences and noted specific mutations that overlap with CD4 and CH103 contact residues, including the D loop, the V1 loop, β23-V5 loop β24 and the CD4-biding loop of Env [187]. Given the high degree of amino acid sequence conservation of the CD4bs, mutations in these specific regions in response to immune pressure could affect the binding of other bNAbs that share the relevant overlapping contact residues.

The second ELISA format analysed biofunctionality of the CH505 Env CD4bs further, using the 17b antibody and 1dCD4, the minimal functional domain of CD4 as described by [266]. This antibody recognizes a CD4 induced (CD4i) epitope, which overlaps with the coreceptor binding site on gp120 [303]. Priming of the BaLgp120 Env with CD4 (1dCD4) effectively induced the 17b epitope relative to the unbound BaLgp120 Env alone (Figure 3.8F). However,

this preferential increase in binding to the CD4-bound conformation of Env was observed to a lesser extent for the FVgp140 control and CH505 Envs (Figure 3.8A-E). Thus, it appears the that the 17b epitope is constitutively exposed on the FVgp140 and CH505 Envs and is far less dependent on the engagement of CD4 to induce the required conformational change to expose the targeted CD4i epitope, compared to the BaLgp120 Env. This result was unable to confirm CD4 binding to the CH505 Envs, but given the antigenicity ELISA data, these results indicate that the CD4bs on the CH505 Envs is conformationally intact.

Although it falls outside the scope of this current project, the findings mentioned above could be strengthened by further evaluation of Env binding with a broader panel of antibodies, directed towards additional vulnerable sites on Env, including PG9, PG16, other VRC01-like antibodies, the PGT family, and the CH103 lineage antibodies using surface plasmon resonance to determine binding kinetics.

4.4) Generation of recombinant AAV vector containing the HIV-1 CH505 Env transgenes

Recombinant AAV have successfully been used for gene therapy in humans and show promise in many vaccine applications [241, 242, 304-306]. The rAAV serotype 2 has been the main focus of this research, and as such is usually a starting point for most rAAV designs [232, 307, 308]. Balazs and colleagues [243] designed a rAAV plasmid with a novel promoter, CASI, that combined the cytomegalovirus immediate early promoter (CMV), the chimeric chicken-β-actin (CAG), and ubiquitin C (UBC) promoters to facilitate long-term transgene expression. They demonstrated improved expression over the regular CAG promoter alone. They further incorporated antibody genes (VRC01 or b12) or luciferase as a control into these vectors for use as vectored immunoprophylaxis studies in small animals. The rAAV delivery method of these antibody genes allowed for long-term bNAbs expression following intramuscular injection of humanised mice. Furthermore the humanised mice that received the vectored immunoprophylaxis were shown to be fully protected following viral challenge [243].

Based on the successful expression described above, the pAAV-CASI-Luc2-W-SV40 plasmid (pAAV-Luc) [243] , was used as a basis for our novel pAAV design to express the CH505-Env glycoproteins as potential vaccine immunogens. Restriction enzyme digestion cloning was successfully performed using this plasmid and our pcDNA3.3-CH505 plasmids using the *Bam*HI and *Not*I restriction sites as described. Following cloning and transformations, initial isolations of the pAAV-CH505 and pAAV-GFP plasmids were performed according to

standard protocols, with some modifications. These included the use of *E. coli* XL10 cells and temperature conditions of 30°C. This was to ensure the retention of the ITR sequences flanking the transgene cassettes, which is necessary for rAAV production [231, 233, 308-310]. These sequences form hairpin-loop secondary structures, that are unstable in *E. coli* cells and prone to deletion during bacterial replication [233, 310]. To prevent this from occurring, endonuclease- and recombinase-deficient *E. coli* cells are used allowing the ITRs to be retained. Despite the use of the *E. coli* XL10 cells and lower culturing temperatures, insufficient DNA yields were obtained for downstream rAAV production and during screening, ITR retention varied (data not shown), These low yields could be a result of the origin of replication being a low-copy number (pMB1) and the lower temperatures used during bacterial growth.

Further optimization was performed with new modifications. Firstly, the SURE2 *E. coli* cells replaced the XL10s, as they were able to consistently retain the ITR sequences (data not shown). Secondly, the ampicillin used during isolation was substituted with carbenicillin, as it is a more stable antibiotic and allows for more effective growth at normal temperatures (37°C) [269]. For large-scale plasmid isolations, chloramphenicol was added during the last 12 hours (see Methods) to further increase DNA yields, as this antibiotic inhibits bacterial host protein synthesis, while allowing for plasmid replication to continue [269]. On average, following optimization, DNA yields increased approximately 20-fold (from ~200ng/ µl to ~4000 ng/ µl; data not shown). This optimized protocol was used for all subsequent DNA isolations and purifications necessary for rAAV production (pAAV-CH505, pAAV-GFP, Adenohelper, rep/cap2 plasmids). Integrity confirmation, of the transgenes present in the plasmids (Figure 3.9A; Figure 3.10) and further *Sma*I restriction enzyme digests revealed that the ITRs were consistently intact (Figure 3.9B; Figure 3.10). Overall, results confirm that the CH505 env sequences were successfully cloned into the pAAV backbone, and through an optimised plasmid culturing protocol we were able to obtain sufficient quantities for the *in vivo* production of the rAAV.

4.5) Quantification of rAAV CH505 vectors

In the past, the determination of rAAV titres relied on DNA dot-blot [310, 311], but with the advent of quantitative, real-time PCR strategies, enhanced assays were soon developed that had improved accuracy and simplicity, and were more robust [312]. These qPCR based-methods have become the standard for rAAV titre assays [243, 270, 310, 313-317], however concerns have been raised about the use of these methods for determining the titres of self-

complementary AAV vector genomes due to primer-probe exclusion or packaging of defective interfering (DI) genomes, which can result in the over-estimation of genome titres [272]. Improvements to digital PCR (dPCR) techniques [318-320] have allowed for the compartmentalization of the DNA molecules, such that the reaction is fractionated into approximately 15 000 individual droplets, which are run in parallel for droplet digital PCR (ddPCR) [272]. Standard "TaqMan" primer-probe sets are used, which are scored as either positive or negative based on probe-derived fluorescence, and allow for absolute quantification, with improved sensitivity and specificity.

Using this information, we designed a ddPCR assay to quantify our vector genomes, based off two primer-probe sets: one to exclusively quantify rAAV-GFP genomes (by targeting the GFP transgene) and one to quantify rAAV genomes by targeting the SV40 polyadenylation signal [272]. Ultimately, the goal was to determine the absolute genome copies/ ml for the rAAVs, as well as to observe if there were any differences in genome titres with the different primer-probe sets used. The tires obtained from the GFP primer probe set were 1.5 times higher than those obtained for the SV40 set (for rAAV-GFP); and these titres were on average 5 times higher than those obtained for the rAAV-CH505 vectors, although all the titres were consistent when experiments were repeated, and were within reported values [271]. These results could potentially be from the GFP primer-probe set being further away from the ITRs, as it has been reported that primer-probe sets closer to and within ITRs can lead to underreporting of genome titres [272]. Additional optimization may be required to improve the vector titres for the rAAV-CH505 vectors, such as scaling-up of production, optimizing the transfection ratios of the 3 plasmids, or potentially using a helper-free system [270, 310]. Overall, despite the lower titres obtained, they were sufficient for *in vitro* assays to determine whether they were capable of recombinant protein expression.

4.6) rAAV mediated transgenic expression of CH505 Envs *in vitro*

As stated previously, the goal of rAAV delivery is the successful expression of the encoded proteins, and when used for vaccine strategies to have an immune response directed against these proteins. We have described the development of matched recombinant Env proteins, and the initial production of the rAAV vectors designed to contain these proteins. Lastly, after the initial detection via ddPCR, we explored the expression of the transgenes *in vitro* with fluorescent microscopy and ELISA [270-272].

The positive control rAAV-GFP expressed GFP as expected (Figure 3.12), with an MOI >25 000 being effective. This is consistent with the literature, although it is noted that the rAAV serotype 2 is most effective in *in vitro* assays, and that assays done for larger-scale transductions may require further optimization. Although the experiment was only continued for 8 days post-transduction (due to media exhaustion and time constraints), under different culture conditions, it is likely that the transgenically expressed protein would continue to be visible for much longer. The rAAV-CH505 Envs were subsequently transduced in HEK 293 T cells, and protein expression levels were confirmed via ELISA from the w20, w30, w53, and w78 rAAV. While the CH505 Envs concentrations were determined to be on average, higher than those achieved during transient transfection (Table 3.1), this is most likely as a result of the substitution of VRC01 with IgG1b12 primary antibody used for detection in the ELISA. As determined in Figure 3.7, IgG1b12 showed increased binding sensitivity to the CH505 Envs compared to VRC01. The lack of expression of the CH505 w4 Env was again confirmed, reiterating, a as of yet unknown aberration in this particular Env sequence/ construct.

A general increase in the HIV-1 CH505 Env expression was noted following rAAV transduction of HEK293 T, peaking between day 6 and 8 post infection (Figure 3.13b). CH505 w58 and w78 constructs achieved similar Env expression levels over the 8-day period, with peak Env expression of approximately 4 µg/mL achieved (Figure 3.13B blue and red lines, respectively). The w20 construct showed a similar trend in Env expression over the evaluation period, however achieving relatively half the concentration (2 µg/ml) to that of w53 and w78 constructs (Figure 3.13B compare pink line (w20) compared to blue (w53) and red (w78), respectively). In contrast, the rAAVw30 construct achieved the highest, relative Env expression at day 2 and subsequently decreased over following 6-day period of evaluation. These results were repeated, and confirm the above result indicating harvest time points were not mixed up during setup of the ELISA and is true reflection of the relative Env concentrations over the 8-day period. Is unclear why this discrepancy between initial Env expression concentration and duration of the relative CH505 Env constructs exist. However, it was noted that the rAAV-w30gp140 produced the lowest viral tires (Table 3.2), and during the transduction of HEK293T cell assay, this translates into a to an approximate 3-fold greater addition in the volume of virus compared to the rAAV-w20, w53 and w78 virus to achieve an MOI of 50 000 (Table 3.2). This increased volume (approximately 100 µl of purified AAV-w30 in final assay volume of 200 µl) may have inadvertently affect the cell survivability of these transduced cell due dilution of growth medium (although this was not evident by

microscopic evaluation). Alternatively, the increased iodixanol concentration within the transduction assay (as the purified rAAVs are contained within the 40% iodixanol gradient) may favour viral entry, and these conditions will need to be controlled for adequately in future experiments to delineate the potential affect iodixanol may have in these transduction assays. Overall, the results provide evidence that demonstrates the feasibility of constructing rAAV to express HIV-1 Env.

4.7) Concluding remarks and future directions

It has become increasingly evident that current immunogens used for HIV-1 vaccine design are not sufficient to elicit bNAb responses that can protect against acquisition of infection. However, vital research into the co-evolution between viral Env and host antibody sequences have revealed important information regarding the virological and immunological characteristics of bNAb development. [103, 187, 216-218]. These studies indicate the importance of engaging specific naïve B cell repertoires with a specific Env sequence to initiate bNAb development and maturation activity [103, 187, 215-220]. Thus, there has been renewed interest in the development of alternative strategies that may better replicate these kinds of responses, using a lineage-based design such as sequential immunization.

Other groups have previously described the use of rAAVs for the delivery of antibody-related genes for vectored immunoprophylaxis [95, 243, 244] and other HIV-1 genes [108, 246]. The rAAV-Env delivery mechanism described in this dissertation offers a viable method for Env immunogen delivery for a sequential immunization strategy. To the best of our knowledge, this is the first report to provide proof-of-concept that rAAVs can be used for the delivery and expression of sequentially-derived HIV-1 Env immunogens in mammalian cells. Future work will focus on testing the sequential matched rAAV-Env and purified recombinant Env in novel prime-boost vaccine regimens in small animal models.

References

1. Barré-Sinoussi, F., Chermann, J.C., Rey, F., Nugeyre, M.T., Chamaret, S., Gruest, J., Dauguet, C., Axler-Blin, C., Vézinet-Brun, F., Rouzioux, C., Rozenbaum, W., and Montagnier, L., *Isolation of a T-lymphotropic retrovirus from a patient at risk for acquired immune deficiency syndrome (AIDS).* Science, 1983. **220**(4599): p. 868-871.
2. Gallo, R.C., Salahuddin, S.Z., Popovic, M., Shearer, G.M., Kaplan, M., Haynes, B.F., Palker, T.J., Redfield, R., Oleske, J., Safai, B., et, al., *Frequent detection and isolation of cytopathic retroviruses (HTLV-III) from patients with AIDS and at risk for AIDS.* Science, 1984. **224**(4648): p. 500-503.
3. WHO. *HIV/ AIDS Factsheet*. 2017 July 2017 [cited 2017 18/10/2017]; Available from: http://www.who.int/mediacentre/factsheets/fs360/en/.
4. UNAIDS. *Fact sheet - Latest statistics on the status of the AIDS epidemic*. 2017 [cited 2018 10/01/2018]; Available from: http://www.unaids.org/sites/default/files/media_asset/UNAIDS_FactSheet_en.pdf.
5. UNAIDS. *South Africa: HIV & AIDS estimates*. 2017 [cited 2018 10/01/2018]; Available from: http://www.unaids.org/en/regionscountries/countries/southafrica.
6. WHO. *Global Health Observatory (GHO) data: HIV/ AIDS*. 2016 [cited 2017 18/10/2017]; Available from: http://www.who.int/gho/hiv/en/.
7. WHO. *HIV/ AIDS Factsheet*. 2016 November 2017 [cited 2018 10/01/2018]; Available from: http://www.who.int/mediacentre/factsheets/fs360/en/.
8. UNAIDS., *Combination HIV prevention: tailoring and coordinating biomedical, behavioural and structural strategies to reduce new HIV infections: a UNAIDS discussion paper.* . 2010: Geneva, Switzerland.
9. Hankins, C.A., and de Zalduondo, B.O., *Combination prevention: a deeper understanding of effective HIV prevention.* AIDS, 2010. **24**(Supplement 4): p. S70-80.
10. Cluver, L.D., Orkin, M.F., Yakubovich, A.R., and Lorraine Sherr, L. , *Combination social protection for reducing HIV-risk behavior amongst adolescents in South Africa.* Journal of Acquired Immune Deficiency Syndromes, 2016. **72**(1): p. 96–104.
11. Hargreaves, J.R., Delany-Moretlwe, S., Hallett, T.B., Johnson, S., Kapiga, S., Bhattacharjee, P., Dallabetta, G., and Garnett, G.P., *The HIV prevention cascade: integrating theories of epidemiological, behavioural, and social science into programme design and monitoring.* The Lancet HIV, 2016. **3**(7): p. e318-322.
12. Krishnaratne, S., Hensen, B., Cordes, J., Enstone, J., and Hargreaves, J.R., *Interventions to strengthen the HIV prevention cascade: a systematic review of reviews.* The Lancet HIV, 2016. **3**(7): p. e307-317.
13. Auvert, B., Taljaard, D., Lagarde, E., Sobngwi-Tambekou, J., Sitta, R., and Puren, A., *Randomized, Controlled Intervention Trial of Male Circumcision for Reduction of HIV Infection Risk: The ANRS 1265 Trial.* PLoS Medicine, 2005. **2**(11): p. e298.
14. Bailey, R.C., Moses, S., Parker, C.B., Agot, K., Maclean, I., Krieger, J.N., Williams, C.F.M., Campbell, R.T., and Ndinya-Achola, J.O., *Male circumcision for HIV prevention in young men in Kisumu, Kenya: a randomised controlled trial.* The Lancet, 2007. **369**(9562): p. 643-656.
15. Gray, R.H., Kigozi, G., Serwadda, D., Makumbi, F., Watya, S., Nalugoda, F., Kiwanuka, N., Moulton, L.H., Chaudhary, M.A., Chen, M.Z., Sewankambo, N.K., Wabwire-Mangen, F., Bacon, M.C., Williams, C.F., Opendi, P., Reynolds, S.J., Laeyendecker, O., Quinn, T.C. and Wawer, M.J., *Male circumcision for HIV prevention in men in Rakai, Uganda: a randomised trial.* The Lancet, 2007. **369**(9562): p. 657–666.

16. Grant, R.M., Lama, J.R., Anderson, P.L., McMahan, V., Liu, A.Y., Vargas, L., Goicochea, P., Casapía, M., Guanira-Carranza, J.V., Ramirez-Cardich, M.E., Montoya-Herrera, O., Fernández, T., Veloso, V.G., Buchbinder, S.P., Chariyalertsak, S., Schechter, M., Bekker, L.G., Mayer, K.H., Kallás, E.G., Amico, K.R., Mulligan, K., Bushman, L.R., Hance, R.J., Ganoza, C., Defechereux, P., Postle, B., Wang, F., McConnell, J.J., Zheng, J.H., Lee, J., Rooney, J.F., Jaffe, H.S., Martinez, A.I., Burns, D.N., Glidden, D.V. and iPrEx Study Team., *Preexposure chemoprophylaxis for HIV prevention in men who have sex with men.* The New England Journal of Medicine, 2010. **363**(27): p. 2587-2599.
17. Choopanya, K., Martin, M., Suntharasamai, P., Sangkum, U., Mock, P.A., Leethochawalit, M., Chiamwongpaet, S., Kitisin, P., Natrujirote, P., Kittimunkong, S., Chuachoowong, R., Gvetadze, R.J., McNicholl, J.M., Paxton, L.A., Curlin, M.E., Hendrix, C.W., Vanichseni, S., and Bangkok Tenofovir Study Group., *Antiretroviral prophylaxis for HIV infection in injecting drug users in Bangkok, Thailand (the Bangkok Tenofovir Study): a randomised, double-blind, placebo-controlled phase 3 trial.* The Lancet, 2013. **381**(9883): p. 2083-2090.
18. Goto, T., Nakai, M. and Ikuta, K. , *The life-cycle of human immunodeficiency virus type 1.* Micron, 1998. **29**(2-3): p. 123-138.
19. Watts, J.M., Dang, K.K., Gorelick, R.J., Leonard, C.W., Bess Jr, J.W., Swanstrom, R., Burch, C.L., and Weeks, K.M, *Architecture and secondary structure of an entire HIV-1 RNA genome.* Nature, 2009. **460**(7256): p. 711-716.
20. LosAlamos. *Landmarks of the HIV-1 genome*. 2014 27 May 2014 [cited 2015 11 August 2017]; Available from: https://www.hiv.lanl.gov/content/sequence/HIV/MAP/landmark.html.
21. Gelderblom, H.R., Özel, M., and Pauli, G. , *Morphogenesis and morphology of HIV structure-function relations.* Archives of Virology, 1989. **106**(1): p. 1-13.
22. Steckbeck, J.D., Kuhlmann, A.S., and Montelaro, R.C., *C-terminal tail of human immunodeficiency virus gp41: functionally rich and structurally enigmatic.* Journal of General Virology, 2013. **94**: p. 1-19.
23. Joseph, S.B., Arrildt, K.T., Swanstrom, A.E., Schnell, G., Lee, B., Hoxie, J.A., and Swanstrom, R., *Quantification of Entry Phenotypes of Macrophage-Tropic HIV-1 across a Wide Range of CD4 Densities.* Journal of Virology, 2014. **88**(4): p. 1858–1869.
24. da Silva, E.S., Mulinge, M., and Bercoff, D.P., *The frantic play of the concealed HIV envelope cytoplasmic tail.* Retrovirology, 2013. **10**(54): p. 1-24.
25. Checkley, M.A., Luttge, B.G., and Freed, E.O., *HIV-1 Envelope Glycoprotein Biosynthesis, Trafficking, and Incorporation.* Journal of Molecular Biology, 2011. **410**(4): p. 1-40.
26. Clapham, P.R. and Á. McKnight, *HIV-1 receptors and cell tropism.* British Medical Bulletin, 2001. **58**(1): p. 43-59.
27. Moore, J.P., A. Trkola, and T. Dragic, *Co-receptors for HIV-1 entry.* Current Opinion in Immunology, 1997. **9**(4): p. 551-562.
28. Pollakis, G., and Paxton, W.A., *Use of (alternative) coreceptors for HIV entry.* Current Opinion in HIV and AIDS, 2012. **7**(5): p. 440-449.
29. Patel, P., Borkowf, C.B., Brooks, J.T., Lasry, A., Lansky, A., and Mermin, J., *Estimating per-act HIV transmission risk: a systematic review.* AIDS, 2014. **28**(10): p. 1509–1519.
30. Joseph, S.B., Swanstrom, R., Kashuba, A.D.M., and Cohen, M.S., *Bottlenecks in HIV-1 transmission: insights from the study of founder viruses.* Nature Reveiws Microbiology, 2015. **13**(7): p. 414-425.

31. Keele, B.F., Giorgi, E.E., Salazar-Gonzalez, J.F., Decker, J.M., Pham, K.T., Salazar, M.G., Sun, C., Grayson, T., Wang, S., Li, H., Wei, X., Jiang, C., Kirchherr, J.L., Gao, F., Anderson, J.A., Ping, L.H., Swanstrom, R., Tomaras, G.D., Blattner, W.A., Goepfert, P.A., Kilby, J.M., Saag, M.S., Delwart, E.L., Busch, M.P., Cohen, M.S., Montefiori, D.C., Haynes, B.F., Gaschen, B., Athreya, G.S., Lee, H.Y., Wood, N., Seoighe, C., Perelson, A.S., Bhattacharya, T., Korber, B.T., Hahn, B.H., and Shaw, G.M., *Identification and characterization of transmitted and early founder virus envelopes in primary HIV-1 infection.* Proceedings of the National Academy of Sciences of the United States of America, 2008. **105**(21): p. 7552-7557.
32. McMichael, A.J., Borrow, P., Tomaras, G.D., Goonetilleke, N., and Haynes, B.F., *The immune response during acute HIV-1 infection: clues for vaccine development.* Nature Reveiws Immunology, 2010. **10**(1): p. 11-23.
33. Derdeyn, C.A., Decker, J.M., Bibollet-Ruche, F., Mokili, J.L., Muldoon, M., Denham, S.A., Heil, M.L., Kasolo, F., Musonda, R., Hahn, B.H., Shaw, G.M., Korber, B.T., Allen, S., and Hunter, E., *Envelope-constrained neutralization-sensitive HIV-1 after heterosexual transmission.* Science, 2004. **303**(5666): p. 2019-2022.
34. Hollingsworth, T.D., Anderson, R.M., and Fraser, C., *HIV-1 Transmission, by Stage of Infection.* The Journal of Infectious Diseases, 2008. **198**(5): p. 687-693.
35. Fox, J., and Fidler, S., *Sexual transmission of HIV-1.* Antiviral Research, 2010. **85**(1): p. 276-285.
36. Pudney, J., A.J. Quayle, and D.J. Anderson, *Immunological Microenvironments in the Human Vagina and Cervix: Mediators of Cellular Immunity Are Concentrated in the Cervical Transformation Zone1.* Biology of Reproduction, 2005. **73**(6): p. 1253-1263.
37. Zhang, Z.-Q., S.W. Wietgrefe, Q. Li, M.D. Shore, L. Duan, C. Reilly, J.D. Lifson, and A.T. Haase, *Roles of substrate availability and infection of resting and activated CD4+ T cells in transmission and acute simian immunodeficiency virus infection.* Proceedings of the National Academy of Sciences of the United States of America, 2004. **101**(15): p. 5640-5645.
38. Février, M., Dorgham, K., and Rebollo, A., *CD4+ T Cell Depletion in Human Immunodeficiency Virus (HIV) Infection: Role of Apoptosis.* Viruses, 2011. **3**(5): p. 586–612.
39. Hearps, A.C., Tyssen, D., Srbinovski, D., Bayigga, L., Diaz, D.J., Aldunate, M., Cone, R.A., Gugasyan, R., Anderson, D.J., and Tachedjian, G., *Vaginal lactic acid elicits an anti-inflammatory response from human cervicovaginal epithelial cells and inhibits production of pro-inflammatory mediators associated with HIV acquisition.* Mucosal Immunology, 2017.
40. Stebbing , J., Gazzard , B., and Douek , D.C. , *Where Does HIV Live?* New England Journal of Medicine, 2004. **350**(18): p. 1872-1880.
41. Maartens, G., Celum, C., and Lewin, S.R., *HIV infection: epidemiology, pathogenesis, treatment, and prevention.* The Lancet, 2014. **384**(9939): p. 258-271.
42. Hernandez-Vargas, E.A., and Middleton, R.H. , *Modeling the three stages in HIV infection.* Journal of Theoretical Biology, 2013. **320**: p. 33–40.
43. Mehandru, S., Poles, M.A., Tenner-Racz, K., Manuelli, V., Jean-Pierre, P., Lopez, P., Shet, A., Low, A., Mohri, H., Boden, D., Racz, P., and Markowitz, M., *Mechanisms of gastrointestinal CD4+ T-cell depletion during acute and early human immunodeficiency virus type 1 infection.* Journal of Virology, 2007. **81**(2): p. 599-612.
44. Veazey, R.S., DeMaria, M., Chalifoux, L.V., Shvetz, D.E., Pauley, D.R., Knight, H.L., Rosenzweig, M., Johnson, R.P., Desrosiers, R.C., and Lackner, A.A., *Gastrointestinal tract as a major site of CD4+ T cell depletion and viral replication in SIV infection.* Science, 1998. **280**(5362): p. 427-431.

45. Brenchley, J.M., Schacker, T.W., Ruff, L.E., Price, D.A., Taylor, J.H., Beilman, G.J., Nguyen, P.L., Khoruts, A., Larson, M., Haase, A.T., and Douek, D.C., *CD4(+) T Cell Depletion during all Stages of HIV Disease Occurs Predominantly in the Gastrointestinal Tract.* The Journal of Experimental Medicine, 2004. **200**(6): p. 749-759.
46. Barre-Sinoussi, F., Ross, A.L., and Delfraissy, J-F., *Past, present and future: 30 years of HIV research.* Nat Rev Micro, 2013. **11**(12): p. 877-883.
47. Carter, C.C., Onafuwa-Nuga, A., McNamara, L.A., Riddell, J., Bixby, D., Savona, M.R., and Collins, K.L., *HIV-1 infects multipotent progenitor cells causing cell death and establishing latent cellular reservoirs.* Nature Medicine, 2010. **16**(4): p. 446-451.
48. Chun, T.-W., Stuyver, L., Mizell, S.B., Ehler, L.A., Mican, J.A.M., Baseler, M., Lloyd, A.L., Nowak, M.A., and Fauci, A.S., *Presence of an inducible HIV-1 latent reservoir during highly active antiretroviral therapy.* Proceedings of the National Academy of Sciences of the United States of America, 1997. **94**(24): p. 13193–13197.
49. Hraber, P., Korber, B., Wagh, K., Giorgi, E.E., Bhattacharya, T., Gnanakaran, S., Lapedes, A.S., Learn, G.H., Kreider, E.F., Li, Y., Shaw, G.M., Hahn, B.H., Montefiori, D.C., Munir Alam, S., Bonsignori, M., Anthony Moody, M., Liao, H-X., Gao, F., Haynes, B.F., *Longitudinal Antigenic Sequences and Sites from Intra-Host Evolution (LASSIE) Identifies Immune-Selected HIV Variants.* Viruses, 2015. **7**(10): p. 5443-5475.
50. Grossman, Z., Meier-Schellersheim, M., Paul, W.E., and Picker, L.J., *Pathogenesis of HIV infection: what the virus spares is as important as what it destroys.* Nature Medicine, 2006. **12**(3): p. 289-295.
51. Hazenberg, M.D., Otto, S.A., van Benthem, B.H.B., Roos, M.T.L., Coutinho, R.A., Lange, J.M.A., Hamann, D., Prins, M., and Miedema, F., *Persistent immune activation in HIV-1 infection is associated with progression to AIDS.* AIDS, 2003. **17**(13): p. 1881-1888.
52. Peretz, Y., Cameron, C., and Sékaly, R-P., *Dissecting the HIV-specific immune response: a systems biology approach.* Current Opinion in HIV and AIDS, 2012. **7**(1): p. 17–23.
53. Anzala, O.A., Nagelkerke, N.J.D., Bwayo, J.J., Holton, D., Moses, S., Ngugi, E.N., Ndinya-Achola, J.O., and Plummer, F.A. , *Rapid progression to disease in African sex workers with human immunodeficiency virus type 1 infection.* Journal of Infectious Diseases, 1995. **171**(3): p. 686–689.
54. Mogensen, T.H., Melchjorsen, J., Larsen, C.S., and Paludan, S.R., *Innate immune recognition and activation during HIV infection.* Retrovirology, 2010. **7**(54): p. 1-19.
55. Iwasaki, A., *Innate Immune Recognition of HIV-1.* Immunity, 2012. **37**(3): p. 389-398.
56. Borrow, P., Lewicki, H., Hahn, B.H., Shaw, G.M., and Oldstone, M.B., *Virus-specific CD8+ cytotoxic T-lymphocyte activity associated with control of viremia in primary human immunodeficiency virus type 1 infection.* Journal of Virology, 1994. **68**(9): p. 6103-6110.
57. Chang, J.J., and Marcus, A., *Innate Immune Activation in Primary HIV-1 Infection.* The Journal of Infectious Diseases, 2010. **202**(Supplement_2): p. S297-S301.
58. Iwasaki, A., and Medzhitov, R., *Regulation of Adaptive Immunity by the Innate Immune System.* Science, 2010. **327**(5963): p. 291-295.
59. Altfeld, M., and Gale Jr, M., *Innate immunity against HIV-1 infection.* Nature Immunology, 2015. **16**: p. 554.
60. Kaul, M., Garden, G., and Lipton, S.A., *Pathways to neuronal injury and apoptosis in HIV-associated dementia.* Nature, 2001. **410**: p. 988.

61. Medders, K.E., and Kaul, M., *Mitogen-Activated Protein Kinase p38 in HIV Infection and Associated Brain Injury.* Journal of neuroimmune pharmacology : the official journal of the Society on NeuroImmune Pharmacology, 2011. **6**(2): p. 202-215.
62. Yang, X., and Gabuzda, G., *Regulation of Human Immunodeficiency Virus Type 1 Infectivity by the ERK Mitogen-Activated Protein Kinase Signaling Pathway.* Journal of Virology, 1999. **73**(4): p. 3460–3466.
63. Hiscott, J., Kwon, H., and Génin, P.,, *Hostile takeovers: viral appropriation of the NF-kB pathway.* Journal of Clinical Investigation, 2001. **107**(2): p. 143-151.
64. Fiume, G., Vecchio, E., De Laurentiis, A., Trimboli, F., Palmieri, C., Pisano, A., Falcone, C., Pontoriero, M., Rossi, A., Scialdone, A., Fasanella Masci, F., Scala, G., and Quinto, I.,, *Human immunodeficiency virus-1 Tat activates NF-κB via physical interaction with IκB-α and p65.* Nucleic Acids Research, 2012. **40**(8): p. 3548-3562.
65. Stacey, A.R., Norris, P.J., Qin, L., Haygreen, E.A., Taylor, E., Heitman, J., Lebedeva, M., DeCamp, A., Li, D., Grove, D., Self, S.G., and Borrow, P., *Induction of a striking systemic cytokine cascade prior to peak viremia in acute human immunodeficiency virus type 1 infection, in contrast to more modest and delayed responses in acute hepatitis B and C virus infections.* Journal of Virology, 2009. **83**(8): p. 3719-3733.
66. Tsang, J., Chain, B.M., Miller, R.F., Webb, B.L., Barclay, W., Towers, G.J., Katz, D.R., and Noursadeghi, M., *HIV-1 infection of macrophages is dependent on evasion of innate immune cellular activation.* AIDS, 2009. **23**(17): p. 2255-2263.
67. Doehle, B.P., Hladik, F., McNevin, J.P., McElrath, M.J., and Gale, M. Jr., *Human immunodeficiency virus type 1 mediates global disruption of innate antiviral signaling and immune defenses within infected cells.* Journal of Virology, 2009. **83**(20): p. 10395-10405.
68. Klein, E., and Ho, R.J.Y., *Challenges in the development of an effective HIV vaccine: Current approaches and future directions.* Clinical Therapeutics, 2000. **22**(3): p. 295–314.
69. Price, D.A., Goulder, P.J.R., Klenerman, P., Sewell, A.K., Easterbrook, P.J., Troop, M., Bangham, C.R.M., and Phillips, R.E., *Positive selection of HIV-1 cytotoxic T lymphocyte escape variants during primary infection.* Proceedings of the National Academy of Sciences of the United States of America, 1997. **94**(5): p. 1890-1895.
70. Borrow, P., and Bhardwaj, N., *Innate immune responses in primary HIV-1 infection.* Current Opinion in HIV and AIDS, 2008. **3**(1): p. 36-44.
71. Euler, Z. and H. Schuitemaker, *Cross-reactive broadly neutralizing antibodies: timing is everything.* Frontiers in Immunology, 2012. **3**(215).
72. Klein, F., Mouquet, H., Dosenovic, P., Scheid, J.F., Scharf, L., and Nussenzweig, M.C., *Antibodies in HIV-1 Vaccine Development and Therapy.* Science, 2013. **341**(6151): p. 1199-1204.
73. Forthal, D.N., *Functions of Antibodies.* Microbiology spectrum, 2014. **2**(4): p. 1-17.
74. Tomaras, G.D., Yates, N.L., Liu, P., Qin, L., Fouda, G.G., Chavez, L.L., Decamp, A.C., Parks, R.J., Ashley, V.C., Lucas, J.T., Cohen, M., Eron, J., Hicks, C.B., Liao, H.X., Self, S.G., Landucci, G., Forthal, D.N., Weinhold, K.J., Keele, B.F., Hahn, B.H., Greenberg, M.L., Morris, L., Karim, S.S., Blattner, W.A., Montefiori, D.C., Shaw, G.M., Perelson, A.S., and Haynes, B.F., *Initial B-cell responses to transmitted human immunodeficiency virus type 1: virion-binding immunoglobulin M (IgM) and IgG antibodies followed by plasma anti-gp41 antibodies with ineffective control of initial viremia.* Journal of Virology 2008. **82**(24): p. 12449-12463.
75. Richman, D.D., Wrin, T., Little, S.J., and Petropoulos, C.J., *Rapid evolution of the neutralizing antibody response to HIV type 1 infection.* Proceedings of the National Academy of Sciences of the United States of America, 2003. **100**(7): p. 4144-4149.

76. Wei, X., Decker, J.M., Wang, S., Hui, H., Kappes, J.C., Wu, X., Salazar-Gonzalez, J.F., Salazar, M.G., Kilby, J.M., Saag, M.S., Komarova, N.L., Nowak, M.A., Hahn, B.H., Kwong, P.D., and Shaw, G.M., *Antibody neutralization and escape by HIV-1*. Nature, 2003. **422**: p. 307-312.
77. Frost, S.D.W., Wrin, T., Smith, D.M., Kosakovsky Pond, S.L., Liu, Y., Paxinos, E., Chappey, C., Galovich, J., Beauchaine, J., Petropoulos, C.J., Little, S.J., and Richman, D.D., *Neutralizing antibody responses drive the evolution of human immunodeficiency virus type 1 envelope during recent HIV infection.* Proceedings of the National Academy of Sciences of the United States of America, 2005. **102**(51): p. 18515-18519.
78. Gray, E.S., Moore, P.L., Choge, I.A., Decker, J.M., Bibollet-Ruche, F., Li, H., Leseka, N., Treurnicht, F., Mlisana,K., Shaw, G.M., Abdool Karim, S.S., Williamson, C., Morris, L., and the CAPRISA 002 Study Team., *Neutralizing Antibody Responses in Acute Human Immunodeficiency Virus Type 1 Subtype C Infection.* Journal of Virology, 2007. **81**(12): p. 6187–6196.
79. Murphy, M.K., Yue, L., Pan, R., Boliar, S., Sethi, A., Tian, J., Pfafferot, K., Karita, E., Allen, S.A., Cormier, E., Goepfert, P.A., Borrow, P., Robinson J.E., Gnanakaran, S., Hunter, E., Kong, X-P., and Derdeyn, C.A., *Viral Escape from Neutralizing Antibodies in Early Subtype A HIV-1 Infection Drives an Increase in Autologous Neutralization Breadth.* PLOS Pathogens, 2013. **9**(2).
80. Stamatatos, L., Morris, L., Burton, D.R., and Mascola, J.R., *Neutralizing antibodies generated during natural HIV-1 infection: good news for an HIV-1 vaccine?* Nature Medicine, 2009. **15**(8): p. 866-870.
81. Gray, E.S., Madiga, M.C., Hermanus, T., Moore, P.L., Kurt Wibmer, C., Tumba, N.L., Werner, L., Mlisana, K., Sibeko, S., Williamson, C., Abdool Karim, S.S., Morris, L., and the CAPRISA 002 Study Team., *The Neutralization Breadth of HIV-1 Develops Incrementally over Four Years and Is Associated with CD4+T Cell Decline and High Viral Load during Acute Infection.* Journal of Virology, 2011. **85**(10): p. 4828–4840.
82. Graziano, R.F., and Guyre, P.M., *Antibody-dependent Cell-mediated Cytotoxicity (ADCC),* in *Encyclopedia of Life Sciences*. 2006. p. 1-5.
83. Forthal, D.N., Landucci, G., Haubrich, R., Keenan, B., Kuppermann, B.D., Tilles, J.G., and Kaplan, J., *Antibody-dependent cellular cytotoxicity independently predicts survival in severely immunocompromised human immunodeficiency virus-infected patients.* The Journal of Infectious Diseases, 1999. **180**(4): p. 1338-1341.
84. Haynes, B.F., Gilbert, P.B., McElrath, M.J., Zolla-Pazner, S., Tomaras, G.D., Alam, S.M., Evans, D.T., Montefiori, D.C., Karnasuta, C., Sutthent, R., Liao, H.X., DeVico, A.L., Lewis, G.K., Williams, C., Pinter, A., Fong, Y., Janes, H., DeCamp, A., Huang, Y., Rao, M., Billings, E., Karasavvas, N., Robb, M.L., Ngauy, V., de Souza, M.S., Paris, R., Ferrari, G., Bailer, R.T., Soderberg, K.A., Andrews, C., Berman, P.W., Frahm, N., De Rosa, S.C., Alpert, M.D., Yates, N.L., Shen, X., Koup, R.A., Pitisuttithum, P., Kaewkungwal, J., Nitayaphan, S., Rerks-Ngarm, S., Michael, N.L., and Kim, J.H., *Immune-correlates analysis of an HIV-1 vaccine efficacy trial.* The New England Journal of Medicine, 2012. **366**(14): p. 1275-1286.
85. Pantaleo, G., and Koup, R.A., *Correlates of immune protection in HIV-1 infection: what we know, what we don't know, what we should know.* Nature Medicine, 2004. **10**(8): p. 806-810.
86. Tomaras, G.D., and Plotkin, S.A., *Complex immune correlates of protection in HIV-1 vaccine efficacy trials.* Immunological Reviews, 2017. **275**(1): p. 245–261.
87. Kuri-Cervantes, L., Fourati, S., Canderan, G., and Sekaly, R-P., *Systems biology and the quest for correlates of protection to guide the development of an HIV vaccine.* Current Opinion in Immunology, 2016. **41**: p. 91–97.

88. Montefiori, D.C., Karnasuta, C., Huang, Y., Ahmed, H., Gilbert, P., de Souza, M.S., McLinden, R., Tovanabutra, S., Laurence-Chenine, A., Sanders-Buell, E., Moody, M.A., Bonsignori, M., Ochsenbauer, C., Kappes, J., Tang, H., Greene, K., Gao, H., LaBranche, C.C., Andrews, C., Polonis, V.R., Rerks-Ngarm, S., Pitisuttithum, P., Nitayaphan, S., Kaewkungwal, J., Self, S.G., Berman, P.W., Francis, D., Sinangil, F., Lee, C., Tartaglia, J., Robb, M.L., Haynes, B.F., Michael, N.L., and Kim, J.H., *Magnitude and breadth of the neutralizing antibody response in the RV144 and Vax003 HIV-1 vaccine efficacy trials.* The Journal of Infectious Diseases, 2012. **206**(3): p. 431-441.
89. Nitayaphan, S., Pitisuttithum, P., Karnasuta, C., Eamsila, C., de Souza, M., Morgan, P., Polonis, V., Benenson, M., VanCott, T., Ratto-Kim, S., Kim, J., Thapinta, D., Garner, R., Bussaratid, V., Singharaj, P., el Habib, R., Gurunathan, S., Heyward, W., Birx, D., McNeil, J., and Brown, A.E., *Safety and immunogenicity of an HIV subtype B and E prime-boost vaccine combination in HIV-negative Thai adults.* The Journal of Infectious Diseases, 2004. **190**(4): p. 702-706.
90. Pitisuttithum, P., Gilbert, P., Gurwith, M., Heyward, W., Martin, M., van Griensven, F., Hu, D., Tappero, J.W., Choopanya, K.; Bangkok Vaccine Evaluation Group., *Randomized, double-blind, placebo-controlled efficacy trial of a bivalent recombinant glycoprotein 120 HIV-1 vaccine among injection drug users in Bangkok, Thailand.* The Journal of Infectious Diseases, 2006. **194**(12): p. 1661-1671.
91. Rerks-Ngarm, S., Pitisuttithum, P., Nitayaphan, S., Kaewkungwal, J., Chiu, J., Paris, R., Premsri, N., Namwat, C., de Souza, M., Adams, E., Benenson, M., Gurunathan, S., Tartaglia, J., McNeil, J.G., Francis, D.P., Stablein, D., Birx, D.L., Chunsuttiwat, S., Khamboonruang, C., Thongcharoen, P., Robb, M.L., Michael, N.L., Kunasol, P., and Kim, J.H., *Vaccination with ALVAC and AIDSVAX to Prevent HIV-1 Infection in Thailand.* The New England Journal of Medicine, 2009. **361**(23): p. 2209-2220.
92. Robb, M.L., Rerks-Ngarm, S., Nitayaphan, S., Pitisuttithum, P., Kaewkungwal, J., Kunasol, P., Khamboonruang, C., Thongcharoen, P., Morgan, P., Benenson, M., Paris, R.M., Chiu, J., Adams, E., Francis, D., Gurunathan, S., Tartaglia, J., Gilbert, P., Stablein, D., Michael, N.L., and Kim, J.H., *Risk behaviour and time as covariates for efficacy of the HIV vaccine regimen ALVAC-HIV (vCP1521) and AIDSVAX B/E: a post-hoc analysis of the Thai phase 3 efficacy trial RV 144.* The Lancet Infectious Diseases, 2012. **12**(7): p. 531–537.
93. Girard, M.P., Osmanov, S., Assossou, O.M., and Kieny, M-P., *Human immunodeficiency virus (HIV) immunopathogenesis and vaccine development: A review.* Vaccine, 2011. **29**(37): p. 6191-6218.
94. Balazs, A.B., Ouyang, Y., Hong, C.M., Chen, J., Nguyen, S.M., Rao, D. S., An, D.S., and Baltimore, D., *Vectored immunoprophylaxis protects humanized mice from mucosal HIV transmission.* Nature Medicine, 2014. **20**(3): p. 296–300.
95. Johnson, P.R., Schnepp, B.C., Zhang, J., Connell, M.J., Greene, S.M., Yuste, E., Desrosiers, R.C., and Clark, K.R., *Vector-mediated gene transfer engenders long-lived neutralizing activity and protection against SIV infection in monkeys.* Nature Medicine, 2009. **15**(8): p. 901–906.
96. Barouch, D.H., Whitney, J.B., Moldt, B., Klein, F., Oliveira, T.Y., Liu, J., Stephenson, K.E., Chang, H-W., Shekhar, K., Gupta, S., Nkolola, J.P., Seaman, M.S., Smith, K.M., Borducchi, E.N., Cabral, C., Smith, J.Y., Blackmore, S., Sanisetty, S., Perry, J.R., Beck, M., Lewis, M.G., Rinaldi, W., Chakraborty, A.K., Poignard, P., Nussenzweig, M.C., and Burton, D.R., *Therapeutic efficacy of potent neutralizing HIV-1-specific monoclonal antibodies in SHIV-infected rhesus monkeys.* Nature, 2013. **503**(7475): p. 224-228.

97. Hessell, A.J., Rakasz, E.G., Poignard, P., Hangartner, L., Landucci, G., Forthal, D.N., Koff, W.C., Watkins, D.I., and Burton, D.R., *Broadly Neutralizing Human Anti-HIV Antibody 2G12 Is Effective in Protection against Mucosal SHIV Challenge Even at Low Serum Neutralizing Titers.* PLoS Pathogens, 2009. **5**(5): p. e1000433.
98. Mascola, J.R., Lewis, M.G., Stiegler, G., Harris, D., VanCott, T.C., Hayes, D., Louder, M.K., Brown, C.R., Sapan, C.V., Frankel, S.S., Lu, Y., Robb, M.L., Katinger, H., and Birx, D.L., *Protection of Macaques against Pathogenic Simian/Human Immunodeficiency Virus 89.6PD by Passive Transfer of Neutralizing Antibodies.* Journal of Virology, 1999. **73**(5): p. 4009–4018.
99. Mascola, J.R., Stiegler, G., VanCott, T.C., Katinger, H., Carpenter, C.B., Hanson, C.E., Beary, H., Hayes, D., Frankel, S.S., Birx, D.L., and Lewis, M.G., *Protection of macaques against vaginal transmission of a pathogenic HIV-1/SIV chimeric virus by passive infusion of neutralizing antibodies.* Nature Medicine, 2000. **6**(2): p. 207-210.
100. Parren, P.W.H.I., Marx, P.A., Hessell, A.J., Luckay, A., Harouse, J., Cheng-Mayer, C., Moore, J.P., and Burton, D.R., *Antibody Protects Macaques against Vaginal Challenge with a Pathogenic R5 Simian/Human Immunodeficiency Virus at Serum Levels Giving Complete Neutralization In Vitro.* Journal of Virology, 2001. **75**(17): p. 8340–8347.
101. Hussein, I.H., Chams, N., Chams, S., Sayegh, S.E., Badran, R., Raad, M., Gerges-Geagea, A., Leone, A., and Jurjus, A., *Vaccines Through Centuries: Major Cornerstones of Global Health.* Frontiers in Public Health, 2015. **3**: p. 1-16.
102. Ellis, R.W., Rappuoli, R., and Ahmed, S., *Technologies for making new vaccines*, in *Vaccines*. 2013, Elsevier. p. 1182–1199.
103. Doria-Rose, N.A., Schramm, C.A., Gorman, J., Moore, P.L., Bhiman, J.N., DeKosky, B.J., Ernandes, M.J., Georgiev, I.S., Kim, H.J., Pancera, M., Staupe, R.P., Altae-Tran, H.R., Bailer, R.T., Crooks, E.T., Cupo, A., Druz, A., Garrett, N.J., Hoi, K.H., Kong, R., Louder, M.K., Longo, N.S., McKee, K., Nonyane, M., O'Dell, S., Roark, R.S., Rudicell, R.S., Schmidt, S.D., Sheward, D.J., Soto, C., Wibmer, C.K., Yang, Y., Zhang, Z., NISC Comparative Sequencing Mullikin, J.C., Binley, J.M., Sanders, R.W., Wilson, I.A., Moore, J.P., Ward, A.B., Georgiou, G., Williamson, C., Abdool Karim, S.S., Morris, L., Kwong, P.D., Shapiro, L., and Mascola, J.R., *Developmental pathway for potent V1V2-directed HIV-neutralizing antibodies.* Nature, 2014. **509**(7498): p. 55-62.
104. Moore, P.L., Gray, E.S., Sheward, D., Madiga, M., Ranchobe, N., Lai, Z., Honnen, W.J., Nonyane, M., Tumba, N., Hermanus, T., Sibeko, S., Mlisana, K., Abdool Karim, S.S., Williamson, C., Pinter, A., Morris, L., and the CAPRISA 002 Study., *Potent and Broad Neutralization of HIV-1 Subtype C by Plasma Antibodies Targeting a Quaternary Epitope Including Residues in the V2 Loop.* Journal of Virology, 2011. **85**(7): p. 3128–3141.
105. Bhiman, J.N., C. Anthony, N.A. Doria-Rose, O. Karimanzira, C.A. Schramm, T. Khoza, D. Kitchin, G. Botha, J. Gorman, N.J. Garrett, S.S. Abdool Karim, L. Shapiro, C. Williamson, P.D. Kwong, J.R. Mascola, L. Morris, and P.L. Moore, *Viral variants that initiate and drive maturation of V1V2-directed HIV-1 broadly neutralizing antibodies.* Nature Medicine, 2015. **21**: p. 1332.
106. Esparza, J., *A brief history of the global effort to develop a preventive HIV vaccine.* Vaccine, 2013. **31**(35): p. 3502–3518.
107. Martin, A.R., and Siliciano, R.F., *Progress Toward HIV Eradication: Case Reports, Current Efforts, and the Challenges Associated with Cure.* Annual Review of Medicine, 2016. **67**: p. 215–228.
108. Xin, K.-Q., Urabe, M., Yang, J., Nomiyama, K., Mizukami, H., Hamajima, K., Nomiyama, H., Saito, T., Imai, M., Monahan, J., Okuda, K., Ozawa, K., and Okuda,

K., *A Novel Recombinant Adeno-Associated Virus Vaccine Induces a Long-Term Humoral Immune Response to Human Immunodeficiency Virus.* Human Gene Therapy, 2001. **12**(9): p. 1047-1061.
109. Choi, E., Michalski, C.J., Choo, S.H., Kim, G.N., Banasikowska, E., Lee, S., Wu, K., An, H.Y., Mills, A., Schneider, S., Bredeek, U.F., Coulston, D.R., Ding, S., Finzi, A., Tian, M., Klein, K., Arts, E.J., Mann, J.F., Gao, Y., and Kang, C.Y., *First Phase I human clinical trial of a killed whole-HIV-1 vaccine: demonstration of its safety and enhancement of anti-HIV antibody responses.* Retrovirology, 2016. **13**(82): p. 1-16.
110. Tang, D.C., DeVit, M., and Johnston, S.A., *Genetic immunization is a simple method for eliciting an immune response.* Nature 1992. **356**(6365): p. 152-154.
111. Nieto, K., and Salvetti, A., *AAV vector vaccines against infectious diseases.* Frontiers in Immunology, 2014. **5**: p. 1-9.
112. Fynan, E.F., R.G. Webster, D.H. Fuller, J.R. Haynes, J.C. Santoro, and H.L. Robinson, *DNA vaccines: protective immunizations by parenteral, mucosal, and gene-gun inoculations.* Proceedings of the National Academy of Sciences of the United States of America, 1993. **90**(24): p. 11478-11482.
113. Wang, B., K.E. Ugen, V. Srikantan, M.G. Agadjanyan, K. Dang, Y. Refaeli, A.I. Sato, J. Boyer, W.V. Williams, and D.B. Weiner, *Gene inoculation generates immune responses against human immunodeficiency virus type 1.* Proceedings of the National Academy of Sciences of the United States of America, 1993. **90**(9): p. 4156-4160.
114. Muthumani, K., S. Kudchodkar, D. Zhang, M.L. Bagarazzi, J.J. Kim, J.D. Boyer, V. Ayyavoo, G.N. Pavlakis, and D.B. Weiner, *Issues for improving multiplasmid DNA vaccines for HIV-1.* Vaccine, 2002. **20**(15): p. 1999-2003.
115. Lambricht, L., K. Vanvarenberg, A. De Beuckelaer, L. Van Hoecke, J. Grooten, B. Ucakar, P. Lipnik, N.N. Sanders, S. Lienenklaus, V. Préat, and G. Vandermeulen, *Coadministration of a Plasmid Encoding HIV-1 Gag Enhances the Efficacy of Cancer DNA Vaccines.* Molecular Therapy, 2016. **24**(9): p. 1686-1696.
116. Melnychuk, L., L. Ajamian, P. Jean-Pierre, J. Liang, R. Gheorghe, M.A. Wainberg, and G.J. Zaharatos, *Development of a DNA vaccine expressing a secreted HIV-1 gp41 ectodomain that includes the membrane-proximal external region.* Vaccine, 2017. **35**(20): p. 2736-2744.
117. Barouch, D.H., and Nabel, G.J., *Adenovirus vector-based vaccines for human immunodeficiency virus type 1.* Human Gene Therapy, 2005. **16**(2): p. 149-56.
118. Franchini, G., S. Gurunathan, L. Baglyos, S. Plotkin, and J. Tartaglia, *Poxvirus-based vaccine candidates for HIV: two decades of experience with special emphasis on canarypox vectors.* Expert Review of Vaccines, 2004. **3**(sup1): p. S75-S88.
119. Graham, F.L., *Adenoviruses as expression vectors and recombinant vaccines.* Trends in Biotechnology, 1990. **8**: p. 85-87.
120. Marovich, M.A., *ALVAC-HIV vaccines: clinical trial experience focusing on progress in vaccine development.* Expert Review of Vaccines, 2004. **3**(sup1): p. S99-S104.
121. Tartaglia, J., Pincus, S., and Paoletti, E., *Poxvirus-based vectors as vaccine candidates.* Critical Reviews in Immunology, 1990. **10**(1): p. 13-30.
122. Puaux, A.-L., and Michel, M-L., *New gene-based approaches for an AIDS vaccine.* Comparative Immunology, Microbiology and Infectious Diseases, 2003. **26**(5-6): p. 357–372.
123. Robinson, H.L., and Torres, C.A.T., *DNA vaccines.* Seminars in Immunology, 1997. **9**(5): p. 271–283.
124. Letvin, N.L., Montefiori, D.C., Yasutomi, Y., Perry, H.C., Davies, M-E., Lekutis, C., Alroy, M., Freed, D.C., Lord, C.I., Handt, L.K., Liu, M.A., and Shiver, J.W., *Potent, protective anti-HIV immune responses generated by bimodal HIV envelope DNA plus*

protein vaccination. Proceedings of the National Academy of Sciences of the United States of America, 1997. **94**(17): p. 9378–9383.
125. Weiner, D.B., and Nabel, G.J., *The development of gene-based vectors for immunization*, in *Vaccines: Sixth Edition*. 2012, Elsevier. p. 1232–1242.
126. Amara, R.R., F. Villinger, J.D. Altman, S.L. Lydy, S.P. Neil, S.I. Staprans, D.C. Montefiori, Y. Xu, J.G. Herndon, L.S. Wyatt, M.A. Candido, N.L. Kozyr, P.L. Earl, J.M. Smith, H.-L. Ma, B.D. Grimm, M.L. Hulsey, J. Miller, H.M. McClure, J.M. McNicholl, B. Moss, and H.L. Robinson, *Control of a Mucosal Challenge and Prevention of AIDS by a Multiprotein DNA/MVA Vaccine.* Science, 2001. **292**(5514): p. 69.
127. Cox, K.S., J.H. Clair, M.T. Prokop, K.J. Sykes, S.A. Dubey, J.W. Shiver, M.N. Robertson, and D.R. Casimiro, *DNA gag/Adenovirus Type 5 (Ad5) gag and Ad5 gag/Ad5 gag Vaccines Induce Distinct T-Cell Response Profiles.* Journal of Virology, 2008. **82**(16): p. 8161-8171.
128. Goepfert, P.A., M.L. Elizaga, A. Sato, L. Qin, M. Cardinali, C.M. Hay, J. Hural, S.C. DeRosa, O.D. DeFawe, G.D. Tomaras, D.C. Montefiori, Y. Xu, L. Lai, S.A. Kalams, L.R. Baden, S.E. Frey, W.A. Blattner, L.S. Wyatt, B. Moss, H.L. Robinson, A. the National Institute of, and H.I.V.V.T.N. Infectious Diseases, *Phase 1 Safety and Immunogenicity Testing of DNA and Recombinant Modified Vaccinia Ankara Vaccines Expressing HIV-1 Virus-like Particles.* The Journal of Infectious Diseases, 2011. **203**(5): p. 610-619.
129. Graham, B.S., R.A. Koup, M. Roederer, R.T. Bailer, M.E. Enama, Z. Moodie, J.E. Martin, M.M. McCluskey, B.K. Chakrabarti, L. Lamoreaux, C.A. Andrews, P.L. Gomez, J.R. Mascola, G.J. Nabel, and T. Vaccine Research Center 004 Study, *Phase 1 Safety and Immunogenicity Evaluation of a Multiclade HIV-1 DNA Candidate Vaccine.* The Journal of infectious diseases, 2006. **194**(12): p. 1650-1660.
130. Gurunathan, S., Wu, C-Y., Freidag, B.L., and Seder, R.A., *DNA vaccines: a key for inducing long-term cellular immunity.* Current Opinion in Immunology, 2000. **12**(4): p. 442–447.
131. Kent, S.J., A. Zhao, S.J. Best, J.D. Chandler, D.B. Boyle, and I.A. Ramshaw, *Enhanced T-Cell Immunogenicity and Protective Efficacy of a Human Immunodeficiency Virus Type 1 Vaccine Regimen Consisting of Consecutive Priming with DNA and Boosting with Recombinant Fowlpox Virus.* Journal of Virology, 1998. **72**(12): p. 10180-10188.
132. Letvin, N.L., D.C. Montefiori, Y. Yasutomi, H.C. Perry, M.-E. Davies, C. Lekutis, M. Alroy, D.C. Freed, C.I. Lord, L.K. Handt, M.A. Liu, and J.W. Shiver, *Potent, protective anti-HIV immune responses generated by bimodal HIV envelope DNA plus protein vaccination.* Proceedings of the National Academy of Sciences of the United States of America, 1997. **94**(17): p. 9378-9383.
133. Lu, S., J. Arthos, D.C. Montefiori, Y. Yasutomi, K. Manson, F. Mustafa, E. Johnson, J.C. Santoro, J. Wissink, J.I. Mullins, J.R. Haynes, N.L. Letvin, M. Wyand, and H.L. Robinson, *Simian immunodeficiency virus DNA vaccine trial in macaques.* Journal of Virology, 1996. **70**(6): p. 3978-3991.
134. Wang, H.B., Kondo, A., Yoshida, A., Yoshizaki, S., Abe, S., Bao, L. L., Mizuki, N., Ichino, M., Klinman, D., Okuda, K., and Shimada, M., *Partial protection against SIV challenge by vaccination of adenovirus and MVA vectors in rhesus monkeys.* Gene Therapy, 2010. **17**(1): p. 4-13.
135. Yasutomi, Y., H.L. Robinson, S. Lu, F. Mustafa, C. Lekutis, J. Arthos, J.I. Mullins, G. Voss, K. Manson, M. Wyand, and N.L. Letvin, *Simian immunodeficiency virus-specific cytotoxic T-lymphocyte induction through DNA vaccination of rhesus monkeys.* Journal of Virology, 1996. **70**(1): p. 678-681.

136. Johnson, P.R., Schnepp, B.C., Connell, M.J., Rohne, D., Robinson, S., Krivulka, G.R., Lord, C.I., Zinn, R., Montefiori, D.C., Letvin, N.L., and Clark, K.R., *Novel Adeno-Associated Virus Vector Vaccine Restricts Replication of Simian Immunodeficiency Virus in Macaques.* Journal of Virology, 2005. **79**(2): p. 955–965.
137. Tenenbaum, L., Lehtonen, E., and Monahan, P.E., *Evaluation of Risks Related to the Use of Adeno-Associated Virus-Based Vectors.* Current Gene Therapy, 2003. **3**(6): p. 545-565.
138. Zincarelli, C., Soltys, S., Rengo, G., and Rabinowitz, J.E., *Analysis of AAV Serotypes 1-9 Mediated Gene Expression and Tropism in Mice After Systemic Injection.* Molecular Therapy, 2008. **16**(6): p. 1073-1080.
139. Cohen, Y.Z., and Dolin, R., *Novel HIV vaccine strategies: overview and perspective.* Therapeutic Advances in Vaccines, 2013. **1**(3): p. 99-112.
140. Safrit, J.T., P.E. Fast, L. Gieber, H. Kuipers, H. Dean, and, and W.C. Koff, *Status of vaccine research and development of vaccines for HIV-1.* Vaccine, 2016. **34**(26): p. 2921-2925.
141. Gilbert, P., Wang, M., Wrin, T., Petropoulos, C., Gurwith, M., Sinangil, F., D'Souza, P., Rodriguez-Chavez, I.R., DeCamp, A., Giganti, M., Berman, P.W., Self, S.G., and Montefiori, D.C., *Magnitude and breadth of a nonprotective neutralizing antibody response in an efficacy trial of a candidate HIV-1 gp120 vaccine.* The Journal of Infectious Diseases, 2010. **202**(4): p. 595-605.
142. Flynn, N.M., Forthal, D.N., Harro, C.D., Judson, F.N., Mayer, K.H., Para, M.F.; rgp120 HIV Vaccine Study Group., *Placebo-controlled phase 3 trial of a recombinant glycoprotein 120 vaccine to prevent HIV-1 infection.* The Journal of Infectious Diseases, 2005. **191**(5): p. 654-665.
143. Buchbinder, S.P., Mehrotra, D.V., Duerr, A., Fitzgerald, D.W., Mogg, R., Li, D., Gilbert, P.B., Lama, J.R., Marmor, M., del Rio, C., McElrath, M.J., Casimiro, D.R., Gottesdiener, K.M., Chodakewitz, J.A., Corey, L., Robertson, M.N., and and t.S.S.P. Team., *Efficacy assessment of a cell-mediated immunity HIV-1 vaccine (the Step Study): a double-blind, randomised, placebo-controlled, test-of-concept trial.* The Lancet, 2008. **372**(9653): p. 1881–1893.
144. Duerr, A., Huang, Y., Buchbinder, S., Coombs, R.W., Sanchez, J., del Rio, C., Casapia, M., Santiago, S., Gilbert, P., Corey, L., Robertson, M.N.; Step/HVTN 504 Study Team., *Extended follow-up confirms early vaccine-enhanced risk of HIV acquisition and demonstrates waning effect over time among participants in a randomized trial of recombinant adenovirus HIV vaccine (Step Study).* The Journal of Infectious Diseases, 2012. **206**(2): p. 258-266.
145. McElrath, M.J., De Rosa, S.C., Moodie, Z., Dubey, S., Kierstead, L., Janes, H., Defawe, O.D., Carter, D.K., Hural, J., Akondy, R., Buchbinder, S.P., Robertson, M.N., Mehrotra, D.V., Self, S.G., Corey, L., Shiver, J.W., Casimiro, D.R.; Step Study Protocol Team., *HIV-1 vaccine-induced immunity in the test-of-concept Step Study: a case-cohort analysis.* The Lancet, 2008. **372**(9653): p. 1894-1905.
146. Fitzgerald, D.W., Janes, H., Robertson, M., Coombs, R., Frank, I., Gilbert, P., Loufty, M., Mehrotra, D., and Duerr, A., for and t.S.S.P. Team., *An Ad5-Vectored HIV-1 Vaccine Elicits Cell-mediated Immunity but does not Affect Disease Progression in HIV-1–infected Male Subjects: Results From a Randomized Placebo-Controlled Trial (The Step Study).* The Journal of Infectious Diseases, 2011. **203**(6): p. 765–772.
147. Gray, G.E., Allen, M., Moodie, Z., Churchyard, G., Bekker, L-G., Nchabeleng, M., Mlisana, K., Metch, B., de Bruyn, G., Latka, M.H., Roux, S., Mathebula, M., Naicker, N., Ducar, C., Carter, D.K., Puren, A., Eaton, N., McElrath, M.J., Robertson, M., Corey, L., and Kublin, J.G. , *Safety and efficacy assessment of the HVTN 503/Phambili Study:*

A double-blind randomized placebo-controlled test-of-concept study of a Clade B-based HIV-1 vaccine in South Africa. The Lancet Infectious Diseases, 2011. **11**(7): p. 507–515.

148. Rerks-Ngarm, S., Paris, R.M., Chunsutthiwat, S., Premsri, N., Namwat, C., Bowonwatanuwong, C., Li, S.S., Kaewkungkal, J., Trichavaroj, R., Churikanont, N., de Souza, M.S., Andrews, C., Francis, D., Adams, E., Flores, J., Gurunathan, S., Tartaglia, J., O'Connell, R.J., Eamsila, C., Nitayaphan, S., Ngauy, V., Thongcharoen, P., Kunasol, P., Michael, N.L., Robb, M.L., Gilbert, P.B., and Kim, J.H., *Extended evaluation of the virologic, immunologic, and clinical course of volunteers who acquired HIV-1 infection in a phase III vaccine trial of ALVAC-HIV and AIDSVAX B/E.* The Journal of Infectious Diseases, 2013. **207**(8): p. 1195-1205.
149. de Souza, M.S., Ratto-Kim, S., Chuenarom, W., Schuetz, A., Chantakulkij, S., Nuntapinit, B., Valencia-Micolta, A., Thelian, D., Nitayaphan, S., Pitisuttithum, P., Paris, R.M., Kaewkungwal, J., Michael, N.L., Rerks-Ngarm, S., Mathieson, B., Marovich, M., Currier, J.R., Kim, J.H.; Ministry of Public Health–Thai AIDS Vaccine Evaluation Group Collaborators., *The Thai phase III trial (RV144) vaccine regimen induces T cell responses that preferentially target epitopes within the V2 region of HIV-1 envelope.* Journal of Immunology, 2012. **188**(10): p. 5166-5176.
150. Hammer, S.M., Sobieszczyk, M.E., Janes, H., Karuna, S.T., Mulligan, M.J., Grove, D., Koblin, B.A., Buchbinder, S.P., Keefer, M.C., Tomaras, G.D., Frahm, N., Hural, J., Anude, C., Graham, B.S., Enama, M.E., Adams, E., DeJesus, E., Novak, R.M., Frank, I., Bentley, C., Ramirez, S., Fu, R., Koup, R.A., Mascola, J.R., Nabel, G.J., Montefiori, D.C., Kublin, J., McElrath, M.J., Corey, L., Gilbert, P.B.; HVTN 505 Study Team., *Efficacy trial of a DNA/rAd5 HIV-1 preventive vaccine.* The New England Journal of Medicine, 2013. **369**(22): p. 2083-2092.
151. Diseases, N.I.o.A.a.I., *Large-Scale HIV Vaccine Trial to Launch in South Africa*, in *NIH-Funded Study Will Test Safety, Efficacy of Vaccine Regimen*. 2016.
152. Wyatt, R., and Sodroski, J., *The HIV-1 Envelope Glycoproteins: Fusogens, Antigens, and Immunogens.* Science, 1998. **280**(5371): p. 1884-1888.
153. Postler, T.S., and Desrosiers, R.C., *The Tale of the Long Tail: the Cytoplasmic Domain of HIV-1 gp41.* Journal of Virology, 2013. **87**(1): p. 2-15.
154. Stein, B.S., and Engleman, E.G., *Intracellular Processing of the gp160 HIV- 1 Envelope Precursor.* The Journal of Biological Chemistry, 1990. **265**(5): p. 2640-2649.
155. Zhu, P., E. Chertova, J. Bess, J.D. Lifson, L.O. Arthur, J. Liu, K.A. Taylor, and K.H. Roux, *Electron tomography analysis of envelope glycoprotein trimers on HIV and simian immunodeficiency virus virions.* Proceedings of the National Academy of Sciences of the United States of America, 2003. **100**(26): p. 15812-15817.
156. Zanetti, G., J.A.G. Briggs, K. Grünewald, Q.J. Sattentau, and S.D. Fuller, *Cryo-Electron Tomographic Structure of an Immunodeficiency Virus Envelope Complex In Situ.* PLOS Pathogens, 2006. **2**(8): p. e83.
157. Dintzis, H.M., R.Z. Dintzis, and B. Vogelstein, *Molecular determinants of immunogenicity: the immunon model of immune response.* Proceedings of the National Academy of Sciences of the United States of America, 1976. **73**(10): p. 3671-3675.
158. Bachmann, M.F., U.H. Rohrer, T.M. Kundig, K. Burki, H. Hengartner, and R.M. Zinkernagel, *The influence of antigen organization on B cell responsiveness.* Science, 1993. **262**(5138): p. 1448.
159. Willey, R.L., R.A. Rutledge, S. Dias, T. Folks, T. Theodore, C.E. Buckler, and M.A. Martin, *Identification of conserved and divergent domains within the envelope gene of the acquired immunodeficiency syndrome retrovirus.* Proceedings of the National Academy of Sciences of the United States of America, 1986. **83**(14): p. 5038-5042.

160. Starcich, B.R., B.H. Hahn, G.M. Shaw, P.D. McNeely, S. Modrow, H. Wolf, E.S. Parks, W.P. Parks, S.F. Josephs, R.C. Gallo, and F. Wong-Staal, *Identification and characterization of conserved and variable regions in the envelope gene of HTLV-III/LAV, the retrovirus of AIDS.* Cell, 1986. **45**(5): p. 637-648.
161. Wyatt, R., and Sodroski, J., *The HIV-1 envelope glycoproteins: fusogens, antigens, and immunogens.* Science, 1998. **280**(5371): p. 1884-1888.
162. Munro, J.B., and Mothes, W., *Structure and Dynamics of the Native HIV-1 Env Trimer.* Journal of Virology, 2015. **89**(11): p. 5752-5755.
163. Munro, J.B., Gorman, J., Ma, X., Zhou, Z., Arthos, J., Burton, D.R., Courter, J.C., Koff, W.C., Smith, A.B., Kwong, P.D., Blanchard, S.C., and Mothes, W. , *Conformational dynamics of single HIV-1 Env trimers on the surface of native virions.* Science, 2014. **346**: p. 795-763.
164. Moore, P.L., Crooks, E.T., Porter, L., Zhu, P., Cayanan, C.S., Grise, H., Corcoran, P., Zwick, M.B., Franti, M., Morris, L., Roux, K.H., Burton, D.R., and Binley, J.M., *Nature of nonfunctional envelope proteins on the surface of human immunodeficiency virus type 1.* Journal of Virology, 2006. **80**(5): p. 2515–2528.
165. Lin, J., Zhi, Y., Mays, L., and Wilson, J.M., *Vaccines Based on Novel Adeno-Associated Virus Vectors Elicit Aberrant CD8+ T-Cell Responses in Mice.* Journal of Virology, 2007. **81**(21): p. 11840–11849.
166. Xiang, S., *Recent Advances on the Use of Structural Biology for the Design of Novel Envelope Immunogens of HIV-1.* Current HIV Research, 2013. **11**(6): p. 464-472.
167. Blattner, C., J.H. Lee, K. Sliepen, R. Derking, E. Falkowska, A.T. de la Peña, A. Cupo, J.-P. Julien, M. van Gils, P.S. Lee, W. Peng, J.C. Paulson, P. Poignard, D.R. Burton, J.P. Moore, R.W. Sanders, I.A. Wilson, and A.B. Ward, *Structural delineation of a quaternary, cleavage-dependent epitope at the gp41-gp120 interface on intact HIV-1 Env trimers.* Immunity, 2014. **40**(5): p. 669-680.
168. Burton, D.R., J. Pyati, R. Koduri, S.J. Sharp, G.B. Thornton, P.W. Parren, L.S. Sawyer, R.M. Hendry, N. Dunlop, P.L. Nara, and a. et, *Efficient neutralization of primary isolates of HIV-1 by a recombinant human monoclonal antibody.* Science, 1994. **266**(5187): p. 1024.
169. Falkowska, E., K.M. Le, A. Ramos, K.J. Doores, J.H. Lee, C. Blattner, A. Ramirez, R. Derking, M.J. van Gils, C.-H. Liang, R. McBride, B. von Bredow, S.S. Shivatare, C.-Y. Wu, P.-Y. Chan-Hui, Y. Liu, T. Feizi, M.B. Zwick, W.C. Koff, M.S. Seaman, K. Swiderek, J.P. Moore, D. Evans, J.C. Paulson, C.-H. Wong, A.B. Ward, I.A. Wilson, R.W. Sanders, P. Poignard, and D.R. Burton, *Broadly neutralizing HIV antibodies define a glycan-dependent epitope on the pre-fusion conformation of the gp41 protein on cleaved Envelope trimers.* Immunity, 2014. **40**(5): p. 657-668.
170. Georgiev, I.S., N.A. Doria-Rose, T. Zhou, Y. Do Kwon, R.P. Staupe, S. Moquin, G.-Y. Chuang, M.K. Louder, S.D. Schmidt, H.R. Altae-Tran, R.T. Bailer, K. McKee, M. Nason, S. O'Dell, G. Ofek, M. Pancera, S. Srivatsan, L. Shapiro, M. Connors, S.A. Migueles, L. Morris, Y. Nishimura, M.A. Martin, J.R. Mascola, and P.D. Kwong, *Delineating Antibody Recognition in Polyclonal Sera from Patterns of HIV-1 Isolate Neutralization.* Science, 2013. **340**(6133): p. 751.
171. Huang, J., B.H. Kang, M. Pancera, J.H. Lee, T. Tong, Y. Feng, I.S. Georgiev, G.-Y. Chuang, A. Druz, N.A. Doria-Rose, L. Laub, K. Sliepen, M.J. van Gils, A.T. de la Peña, R. Derking, P.-J. Klasse, S.A. Migueles, R.T. Bailer, M. Alam, P. Pugach, B.F. Haynes, R.T. Wyatt, R.W. Sanders, J.M. Binley, A.B. Ward, J.R. Mascola, P.D. Kwong, and M. Connors, *Broad and potent HIV-1 neutralization by a human antibody that binds the gp41-120 interface.* Nature, 2014. **515**(7525): p. 138-142.

172. Huang, J., G. Ofek, L. Laub, M.K. Louder, N.A. Doria-Rose, N.S. Longo, H. Imamichi, R.T. Bailer, B. Chakrabarti, S.K. Sharma, S.M. Alam, T. Wang, Y. Yang, B. Zhang, S.A. Migueles, R. Wyatt, B.F. Haynes, P.D. Kwong, J.R. Mascola, and M. Connors, *Broad and potent neutralization of HIV-1 by a gp41-specific human antibody.* Nature, 2012. **491**(7424): p. 406-412.
173. Kong, R., K. Xu, T. Zhou, P. Acharya, T. Lemmin, K. Liu, G. Ozorowski, C. Soto, J.D. Taft, R.T. Bailer, E.M. Cale, L. Chen, C.W. Choi, G.-Y. Chuang, N.A. Doria-Rose, A. Druz, I.S. Georgiev, J. Gorman, J. Huang, M.G. Joyce, M.K. Louder, X. Ma, K. McKee, S. O'Dell, M. Pancera, Y. Yang, S.C. Blanchard, W. Mothes, D.R. Burton, W.C. Koff, M. Connors, A.B. Ward, P.D. Kwong, and J.R. Mascola, *Fusion peptide of HIV-1 as a site of vulnerability to neutralizing antibody.* Science (New York, N.Y.), 2016. **352**(6287): p. 828-833.
174. McLellan, J.S., M. Pancera, C. Carrico, J. Gorman, J.-P. Julien, R. Khayat, R. Louder, R. Pejchal, M. Sastry, K. Dai, S. O'Dell, N. Patel, S. Shahzad-ul-Hussan, Y. Yang, B. Zhang, T. Zhou, J. Zhu, J.C. Boyington, G.-Y. Chuang, D. Diwanji, I. Georgiev, Y.D. Kwon, D. Lee, M.K. Louder, S. Moquin, S.D. Schmidt, Z.-Y. Yang, M. Bonsignori, J.A. Crump, S.H. Kapiga, N.E. Sam, B.F. Haynes, D.R. Burton, W.C. Koff, L.M. Walker, S. Phogat, R. Wyatt, J. Orwenyo, L.-X. Wang, J. Arthos, C.A. Bewley, J.R. Mascola, G.J. Nabel, W.R. Schief, A.B. Ward, I.A. Wilson, and P.D. Kwong, *Structure of HIV-1 gp120 V1/V2 domain with broadly neutralizing antibody PG9.* Nature, 2011. **480**(7377): p. 336-343.
175. Pejchal, R., K.J. Doores, L.M. Walker, R. Khayat, P.-S. Huang, S.-K. Wang, R.L. Stanfield, J.-P. Julien, A. Ramos, M. Crispin, R. Depetris, U. Katpally, A. Marozsan, A. Cupo, S. Maloveste, Y. Liu, R. McBride, Y. Ito, R.W. Sanders, C. Ogohara, J.C. Paulson, T. Feizi, C.N. Scanlan, C.-H. Wong, J.P. Moore, W.C. Olson, A.B. Ward, P. Poignard, W.R. Schief, D.R. Burton, and I.A. Wilson, *A Potent and Broad Neutralizing Antibody Recognizes and Penetrates the HIV Glycan Shield.* Science, 2011. **334**(6059): p. 1097.
176. Purtscher, M., A. Trkola, G. Gruber, A. Buchacher, R. Predl, F. Steindl, C. Tauer, R. Berger, N. Barrett, A. Jungbauer, and H. Katinger, *A Broadly Neutralizing Human Monoclonal Antibody against gp41 of Human Immunodeficiency Virus Type 1.* AIDS Research and Human Retroviruses, 1994. **10**(12): p. 1651-1658.
177. Scharf, L., J.F. Scheid, J.H. Lee, A.P. West, C. Chen, H. Gao, P.N.P. Gnanapragasam, R. Mares, M.S. Seaman, A.B. Ward, M.C. Nussenzweig, and P.J. Bjorkman, *Antibody 8ANC195 Reveals a Site of Broad Vulnerability on the HIV-1 Envelope Spike.* Cell reports, 2014. **7**(3): p. 785-795.
178. Scheid, J.F., H. Mouquet, B. Ueberheide, R. Diskin, F. Klein, T.Y.K. Oliveira, J. Pietzsch, D. Fenyo, A. Abadir, K. Velinzon, A. Hurley, S. Myung, F. Boulad, P. Poignard, D.R. Burton, F. Pereyra, D.D. Ho, B.D. Walker, M.S. Seaman, P.J. Bjorkman, B.T. Chait, and M.C. Nussenzweig, *Sequence and Structural Convergence of Broad and Potent HIV Antibodies That Mimic CD4 Binding.* Science (New York, N.y.), 2011. **333**(6049): p. 1633-1637.
179. Stiegler, G., R. Kunert, M. Purtscher, S. Wolbank, R. Voglauer, F. Steindl, and H. Katinger, *A Potent Cross-Clade Neutralizing Human Monoclonal Antibody against a Novel Epitope on gp41 of Human Immunodeficiency Virus Type 1.* AIDS Research and Human Retroviruses, 2001. **17**(18): p. 1757-1765.
180. Walker, L.M., M. Huber, K.J. Doores, E. Falkowska, R. Pejchal, J.-P. Julien, S.-K. Wang, A. Ramos, P.-Y. Chan-Hui, M. Moyle, J.L. Mitcham, P.W. Hammond, O.A. Olsen, P. Phung, S. Fling, C.-H. Wong, S. Phogat, T. Wrin, M.D. Simek, G.P.I. Protocol, W.C. Koff, I.A. Wilson, D.R. Burton, and P. Poignard, *Broad neutralization*

coverage of HIV by multiple highly potent antibodies. Nature, 2011. **477**(7365): p. 466-470.
181. Walker, L.M., S.K. Phogat, P.-Y. Chan-Hui, D. Wagner, P. Phung, J.L. Goss, T. Wrin, M.D. Simek, S. Fling, J.L. Mitcham, J.K. Lehrman, F.H. Priddy, O.A. Olsen, S.M. Frey, P.W. Hammond, G.P.I. Protocol, S. Kaminsky, T. Zamb, M. Moyle, W.C. Koff, P. Poignard, and D.R. Burton, *Broad and Potent Neutralizing Antibodies from an African Donor Reveal a New HIV-1 Vaccine Target.* Science (New York, N.y.), 2009. **326**(5950): p. 285-289.
182. Burton, D.R., and Hangartner, L., *Broadly Neutralizing Antibodies to HIV and Their Role in Vaccine Design.* Annual Review of Immunology, 2016. **34**: p. 635-659.
183. Sanders, R.W., van Gils, M.J., Derking, R., Sok, D., Ketas, T.J., Burger, J.A., Ozorowski, G., Cupo, A., Simonich, C., Goo, L., Arendt, H., Kim, H.J., Hyun Lee, J., Pugach, P., Williams, M., Debnath, G., Moldt, B., van Breemen, M.J., Isik, G., Medina-Ramírez, M., Willem Back, J., Koff, W.C., Julien, J-P., Rakasz, E.G., Seaman, M.S., Guttman, M., Lee, K.K., Johan Klasse, P., LaBranche, C., Schief, W.R., Wilson, I.A., Overbaugh, J., Burton, D.R., Ward, A.B., Montefiori, D.C., Dean, H., and Moore, J.P., *HIV-1 neutralizing antibodies induced by native-like envelope trimers.* Science, 2015. **349**(6244): p. aac4223-1 - aac4223-10.
184. Hraber, P., M.S. Seaman, R.T. Bailer, J.R. Mascola, D.C. Montefiori, and B.T. Korber, *Prevalence of broadly neutralizing antibody responses during chronic HIV-1 infection.* AIDS (London, England), 2014. **28**(2): p. 163-169.
185. Yamada, M., S. Hudson, O. Tournay, S. Bittenbender, S.S. Shane, B. Lange, Y. Tsujimoto, A.J. Caton, and G. Rovera, *Detection of minimal disease in hematopoietic malignancies of the B-cell lineage by using third-complementarity-determining region (CDR-III)-specific probes.* Proceedings of the National Academy of Sciences, 1989. **86**(13): p. 5123.
186. Lee, C.C., J.M. Perchiacca, and P.M. Tessier, *Toward aggregation-resistant antibodies by design.* Trends in Biotechnology. **31**(11): p. 612-620.
187. Liao, H.-X., Lynch, R., Zhou, T., Gao, F., Alam, S.M., Boyd, S.D., Fire, A.Z., Roskin, K.M., Schramm, C.A., Zhang, Z., Zhu, J., Shapiro, L., Mullikin, J.C., Gnanakaran, S., Hraber, P., Wiehe, K., Kelsoe, G., Yang, G., Xia, S-M., Montefiori, D.C., Parks, R., Lloyd, K.E., Scearce, R.M., Soderberg, K.A., Cohen, M., Kamanga, G., Louder, M.K., Tran, L.M., Chen, Y., Cai, F., Chen, S., Moquin, S., Du, X., Joyce, M.G., Srivatsan, S., Zhang, B., Zheng, A., Shaw, G.M., Hahn, B.H., Kepler, T.B., Korber, B.T.M., Kwong, P.D., Mascola, J.R., and Haynes, B.F., *Co-evolution of a broadly neutralizing HIV-1 antibody and founder virus.* Nature, 2013. **496**(7446): p. 469-476.
188. Williams, L.D., G. Ofek, S. Schätzle, J.R. McDaniel, X. Lu, N.I. Nicely, L. Wu, C.S. Lougheed, T. Bradley, M.K. Louder, K. McKee, R.T. Bailer, S. O'Dell, I.S. Georgiev, M.S. Seaman, R.J. Parks, D.J. Marshall, K. Anasti, G. Yang, X. Nie, N.L. Tumba, K. Wiehe, K. Wagh, B. Korber, T.B. Kepler, S. Munir Alam, L. Morris, G. Kamanga, M.S. Cohen, M. Bonsignori, S.-M. Xia, D.C. Montefiori, G. Kelsoe, F. Gao, J.R. Mascola, M.A. Moody, K.O. Saunders, H.-X. Liao, G.D. Tomaras, G. Georgiou, and B.F. Haynes, *Potent and broad HIV-neutralizing antibodies in memory B cells and plasma.* Science Immunology, 2017. **2**(7).
189. Sadanand, S., Suscovich, T.J., and Alter, G., *Broadly Neutralizing Antibodies Against HIV: New Insights to Inform Vaccine Design.* Annual Review of Medicine, 2016. **67**: p. 185–200.
190. Baba, T.W., V. Liska, R. Hofmann-Lehmann, J. Vlasak, W. Xu, S. Ayehunie, L.A. Cavacini, M.R. Posner, H. Katinger, G. Stiegler, B.J. Bernacky, T.A. Rizvi, R. Schmidt, L.R. Hill, M.E. Keeling, Y. Lu, J.E. Wright, T.-C. Chou, and R.M. Ruprecht, *Human*

neutralizing monoclonal antibodies of the IgG1 subtype protect against mucosal simian–human immunodeficiency virus infection. Nature Medicine, 2000. **6**: p. 200.

191. Hessell, A.J., E.G. Rakasz, D.M. Tehrani, M. Huber, K.L. Weisgrau, G. Landucci, D.N. Forthal, W.C. Koff, P. Poignard, D.I. Watkins, and D.R. Burton, *Broadly Neutralizing Monoclonal Antibodies 2F5 and 4E10 Directed against the Human Immunodeficiency Virus Type 1 gp41 Membrane-Proximal External Region Protect against Mucosal Challenge by Simian-Human Immunodeficiency Virus SHIV(Ba-L).* Journal of Virology, 2010. **84**(3): p. 1302-1313.
192. Shibata, R., T. Igarashi, N. Haigwood, A. Buckler–White, R. Ogert, W. Ross, R. Willey, M.W. Cho, and M.A. Martin, *Neutralizing antibody directed against the HIV–1 envelope glycoprotein can completely block HIV–1/SIV chimeric virus infections of macaque monkeys.* Nature Medicine, 1999. **5**: p. 204.
193. Trkola, A., H. Kuster, P. Rusert, B. Joos, M. Fischer, C. Leemann, A. Manrique, M. Huber, M. Rehr, A. Oxenius, R. Weber, G. Stiegler, B. Vcelar, H. Katinger, L. Aceto, and H.F. Günthard, *Delay of HIV-1 rebound after cessation of antiretroviral therapy through passive transfer of human neutralizing antibodies.* Nature Medicine, 2005. **11**: p. 615.
194. Moldt, B., E.G. Rakasz, N. Schultz, P.-Y. Chan-Hui, K. Swiderek, K.L. Weisgrau, S.M. Piaskowski, Z. Bergman, D.I. Watkins, P. Poignard, and D.R. Burton, *Highly potent HIV-specific antibody neutralization in vitro translates into effective protection against mucosal SHIV challenge in vivo.* Proceedings of the National Academy of Sciences of the United States of America, 2012. **109**(46): p. 18921-18925.
195. Saunders, K.O., L. Wang, M.G. Joyce, Z.-Y. Yang, A.B. Balazs, C. Cheng, S.-Y. Ko, W.-P. Kong, R.S. Rudicell, I.S. Georgiev, L. Duan, K.E. Foulds, M. Donaldson, L. Xu, S.D. Schmidt, J.-P. Todd, D. Baltimore, M. Roederer, A.T. Haase, P.D. Kwong, S.S. Rao, J.R. Mascola, and G.J. Nabel, *Broadly Neutralizing Human Immunodeficiency Virus Type 1 Antibody Gene Transfer Protects Nonhuman Primates from Mucosal Simian-Human Immunodeficiency Virus Infection.* Journal of Virology, 2015. **89**(16): p. 8334-8345.
196. Shingai, M., O.K. Donau, R.J. Plishka, A. Buckler-White, J.R. Mascola, G.J. Nabel, M.C. Nason, D. Montefiori, B. Moldt, P. Poignard, R. Diskin, P.J. Bjorkman, M.A. Eckhaus, F. Klein, H. Mouquet, J.C. Cetrulo Lorenzi, A. Gazumyan, D.R. Burton, M.C. Nussenzweig, M.A. Martin, and Y. Nishimura, *Passive transfer of modest titers of potent and broadly neutralizing anti-HIV monoclonal antibodies block SHIV infection in macaques.* The Journal of Experimental Medicine, 2014. **211**(10): p. 2061-2074.
197. Shingai, M., Y. Nishimura, F. Klein, H. Mouquet, O.K. Donau, R. Plishka, A. Buckler-White, M. Piatak, J.D. Lifson, D. Dimitrov, M.C. Nussenzweig, and M.A. Martin, *Antibody-mediated immunotherapy of macaques chronically infected with SHIV suppresses viraemia.* Nature, 2013. **503**(7475): p. 277-280.
198. Gruell, H., S. Bournazos, J.V. Ravetch, A. Ploss, M.C. Nussenzweig, and J. Pietzsch, *Antibody and Antiretroviral Preexposure Prophylaxis Prevent Cervicovaginal HIV-1 Infection in a Transgenic Mouse Model.* Journal of Virology, 2013. **87**(15): p. 8535-8544.
199. Halper-Stromberg, A., C.-L. Lu, F. Klein, J.A. Horwitz, S. Bournazos, L. Nogueira, T.R. Eisenreich, C. Liu, A. Gazumyan, U. Schaefer, R.C. Furze, M.S. Seaman, R. Prinjha, A. Tarakhovsky, J.V. Ravetch, and M.C. Nussenzweig, *Broadly Neutralizing Antibodies and Viral inducers decrease rebound from HIV-1 latent reservoirs in humanized mice.* Cell, 2014. **158**(5): p. 989-999.
200. Klein, F., A. Halper-Stromberg, J.A. Horwitz, H. Gruell, J.F. Scheid, S. Bournazos, H. Mouquet, L.A. Spatz, R. Diskin, A. Abadir, T. Zang, M. Dorner, E. Billerbeck, R.N.

Labitt, C. Gaebler, P. Marcovecchio, R.-B. Incesu, T.R. Eisenreich, P.D. Bieniasz, M.S. Seaman, P.J. Bjorkman, J.V. Ravetch, A. Ploss, and M.C. Nussenzweig, *HIV therapy by a combination of broadly neutralizing antibodies in humanized mice.* Nature, 2012. **492**(7427): p. 10.1038/nature11604.

201. Pietzsch, J., H. Gruell, S. Bournazos, B.M. Donovan, F. Klein, R. Diskin, M.S. Seaman, P.J. Bjorkman, J.V. Ravetch, A. Ploss, and M.C. Nussenzweig, *A mouse model for HIV-1 entry.* Proceedings of the National Academy of Sciences, 2012. **109**(39): p. 15859.
202. Caskey, M., F. Klein, J.C.C. Lorenzi, M.S. Seaman, A.P. West, N. Buckley, G. Kremer, L. Nogueira, M. Braunschweig, J.F. Scheid, J.A. Horwitz, I. Shimeliovich, S. Ben Avraham-Shulman, M. Witmer-Pack, M. Platten, C. Lehmann, L.A. Burke, T. Hawthorne, R.J. Gorelick, B.D. Walker, T. Keler, R.M. Gulick, G. Fätkenheuer, S.J. Schlesinger, and M.C. Nussenzweig, *3BNC117 a Broadly Neutralizing Antibody Suppresses Viremia in HIV-1-Infected Humans.* Nature, 2015. **522**(7557): p. 487-491.
203. Ledgerwood, J.E., E.E. Coates, G. Yamshchikov, J.G. Saunders, L. Holman, M.E. Enama, A. DeZure, R.M. Lynch, I. Gordon, S. Plummer, C.S. Hendel, A. Pegu, M. Conan-Cibotti, S. Sitar, R.T. Bailer, S. Narpala, A. McDermott, M. Louder, S. O'Dell, S. Mohan, J.P. Pandey, R.M. Schwartz, Z. Hu, R.A. Koup, E. Capparelli, J.R. Mascola, B.S. Graham, and V.R.C.S.T. the, *Safety, pharmacokinetics and neutralization of the broadly neutralizing HIV-1 human monoclonal antibody VRC01 in healthy adults.* Clinical and Experimental Immunology, 2015. **182**(3): p. 289-301.
204. Mayer, K.H., K.E. Seaton, Y. Huang, N. Grunenberg, A. Isaacs, M. Allen, J.E. Ledgerwood, I. Frank, M.E. Sobieszczyk, L.R. Baden, B. Rodriguez, H. Van Tieu, G.D. Tomaras, A. Deal, D. Goodman, R.T. Bailer, G. Ferrari, R. Jensen, J. Hural, B.S. Graham, J.R. Mascola, L. Corey, D.C. Montefiori, H.P.T. on behalf of the, and N.H.I.V.V.T.N. and the, *Safety, pharmacokinetics, and immunological activities of multiple intravenous or subcutaneous doses of an anti-HIV monoclonal antibody, VRC01, administered to HIV-uninfected adults: Results of a phase 1 randomized trial.* PLoS Medicine, 2017. **14**(11): p. e1002435.
205. Wibmer, C.K., P.L. Moore, and L. Morris, *HIV broadly neutralizing antibody targets.* Current opinion in HIV and AIDS, 2015. **10**(3): p. 135-143.
206. Wu, X., Z.-Y. Yang, Y. Li, C.-M. Hogerkorp, W.R. Schief, M.S. Seaman, T. Zhou, S.D. Schmidt, L. Wu, L. Xu, N.S. Longo, K. McKee, S. O'Dell, M.K. Louder, D.L. Wycuff, Y. Feng, M. Nason, N. Doria-Rose, M. Connors, P.D. Kwong, M. Roederer, R.T. Wyatt, G.J. Nabel, and J.R. Mascola, *Rational Design of Envelope Identifies Broadly Neutralizing Human Monoclonal Antibodies to HIV-1.* Science (New York, N.Y.), 2010. **329**(5993): p. 856-861.
207. Huang, J., Kang, B.H., Ishida, E., Zhou, T., Griesman, T., Sheng, Z., Wu, F., Doria-Rose, N.A., Zhang, B., McKee, K., O'Dell, S., Chuang, G.Y., Druz, A., Georgiev, I.S., Schramm, C.A., Zheng, A., Joyce, M.G., Asokan, M., Ransier, A., Darko, S., Migueles, S.A., Bailer, R.T., Louder, M.K., Alam, S.M., Parks, R., Kelsoe, G., Von Holle, T., Haynes, B.F., Douek, D.C., Hirsch, V., Seaman, M.S., Shapiro, L., Mascola, J.R., Kwong, P.D., and Connors, M., *Identification of a CD4-Binding-Site Antibody to HIV that Evolved Near-Pan Neutralization Breadth.* Immunity, 2016. **45**(5): p. 1108-1121.
208. Buchacher, A., R. Predl, K. Strutzenberger, W. Steinfellner, A. Trkola, M. Purtscher, G. Gruber, C. Tauer, F. Steindl, A. Jungbauer, and H. Katinger, *Generation of Human Monoclonal Antibodies against HIV-1 Proteins; Electrofusion and Epstein-Barr Virus Transformation for Peripheral Blood Lymphocyte Immortalization.* AIDS Research and Human Retroviruses, 1994. **10**(4): p. 359-369.
209. Zwick, M.B., A.F. Labrijn, M. Wang, C. Spenlehauer, E.O. Saphire, J.M. Binley, J.P. Moore, G. Stiegler, H. Katinger, D.R. Burton, and P.W.H.I. Parren, *Broadly*

Neutralizing Antibodies Targeted to the Membrane-Proximal External Region of Human Immunodeficiency Virus Type 1 Glycoprotein gp41. Journal of Virology, 2001. **75**(22): p. 10892-10905.

210. Bonsignori, M., Hwang, K-K., Chen, X., Tsao, C-Y., Morris, L., Gray, E., Marshall, D.J., Crump, J.A., Kapiga, S.H., Sam, N.E., Sinangil, F., Pancera, M., Yongping, Y., Zhang, B., Zhu, J., Kwong, P.D., O'Dell, S., Mascola, J.R., Wu, L., Nabel, G.J., Phogat, S., Seaman, M.S., Whitesides, J.F., Moody, M.A., Kelsoe, G., Yang, X., Sodroski, J., Shaw, G.M., Montefiori, D.C., Kepler, T.B., Tomaras, G.D., Alam, S.M., Liao, H-X., and Haynes, B.F., *Analysis of a Clonal Lineage of HIV-1 Envelope V2/V3 Conformational Epitope-Specific Broadly Neutralizing Antibodies and Their Inferred Unmutated Common Ancestors.* Journal of Virology, 2011. **85**(19): p. 9998–10009.
211. Meyer-Hermann, M., E. Mohr, N. Pelletier, Y. Zhang, Gabriel D. Victora, and K.-M. Toellner, *A Theory of Germinal Center B Cell Selection, Division, and Exit.* Cell Reports, 2012. **2**(1): p. 162-174.
212. Robert, P.A., A.L.J. Marschall, and M. Meyer-Hermann, *Induction of broadly neutralizing antibodies in Germinal Centre simulations.* Current Opinion in Biotechnology, 2018. **51**: p. 137-145.
213. Sheng, Z., Schramm, C.A., Connors, M., Morris, L., Mascola, J.R., Kwong, P.D., and Shapiro, L., *Effects of Darwinian Selection and Mutability on Rate of Broadly Neutralizing Antibody Evolution during HIV-1 Infection.* PLoS Computational Biology, 2016. **12**(5): p. e1004940.
214. Klein, F., Diskin, R., Scheid, J.F., Gaebler, C., Mouquet, H., Georgiev, I.S., Pancera, M., Zhou, T., Incesu, R.B., Fu, B.Z., Gnanapragasam, P.N., Oliveira, T.Y., Seaman, M.S., Kwong, P.D., Bjorkman, P.J., and Nussenzweig, M.C., *Somatic mutations of the immunoglobulin framework are generally required for broad and potent HIV-1 neutralization.* Cell, 2013. **153**(1): p. 126-138.
215. Gao, F., Bonsignori, M., Liao, H.X., Kumar, A., Xia, S.M., Lu, X., Cai, F., Hwang, K.K., Song, H., Zhou, T., Lynch, R.M., Alam, S.M., Moody, M.A., Ferrari, G., Berrong, M., Kelsoe, G., Shaw, G.M., Hahn, B.H., Montefiori, D.C., Kamanga, G., Cohen, M.S., Hraber, P., Kwong, P.D., Korber, B.T., Mascola, J.R., Kepler, T.B., and Haynes, B.F., *Cooperation of B cell lineages in induction of HIV-1-broadly neutralizing antibodies.* Cell, 2014. **158**(3): p. 481-491.
216. Bonsignori, M., E.F. Kreider, D. Fera, R.R. Meyerhoff, T. Bradley, K. Wiehe, S.M. Alam, B. Aussedat, W.E. Walkowicz, K.-K. Hwang, K.O. Saunders, R. Zhang, M.A. Gladden, A. Monroe, A. Kumar, S.-M. Xia, M. Cooper, M.K. Louder, K. McKee, R.T. Bailer, B.W. Pier, C.A. Jette, G. Kelsoe, W.B. Williams, L. Morris, J. Kappes, K. Wagh, G. Kamanga, M.S. Cohen, P.T. Hraber, D.C. Montefiori, A. Trama, H.-X. Liao, T.B. Kepler, M.A. Moody, F. Gao, S.J. Danishefsky, J.R. Mascola, G.M. Shaw, B.H. Hahn, S.C. Harrison, B.T. Korber, and B.F. Haynes, *Staged induction of HIV-1 glycan–dependent broadly neutralizing antibodies.* Science translational medicine, 2017. **9**(381): p. eaai7514.
217. MacLeod, D.T., N.M. Choi, B. Briney, F. Garces, L.S. Ver, E. Landais, B. Murrell, T. Wrin, W. Kilembe, C.-H. Liang, A. Ramos, C.B. Bian, L. Wickramasinghe, L. Kong, K. Eren, C.-Y. Wu, C.-H. Wong, I.P.C.I. The, I.A.H.I.V.R. The, S.L. Kosakovsky Pond, I.A. Wilson, D.R. Burton, and P. Poignard, *Early Antibody Lineage Diversification and Independent Limb Maturation Lead to Broad HIV-1 Neutralization Targeting the Env High-Mannose Patch.* Immunity, 2016. **44**(5): p. 1215-1226.
218. Simonich, C.A., K.L. Williams, H.P. Verkerke, J.A. Williams, R. Nduati, K.K. Lee, and J. Overbaugh, *HIV-1 neutralizing antibodies with limited hypermutation from an infant.* Cell, 2016. **166**(1): p. 77-87.

219. Bonsignori, M., Zhou, T., Sheng, Z., Chen, L., Gao, F., Joyce, M.G., Ozorowski, G., Chuang, G.Y., Schramm, C.A., Wiehe, K., Alam, S.M., Bradley, T., Gladden, M.A., Hwang, K.K., Iyengar, S., Kumar, A., Lu, X., Luo, K., Mangiapani, M.C., Parks, R.J., Song, H., Acharya, P., Bailer, R.T., Cao, A., Druz, A., Georgiev, I.S., Kwon, Y.D., Louder, M.K., Zhang, B., Zheng, A., Hill, B.J., Kong, R., Soto, C.; NISC Comparative Sequencing Program, Mullikin, J.C., Douek, D.C., Montefiori, D.C., Moody, M.A., Shaw, G.M., Hahn, B.H., Kelsoe, G., Hraber, P.T., Korber, B.T., Boyd, S.D., Fire, A.Z., Kepler, T.B., Shapiro, L., Ward, A.B., Mascola, J.R., Liao, H.X., Kwong, P.D., and Haynes, B.F., *Maturation Pathway from Germline to Broad HIV-1 Neutralizer of a CD4-Mimic Antibody.* Cell, 2016. **165**(2): p. 449-463.
220. Bonsignori, M., Liao, H.X., Gao, F., Williams, W.B., Alam, S.M., Montefiori, D.C., and Haynes, B.F., *Antibody-virus co-evolution in HIV infection: paths for HIV vaccine development.* Immunological Reviews, 2017. **275**(1): p. 145-160.
221. Malherbe, D.C., Doria-Rose, N.A., Misher, L., Beckett, T., Puryear, W.B., Schuman, J.T., Kraft, Z., O'Malley, J., Mori, M., Srivastava, I., Barnett, S., Stamatatos, L., and Haigwood, N.L., *Sequential Immunization with a Subtype B HIV-1 Envelope Quasispecies Partially Mimics the In Vivo Development of Neutralizing Antibodies.* Journal of Virology, 2011. **85**(11): p. 5262–5274.
222. Pissani, F., Malherbe, D.C., Robins, H., DeFilippis, V.R., Park, B., Sellhorn, G., Stamatatos, L., Overbaugh, J., and Haigwood, N.L., *Motif-optimized subtype A HIV envelope-based DNA vaccines rapidly elicit neutralizing antibodies when delivered sequentially.* Vaccine, 2012. **30**(37): p. 5519–5526.
223. Malherbe, D.C., Pissani, F., Sather, D.N., Guo, B., Pandey, S., Sutton, W.F., Stuart, A.B., Robins, H., Park, B., Krebs, S.J., Schuman, J.T., Kalams, S., Hessell, A.J., and Haigwood, N.L., *Envelope Variants Circulating as Initial Neutralization Breadth Developed in Two HIV-Infected Subjects Stimulate Multiclade Neutralizing Antibodies in Rabbits.* Journal of Virology, 2014. **88**(22): p. 12949–12967.
224. Dosenovic, P., L. von Boehmer, A. Escolano, J. Jardine, Natalia T. Freund, Alexander D. Gitlin, Andrew T. McGuire, Daniel W. Kulp, T. Oliveira, L. Scharf, J. Pietzsch, Matthew D. Gray, A. Cupo, Marit J. van Gils, K.-H. Yao, C. Liu, A. Gazumyan, Michael S. Seaman, Pamela J. Björkman, Rogier W. Sanders, John P. Moore, L. Stamatatos, William R. Schief, and Michel C. Nussenzweig, *Immunization for HIV-1 Broadly Neutralizing Antibodies in Human Ig Knockin Mice.* Cell, 2015. **161**(7): p. 1505-1515.
225. Wang, S., Mata-Fink, J., Kriegsman, B., Hanson, M., Irvine, D.J., Eisen, H.N., Burton, D.R., Wittrup, K.D., Kardar, M., and Chakraborty, A.K., *Manipulating the Selection Forces during Affinity Maturation to Generate Cross-Reactive HIV Antibodies.* Cell, 2015. **160**(4): p. 785–797.
226. Briney, B., Sok, D., Jardine, J.G., Kulp, D.W., Skog, P., Menis, S., Jacak, R., Kalyuzhniy, O., de Val, N., Sesterhenn, F., Le, K.M., Ramos, A., Jones, M., Saye-Francisco, K.L., Blane, T.R., Spencer, S., Georgeson, E., Hu, X., Ozorowski, G., Adachi, Y., Kubitz, M., Sarkar, A., Wilson, I.A., Ward, A.B., Nemazee, D., Burton, D.R., and Schief, W.R., *Tailored Immunogens Direct Affinity Maturation toward HIV Neutralizing Antibodies.* Cell, 2016. **166**(6): p. 1459-1470.
227. Escolano, A., Steichen, J.M., Dosenovic, P., Kulp, D.W., Golijanin, J., Sok, D., Freund, N.T., Gitlin, A.D., Oliveira, T., Araki, T., Lowe, S., Chen, S.T., Heinemann, J., Yao, K.H., Georgeson, E., Saye-Francisco, K.L., Gazumyan, A., Adachi, Y., Kubitz, M., Burton, D.R., Schief, W.R., and Nussenzweig, M.C., *Sequential Immunization Elicits Broadly Neutralizing Anti-HIV-1 Antibodies in Ig Knockin Mice.* Cell, 2016. **166**(6): p. 1445-1458.

228. Steichen, Jon M., Daniel W. Kulp, T. Tokatlian, A. Escolano, P. Dosenovic, Robyn L. Stanfield, Laura E. McCoy, G. Ozorowski, X. Hu, O. Kalyuzhniy, B. Briney, T. Schiffner, F. Garces, Natalia T. Freund, Alexander D. Gitlin, S. Menis, E. Georgeson, M. Kubitz, Y. Adachi, M. Jones, Andrew A. Mutafyan, Dong S. Yun, Christian T. Mayer, Andrew B. Ward, Dennis R. Burton, Ian A. Wilson, Darrell J. Irvine, Michel C. Nussenzweig, and William R. Schief, *HIV Vaccine Design to Target Germline Precursors of Glycan-Dependent Broadly Neutralizing Antibodies.* Immunity, 2016. **45**(3): p. 483-496.
229. Tian, M., Cheng, C., Chen, X., Duan, H., Cheng, H.L., Dao, M., Sheng, Z., Kimble, M., Wang, L., Lin, S., Schmidt, S.D., Du, Z., Joyce, M.G., Chen, Y., DeKosky, B.J., Chen, Y., Normandin, E., Cantor, E., Chen, R.E., Doria-Rose, N.A., Zhang, Y., Shi, W., Kong, W.P., Choe, M., Henry, A.R., Laboune, F., Georgiev, I.S., Huang, P.Y., Jain, S., McGuire, A.T., Georgeson, E., Menis, S., Douek, D.C., Schief, W.R., Stamatatos, L., Kwong, P.D., Shapiro, L., Haynes, B.F., Mascola, J.R., and Alt, F.W., *Induction of HIV Neutralizing Antibody Lineages in Mice with Diverse Precursor Repertoires.* Cell, 2016. **166**(6): p. 1471-1484.
230. Williams, W.B., J. Zhang, C. Jiang, N.I. Nicely, D. Fera, K. Luo, M.A. Moody, H.-X. Liao, S.M. Alam, T.B. Kepler, A. Ramesh, K. Wiehe, J.A. Holland, T. Bradley, N. Vandergrift, K.O. Saunders, R. Parks, A. Foulger, S.-M. Xia, M. Bonsignori, D.C. Montefiori, M. Louder, A. Eaton, S. Santra, R. Scearce, L. Sutherland, A. Newman, H. Bouton-Verville, C. Bowman, H. Bomze, F. Gao, D.J. Marshall, J.F. Whitesides, X. Nie, G. Kelsoe, S.G. Reed, C.B. Fox, K. Clary, M. Koutsoukos, D. Franco, J.R. Mascola, S.C. Harrison, B.F. Haynes, and L. Verkoczy, *Initiation of HIV neutralizing B cell lineages with sequential envelope immunizations.* Nature Communications, 2017. **8**(1): p. 1732.
231. Hastie, E. and R.J. Samulski, *Adeno-Associated Virus at 50: A Golden Anniversary of Discovery, Research, and Gene Therapy Success—A Personal Perspective.* Human Gene Therapy, 2015. **26**(5): p. 257-265.
232. Russell, D.W. and M.A. Kay, *Adeno-Associated Virus Vectors and Hematology.* Blood, 1999. **94**(3): p. 864-874.
233. Yan, Z., Zak, R., Zhang, Y., and Engelhardt, J.F., *Inverted Terminal Repeat Sequences Are Important for Intermolecular Recombination and Circularization of Adeno-Associated Virus Genomes.* Journal of Virology, 2005. **79**(1): p. 364–379.
234. Walsh, C.E., J.M. Liu, X. Xiao, N.S. Young, A.W. Nienhuis, and R.J. Samulski, *Regulated High Level Expression of a Human γ-Globin Gene Introduced Into Erythroid Cells by an Adeno-Associated Virus Vector.* Proceedings of the National Academy of Sciences of the United States of America, 1992. **89**(15): p. 7257-7261.
235. Flotte, T.R., S.A. Afione, C. Conrad, S.A. McGrath, R. Solow, H. Oka, P.L. Zeitlin, W.B. Guggino, and B.J. Carter, *Stable in vivo expression of the cystic fibrosis transmembrane conductance regulator with an adeno-associated virus vector.* Proceedings of the National Academy of Sciences of the United States of America, 1993. **90**(22): p. 10613-10617.
236. Miller, J.L., C.E. Walsh, P.A. Ney, R.J. Samulski, and A.W. Nienhuis, *Single-copy transduction and expression of human gamma-globin in K562 erythroleukemia cells using recombinant adeno-associated virus vectors: the effect of mutations in NF-E2 and GATA-1 binding motifs within the hypersensitivity site 2 enhancer [published erratum appears in Blood 1995 Feb 1;85(3):862]*. Blood, 1993. **82**(6): p. 1900.
237. Kaplitt, M.G., P. Leone, R.J. Samulski, X. Xiao, D.W. Pfaff, K.L. O'Malley, and M.J. During, *Long-term gene expression and phenotypic correction using adeno-associated virus vectors in the mammalian brain.* Nature Genetics, 1994. **8**: p. 148.

238. Kaplitt, M.G., Xiao, X., Samulski, R.J., Li, J., Ojamaa, K., Klein, I.L., Makimura, H., Kaplitt, M.J., Strumpf, R.K., and Diethrich, E.B. and *Long-Term Gene Transfer in Porcine Myocardium After Coronary Infusion of an Adeno-Associated Virus Vector.* Annuals Thoracic Surgery, 1996. **62**: p. 1669-1676.
239. Manning, W.C., Paliard, X., Zhou, S., Pat Bland, M., Lee, A.Y., Hong, K., Walker, C.M., Escobedo, J.A., and Dwarki, V., *Genetic Immunization with Adeno-Associated Virus Vectors Expressing Herpes Simplex Virus Type 2 Glycoproteins B and D.* Journal of Virology, 1997. **71**(10): p. 7960–7962.
240. Bartlett, J.S., R.J. Samulski, and T.J. McCown, *Selective and Rapid Uptake of Adeno-Associated Virus Type 2 in Brain.* Human Gene Therapy, 1998. **9**(8): p. 1181-1186.
241. Carter, B.J., *Adeno-Associated Virus Vectors in Clinical Trials.* Human Gene Therapy, 2005. **16**(5): p. 541-550.
242. Naso, M.F., B. Tomkowicz, W.L. Perry, and W.R. Strohl, *Adeno-Associated Virus (AAV) as a Vector for Gene Therapy.* Biodrugs, 2017. **31**(4): p. 317-334.
243. Balazs, A.B., Chen, J., Hong, C.M., Rao, D.S., Yang, L., and Baltimore, D., *Antibody-based protection against HIV infection by vectored immunoprophylaxis.* Nature, 2012. **481**(7379): p. 81-84.
244. Lewis, A.D., Chen, R., Montefiori, D.C., Johnson, P.R., and Clark, K.R., *Generation of Neutralizing Activity against Human Immunodeficiency Virus Type 1 in Serum by Antibody Gene Transfer.* Journal of Virology, 2002. **76**(17): p. 8769–8775.
245. Gardner, M.R., Kattenhorn, L.M., Kondur, H.R., von Schaewen, M., Dorfman, T., Chiang, J.J., Haworth, K.G., Decker, J.M., Alpert, M.D., Bailey, C.C., Neale Jr, E.S., Fellinger, C.H., Joshi, V.R., Fuchs, S.P., Martinez-Navio, J.M., Quinlan, B.D., Yao, A.Y., Mouquet, H., Gorman, J., Zhang, B., Poignard, P., Nussenzweig, M.C., Burton, D.R., Kwong, P.D., Piatak Jr, M., Lifson, J.D., Gao, G., Desrosiers, R.C., Evans, D.T., Hahn, B.H., Ploss, A., Cannon, P.M., Seaman, M.S., and Farzan, M., *AAV-expressed eCD4-Ig provides durable protection from multiple SHIV challenges.* Nature 2015. **5**(519): p. 87-91.
246. Lin, J., Calcedo, R., Vandenberghe, L.H., Bell, P., Somanathan, S., and Wilson, J.M., *A New Genetic Vaccine Platform Based on an Adeno-Associated Virus Isolated from a Rhesus Macaque.* Journal Of Virology, 2009. **83**(24): p. 12738–12750.
247. Killick, M., Capovilla, A., and Papathanasopoulos, M.A. , *Generation and Characterization of an HIV-1 Subtype C Transmitted and Early Founder Virus Consensus Sequence.* AIDS Research and Human Retroviruses, 2014. **30**(10): p. 1001-1005.
248. Liu, Y., McNevin, J., Cao, J., Zhao, H., Genowati, I., Wong, K., McLaughlin, S., McSweyn, M.D., Diem, K., Stevens, C.E., Maenza, J., He, H., Nickle, D.C., Shriner, D., Holte, S.E., Collier, A.C., Corey, L., McElrath, M.J., and Mullins, J.I., *Selection on the Human Immunodeficiency Virus Type 1 Proteome following Primary Infection.* Journal of Virology, 2006. **80**(19): p. 9519–9529.
249. Bunnik, E.M., Pisas, L., van Nuenen, A.C., and Schuitemaker, H., *Autologous Neutralizing Humoral Immunity and Evolution of the Viral Envelope in the Course of Subtype B Human Immunodeficiency Virus Type 1 Infection.* Journal of Virology, 2008. **82**(16): p. 7932–7941.
250. Carvajal-Rodriguez, A., Posada, D., Pe´rez-Losada, M., Keller, E., Abrams, E.J., Viscidi, R.P., and Crandall, K.A., *Disease progression and evolution of the HIV-1 env gene in 24 infected infants.* Infection, Genetics and Evolution, 2008. **8**(2): p. 110-120.
251. Coetzer, M., Cilliers, T., Papathanasopoulos, M., Ramjee, G., Abdool Karim, S., Williamson, C., and Morris, L., *Longitudinal Analysis of HIV Type 1 Subtype C*

Envelope Sequences from South Africa. AIDS Research and Human Retroviruses, 2007. **23**(2): p. 316-321.
252. Shankarappa, R., Margolick, J.B., Gange, S.J., Rodrigo, A.G., Upchurch, D., Farzadegan, H., Gupta, P., Rinaldo, C.R., Learn, G.H., He, X., Huang, X.L., and Mullins, J.I., *Consistent viral evolutionary changes associated with the progression of human immunodeficiency virus type 1 infection.* Journal of Virology, 1999. **73**(12): p. 10489-10502.
253. Shriner, D., Shankarappa, R., Jensen, M.A., Nickle, D.C., Mittler, J.E., Margolick, J.B., and Mullins, J.I., *Influence of Random Genetic Drift on Human Immunodeficiency Virus Type 1 env Evolution During Chronic Infection.* Genetics, 2004. **166**(3): p. 1155-1164.
254. Larkin, M.A., Blackshields, G., Brown, N.P., Chenna, R., McGettigan, P.A., McWilliam, H., Valentin, F., Wallace, I.M., Wilm, A., Lopez, R., Thompson, J.D., Gibson, T.J. and Higgins, D.G., *Clustal W and Clustal X version 2.0. .* Bioinformatics, 2007. **23**(21): p. 1596-1599.
255. Nicholas, K.B., Nicholas, H.B.J., and Deerfield, D.W.I., *GeneDoc: Analysis and Visualization of Genetic Variation.* Embnew.news 1997. **4**(14).
256. Harbury, P.B., Zhang, T., Kim, P.S. and Alber, T., *A switch between two-, three-, and four-stranded coiled coils in GCN4 leucine zipper mutants.* Science, 1993. **262**(5138): p. 1401-1407.
257. Yang, X., Florin, L., Farzan, M., Kolchinsky, P., Kwong, P.D., Sodroski, J., and Wyatt, R., *Modifications that stabilize human immunodeficiency virus envelope glycoprotein trimers in solution.* Journal of Virology 2000. **74**(10): p. 4746–4754.
258. Yang, X., Farzan, M., Wyatt, R., and Sodroski, J., *Characterization of Stable, Soluble Trimers Containing Complete Ectodomains of Human Immunodeficiency Virus Type 1 Envelope Glycoproteins.* Journal of Virology, 2000. **74**(12): p. 5716–5725.
259. Aruffo, A., Stamenkovic, I., Melnick, M., Underhill, C.B. and Seed, B., *CD44 is the principal cell surface receptor for hyaluronate.* Cell, 1990. **61**(7): p. 1303-1313.
260. Haas, J., Park, E-C., and Seed, B., *Codon usage limitation in the expression of HIV-1 envelope glycoprotein.* Current Biology, 1996. **6**(3): p. 315-324.
261. Kibbe, W.A., *OligoCalc: an online oligonucleotide properties calculator.* Nucleic Acids Research, 2007. **35**: p. W43–W46.
262. Killick, M.A., Grant, M.L., Cerutti, N.M., Capovilla, A., and Papathanasopoulos, M.A., *Env-2dCD4 S60C complexes act as super immunogens and elicit potent, broadly neutralizing antibodies against clinically relevant human immunodeficiency virus type 1 (HIV-1).* Vaccine, 2015. **33**(46): p. 6298-6306.
263. Thomas, P., and Smart, T.G. 2005. HEK293 cell line: A vehicle for the expression of recombinant proteins. Journal of Pharmacological and Toxicological Methods, 51, 187-200., *HEK293 cell line: A vehicle for the expression of recombinant proteins.* Journal of Pharmacological and Toxicological Methods, 2005. **51**(3): p. 187-200.
264. Feng, Y., K. McKee, K. Tran, S. O'Dell, S.D. Schmidt, A. Phogat, M.N. Forsell, G.B. Karlsson Hedestam, J.R. Mascola, and R.T. Wyatt, *Biochemically Defined HIV-1 Envelope Glycoprotein Variant Immunogens Display Differential Binding and Neutralizing Specificities to the CD4-binding Site.* The Journal of Biological Chemistry, 2012. **287**(8): p. 5673-5686.
265. Hoefer, *Protein Electrophoresis Apllications Guide*. 1994: Hoefer Scientific Instruments
266. Chen, W., Y. Feng, R. Gong, Z. Zhu, Y. Wang, Q. Zhao, and D.S. Dimitrov, *Engineered Single Human CD4 Domains as Potent HIV-1 Inhibitors and Components of Vaccine Immunogens.* Journal of Virology, 2011. **85**(18): p. 9395-9405.

267. Thali, M., Moore, J. P., Furman, C., Charles, M., Ho, D. D., Robinson, J. and Sodroski, J., *Characterization of conserved human immunodeficiency virus type 1 gp120 neutralization epitopes exposed upon gp120-CD4 binding.* Journal of Virology, 1993. **67**(7): p. 3978-3988.
268. Kwong, P.D., R. Wyatt, J. Robinson, R.W. Sweet, J. Sodroski, and W.A. Hendrickson, *Structure of an HIV gp120 envelope glycoprotein in complex with the CD4 receptor and a neutralizing human antibody.* Nature, 1998. **393**(6686): p. 648-659.
269. Sambrook, J.F., and Russell, D.W., *Molecular Cloning: A Laboratory Manual*. Vol. 1, 2, and 3. 2001, Cold Spring Harbor, N.Y.: Cold Spring Harbor Laboratory Press.
270. Lock, M., Alvira, M., Vandenberghe, L.H., Samanta, A., Toelen, J., Debyser, Z., and Wilson, J.M., *Rapid, Simple, and Versatile Manufacturing of Recombinant Adeno-Associated Viral Vectors at Scale.* Human Gene Therapy, 2010. **21**(10): p. 1259-1271.
271. Hermens, W.T.J.M.C., Ter Brake, O., Dijkhuizen, P.A., Sonnemans, M.A.F., Grimm, D., Kleinschmidt, J.A., and Verhaagen, J., *Purification of Recombinant Adeno-Associated Virus by Iodixanol Gradient Ultracentrifugation Allows Rapid and Reproducible Preparation of Vector Stocks for Gene Transfer in the Nervous System.* Human Gene Therapy, 1999. **10**(11): p. 1885-1891.
272. Lock, M., Alvira, M.R., Chen, S-J., and Wilson, J.M., *Absolute Determination of Single-Stranded and Self-Complementary Adeno-Associated Viral Vector Genome Titers by Droplet Digital PCR.* Human Gene Therapy Methods, 2013. **25**(2): p. 115–125.
273. Untergasser, A., H. Nijveen, X. Rao, T. Bisseling, R. Geurts, and J.A.M. Leunissen, *Primer3Plus, an enhanced web interface to Primer3.* Nucleic Acids Research, 2007. **35**(Web Server issue): p. W71-W74.
274. Rozen, S., and Skaletsky, H.J., *Primer3 on the WWW for general users and for biologist programmers.*, in *Bioinformatics Methods and Protocols: Methods in Molecular Biology.*, S. Krawetz, and Misener, S., Editor. 2000, Humana Press: Totowa, NJ. p. 365-386.
275. Araújo, L.A.L., and Almeida, S.E.M., *HIV-1 Diversity in the Envelope Glycoproteins: Implications for Viral Entry Inhibition.* Viruses, 2013. **5**: p. 595-604.
276. Hemelaar, J., *Implications of HIV diversity for the HIV-1 pandemic.* Journal of Infection, 2013. **66**(5): p. 391–400.
277. Frost, S.D.W., Y. Liu, S.L.K. Pond, C. Chappey, T. Wrin, C.J. Petropoulos, S.J. Little, and D.D. Richman, *Characterization of Human Immunodeficiency Virus Type 1 (HIV-1) Envelope Variation and Neutralizing Antibody Responses during Transmission of HIV-1 Subtype B.* Journal of Virology, 2005. **79**(10): p. 6523-6527.
278. Olshevsky, U., E. Helseth, C. Furman, J. Li, W. Haseltine, and J. Sodroski, *Identification of individual human immunodeficiency virus type 1 gp120 amino acids important for CD4 receptor binding.* Journal of Virology, 1990. **64**(12): p. 5701-5707.
279. Pantophlet, R., E. Ollmann Saphire, P. Poignard, P.W.H.I. Parren, I.A. Wilson, and D.R. Burton, *Fine Mapping of the Interaction of Neutralizing and Nonneutralizing Monoclonal Antibodies with the CD4 Binding Site of Human Immunodeficiency Virus Type 1 gp120.* Journal of Virology, 2003. **77**(1): p. 642-658.
280. Li, Y., S. O'Dell, L.M. Walker, X. Wu, J. Guenaga, Y. Feng, S.D. Schmidt, K. McKee, M.K. Louder, J.E. Ledgerwood, B.S. Graham, B.F. Haynes, D.R. Burton, R.T. Wyatt, and J.R. Mascola, *Mechanism of Neutralization by the Broadly Neutralizing HIV-1 Monoclonal Antibody VRC01.* Journal of Virology, 2011. **85**(17): p. 8954-8967.
281. Khattar, S.K., Samal, S., LaBranche, C.C., Montefiori, D.C., Collins, P.L., and Samal, S.K., *Comparative Immunogenicity of HIV-1 gp160, gp140 and gp120 Expressed by Live Attenuated Newcastle Disease Virus Vector.* PLOS One, 2013. **8**(10): p. 1-13.

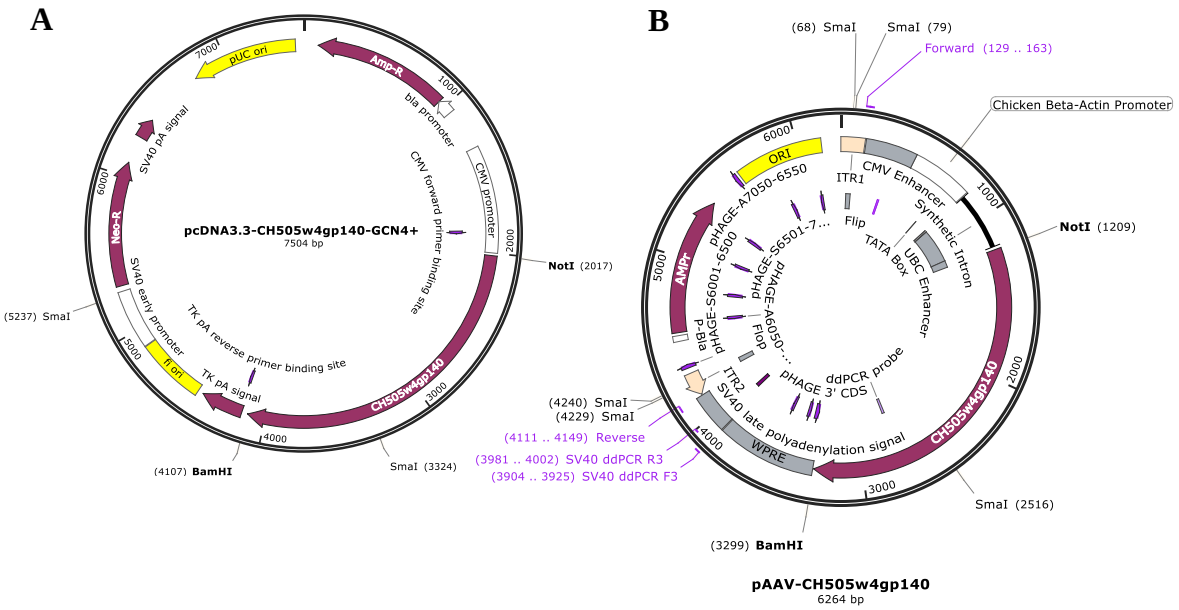
282. Mascola, J.R., Snyder, S.W., Weislow, O.S., Belay, S.M., Belshe, R.B., Schwartz, D.H., Clements, M.L., Dolin, R., Graham, B.S., Gorse, G.J., Keefer, M.C., McElrath, M.J., Walker, M.C., Wagner, K.F., McNeil, J.G., McCutchan, F.E., and Burke, D.S., *Immunization with envelope subunit vaccine products elicits neutralizing antibodies against laboratory-adapted but not primary isolates of human immunodeficiency virus type 1. The National Institute of Allergy and Infectious Diseases AIDS Vaccine Evaluation Group.* The Journal of Infectious Diseases, 1996. **173**(2): p. 340-348.
283. Burton, D.R., Desrosiers, R.C., Doms, R.W., Koff, W.C., Kwong, P.D., Moore, J.P., Nabel, G.J., Sodroski, J., Wilson, I.A., and Wyatt, R.T., *HIV vaccine design and the neutralizing antibody problem.* Nature Immunology, 2004. **5**(3): p. 233-236.
284. Schülke, N., M.S. Vesanen, R.W. Sanders, P. Zhu, M. Lu, D.J. Anselma, A.R. Villa, P.W.H.I. Parren, J.M. Binley, K.H. Roux, P.J. Maddon, J.P. Moore, and W.C. Olson, *Oligomeric and Conformational Properties of a Proteolytically Mature, Disulfide-Stabilized Human Immunodeficiency Virus Type 1 gp140 Envelope Glycoprotein.* Journal of Virology, 2002. **76**(15): p. 7760-7776.
285. Srivastava, I.K., L. Stamatatos, E. Kan, M. Vajdy, Y. Lian, S. Hilt, L. Martin, C. Vita, P. Zhu, K.H. Roux, L. Vojtech, D. C. Montefiori, J. Donnelly, J.B. Ulmer, and S.W. Barnett, *Purification, Characterization, and Immunogenicity of a Soluble Trimeric Envelope Protein Containing a Partial Deletion of the V2 Loop Derived from SF162, an R5-Tropic Human Immunodeficiency Virus Type 1 Isolate.* Journal of Virology, 2003. **77**(20): p. 11244-11259.
286. Yang, X., J. Lee, E.M. Mahony, P.D. Kwong, R. Wyatt, and J. Sodroski, *Highly Stable Trimers Formed by Human Immunodeficiency Virus Type 1 Envelope Glycoproteins Fused with the Trimeric Motif of T4 Bacteriophage Fibritin.* Journal of Virology, 2002. **76**(9): p. 4634-4642.
287. Zhang, P.F., F. Cham, M. Dong, A. Choudhary, P. Bouma, Z. Zhang, Y. Shao, Y.-R. Feng, L. Wang, N. Mathy, G. Voss, C.C. Broder, and G.V. Quinnan, *Extensively cross-reactive anti-HIV-1 neutralizing antibodies induced by gp140 immunization.* Proceedings of the National Academy of Sciences of the United States of America, 2007. **104**(24): p. 10193-10198.
288. Binley, J.M., Sanders, R.W., Clas, B., Schuelke, N., Master, A., Guo, Y., Kajumo, F., Anselma, D.J., Maddon, P.J., Olson, W.C., and Moore, J.P., *A recombinant human immunodeficiency virus type 1 envelope glycoprotein complex stabilized by an intermolecular disulfide bond between the gp120 and gp41 subunits is an antigenic mimic of the trimeric virion-associated structure.* Journal of Virology, 2000. **74**(2): p. 627-643.
289. Sanders, R.W., Vesanen, M., Schuelke, N., Master, A., Schiffner, L., Kalyanaraman, R., Paluch, M., Berkhout, B., Maddon, P.J., Olson, W.C., Lu, M., and Moore, J.P., *Stabilization of the soluble, cleaved, trimeric form of the envelope glycoprotein complex of human immunodeficiency virus type 1.* Journal of Virology, 2002. **76**(17): p. 8875-8889.
290. Pancera, M., J. Lebowitz, A. Schön, P. Zhu, E. Freire, P.D. Kwong, K.H. Roux, J. Sodroski, and R. Wyatt, *Soluble Mimetics of Human Immunodeficiency Virus Type 1 Viral Spikes Produced by Replacement of the Native Trimerization Domain with a Heterologous Trimerization Motif: Characterization and Ligand Binding Analysis.* Journal of Virology, 2005. **79**(15): p. 9954-9969.
291. Du, S.X., R.J. Idiart, E.B. Mariano, H. Chen, P. Jiang, L. Xu, K.M. Ostrow, T. Wrin, P. Phung, J.M. Binley, C.J. Petropoulos, J.A. Ballantyne, and R.G. Whalen, *Effect of Trimerization Motifs on Quaternary Structure, Antigenicity, and Immunogenicity of a Non-cleavable HIV-1 gp140 Envelope Glycoprotein.* Virology, 2009. **395**(1): p. 33-44.

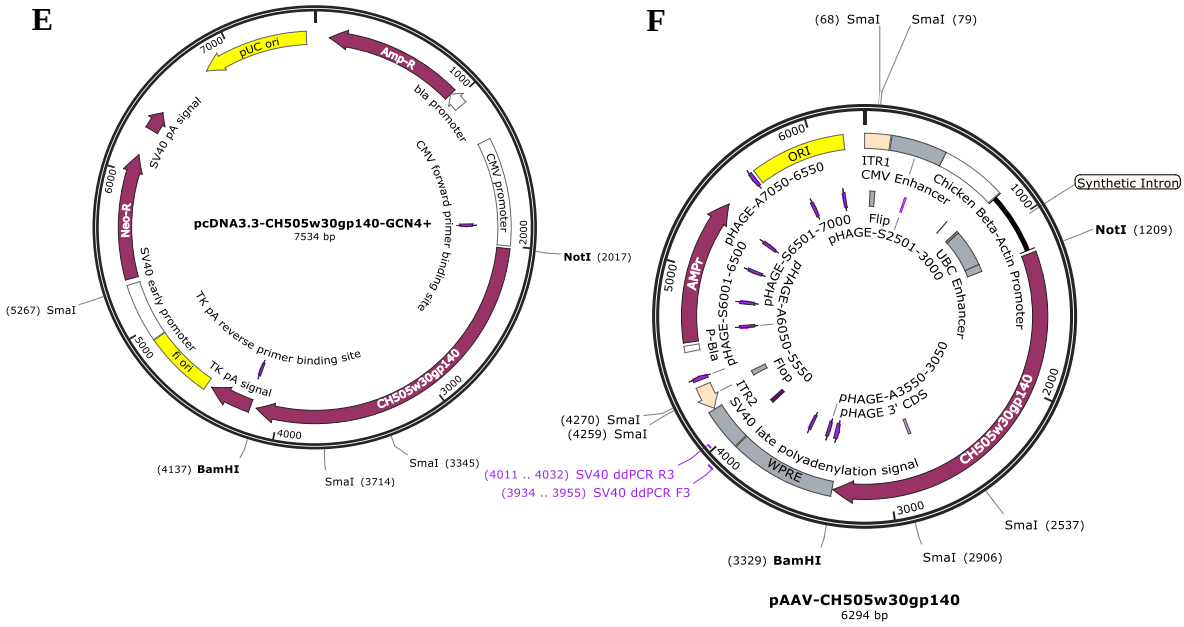
292. Kothe, D.L., Y. Li, J.M. Decker, F. Bibollet-Ruche, K.P. Zammit, M.G. Salazar, Y. Chen, Z. Weng, E.A. Weaver, F. Gao, B.F. Haynes, G.M. Shaw, B.T.M. Korber, and B.H. Hahn, *Ancestral and consensus envelope immunogens for HIV-1 subtype C.* Virology, 2006. **352**(2): p. 438-449.
293. Zhang, W., A.P. Godillot, R. Wyatt, J. Sodroski, and I. Chaiken, *Antibody 17b Binding at the Coreceptor Site Weakens the Kinetics of the Interaction of Envelope Glycoprotein gp120 with CD4.* Biochemistry, 2001. **40**(6): p. 1662-1670.
294. Kothe, D.L., J.M. Decker, Y. Li, Z. Weng, F. Bibollet-Ruche, K.P. Zammit, M.G. Salazar, Y. Chen, J.F. Salazar-Gonzalez, Z. Moldoveanu, J. Mestecky, F. Gao, B.F. Haynes, G.M. Shaw, M. Muldoon, B.T.M. Korber, and B.H. Hahn, *Antigenicity and immunogenicity of HIV-1 consensus subtype B envelope glycoproteins.* Virology, 2007. **360**(1): p. 218-234.
295. Bjellqvist, B., Hughes, G.J., Pasquali, Ch., Paquet, N., Ravier, F., Sanchez, J.-Ch., Frutiger, S. and Hochstrasser, D.F. , *The focusing positions of polypeptides in immobilized pH gradients can be predicted from their amino acid sequences.* . Electrophoresis, 1993. **14**: p. 1023-1031.
296. Bjellqvist, B., Basse, B., Olsen, E. and Celis, J.E. , *Reference points for comparisons of two-dimensional maps of proteins from different human cell types defined in a pH scale where isoelectric points correlate with polypeptide compositions.* . Electrophoresis, 1994. **15**: p. 529-539.
297. Gasteiger E., H.C., Gattiker A., Duvaud S., Wilkins M.R., Appel R.D., and Bairoch A., *Protein Identification and Analysis Tools on the ExPASy Server*, in *The Proteomics Protocols Handbook*, J.M. Walker, Editor. 2005, Humana Press
298. Sanders, R.W., Derking, R., Cupo, A., Julien, J.P., Yasmeen, A., de Val, N., Kim, H.J., Blattner, C., de la Peña, A.T., Korzun, J., Golabek, M., de Los Reyes, K., Ketas, T.J., van Gils, M.J., King, C.R., Wilson, I.A., Ward, A.B., Klasse, P.J., and Moore, J.P., *A next-generation cleaved, soluble HIV-1 Env trimer, BG505 SOSIP.664 gp140, expresses multiple epitopes for broadly neutralizing but not non-neutralizing antibodies.* PLoS Pathogens, 2013. **9**(9): p. e1003618.
299. Julien, J.P., Cupo, A., Sok, D., Stanfield, R.L., Lyumkis, D., Deller, M.C., Klasse, P.J., Burton, D.R., Sanders, R.W., Moore, J.P., Ward, A.B., and Wilson, I.A., *Crystal structure of a soluble cleaved HIV-1 envelope trimer.* Science, 2013. **342**(6165): p. 1477-1483.
300. Klasse, P.J., Depetris, R.S., Pejchal, R., Julien, J.P., Khayat, R., Lee, J.H., Marozsan, A.J., Cupo, A., Cocco, N., Korzun, J., Yasmeen, A., Ward, A.B., Wilson, I.A., Sanders, R.W., and Moore, J.P., *Influences on trimerization and aggregation of soluble, cleaved HIV-1 SOSIP envelope glycoprotein.* Journal of Virology, 2013. **87**(17): p. 9873-9885.
301. Dey, A.K., K.B. David, M. Lu, and J.P. Moore, *Biochemical and biophysical comparison of cleaved and uncleaved soluble, trimeric HIV-1 envelope glycoproteins.* Virology, 2009. **385**(1): p. 275-281.
302. Doria-Rose, N.A., Learn, G.H., Rodrigo, A.G., Nickle, D.C., Li, F., Mahalanabis, M., Hensel, M.T., McLaughlin, S., Edmonson, P.F., Montefiori, D., Barnett, S.W., Haigwood, N.L., and Mullins, J.I., *Human immunodeficiency virus type 1 subtype B ancestral envelope protein is functional and elicits neutralizing antibodies in rabbits similar to those elicited by a circulating subtype B envelope.* Journal of Virology, 2005. **79**(17): p. 11214-11224.
303. Saphire, E.O., P.W.H.I. Parren, R. Pantophlet, M.B. Zwick, G.M. Morris, P.M. Rudd, R.A. Dwek, R.L. Stanfield, D.R. Burton, and I.A. Wilson, *Crystal Structure of a Neutralizing Human IgG Against HIV-1: A Template for Vaccine Design.* Science, 2001. **293**(5532): p. 1155-1159.

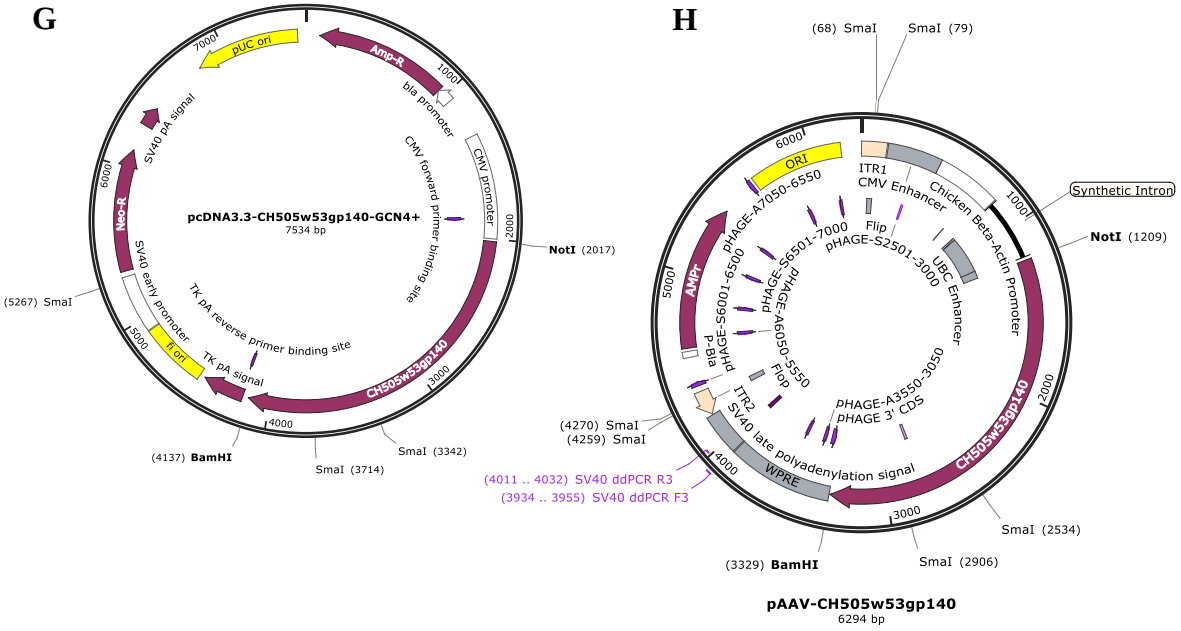
304. Fuchs, S.P., and Desrosiers, R.C., *Promise and problems associated with the use of recombinant AAV for the delivery of anti-HIV antibodies.* Molecular Therapy — Methods & Clinical Development, 2016. **3**: p. 1-18.
305. Loomis, R., and Johnson, P. R., *Emerging Vaccine Technologies.* Vaccines, 2015. **3**(2): p. 429.
306. Ura, T., Okuda, K., and Shimada, M., *Developments in Viral Vector-Based Vaccines.* Vaccines, 2014. **2**(3): p. 624-641.
307. Grimm, D., Kay, M.A., and Kleinschmidt, J.A., *Helper Virus-Free, Optically Controllable, and Two-Plasmid-Based Production of Adeno-associated Virus Vectors of Serotypes 1 to 6.* Mol Ther, 2003. **7**(6): p. 839-850.
308. Daya, S., and Berns, K.I., *Gene Therapy Using Adeno-Associated Virus Vectors.* Clinical Microbiology Reviews, 2008. **21**(4): p. 583–593.
309. Gonçalves, M.A.F.V., *Adeno-associated virus: from defective virus to effective vector.* Virology Journal, 2005. **2**(43): p. 1-17.
310. Gray, S.J., Choi, V.W., Asokan, A., Haberman, R.A., McCown, T.J., and Samulski, R.J., *Production of Recombinant Adeno-Associated Viral Vectors and Use in In Vitro and In Vivo Administration.* Current Protocols in Neuroscience, 2011. **4.17**: p. 1-36.
311. Samulski, R.J., Chang, L.S., and Shenk, T., *Helper-free stocks of recombinant adeno-associated viruses: normal integration does not require viral gene expression.* Journal of Virology, 1989. **63**(9): p. 3822-3828.
312. Clark, K.R., X. Liu, J.P. McGrath, and P.R. Johnson, *Highly Purified Recombinant Adeno-Associated Virus Vectors Are Biologically Active and Free of Detectable Helper and Wild-Type Viruses.* Human Gene Therapy, 1999. **10**(6): p. 1031-1039.
313. Weaver, S., Dube, S., Mir, A., Qin, J., Sun, G., Ramakrishnan, R., Jones, R.C., and Livak, K.J., *Taking qPCR to a higher level: Analysis of CNV reveals the power of high throughput qPCR to enhance quantitative resolution.* Methods, 2010. **50**(4): p. 271–276.
314. Ayuso, E., V. Blouin, M. Lock, S. McGorray, X. Leon, M.R. Alvira, A. Auricchio, S. Bucher, A. Chtarto, K.R. Clark, C. Darmon, M. Doria, W. Fountain, G. Gao, K. Gao, M. Giacca, J. Kleinschmidt, B. Leuchs, C. Melas, H. Mizukami, M. Müller, Y. Noordman, O. Bockstael, K. Ozawa, C. Pythoud, M. Sumaroka, R. Surosky, L. Tenenbaum, I. van der Linden, B. Weins, J.F. Wright, X. Zhang, L. Zentilin, F. Bosch, R.O. Snyder, and P. Moullier, *Manufacturing and Characterization of a Recombinant Adeno-Associated Virus Type 8 Reference Standard Material.* Human Gene Therapy, 2014. **25**(11): p. 977-987.
315. D'Costa, S., V. Blouin, F. Broucque, M. Penaud-Budloo, A. Fçranois, I.C. Perez, C. Le Bec, P. Moullier, R.O. Snyder, and E. Ayuso, *Practical utilization of recombinant AAV vector reference standards: focus on vector genomes titration by free ITR qPCR.* Molecular Therapy - Methods & Clinical Development, 2016. **3**: p. 16019.
316. Ellis, B.L., Hirsch, M.L., Barker, J.C., Connelly, J.P., Steininger III, R.J., and Porteus, M.H., *A survey of ex vivo/in vitro transduction efficiency of mammalian primary cells and cell lines with Nine natural adeno-associated virus (AAV1-9) and one engineered adeno-associated virus serotype.* Virology Journal, 2013. **10**(74).
317. Werling, N.J., S. Satkunanathan, R. Thorpe, and Y. Zhao, *Systematic Comparison and Validation of Quantitative Real-Time PCR Methods for the Quantitation of Adeno-Associated Viral Products.* Human Gene Therapy Methods, 2015. **26**(3): p. 82-92.
318. Sidransky, D., T. Tokino, Hamilton, K. Kinzler, B. Levin, P. Frost, and B. Vogelstein, *Identification of ras oncogene mutations in the stool of patients with curable colorectal tumors.* Science, 1992. **256**(5053): p. 102-105.

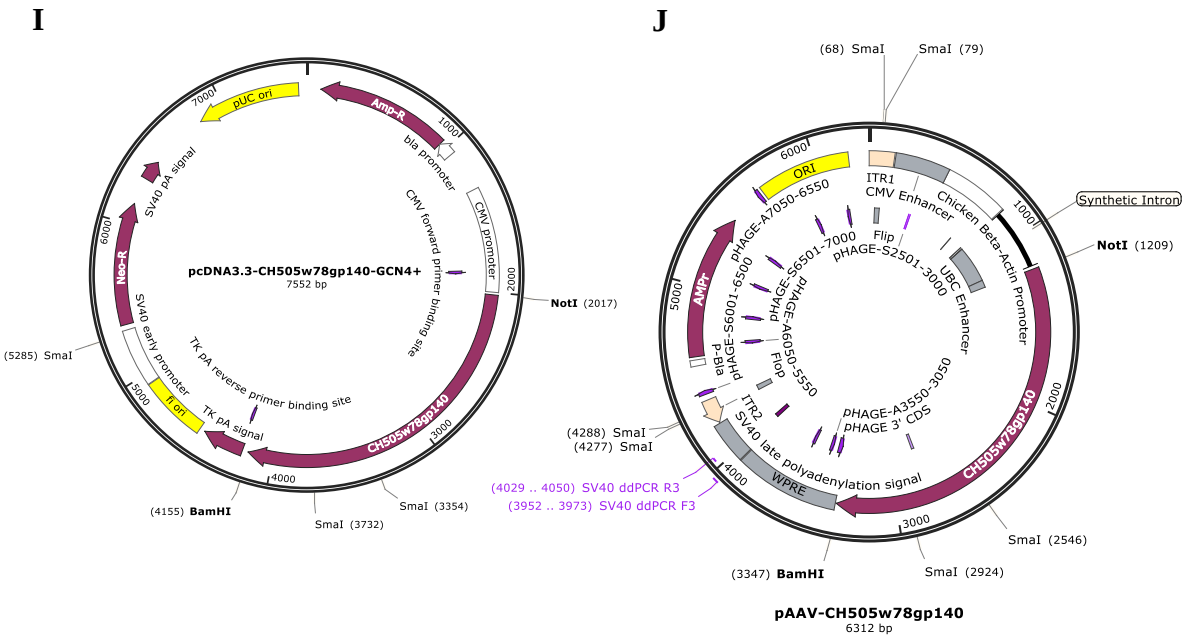
319. Vogelstein, B. and K.W. Kinzler, *Digital PCR.* Proceedings of the National Academy of Sciences, 1999. **96**(16): p. 9236-9241.
320. Morley, A.A., *Digital PCR: A brief history.* Biomolecular Detection and Quantification, 2014. **1**(1): p. 1-2.

Appendix A: Supplementary figures



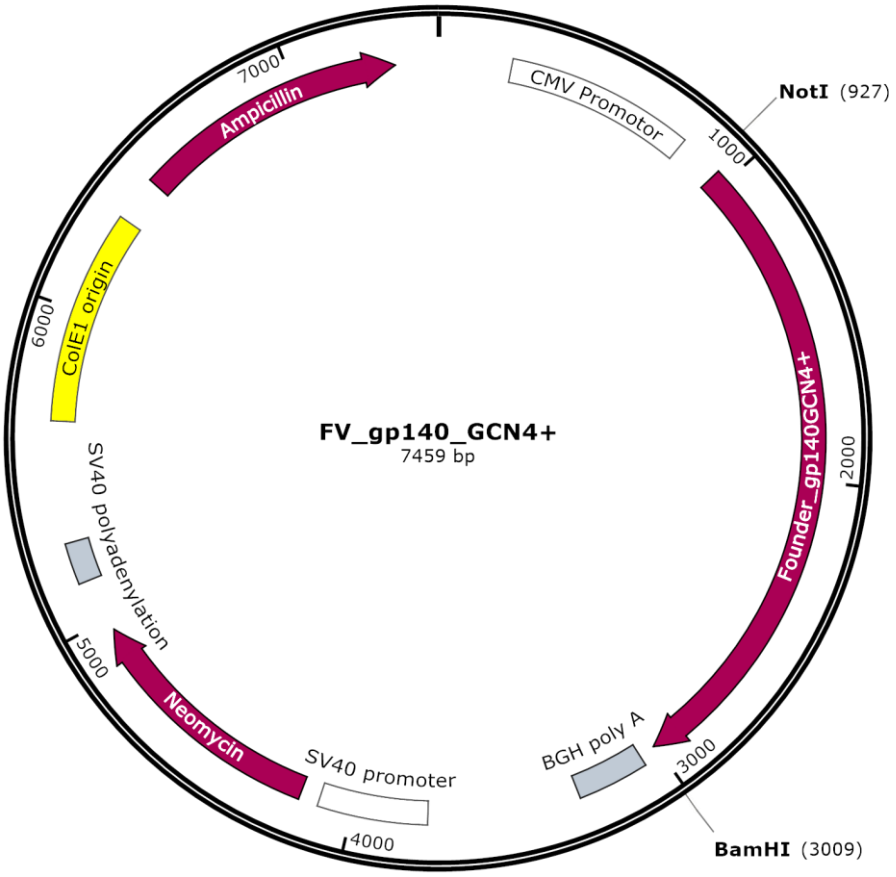

E
pcDNA3.3-CH505w30gp140-GCN4+
7534 bp
pUC ori
Amp-R
bla promoter
CMV forward primer binding site
CMV promoter
NotI (2017)
CH505w30gp140
TK pA reverse primer binding site
TK pA signal
f1 ori
SV40 early promoter
Neo-R
SV40 pA signal
(5267) SmaI
(4137) BamHI
SmaI (3714)
SmaI (3345)
F
(68) SmaI
SmaI (79)
ORI
ITR1
CMV Enhancer
Chicken Beta-Actin Promoter
Synthetic Intron
NotI (1209)
UBC Enhancer
pHAGE-S2501-3000
Flip
pHAGE-S6501-7000
pHAGE-A7050-6550
pHAGE-S6001-6500
pHAGE-A6050-5550
Flop
P-Bla
AMPr
pHAGE-A3550-3050
pHAGE 3' CDS
ITR2
SV40 late polyadenylation signal
WPRE
CH505w30gp140
(4270) SmaI
(4259) SmaI
(4011 .. 4032) SV40 ddPCR R3
(3934 .. 3955) SV40 ddPCR F3
SmaI (2537)
SmaI (2906)
(3329) BamHI
pAAV-CH505w30gp140
6294 bp


G
pcDNA3.3-CH505w53gp140-GCN4+
7534 bp
pUC ori
Amp-R
bla promoter
CMV forward primer binding site
CMV promoter
NotI (2017)
CH505w53gp140
TK pA reverse primer binding site
TK pA signal
f1 ori
SV40 early promoter
Neo-R
SV40 pA signal
(5267) SmaI
(4137) BamHI
SmaI (3714)
SmaI (3342)
H
(68) SmaI
SmaI (79)
ORI
ITR1
CMV Enhancer
Chicken Beta-Actin Promoter
Synthetic Intron
NotI (1209)
UBC Enhancer
pHAGE-S2501-3000
Flip
pHAGE-S6501-7000
pHAGE-A7050-6550
pHAGE-S6001-6500
pHAGE-A6050-5550
Flop
P-Bla
AMPr
pHAGE-A3550-3050
pHAGE 3' CDS
ITR2
SV40 late polyadenylation signal
WPRE
CH505w53gp140
(4270) SmaI
(4259) SmaI
(4011 .. 4032) SV40 ddPCR R3
(3934 .. 3955) SV40 ddPCR F3
SmaI (2534)
SmaI (2906)
(3329) BamHI
pAAV-CH505w53gp140
6294 bp



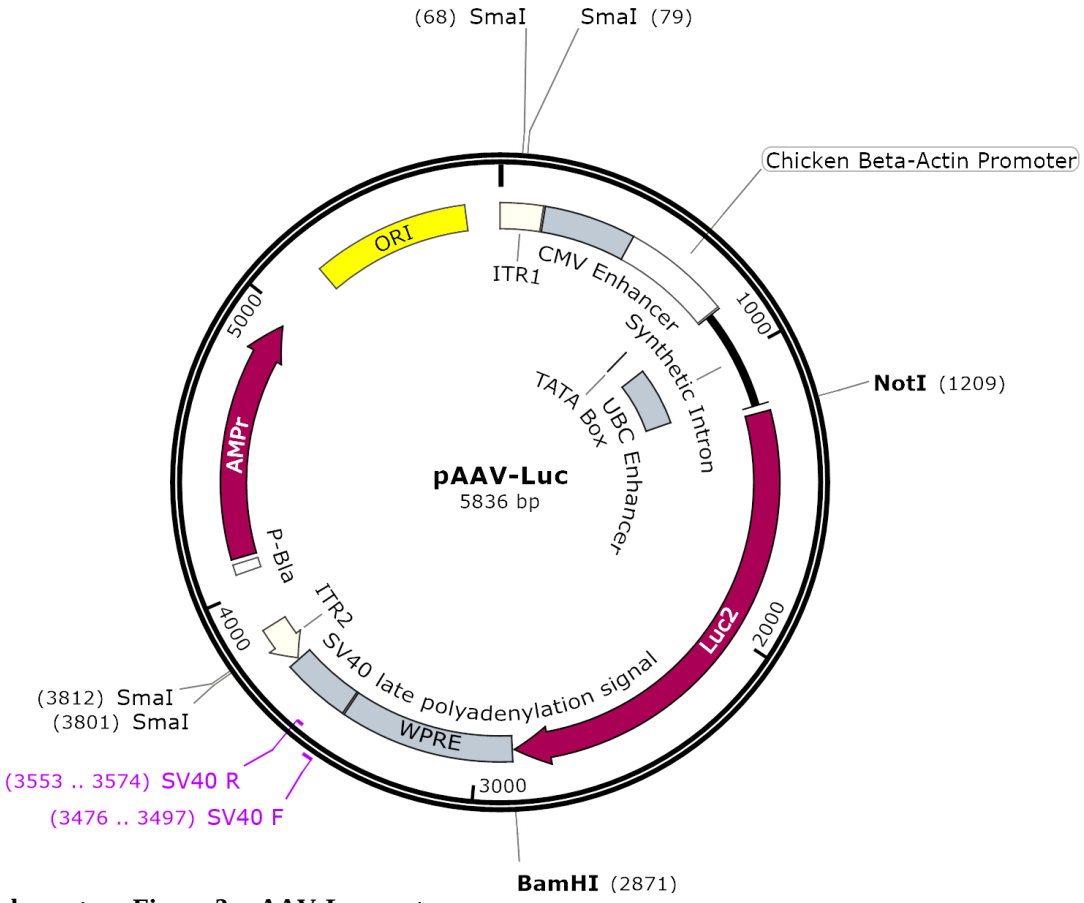
Supplementary Figure 1: pcDNA3.3-CH505w*n*gp140 and corresponding pAAV-CH505w*n*gp140 vector maps.

(A, C, E, G, I) Schematic representations of the pcDNA3.3 expression vectors containing the CH505 Env transgenes (w4, w20, w30, w53, and w78 respectively) flanked by the *Bam*HI and *Not*I restriction sites used for plasmid validation and restriction cloning. Existing *Sma*I restriction sites are also indicated. (B, D, F, H, J) Corresponding schematic representations of the pAAV vectors containing the same CH505 Env transgenes flanked by the *Bam*HI and *Not*I restriction sites used for plasmid validation and restriction cloning. Existing and additional *Sma*I restriction sites are also indicated. The SV40 primers are indicated in purple (R= reverse primer; F = forward primer). (B) includes additional primers used for sequencing done on the w4 construct.



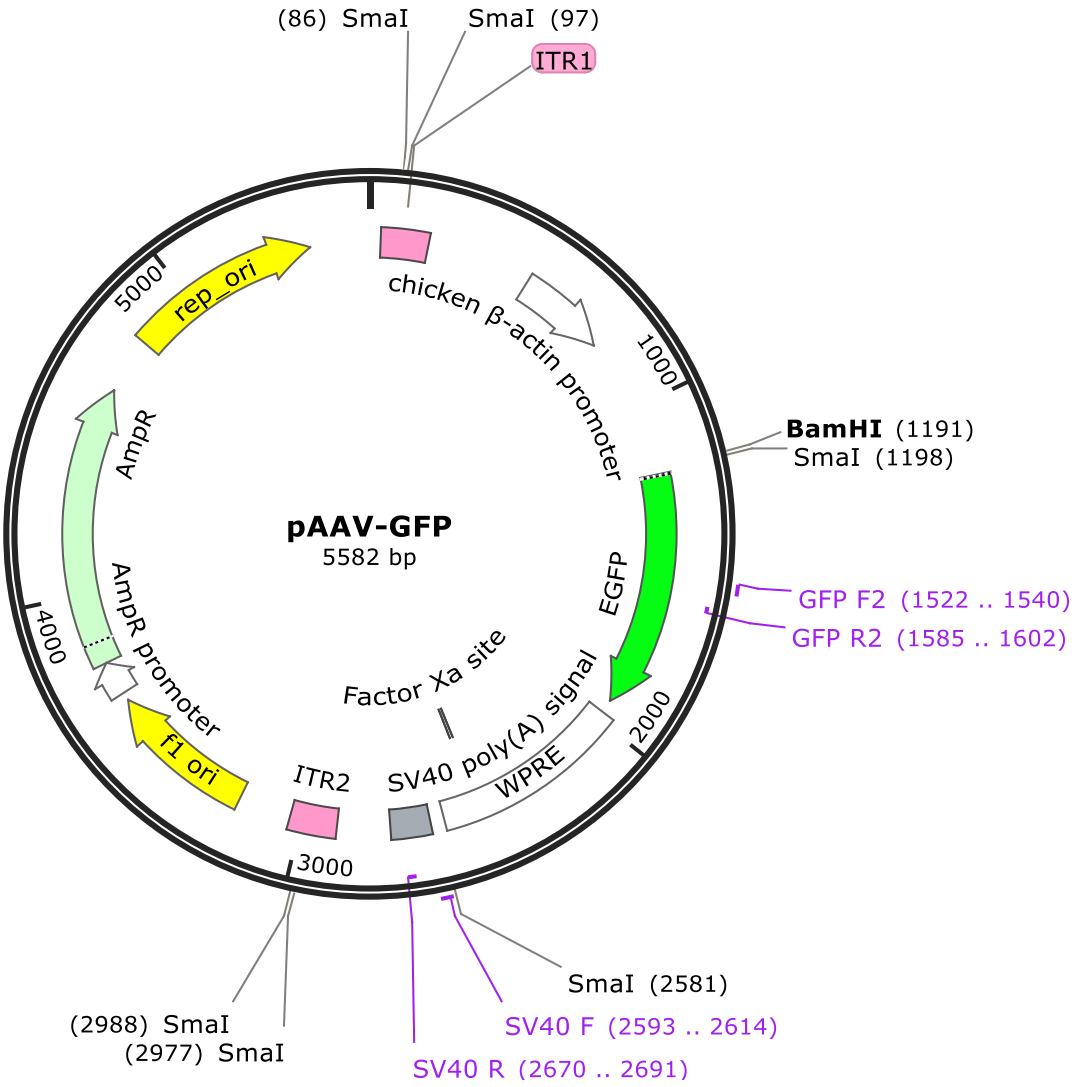
Supplementary Figure 2: pcDNA3.1-FVgp140 vector map.

Schematic representation of the pcDNA3.1 expression vector containing the FV Env transgene flanked by the *Bam*HI and *Not*I restriction sites used for plasmid validation.



Supplementary Figure 3: pAAV-Luc vector map.

Schematic representation of the pAAV vector containing the luciferase (luc) transgene flanked by the *Bam*HI and *Not*I restriction sites used for plasmid validation and restriction cloning. The *Sma*I restriction sites used for further plasmid validation are indicated in the ITR sequences. The SV40 primers are indicated in purple (R= reverse primer; F = forward primer).



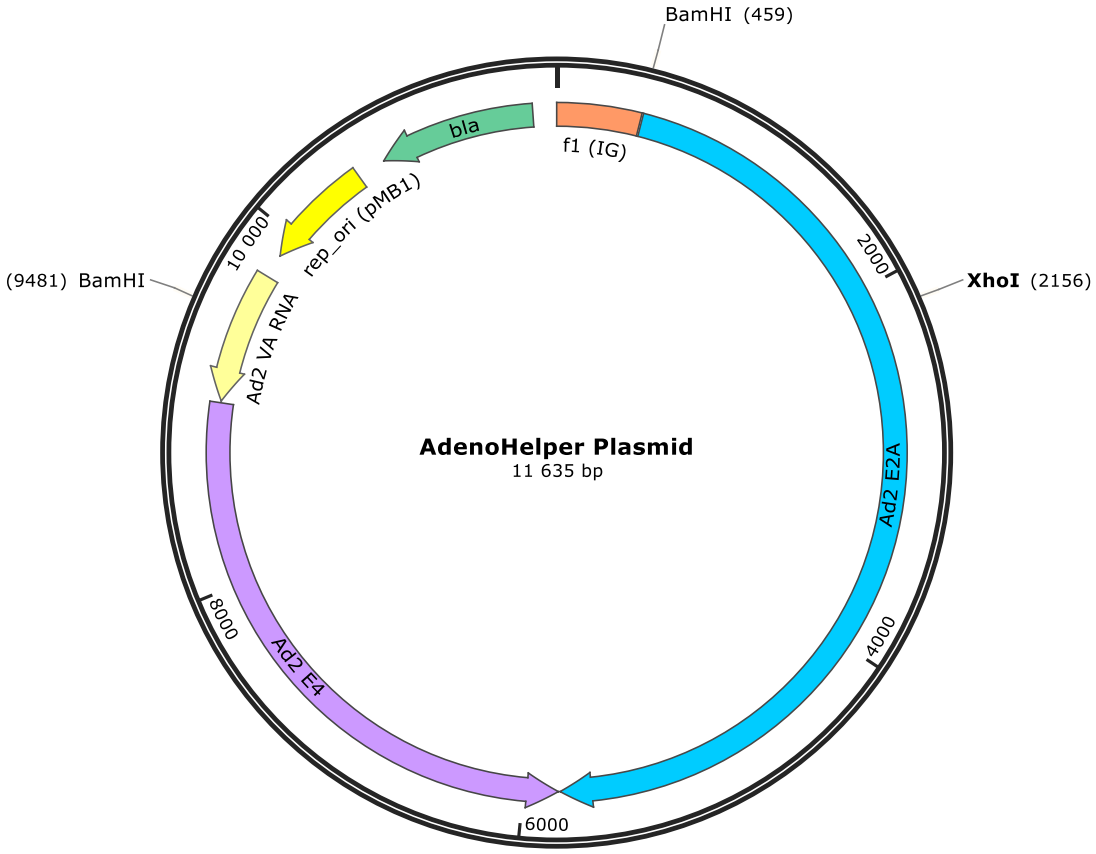
Supplementary Figure 4: pAAV-GFP vector map.

Schematic representation of the pAAV vector containing the enhanced green fluorescent protein (GFP) transgene flanked by the *Bam*HI and *Not*I restriction sites used for plasmid validation. The *Sma*I restriction sites used for further plasmid validation are indicated. The SV40 primers (SV40 R= reverse primer; SV40 F = forward primer) and GFP primers (GFP R2 = reverse primer; GFP F2 = forward primer) are indicated in purple



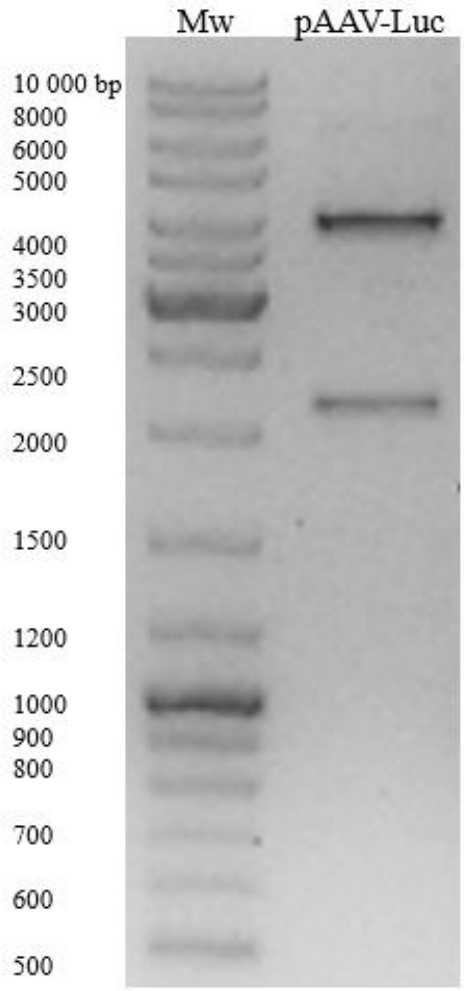
Supplementary Figure 5: Replication/ capsid (rep/cap) serotype 2 vector map.

Schematic representation of the rep/ cap serotype 2 AAV vector, containing the replication and capsid genes from AAV serotype 2. The indicated *Bam*HI and *Nco*I restriction sites were used for plasmid validation.

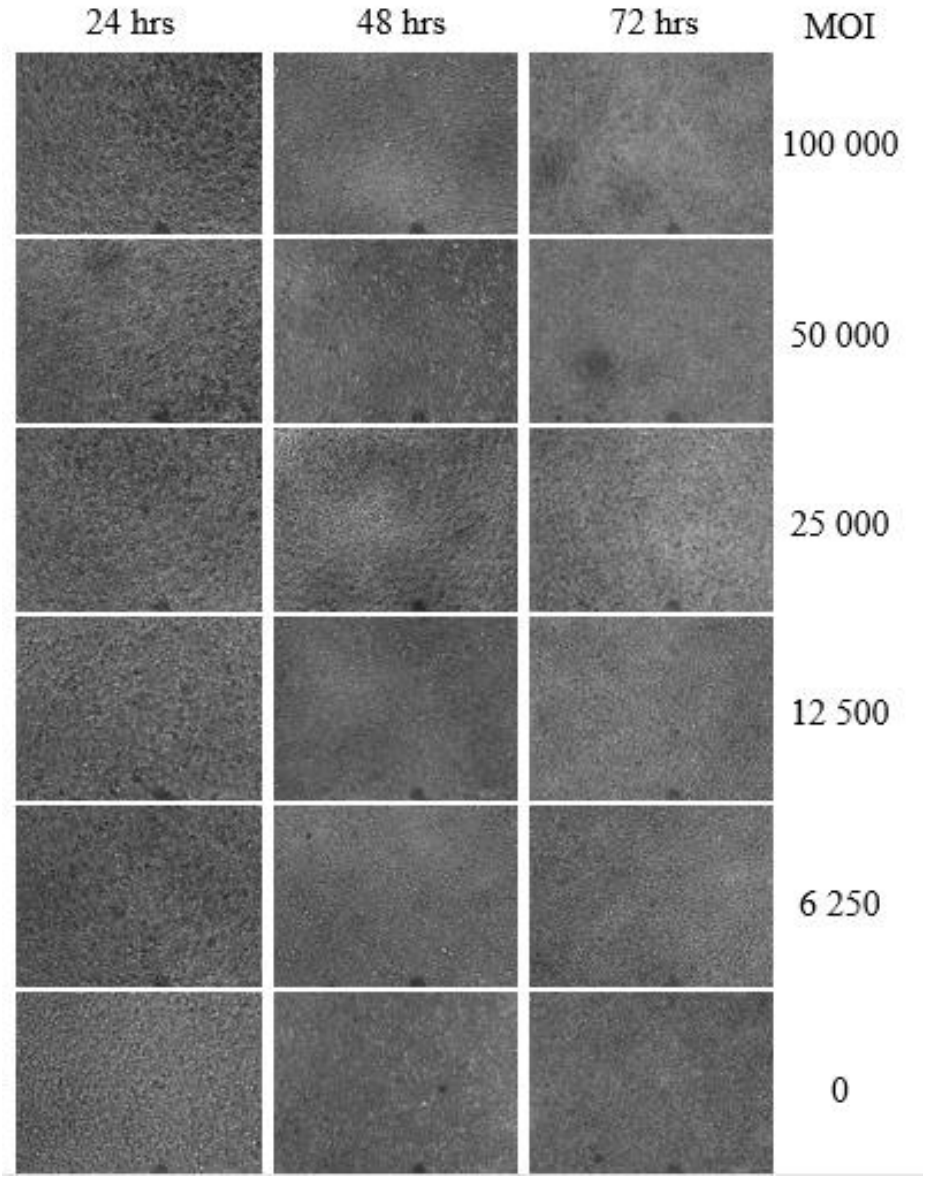


Supplementary Figure 6: AdenoHelper vector map.

Schematic representation of the AdenoHelper vector map, containing the Adeno virus 2 VA RNA, E$, and E2A transgenes required for efficient rAAV production. The indicated *Bam*HI and XhoI restriction sites were used for plasmid validation.



Supplementary Figure 7: Restriction digest analysis of the pAAV-Luc expression vector, showing intact ITRs. DNA samples were run on a 1% agarose gel and visualised under UV light. The pAAV-Luc plasmid was digested with the *Sma*I restriction enzyme (multiple restriction sites) to check ITR integrity. Mw corresponds to the O'Gene Ruler DNA ladder (Thermo Fisher Scientific, Waltham, MA, USA) used; bands are indicated on the left in base pairs (bp).



Supplementary Figure 8: Corresponding bright field images for the relative transduction efficiency of the rAAV-GFP vector *in vitro*. HEK293 T cells were infected in duplicate at various MOIs (range 100 000 - 0). The bright field images were taken at 24, 48, and 72 hours post-transduction (exposure time 5 ms). Magnification = 100x.

Appendix B: Standard protocols and recipes

B1) Bacterial cell culture

B1.1) Transformation buffer (pH 7.00; 100 mM $CaCl_2$, 10 mM PIPES-HCl, 15% Glycerol)

1.4702 g of $CaCl_2$-H_2O (Calbiochem), 0.3024 g PIPES (Merck, South Africa) and 15 ml of glycerol (Merck, South Africa) were mixed with dH_2O to a final volume of 100 ml. The pH was adjusted to 7.00 using NaCl, then autoclaved (121°C, 1 kg/cm^2, 20 minutes), and stored at 4°C until needed.

B1.2) Preparation of chemically competent *E. coli* (DH5α, SURE2) cells

20 ml of LB broth was inoculated with 10 µl of glycerol stock *E. coli* cells, under sterile conditions. This culture was incubated overnight at 37°C in a shaking incubator. The overnight culture was diluted by adding 1 ml to 39 ml of LB broth and grown for a further 2 hours at 37°C in the shaking incubator until log growth phase was reached. Once the A_{600} measurement was between 0.4-0.6, the culture was centrifuged at 6000 x g for 10 minutes at 4°C, to pellet the cells. The supernatant was discarded, and the pellet was re-suspended in 10 ml of ice cold transformation buffer per 50 ml of culture and incubated on ice for 20 minutes. The cells were pelleted again at 6000 x g for 10 minutes at 4°C. The supernatant was discarded, and the pellet was re-suspended in 1 ml of ice cold transformation buffer. One hundred microliter aliquots of the chemically competent *E. coli* cells were stored at -80°C until needed.

B1.3) Transformation of competent *E. coli* (DH5α, SURE2) cells

Half a microliter of plasmid DNA (100ng) was added to 50 µl of chemically competent E. *coli* (DH5α, SURE2) cells, and incubated on ice for 20 minutes. A mock transformation (with no plasmid DNA) was also performed to serve as the negative control. Cells were heat shocked at 42°C for 45 seconds and immediately put back on ice for 5 minutes. Each transformation reaction was spread onto an agar plate (supplemented with 100 µg/ml ampicillin for DH5α cells; or 100 µg/ml carbenicillin for SURE2 cells) under sterile conditions, and incubated overnight at 37°C.

B1.4) Luria-Bertani (LB) media (1 L)

Ten grams of Tryptone powder (Merck, South Africa, South Africa), 5 g yeast extract (Merck, South Africa) and 5 g NaCl (Merck, South Africa) were dissolved in dH_2O to a final volume

of 1 L. The broth was autoclaved (121°C, 1 kg/cm^2, 20 minutes) and stored at room temperature until needed.

B1.5) 2YT Luria-Bertani (LB) media (1 L)

Sixteen grams Tryptone powder (Merck, South Africa, South Africa), 10 g yeast extract (Merck, South Africa) and 5 g NaCl (Merck, South Africa) were dissolved in dH_2O to a final volume of 1 L. The broth was autoclaved (121°C, 1 kg/cm^2, 20 minutes) and stored at room temperature until needed.

B1.6) LB agar plates (1 L)

Seven grams of LB agar powder (Sigma-Aldrich, St. Louis, MO, USA) was dissolved in dH_2O to a final volume of 200 ml. The agar was autoclaved (121°C, 1 kg/ cm^2, 20 minutes) and allowed to cool to approximately 50°C before the addition of 100 µg/ ml ampicillin and poured into 90 mm Petri dishes and allowed to set. Plates were stored at 4°C until used.

B1.7) Antibiotics

B1.7.1) Ampicillin Stock; 100 mg/ ml (use at final concentration 100 µg/ml= 1µl/ml)

One gram of ampicillin (Roche, Basel, Switzerland) was dissolved in 70% ethanol (Sigma-Aldrich, St. Louis, MO, USA) to a final volume of 10 ml, filter sterilised, and stored in 1 ml aliquots at -20°C until needed.

B1.7.2) Carbenicillin Stock; 100 mg/ ml (use at final concentration 100 µg/ml= 1µl/ml)

One gram of carbenicillin (Thermo Fisher Scientific, Waltham, MA, USA) was dissolved in 70% ethanol (Sigma-Aldrich, St. Louis, MO, USA) to a final volume of 10 ml, filter sterilised, and stored in 1 ml aliquots at -20°C until needed.

B1.7.3) Chloramphenicol Stock; 34 mg/ ml (use at final concentration 170 µg/ml)

Three-four milligrams of chloramphenicol (Thermo Fisher Scientific, Waltham, MA, USA Thermo Fisher Scientific, Waltham, MA, USA) was dissolved in 100% ethanol (Sigma-Aldrich, St. Louis, MO, USA) to a final volume of 10 ml, filter sterilised, and stored in 1 ml aliquots at -20°C until needed.

B2) Restriction enzyme digests

Table B1: Restriction enzymes and corresponding buffers used for restriction enzyme digests of plasmids, all from Thermo Fisher Scientific (Waltham, MA, USA).

Enzyme	Corresponding buffer
*Bam*HI	Unique buffer (10x Buffer *Bam*HI)
*Not*I	10x Buffer O (orange)
*Bam*HI + *Not*I double digest	Unique buffer (10x Buffer *Bam*HI)
*Sma*I	10x Buffer Tango
*Xho*I	10x Buffer R (red)
*Nco*I	10x Buffer Tango

B3) Agarose gel electrophoresis

B3.1) 0.5 M EDTA (Ethylenediaminetetraacetic acid; pH 8.0)

93.05 g of EDTA was dissolved in dH_2O to a final volume of 500 ml. The pH of the solution was adjusted to 8.0 by adding 10 M NaOH. This was autoclaved (121°C, 1 kg/cm^2, 20 minutes), and stored at room temperature until needed.

B3.2) 50 x TAE (Tris-acetate-EDTA) buffer

242 g of Tris, 57.1 ml of glacial acetic acid and 100 ml of 0.5 M EDTA were dissolved in dH_2O to a final volume of 1 L and stored at room temperature until needed.

B3.3) 1 X TAE buffer

10 ml of 50 X TAE stock buffer was made up to 500 ml with dH_2O and stored at room temperature until needed

B3.4) Preparation of agarose gels

1% agarose gels were made by adding 1 g of agarose powder (Sigma-Aldrich, St. Louis, MO, USA) to 100 ml of 1 X TAE buffer. The mixture was the heated until the agarose powder had fully dissolved; prior to pouring the gels, a final concentration of 0.5 μg/ml of ethidium bromide (Promega, Fitchburg, WI, USA) was added. Gels were poured into a Bio-Rad gel Chamber System (Bio-Rad, CA, USA) and allowed to set at room temperature.

B3.5) Electrophoresis procedure

Agarose gels were placed in the Bio-Rad Gel Tank System (Bio-Rad, CA, USA), and submerged in 1 X TAE buffer to allow for even heat conduction during DNA separation. All

DNA samples, controls and the MassRuler DNA Ladder mix (Thermo Fisher Scientific, Waltham, MA, USA) or the O'Gene Ruler DNA Ladder mix, Ready-to-use (Thermo Fisher Scientific, Waltham, MA, USA) were mixed with 6x Orange DNA Loading Dye (Thermo Fisher Scientific, Waltham, MA, USA). Gels were run at maximum current, and 50 V for 15 minutes (until samples exited the wells) and then voltage increase to 80 V for 15-20 minutes or until the samples had adequately resolved. DNA bands on the gels were visualised and images captured under UV light using the ChemiDoc™ MP imaging system from Bio-Rad (CA, USA) and the QuantityOne version 4.6.9 Software Programme (Bio-Rad, CA, USA).

B4) Mammalian cell culture

B4.1) Freezing mix (90% [v/v] FCS; 10% [v/v] DMSO)

9 ml foetal calf serum (FCS) (Gibco, Life Technologies, Carlsbad, CA, USA) was added to 1 ml dimethyl sulphoxide (DMSO) (Fluka Chemika, Buchs, Switzerland), filter sterilised, and stored at -20°C until needed.

B4.2) PEIMax Transfection Reagent Stock solution (1 mg/ml)

10 mg of PEImax (Polysciences Inc.) was dissolved in 10 ml of dH_2O, filter sterilised, and stored in 1 ml aliquots at -20°C until needed.

B5) SDS-PAGE

B5.1) Monomer Solution: 30% Acrylamide/ 0.8% Bisacrylamide

30 g of acrylamide (Sigma-Aldrich, St. Louis, MO, USA) and 0.8 g of bisacrylamide (N, N'-methylenebisacrylamide) (Sigma-Aldrich, St. Louis, MO, USA) were dissolved in dH_2O to a final volume of 100 ml. This was stored in the dark at 4°C until needed.

B5.2) Running Gel Buffer: 4X Tris-HCl, pH 8.8 (1.5 M Tris)

91 g Tris (USB, Cleveland, OH, USA) was dissolved in dH_2O to a volume of 300 ml. HCl was used to adjust the pH to 8.8 and made up to a final volume of 500 ml and was thereafter stored in the dark at 4°C until needed.

B5.3) Stacking Gel Buffer: 4X Tris-HCl, pH 6.8 (0.5 M Tris)

6.05 g Tris (USB, Cleveland, OH, USA) was dissolved in dH_2O to a volume of 40 ml. HCl was used to adjust the pH to 6.8 and made up to a final volume of 100 ml and was thereafter stored in the dark at 4°C until needed.

B5.4) 10% Sodium Dodecyl Sulphate (SDS)

10 g of SDS (Calibiochem) was dissolved in dH_2O to a final volume of 100 ml and stored at room temperature until needed.

B5.5) 10% Ammonium Persulphate (APS)

0.1 g of APS (Sigma-Aldrich, St. Louis, MO, USA) was dissolved in dH_2O to a final volume of 1 ml. The solution was made up fresh each time.

B5.6) 2X Laemmli Sample Buffer (0.125 M Tris-HCl, 4% SDS, 20% v/v Glycerol, 0.2 M DTT, 0.02% Bromophenol Blue, pH 6.8)

2.5 ml of 4X stacking gel buffer, 4 ml of 10% SDS, 2 ml of glycerol (Saarchem, Merck, South Africa), 0.31 g DTT (from where) and 2 mg bromophenol blue (Saarchem, Merck, South Africa) were dissolved in dH_2O to a final volume of 10 ml. This was then aliquoted into 1 ml samples that were stored at -20°C until needed.

B5.7) 10X Tank buffer (Electrophoresis buffer)

30.28 g Tris-HCl, 144.13 g of glycine and 10 g SDS were dissolved in dH_2O to a final volume of 1 L. This was stored at room temperature until needed.

B5.8) Preparation of SDS-PAGE gels

SDS-PAGE gels were assembled using the BioRad Gel Casting System (CA, USA). Briefly, the casting chamber was assembled and sealed with parafilm, and the separating gel solution was added to the chamber, followed by a layer of isopropanol (Sigma-Aldrich, St. Louis, MO, USA) to seal and level the gel. Once set, the isopropanol was poured off and the stacking gel solution was added, the comb was inserted, and the gel was allowed to set. Once the gel was fully set, it was wrapped in paper towel, wet, wrapped in cling wrap and stored at 4°C.

Table B2: Running and Stacking gel recipes for 1.5 and 0.75 mm gels [265]**.**

Running gel and stacking gel recipes for 1.5- and 0.75-mm thick gels					
Running gel final concentration (30 ml; 2 ea. 0.75 mm thick SE 600/400 gels)					
	5%	7.5%	10%	12.5%	15%
Monomer solution	5 ml	7.5 ml	10 ml	12.5 ml	15 ml
4X Running gel buffer	7.5 ml	7.5 ml	7.5 ml	7.5 ml	7.5 ml
10% SDS	0.3 ml	0.3 ml	0.3 ml	0.3 ml	0.3 ml
ddH2O	17.1 ml	14.6 ml	12.1 ml	9.6 ml	7.1 ml
10% Ammonium persulphate*	150 µl	150 µl	150 µl	150 µl	150 µl
TEMED*	10 µl	10 µl	10 µl	10 µl	10 µl
Stacking gel solutions (4% Acrylamide; for 2 gels)					
	0.75 mm	1.5 mm			
Monomer solution	1.33 ml	2.66 ml			
4X Stacking gel buffer	2.5 ml	5.0 ml			
10% SDS	0.1 ml	0.2 ml			
ddH2O	6.0 ml	12.0 ml			
10% Ammonium persulphate*	50 µl	100 µl			
TEMED*	5 µl	10 µl			

*Added last.

B5.9) SDS-PAGE electrophoresis procedure

SDS-PAGE gels were run under denaturing conditions using the BioRad Gel System (CA, USA) submerged in 1 X Tank buffer, to allow for even heat conduction. All the samples and controls were mixed with 2 X Treatment buffer, boiled for 5 minutes, and loaded into the wells. The Colour Protein Standard Broad Range (Thermo Fisher Scientific, Waltham, MA, USA) was used for molecular weight calculation. The gels were run at a constant voltage of 150 V.

B5.10) Staining procedures

B5.10.1) Coomassie Stain

0.25 g Coomassie® Brilliant Blue R250 (Sigma-Aldrich, St. Louis, MO, USA) was dissolved in 500 ml methanol (Sigma-Aldrich, St. Louis, MO, USA), 100 ml acetic acid and 400 ml dH_2O. The solution was stored at room temperature until needed.

B5.10.2) Destaining solution 1 (5% Methanol, 7% Acetic acid)

50 ml ethanol (Sigma-Aldrich, St. Louis, MO, USA), 70 ml acetic acid and 880 ml of dH_2O were mixed at stored at room temperature until needed.

B5.10.3) Destaining solution 2 (40% Methanol, 7% Acetic acid)

400 ml methanol (Sigma-Aldrich, St. Louis, MO, USA), 70 ml acetic acid and 530 ml dH_2O were mixed and stored at room temperature until needed.

B5.10.4) Quick destain solution

100 ml acetic acid, 125 ml isopropanol (Sigma-Aldrich, St. Louis, MO, USA) and 775 ml dH_2O were mixed and stored at room temperature until needed.

B5.10.5) Protocol for Coomassie staining

SDS-PAGE gels were stained with Coomassie® Brilliant Blue R250 (Sigma-Aldrich, St. Louis, MO, USA) overnight at room temperature with gentle shaking. The gels were then either destained with destaining solution 1 and 2, or with the quick destain, both at room temperature with gentle shaking. Protein bands were visualised, and images captured under white light using ChemiDoc™ MP imaging system from Bio-Rad (CA, USA) and the Quantity One Version 4.6.1 Software Programme (Bio-Rad, CA, USA).

B6) Western Blot

B6.1) 1X NuPAGE® Transfer buffer

25 ml NuPAGE® Transfer Buffer (20X), 100 ml of methanol (Sigma-Aldrich, St. Louis, MO, USA), were made up to 500 ml with dH_20, mixed and stored at room temperature until needed.

B6.2) 10 X Tris-Buffered Saline (TBS), pH 7.4

10 g NaCl, 30 g Tris-HCl and 2 g KCl were dissolved in 800 ml of dH_2O. HCl was used to adjust the pH to 7.4 and was made up to 1 L with dH_2O, and thereafter it was autoclaved. This was stored at room temperature until needed.

B6.3) Tris- Buffered Saline & Tween 20 (T-TBS)

1 ml of Tween-20 was added to 1 L of TBS (0.1% Tween-20, (v/v)).

B7) ELISA

B7.1) Blocking buffer

1 % (w/v) BSA (Roche, Basel, Switzerland) and 0.05 % Tween-20 (v/v) was added to 50 ml of 1 X PBS, and vortexed thoroughly until BSA was fully dissolved.

B7.2) PBS-T

0.05 % Tween-20 (v/v) was added to 1 L of 1 X PBS.

B8) Lectin Affinity Chromatography

B8.1) 0.5 M NaCl (PBS)

250 ml of 1 M NaCl was added to 250 ml PBS to give 500ml 0.5 M NaCl.

B8.2) 1 M NaCl (PBS)

29.22 g NaCl was dissolved in 750 ml 1 x PBS

B8.3) 1 x PBS

10 x PBS was diluted to 1 x PBS; final volume of 1,5 L.

B8.4) 1 M methyl α-D-mannopyranoside (MMP) (PBS)

3.88 g MMP was dissolved in 20 ml 1 x PBS. This solution was made fresh each time.

B9) rAAV Production Solutions

B9.1) Viral Lysis Buffer; 50 mM Tris-HCl (pH 8.5), 0.15 mM NaCl (1 L)

1M Tris-HCl (pH 8.5) 50 mM

121.14 g Tris base was dissolved in 900 ml milli Q dH_2O. HCl was used to adjust the pH to 7.4 and was made up to 1 L with dH_2O, and thereafter it was autoclaved. This was stored at room temperature until needed.

B9.2) NaCl 0.15M

8.8g NaCl was dissolved in 900 ml milli Q dH_2O. 50 ml of the 50 Mm Tris buffer was added, and the final volume adjusted to 1 L and autoclaved. This was stored at room temperature until needed.

B9.3) 5 x PEG (1 L) (40% PEG [final concentration 8%] in 2.5 M NaCl [final concentration 0.5 M])

146.53 g NaCl was dissolved in 600 ml milli Q dH_2O. Then 400 g of PEG was added to a 1 L bottle, followed by the NaCl solution, and autoclaved. This solution was left on a shaker at 37°C overnight, and then stored in an incubator at 37°C.

B9.4) PBS-MK (1 x PBS; 1 mM $MgCl_2$; 2.5 mM KCl)

1 x PBS tablet, 0.102 g MgCl, and 0.093g KCl were dissolved in 500 ml milli Q dH_2O. Thereafter, it was autoclaved and stored at room temperature until needed.

B9.5) PBS-MK-NaCl (1 x PBS; 1 mM $MgCl_2$; 2.5 mM KCl; 1 M NaCl)

1 x PBS tablet, 0.102 g MgCl, 0.093g KCl, and 29.22 g NaCl were dissolved in 500 ml milli Q dH_2O. Thereafter, it was autoclaved and stored at room temperature until needed.

B9.6) Preparation of Iodixanol Gradients

Table B3: Preparation of iodixanol gradients.

Gradient	Composition	Colour
60% Iodixanol	60 ml iodixanol* + 2,5 µl/ml Phenolred	Yellow
40% Iodixanol	30 ml iodixanol + 15ml PBS-MK	Clear
25% Iodixanol	20 ml iodixanol + 28ml PBS-MK + 120 µl Phenolred	Pink/ red
15% Iodixanol	12 ml iodixanol + 36ml PBS-MK-NaCl	Clear

Make sterile dilutions, and then add Phenolred
* Iodixanol (Opti-Prep, Sigma-Aldrich, St. Louis, MO, USA) is supplied sterile at 60%.

B10) Droplet Digital Polymerase Chain Reaction

B10.1) Fluorescent dyes and quenchers for probes

Table B4: The fluorescent dyes and quencher used in the ddPCR probes, obtained from Thermo Scientific (Waltham, MA, USA).

Fluorescent dye/ quencher	Description	Emission (nm)	Absorption (nm)
6-FAM™	6-Carboxyfluorescein fluorescent reporter dye	520	495
VIC™	6-Carboxyfluorescein fluorescent reporter dye	552	538
QSY™	Succinimidyl ester, amine-reactive quencher.	-	560

B10.2) Dilution buffer

994.8 µl nuclease-free water (Ambion, Thermo Fisher Scientific, Waltham, MA, USA), 0.2 µl Ultra-Pure Salmon sperm DNA (Invitrogen) (final concentration 2 ng/ µl), and 5 µl 10% Pluronic F-68 (final concentration 0.05%), were added to a 1.5 ml microcentrifuge tube and vortexed. The dilution buffer was made fresh for every round of ddPCR.

B11) Antibodies used in this study

Table B5: Primary and secondary antibodies used in this study.

Primary antibody	Epitope	Supplier
VRC01	Anti-HIV-1 gp120	NIH AIDS Reagent Program, Division of AIDS, NIAID, NIH.
10E8	Anti-HIV-1 gp41	NIH AIDS Reagent Program, Division of AIDS, NIAID, NIH.
4E10	Anti-HIV-1 gp41	NIH AIDS Reagent Program, Division of AIDS, NIAID, NIH.
HIV-1 positive patient sera		South African National Blood Service (SANBS) – unpublished data
Rabbit sera	Anti-gp140	HPRU, [262]
CH01	V1V2 region	NIH AIDS Reagent Program, Division of AIDS, NIAID, NIH.
3BNC117	Anti-HIV-1 gp120	NIH AIDS Reagent Program, Division of AIDS, NIAID, NIH.
NIH45-46 G54W	Anti-HIV-1 gp120	NIH AIDS Reagent Program, Division of AIDS, NIAID, NIH.
17b	Anti-HIV-1 gp120	NIH AIDS Reagent Program, Division of AIDS, NIAID, NIH.
IgG1b12	Anti-HIV-1 gp120	NIH AIDS Reagent Program, Division of AIDS, NIAID, NIH.

Secondary antibody	Supplier
ECL™ Anti-rabbit IgG, Horseradish Peroxidase linked whole antibody (from donkey)	GE Healthcare UK Limited, Little Chalfont, Buckinghamshire, United Kingdom.
ECL™ Anti-human IgG, Horseradish Peroxidase linked whole antibody (from sheep)	GE Healthcare UK Limited, Little Chalfont, Buckinghamshire, United Kingdom.

Appendix C: Ethics Approval

UNIVERSITY OF THE WITWATERSRAND, JOHANNESBURG

HUMAN RESEARCH ETHICS COMMITTEE (MEDICAL)

22/03/2016

C&P
Ref: W-~~CPB~~-180322-01

TO WHOM IT MAY CONCERN:

Waiver: This certifies that the following research does not require clearance from the Human Research Ethics Committee (Medical).

Investigator: Ms M Moodie et al
Student No. (if appropriate): 671828
Staff No. (if appropriate):

Supervisor: Professor M Papathanasopoulos

School: Pathology
Department: Molecular Medicine and Haematology
HIV Pathogenisis Research Unit
Medical School
University

Project title: *Sequential adeno-associated virus-delivered HIV-1 envelope glycoproteins as novel vaccine immunogens*

Reason: Laboratory analysis.
No human participants will be involved in the study.

Professor CB Penny
Chairperson: Human Research Ethics Committee (Medical)

Copy – HREC (Medical) Secretariat: Zanele Ndlovu and Rhulani Mkansi

Research Office Secretariat:
Physical address: Phillip Tobias Building, 3rd Floor, Office 302, Corner York Road and Princess of Wales Terrace, Parktown, Johannesburg 2193.
Postal address: Private Bag 3, Wits 2050
Tel Nos. +27 (0)11-717-1234/2656/2700/1252
Office E-mail: HREC-MedicalResearchOffice@wits.ac.za
Website: http://www.wits.ac.za/research/about-our-research/ethics-and-research-integrity/